Electricity System Planning with Distributed Energy Resources: New Methods and Insights for Economics, Regulation, and Policy

by

Jesse D. Jenkins

B.S., Computer & Information Science, University of Oregon (2006)

S.M., Technology & Policy, Massachusetts Institute of Technology (2014)

Submitted to the Institute for Data, Systems & Society

in partial fulfillment of the requirements for the degree of

Doctor of Philosophy in Engineering Systems

at the

MASSACHUSETTS INSTITUTE OF TECHNOLOGY

September 2018

Author .....

Institute for Data, Systems & Society

August 24, 2018

Certified by .....

Ignacio J. Pérez Arriaga

Visiting Professor, Sloan School of Management

Professor, Instituto de Investigacion Tecnológica (IIT), Universidad Pontificia Comillas

Thesis Supervisor

Certified by .....

Richard K. Lester

Professor, Department of Nuclear Science & Engineering

Committee Member

Certified by .....

Richard Schmalenesee

Professor, Sloan School of Management, Emeritus

Committee Member

Certified by .....

William W. Hogan

Professor, Kennedy School of Government, Harvard University

Committee Member

Certified by .....

Carlos Batlle

Associate Professor, Instituto de Investigacion Tecnológica (IIT), Universidad Pontificia Comillas

Committee Member

Accepted by .....

Stephen Graves

IDSS Graduate Officer

Electricity System Planning with Distributed Energy Resources: New Methods and Insights for Economics, Regulation, and Policy

by

Jesse D. Jenkins

Submitted to the Institute for Data, Systems & Society
on August 24, 2018, in partial fulfillment of the
requirements for the degree of
Doctor of Philosophy in Engineering Systems

Abstract

This dissertation demonstrates a novel integrated electric power system planning framework that incorporates distributed energy resources (DERs), flexible and price-responsive demand, and distribution network losses and reinforcement costs. New methods are developed and demonstrated to derive the aggregate impact of demand and DERs on distribution network losses and upgrade costs from detailed distribution network simulations. The results from these simulations are used to parameterize a novel and tractable representation of distribution networks at an aggregate scale in a new formulation of the electricity resource capacity planning problem. A set of case studies demonstrate the utility of this modeling framework for modeling competition amongst distributed and centralized resources, exploring trade-offs between economies of unit scale and locational value of various resources, assessing the value of price-responsive electricity demand, and considering the impact of policy or regulation that drives the adoption of DERs. Methodologically, this dissertation makes a set of contributions, including:

1. A new approach to using AC power flow simulations to accurately derive the effect of aggregate changes in power withdrawals and injections on resistive network losses in large-scale distribution networks.

2. A method for adapting AC optimal power flow simulations to identify the minimum quantity of net reductions in coincident peak demand (achieved either by demand flexibility or distributed generation or storage) necessary to accommodate demand growth in large-scale distribution networks without investment in new network assets (e.g., 'non-wires' alternatives).

3. A method for using a distribution network planning model to determine the cost of traditional network upgrades required to accommodate an equivalent increase in peak demand.

4. An integrated electricity resource capacity planning model that employs results from the above methods to incorporate DERs and flexible demand and consider key sources of locational value or cost, including impacts on transmission and distribution network costs and losses.

Electricity system planning models provide decision support for electric utilities, insight for policy-makers, and a detailed techno-economic framework to evaluate emerging technologies. Collectively, the new methods demonstrated herein expand the capabilities of these important planning tools to keep pace with a rapidly evolving electric power sector.

Thesis Supervisor: Ignacio J. Pérez Arriaga
Title: Visiting Professor, Sloan School of Management
Professor, Instituto de Investigacion Tecnológica (IIT), Universidad Pontificia Comillas

Committee Member: Richard K. Lester
Title: Professor, Department of Nuclear Science & Engineering

Committee Member: Richard Schmalenesee
Title: Professor, Sloan School of Management, Emeritus

Committee Member: William W. Hogan
Title: Professor, Kennedy School of Government, Harvard University

Committee Member: Carlos Batlle
Title: Associate Professor, Instituto de Investigacion Tecnológica (IIT), Universidad Pontificia Comillas

Acknowledgments

In the brief style of an Academy Awards acceptance speech: I would like to thank my advisor, Ignacio Pérez-Arriaga, and constant compatriot, Carlos Batlle; my august committee members, Richard Lester, Richard Schmalensee, and William Hogan; current and former collaborators, Nestor Sepulveda, Scott Burger, Fernando de Sisternes, Max Luke, Claudio Vergara, Sam Huntington, Ashwini Bharatkumar, Raanan Miller, Valerie Karplus, and Audun Botterud; the MIT Energy Initiative Utility of the Future Consortium, GE, Martin Family Society of Fellows for Sustainability, and the National Science Foundation for their financial support during my doctoral studies; and most of all, my wife, Alisha, who has supported me through a six-year marathon while giving us our beloved son (and so much more). And also coffee. I definitely want to thank coffee.

Contents

List of Figures

List of Tables

Chapter 1

Introduction

1.1 A Changing Electricity Landscape

Distributed energy resources (DERs), including distributed generation (e.g., solar photovoltaics, fuel cells, microturbines), electrical and thermal energy storage devices, and flexible or controllable electricity demand, are beginning to proliferate in electricity systems throughout the world. Benefiting from robust public policy support, these distributed technologies are now being deployed amidst several broad drivers of change in power systems, including growth in the use of variable renewable energy sources such as wind and solar energy; efforts to decarbonize the energy system as part of global climate change mitigation efforts; and the proliferation of monitoring, communication, and control technologies throughout electricity distribution systems and end-uses.

Collectively, these trends entail new options for the delivery of electricity services, substantial changes to the mix of electricity generation resources, and new challenges for power system planning and policy making. Over the past decade, improvements in electricity resource planning methods have offered new techniques to better incorporate the impacts of variable renewable energy resources, operational flexibility requirements, and transmission expansion decisions on generation investment decisions (see Section 1.2.2). Yet no current techniques yet adequately capture the potential role and value of DERs or more flexible

electricity demand in a holistic power system planning context. This thesis builds on recent advances and provides new methods for considering DERs, flexible demand, and distribution systems in the power system planning problem.

1.1.1 The Growth of Distributed Energy Resources

For much of the 20th century, the size of electric power generating units steadily increased to leverage economies of unit scale and improved efficiencies associated with larger power stations (Fig. 1-1). More recently, a combination of supportive public polices and improvements in the cost and performance of distributed generation and storage technologies have begun to reverse this trend and led to a proliferation of smaller distributed resources. At the same time, improvements in communication, computing, and control technology have lowered transaction costs associated with demand response and aggregation and control of DERs.

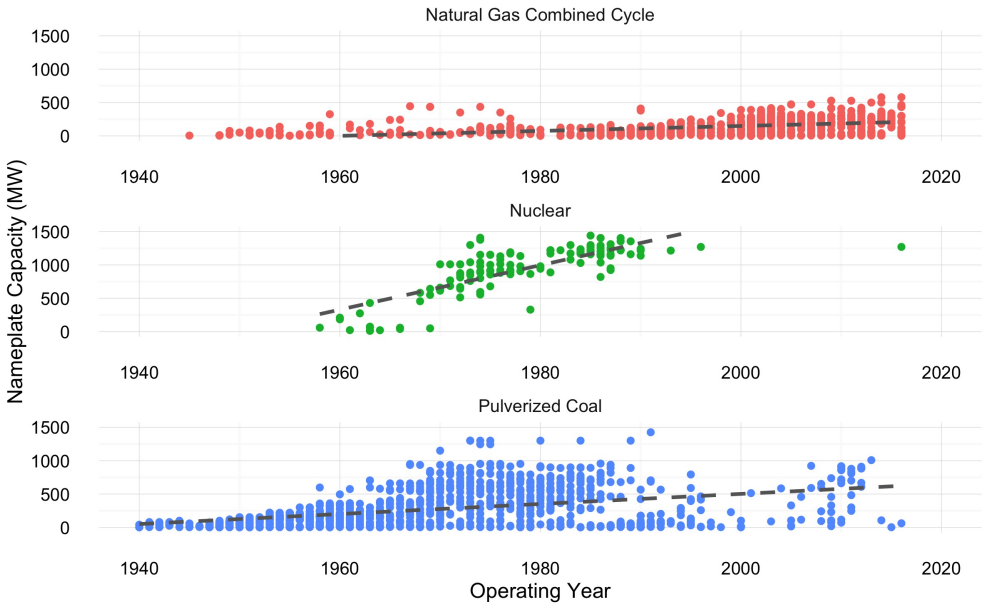

Figure 1-1: U.S. thermal generator unit size over time
Data from U.S. Energy Information Administration Form 860. Includes operating and retired units. For combined cycle plants, capacity of the combustion turbine unit is displayed

While DER adoption remains modest in many jurisdictions, deployment of distributed resources is rapidly increasing, particularly solar PV and battery energy storage systems (Figs. 1-2 & 1-3). Distributed solar PV systems represented nearly 14 percent of all generating capacity additions in the United States in 2017 (Margolis et al., 2018). By the end of 2017, distributed solar systems generated 1 percent of U.S. electricity and 1.6 million residential solar PV systems had been deployed, representing approximately 1.3 percent of U.S. households or 2.1 percent of households living in single-family detached structures (Fig. 1-4; ibid.). Residential solar PV adoption in the United States is concentrated in a handful of states, and DER penetration has therefore reached more significant levels in some power systems. Residential solar PV adoption in Hawaii, California, and Arizona, for example, has reached an estimated 31 percent, 11 percent, and 9 percent of single-family households, respectively (ibid.). Furthermore, distributed solar PV systems generated more than 6 percent of California's electricity in 2017 (ibid.).

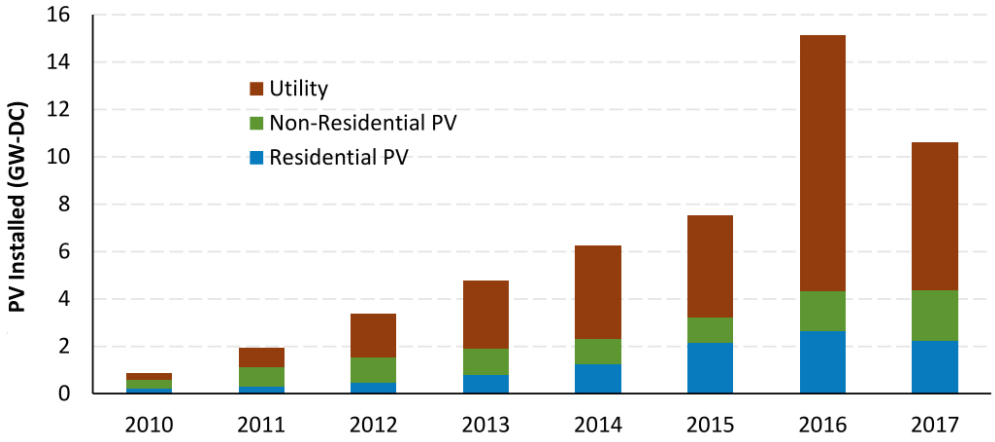

Figure 1-2: Annual U.S. solar PV installations by market segment
Graphic from Margolis et al. (2018). Data from GTM Research/SEIA: U.S. Solar Market Insight 2017 Year-in-Review.

Distributed energy resources enjoy substantial public policy support in a growing number of jurisdictions. Distributed solar PV, in particular, benefits from direct subsidies, favorable tariff design, volumetric 'net metering' policies, and utility purchase requirements (e.g., solar-specific 'carve-outs' in renewable portfolio standards). Installation of distributed PV in all

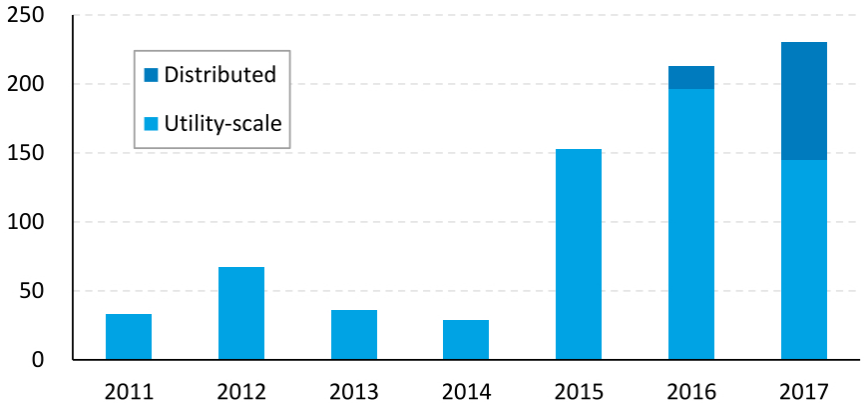

Figure 1-3: Annual U.S. battery energy storage installations by market segment (megawatts)
Graphic from Margolis et al. (2018). Utility-scale data from EIA "Preliminary Monthly Electric Generator Inventory" (December 2017); distributed data from EIA, Form 861M.

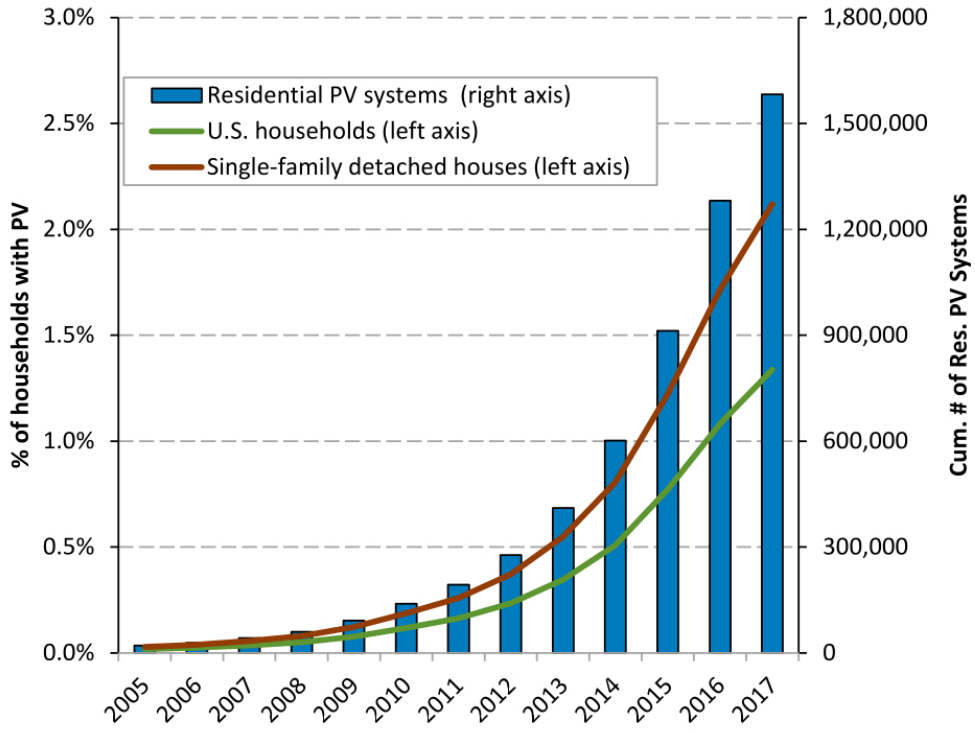

Figure 1-4: U.S. residential solar PV adoption
Graphic from Margolis et al. (2018).

new homes was even enshrined in California's building code in 2018 (Penn, 2018).

The public costs of these policies for electricity ratepayers or taxpayers are not insignificant. The Go Solar California Program, for example, invested $3.35 billion from 2007 to 2016 to drive adoption of 3,000 MW of distributed solar PV across the Golden State (State of California, 2018). Massachusetts has required utilities to purchase a share of their electricity from distributed solar projects up to 6 MW in size since 2010. The solar renewable energy certificates (SRECs) used as compliance with this requirement have historically traded for $200-500 per MWh, and the current annual liability for utility SREC purchase obligations totals nearly $700 million[1] (SRECTrade, 2018). This generous incentive – combined with volumetric net metering at the full retail rate – has driven deployment of nearly 2.5 GW of distributed solar within Massachusetts as of July, 2018, sufficient to supply about four percent of Massachusetts's annual electricity demand (MA DOER, 2018). This compares to only 335 MW of larger, multi-megawatt 'utility-scale' solar PV projects across New England which qualify for the Commonwealth's broader renewable portfolio standard (ibid.). Policy support has likewise spurred distributed solar adoption in a growing number of U.S. states and across Europe, most famously in Germany.

Recently, small-scale distributed battery energy storage systems have also enjoyed policy support. California's Self-Generation Incentive Program has allocated $448 million towards distributed energy storage 'behind the meter' on customer premises, for example. The program is largely designed to support the state's high penetration of distributed solar by reducing stresses on distribution grids caused by exported generation from distributed PV systems. Storage deployment mandates have also been enacted in California, Oregon, Massachusetts, New York, and elsewhere, and many specify a portion of that storage must be located behind the meter or in distribution networks.

Does this public policy support deliver desired ends? Do DERs provide sufficient value to warrant widespread adoption? Should we expect the future of power systems to become distributed, remain predominantly centralized, or a mix of the two? How does support for

[1]This includes roughly $250 million per year for SREC I liabilities, which will continue through the end of 2023, and $440 million in SREC II liabilities that will continue through the end of 2027.

DERs trade off against or interact with other possible policies? What economic gains can be achieved from regulatory reforms that align incentives for network utilities and electricity customers with lower overall power system costs? Should electricity rates be reformed to incentivize more flexible demand?

Answering these questions depends on analytical methods that can identify the role and value of DERs and more flexible demand in power systems. As this thesis will demonstrate, the comparative advantage of distributed resources lies in their ability to capture 'locational value' arising from the impacts of electricity networks on the value of electricity services at different points in transmission and distribution networks. In addition, each of the various DERs compete with each other, with more flexible electricity consumption, and with conventional generators to deliver (or reduce demand for) a limited set of electricity services. Assessing the role and value of DERs therefore requires tools that can span bulk generation, transmission, and distribution, consider the role of flexible and price-responsive electricity demand, and model the various sources of value captured (or costs imposed) by DERs on power systems.

Building on the MIT Energy Initiative *Utility of the Future* report (Pérez-Arriaga et al., 2016), this thesis defines distributed energy resources as any resource capable of providing electricity services[2] that is located in the distribution portion of the power system. In most regions, distribution networks encompass the portion of the electricity grid operating at or below 35 kilovolts (kV). DERs are therefore characterized by relatively small capacities (a few kilowatts to a few megawatts) and include demand response or controllable demand[3] as well as any generation or energy storage devices that are connected to distribution voltages.

Some DERs, including controllable demand such as electric vehicles or building heating, ventilation, and cooling (HVAC) systems, are inherently distributed and exist primarily to provide end-use services (e.g., heating, cooling, lighting, transportation). Other DERs, such

[2]Electricity services are defined and discussed in Section 1.1.2.

[3]Flexible or price-responsive demand can both lower the cost of consuming electricity services for an end user and modify consumption to supply electricity services to other parties, such as network utilities or system operators. In this latter capacity – as a supplier of electricity services – I consider flexible or price-responsive demand to be a DER. Otherwise, reducing the demand for electricity services acts as an alternative to the services provided by other DERs or conventional resources.

as solar PV panels or electric batteries, harness modular technologies that can be deployed at various sizes and voltage levels, ranging from a few kilowatts (kW) at low-voltage distribution to large-scale installations at transmission voltages rated at hundreds of megawatts (MW).

Both types of DERs compete with (and complement) one another as well as conventional electricity generation resources to provide electricity services to end users and power system operators, including energy, firm capacity, and operating reserves. These resources can also support public policy objectives, such as clean energy deployment, resource diversity, or climate mitigation.

At the same time, DERs have very different impacts on electricity transmission and distribution networks as compared to conventional resources, and they can often be deployed at multiple voltage levels and scales. Determining the full value of flexible demand and the optimal size, location, and installed capacity of DERs requires understanding the additional 'locational value' that may be captured by deploying DERs at different network locations (see Section 1.1.3). On the other hand, solar PV, battery energy storage, and other modular distributed resources exhibit significant economies of unit scale, which argues for larger-scale resources with lower unit costs, all else equal (see Section 1.1.4). Distributed resources thus raise several important new considerations and tradeoffs, which are discussed in the following sections.

1.1.2 Electricity Services

As per Pérez-Arriaga et al. (2016), I define electricity services as activities performed in the context of a power system that create economic value by enabling the consumption of electrical energy, lowering the costs associated with consuming electrical energy, or both. Electricity services are thus intermediate services associated with the production and delivery of electrical energy and differ from various end use energy services such as heating, cooling, lighting, transportation, etc. The value of electricity services arises from the satisfaction of various constraints on the supply and delivery of electricity, which may be inherent physical constraints or more subjective simplifying or policy constraints imposed by regulators, system

operators, or policy makers.[4]

Electrical energy is the most fundamental electricity service and power systems' *raison d'être*. Consumers value the useful work or utility that electrical energy can provide (e.g., heating, cooling, lighting, and powering electronics and transport). This leads to a demand for electrical energy which varies over time along with changing demand for end use services. The physical necessity of instantaneously balancing supply and demand in electric power systems at all times is the first constraint and gives rise to a value for electrical energy at a given time (reflecting the marginal cost of supply or the marginal opportunity cost of reduced consumption needed to balance supply and demand)

Electrical energy must also be delivered from the site of production to the site of consumption through electricity transmission and distribution networks, or grids. Alternating current power flows through electricity networks are subject to several physical constraints: current must not exceed thermal limits of conductors or transformers, the frequency of current and voltage waveforms must be maintained within tight bounds, etc. The interaction of the power balance constraint described above with these physical network constraints creates unique values for power injection or withdrawal (conventionally decomposed into real and reactive power) at each point in the network.

With perfect foresight and under other restrictive assumptions (e.g., convex and continuously differentiable costs), the only service that needs to exist is the provision of electrical energy at a location and a point in time. The power balance and power flow constraints above may be used to derive locational marginal prices (Schweppe et al., 1988; Perez-Arriaga and Meseguer, 1997) that could, in theory, coordinate the consumption and production of electricity at all points in the network to respect physical constraints and, over time, motivate actors to invest in generation and network capacity.

In practice, however, the behavior of millions of agents supplying and consuming electricity services must somehow be coordinated within tight physical constraints and in the face of uncertainty on multiple dimensions and time scales. Regulators and power system

[4]In an optimization framework, these values are related to the "shadow price" (aka "dual variable," or "Lagrange multiplier") of the constraint.

operators therefore frequently place additional constraints on the planning and operation of power systems. These 'coordinating and simplifying constraints' are intended to transform complex decision-making processes into simpler formulations that can be easily implemented by power system operators and planners – e.g., the amount of secondary operating reserves should be equal to the rated capacity of the largest generation unit in operation plus 3 percent of the expected demand; power flow in a certain line cannot exceed 90 percent of its thermal rated capacity except in emergency situations; or the amount of firm installed capacity must exceed estimated peak demand by 15 percent. The definition of these simplifying constraints leads to additional electricity services, such as various classes of operating reserves, firm capacity requirements, and electricity network capacity margins.

Finally, policy makers may impose additional constraints on power systems, such as mandates for maximum levels of carbon emitted or minimum levels of energy from renewable sources. Typically, these 'policy constraints' are created to internalize externalities that are not currently accounted for in power systems operation, planning, and associated markets or to further other social objectives.

1.1.3 Locational Value

DERs compete with conventional generation and network assets to provide the range of electricity services resulting from the constraints described above. In this sense, they are no different from other options for electricity service provision. What distinguishes DERs is the ability to deploy these resources closer to the point of electricity consumption and in locations inaccessible to more centralized resources.

This capability is important, because the value of some electricity services changes with the location of provision. This difference in 'locational value' emerges from the physical characteristics of electricity networks, including resistive losses, capacity limits of network components, voltage limits at network nodes, and the potential for network failures that may disrupt delivery of electricity services. There are three main electricity services that exhibit locational value: electrical energy; network capacity (or 'non-wires' alternatives to network

capacity); and enhanced reliability or resilience.[5]

First, due to the impact of network losses and constraints on the delivery of electricity, the value of electrical energy consumption or injection varies at different points in the power system. DERs therefore have the potential to create significant value by supplying energy (or reducing net consumption) at locations where networks are frequently constrained and/or transmission and distribution losses are large. As Fig. 1-5 illustrates, 2015 average locational marginal prices at the transmission level in the PJM Interconnection (the largest electricity market in the United States by volume of electricity generated/sold) primarily varied between $21-40 per MWh, exhibiting up to 100 percent difference in value. Furthermore, roughly 3 percent of nodes in PJM exhibit average prices 3-10 times higher than the PJM mean. The largest differences in locational value at transmission voltages reflect persistent transmission constraints preventing delivery of cheaper energy to these locations.[6] Resources located 'downstream' of these constraints and capable of supplying energy or reducing consumption during periods of network congestion could therefore create much greater value than they could by selling energy at an average location. To capture higher locational value due to network constraints, DERs must be able to operate both *where* and *when* these constraints are binding.

In addition, the majority of resistive losses in electricity networks occur in distribution networks, which operate at much lower voltages than transmission networks (increasing the current associated with a given power flow and thus the associated resistive losses). As DERs can be located within distribution networks close to demand, they offer the possibility to avoide these losses and capture greater locational value. Total transmission and distribution losses averaged 6.2 percent in the United States and 6.7 percent in the European Union in 2014, although average losses can range from as low as a few percent up to double digits

[5]Other services with locational value include power quality management and black-start or system restoration capabilities, although these are typically more niche services

[6]Absent network constraints, differences in LMPs are driven only by resistive losses. The impact of marginal transmission losses on wholesale LMPs is typically a few percent of the cost of the marginal generator. The impact of distribution losses can be larger, as resistive losses are greater in lower voltage networks, as discussed below.

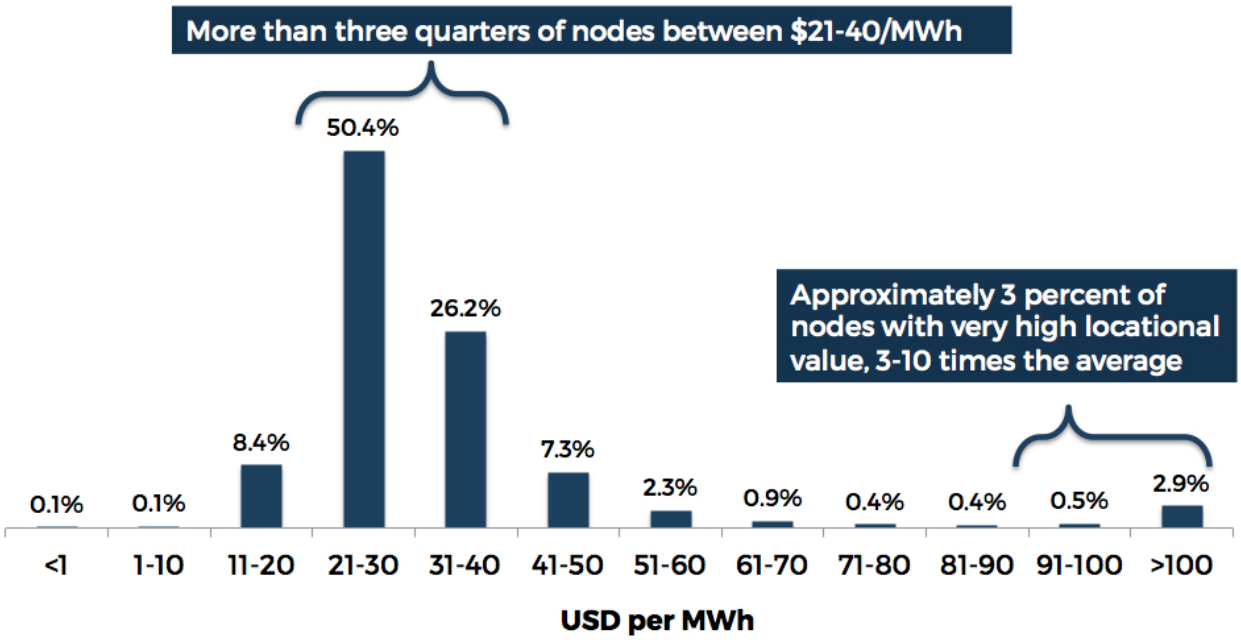

Figure 1-5: Distribution of annual average locational marginal prices at each node in the PJM Interconnection in 2015
Data from PJM Interconnection. Graphic originally published in Pérez-Arriaga et al. (2016).

in some countries (EnerData, 2016).[7] As resistive losses rise quadratically with current or power flow, DERs that generate power (or reduce net consumption) during periods of high demand and therefore high network loading may also capture much greater locational value by avoiding marginal losses during these periods. As an illustrative example, Fig. 1-6 depicts the production-weighted average marginal losses avoided by a solar PV system located in low-voltage distribution in the Texas ERCOT power system for distribution networks exhibiting either 3 percent or 9 percent average losses throughout the year. At initial penetration levels, a distributed solar PV system in these examples delivers roughly 6-19 percent greater locational value by avoiding marginal losses in distribution than a PV system sited at transmission voltages. However, as the figure also illustrates, the marginal locational value of a distributed solar PV system falls as solar penetration on a given distribution network increases and power flows across the network steadily decline during periods of solar PV

[7]These figures include both technical losses (including resistive losses and hysteresis losses in transmission and distribution components) and non-technical losses (e.g., theft). Countries with the highest losses usually reflect a combination of technical and non-technical losses.

production. Eventually, at high enough penetration levels, distributed solar PV systems may even increase marginal losses by creating reverse power flows across lower distribution voltages (Schmalensee et al., 2015, chap. 7).

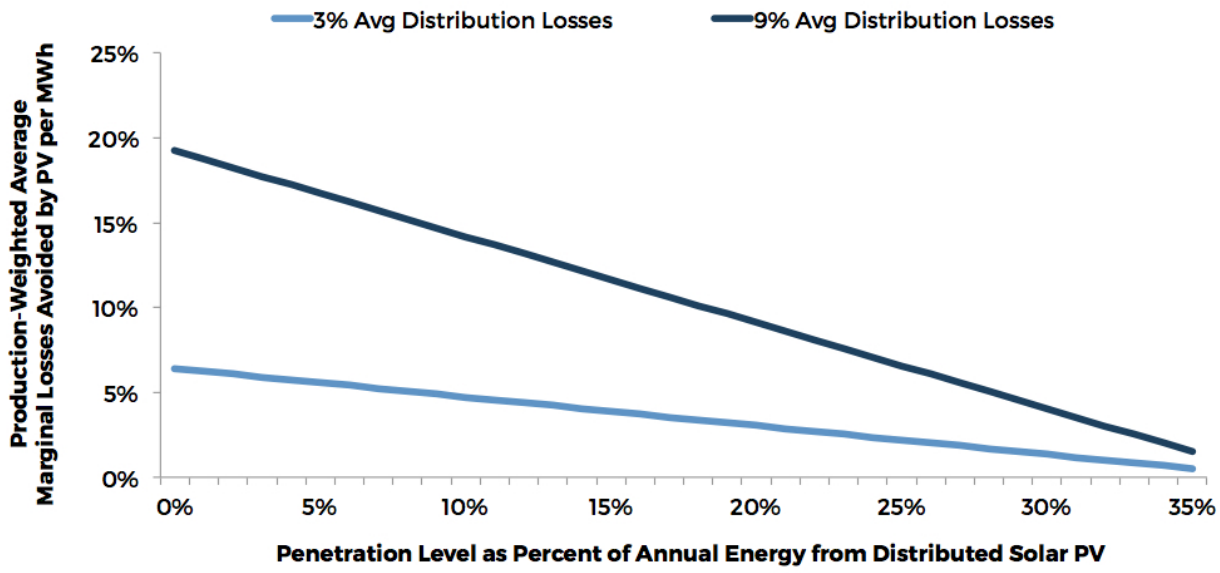

Figure 1-6: An example of the marginal value of distribution network losses avoided by distributed solar PV as penetration increases

Solar PV production and demand profile from the Electricity Reliability Corporation of Texas for 2015. For this illustrative example, I estimate two coefficients for losses as a function of power flows consistent with annual average losses of 3 percent and 9 percent at 0 percent solar penetration given the average ERCOT demand profile. I then calculate marginal hourly losses for different penetrations of solar PV and the generation-weighted average value of marginal losses per megawatt-hour of solar production. Graphic originally published in Pérez-Arriaga et al. (2016).

Second, it is possible for DERs sited in the right locations and operated at the right times to substitute partially or fully for conventional investments in transmission and/or distribution infrastructure (sometimes referred to as a 'non-wires alternative' to traditional upgrades to network 'wires'). For DERs to provide this network capacity value, they must: (1) be located in areas of the network that are experiencing or are projected to experience violations of network constraints that would otherwise necessitate investments in network expansion, such as areas of peak load growth or of reverse power flow;[8] (2) be able to reduce net power withdrawals or injections during periods when network congestion is expected;

[8]Areas of the network with aging assets due for replacement could also afford opportunities for network capacity deferral value, although the cost of asset replacement is generally lower than new construction.

and (3) be able to provide these services reliably, over whatever period of time network investments are to be deferred. Not all locations and not all DERs are likely to meet these conditions, but where they are able to do so, DERs may deliver significantly greater locational value than larger-scale alternatives at transmission voltages (see e.g., Cohen et al. (2016)). This potential benefit is explored further in Chapter 2 Section 2.3.

Finally, DERs may be able to increase the reliability or resilience of power systems. For example, DERs such as batteries, fuel cells, reciprocating engines, and microturbines can provide power during network outages, thus avoiding service interruptions. At present, the benefits of DERs used for reliability purposes (i.e., backup power) flow almost exclusively to the DER owner (all benefits are private). However, pilot programs are developing models to enable communities or wider areas to benefit from the reliability improvements provided by DERs, such as by 'islanding' portions of the distribution network or operating private microgrids that can disconnect from the distribution system during service disruptions.

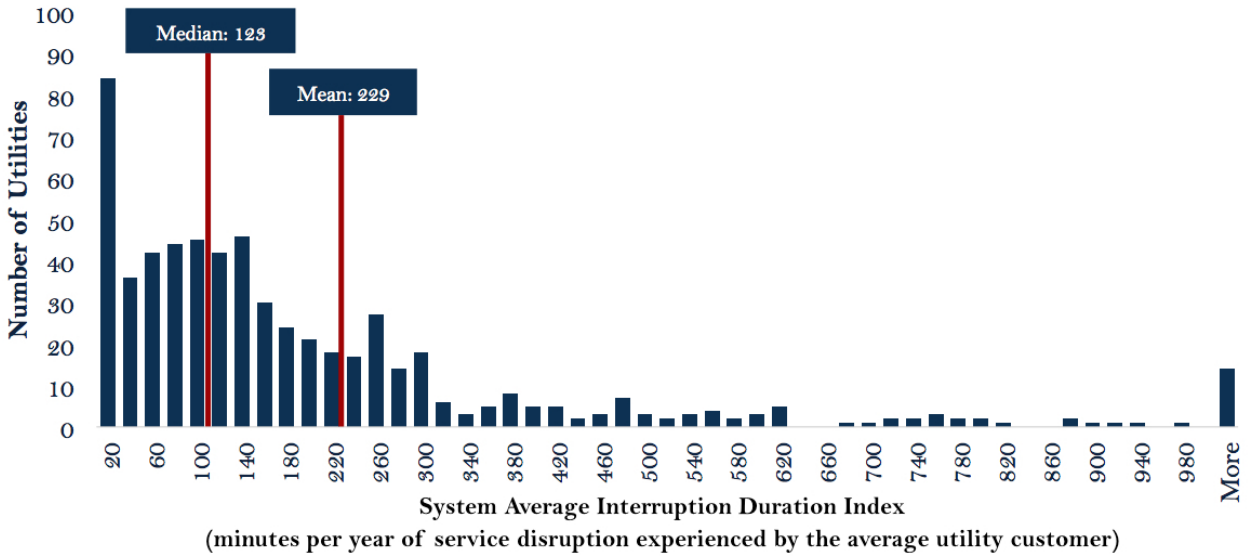

Figure 1-7: Histogram of 2014 system average interruption duration index for U.S. utilities
Data from U.S. Energy Information Administration Form 861. Graphic originally published in Pérez-Arriaga et al. (2016).

The locational value of increased reliability depends on the frequency and duration of service outages experienced at a particular location and consumers' willingness to pay to

avoid such outages (see e.g., Sullivan et al. (2015)). Reliability in developed power systems is generally quite high, with the average customer of the average U.S. utility experiencing less than four hours of total service disruption in 2014, for example (Fig. 1-7). However, a small number of utilities in the United States experience average outages of much longer duration, and individual customers within each utility service territory experience additional variation in outage duration and frequency. Based on a meta-survey of estimated willingness to pay for avoided outages by different customer classes (Sullivan et al., 2015) and the distribution of average outage durations in Fig 1-7, Table 1.1 presents an estimate of the cost of outages for several classes of customers and different cumulative annual outage durations. To the extent that DERs can prevent service interruptions by providing backup power, they can therefore generate additional locational value on the order of the values presented in Table 1.1. As this data indicates, the additional locational value associated with reliability benefits for residential customers may be modest, unless a given DER can provide power for multiple residences during each outage. Sullivan et al. (2015) finds that the cost of services disruptions for commercial and industrial customers is higher, however, and can be significant for smaller commercial and industrial customers. Other opportunities for DERs to provide significant locational value via reliability benefits include specific locations with much greater than average supply disruptions and/or certain high-value or critical loads – facilities such as hospitals, emergency response services, communication networks, data centers, or uninterruptible industrial processes – that exhibit a very high willingness to pay to avoid supply interruptions.[9]

In contrast to services exhibiting locational value, a range of other electricity services, including firm generating capacity, frequency regulation, operating reserves, and price hedging services, are broadly fungible commodities with the same value across the entire power system (or at least across wide area zones of the system). Compliance with policy constraints, such as carbon dioxide emissions cap and trade programs or renewable portfolio standards, also typically lack a locational component. For example, Callaway et al. (2018) find the

[9]Due to this higher value, many such facilities are already equipped with DERs for uninterruptible power supply.

Table 1.1: Estimated reliability value for different customer classes in the United States given different cumulative annual outage durations (2017USD per firm kW per year)

Cumulative annual outage duration	**Residential**	**Small commercial or industrial**	**Large commercial or industrial**
2 hours (median U.S. utility)	$7	$642	$47
4 hours (mean U.S. utility)	$14	$1,284	$95
16 hours (extreme U.S. utility)	$57	$5,135	$379

Cost of service interruptions per kWh from Sullivan et al. (2015) updated to 2017 USD using the Bureau of Labor Statistics CPI inflation calculator and assuming typical outage duration of 1 hour per outage (e.g., the cost of a cumulative annual outage duration of 16 hours equals the cost of a 1-hour interruption multiplied by 16). Note that Sullivan et al. (2015) find shorter-duration outages to be more costly on a per-hour basis – that is, a 16-hour outage would be less costly for a customer than 16 1-hour outages. Value assumes the DER provides a consistent kW of power supply throughout the duration of each service disruption.

quantity of greenhouse gas emissions displaced by wind, solar, and efficiency resources varies significant between different independent system operator regions of the United States, but is limited *within* a given region. Where DERs deliver these services, they do so in direct competition with other conventional resources without the advantage of increased locational value.

1.1.4 Economies of Unit Scale and Distributed Opportunity Costs

While DERs may be sited in the power system to capture additional locational value, there are economic tradeoffs associated with the smaller scale of these distributed resources as well. Many technologies suitable for distributed deployment, including solar PV, electrochemical energy storage, and fuel cells, can be deployed across a range of scales, and each of these resources exhibits varying degrees of economies of unit scale. In other words, costs per unit of capacity decrease as the size of the system increases and vice versa. By failing to exhaust economies of unit scale, smaller-scale deployment of these resources therefore results in incremental unit costs relative to larger-scale systems.

Figures 1-8 and 1-9 illustrate the economies of unit scale exhibited by both solar PV

systems and lithium-ion battery energy storage systems. Despite employing the same small, modular components at their heart (e.g., solar PV cells and lithium-ion battery packs), installed costs of distributed solar and battery storage systems increase substantially as unit size falls. Cost increases reflect decreased economies of scale in installation labor, project development/customer acquisition, interconnection, and balance of system (inverters, racking, etc.) costs. Note that costs depicted in these figures do not reflect additional transmission or distribution network expansion that may be required to accommodate new solar or storage systems (e.g., they reflect only shallow interconnection costs). As these figures demonstrate, the cost of deploying a solar PV or battery storage system at the residential kW-scale in the United States[10] can be roughly twice the cost (or more) of employing these same resources at the MW-scale. Economies of unit scale still matter, even for distributed resources.

For resources that can be deployed at multiple scales, incremental unit costs must therefore be considered alongside possible increases in locational value associated with smaller-scale, distributed installation of these resources. Indeed, in cases where incremental unit costs exceed incremental locational value, society incurs 'distributed opportunity costs' when small-scale DERs are deployed in lieu of more cost-effective, larger-scale installations of the same resource. Understanding trade-offs between locational value on the one hand and incremental unit costs due to economies of unit scale on the other hand are therefore critical to identifying when and where DER deployment would increase or decrease social welfare.

[10]Economies of unit scale differ by location due to variations in the local cost of labor, customer acquisition, materials, etc.

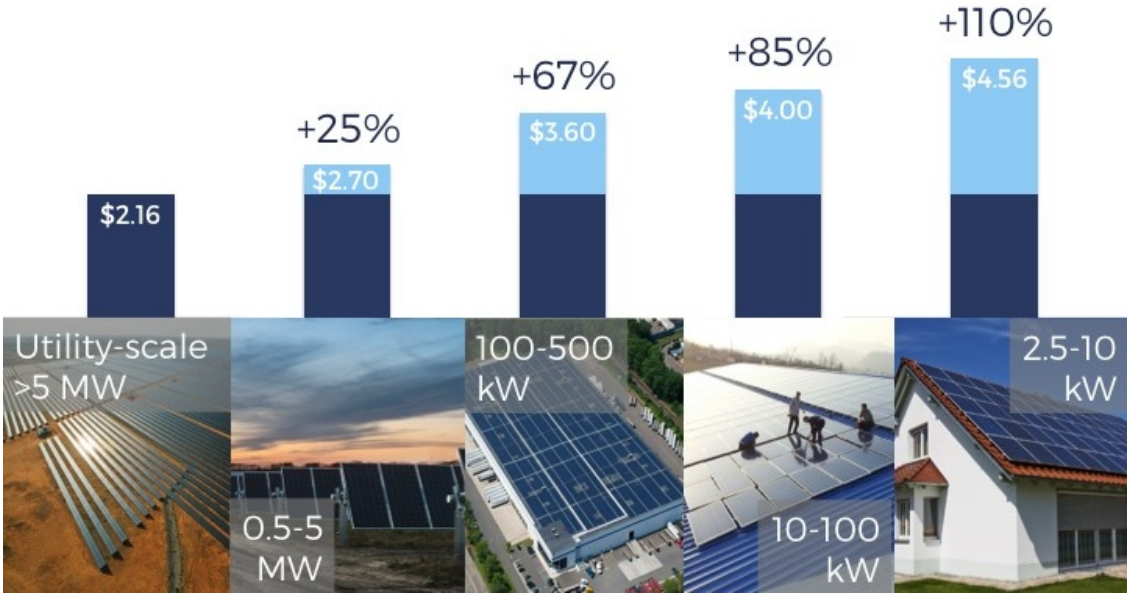

Figure 1-8: Economies of unit scale and incremental unit costs for solar PV systems (First half 2018 costs per kW-ac)
Data from Margolis et al. (2018). Assumes DC to AC ratio (inverter loading ratio) of 1.2 for distributed systems below 5 MW and 1.3 for utility-scale systems above 5 MW. Note that utility-scale PV systems typically have greater productivity per kW of capacity due to use of tracking systems, optimized siting, and more frequent cleaning and upkeep than smaller-scale distributed systems. This graphic may therefore underestimate incremental levelized costs per kWh of generation for distributed solar systems.

Figure 1-9: Economies of unit scale and incremental unit costs for lithium-ion battery energy storage systems (2017 costs per kWh)
Data from Lazard (2017).

1.2 New Challenges for Electricity System Planning, Policy, and Regulation

It is clear that distributed energy resources present both new options for the delivery of electricity services and important economic tradeoffs and system impacts that are distinct from conventional generation resources. As such, the proliferation and increasing cost-effectiveness of DERs presents new challenges for power system planning, including generation and network expansion decisions. Public policies driving DER adoption carry significant costs and should be targeted to maximize public value. At the same time, the growing penetration of DERs is stressing established regulatory paradigms, including electricity rate design practices and regulation and remuneration of distribution network utilities (see Pérez-Arriaga et al. (2016); Jenkins and Pérez-Arriaga (2017)).

To capture the key considerations associated with DERs and to provide decision support for policy makers, regulators, and utility planners, new electricity resource capacity planning models are needed that are capable of: (1) incorporating key network-related impacts of each resource, including transmission and distribution losses, constraints, and expansion costs; (2) considering siting of DERs at multiple scales, locations, and voltage levels to capture tradeoffs between locational value and economies of unit scale, and; (3) fully considering competition between the wide range of distributed and conventional resources now available as well as the potential role of more flexible electricity demand. The remainder of this section describes the role of electricity system planning models in vertically integrated and competitive power system contexts, provides a review of recent developments in electricity resource capacity planning models, and summarizes the limitations of current state of the art approaches to capacity planning modeling. Finally, I briefly outline a new approach to electricity system planning with DERs that is developed further in subsequent chapters and represents the novel methodological contribution of this thesis.

1.2.1 The Role of Electricity System Planning and Capacity Planning Models

Electricity generation, transmission, and distribution assets are long-lived, capital intensive assets. Investment and policy decisions in the electricity sector must therefore be made in the face of considerable uncertainty about the evolution of demand, technology and fuel costs, and macroeconomic conditions over the decades-long lifespan of potential assets. Asset investment and retirement decisions made today will also have lasting impacts on electricity costs, the environmental impacts of electricity systems, and other key policy and regulatory considerations.

For decades, power system capacity planning models (also referred to as capacity expansion models or generation / transmission expansion models) have been employed as decision support tools for electric utilities, power sector investors and market analysts, and policy makers. Capacity planning models are typically formulated as constrained optimization models (based on linear programming or mixed-integer linear programming techniques) that attempt to find the lowest-cost set of power system investment (and retirement) decisions that will meet expected electricity demand in a future planning year while maintaining adequate reliability and complying with environmental regulations and public policy constraints. Due to computational complexity, planners typically employ separate capacity planning models to consider power generation (and energy storage) expansion decisions, detailed operational decisions, and transmission network expansion decisions, although recent work has begun to bridge these three classes of models. Distribution network planning has also been distinct from bulk power system (generation and transmission) planning decisions. As we will see, DERs make these distinctions increasingly untenable, demanding novel methods to expand the scope and capabilities of capacity planning models.

Capacity planning models belong to a large class of models used to design, operate, and plan power systems and to operate competitive electricity markets. Given the engineering and economic complexity of power systems, no single model can tractably consider all levels of detail or relevant decisions in the power system. Electricity models therefore range in scope

and detail from the milliseconds-scale simulation of physical and engineering constraints to multi-decadal planning models with a highly abstracted level of engineering detail (see Fig. 1-10).[11]

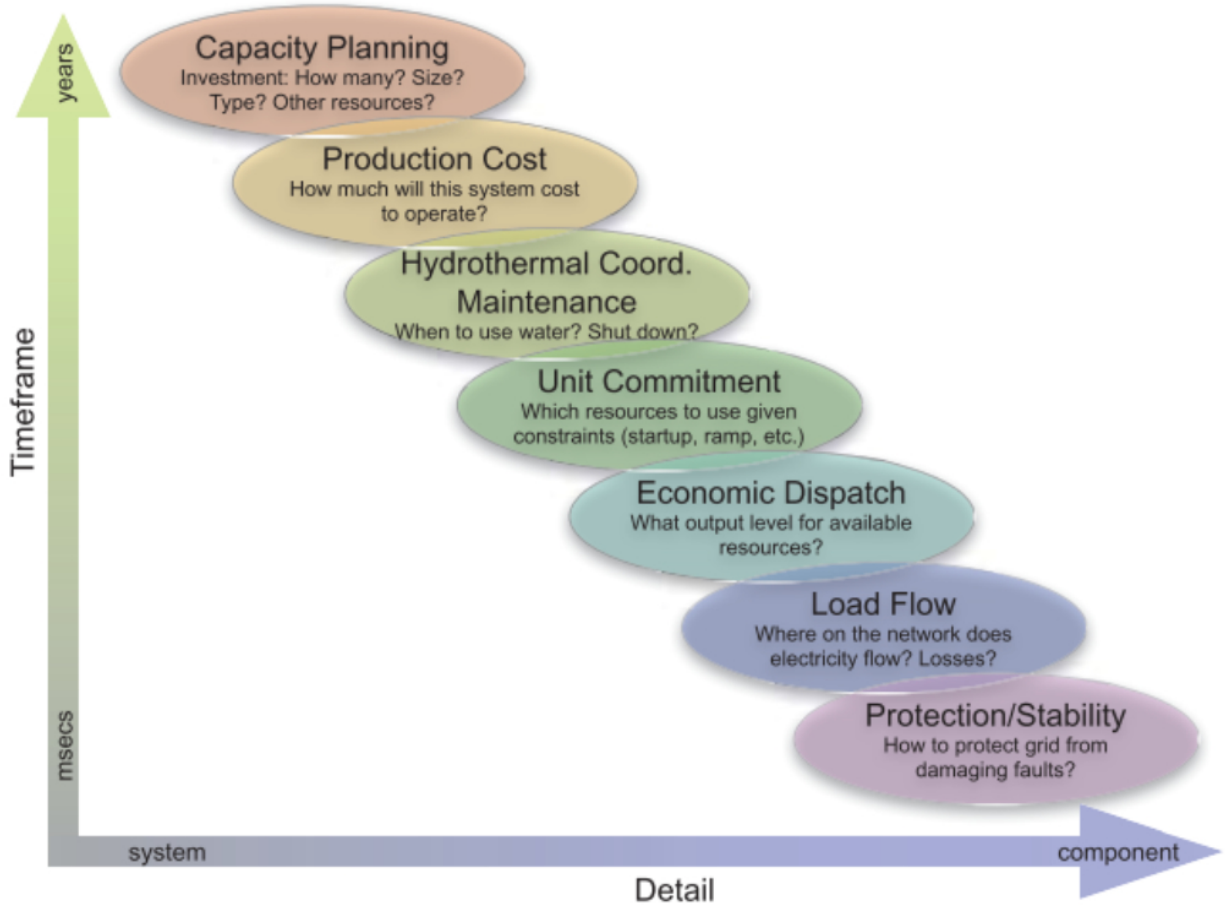

Figure 1-10: Taxonomy of electricity system models
Graphic from Palmintier (2013).

Capacity planning models are also closely related to national energy system models or energy-economic models which are used to consider the evolution of multiple energy and end-use sectors (e.g., electricity, transportation, heat) and generate insight for policy decisions (see e.g., U.S. EIA (2009); Loulou et al. (2016)). Energy system models typically embed an electricity sector planning model (e.g., U.S. EIA (2017) as part of U.S. EIA (2009)), although by virtue of the more expansive scope of the overall model, this embedded model lacks some

[11]See Palmintier (2013) for a taxonomy and brief review of the full range of power system models.

features and detail present in electricity sector-only planning models.[12]

Regulated, vertically-integrated electric utilities have a long tradition of employing capacity planning models to help determine investment and retirement decisions and to justify their decisions to regulators, ratepayers, and other stakeholders (Schweppe and Burke, 1989). In many jurisdictions long-term resource planning is required by regulators and codified in so-called integrated resource planning processes (Wilson and Peterson, 2011; Wilson and Biewald, 2013). Integrated resource planning became common in the United States in the 1980s as the electricity sector began to enter a new and uncertain phase of demand growth, decades of rapid post-war expansion gave way to changing macroeconomic trends, and oil embargoes roiled international energy markets. Significant cost overruns at nuclear and coal-fired power stations, oil price shocks, and bankruptcies of a number of U.S. utilities combined to motivate utility regulators, policy makers, and electricity consumers to exercise closer oversight of utility planning decisions, demand forecasts, and associated risk exposure. State legislatures and utility regulators in many jurisdictions required utilities to perform regular planning processes with varying degrees of stakeholder participation, transparency about assumptions and forecasts, and requirements for consideration of risk and alternatives to new generation or transmission investments (such as demand-side management or energy efficiency). Although much of the world electricity sector has transitioned to restructured and vertically disaggregated markets with competitive generation sectors, utility resource planning remains an essential activity for vertically-integrated utilities. Capacity planning models therefore remain an important input to resource planning processes for many utilities.

In restructured electricity markets, planning functions have become disaggregated, and investment in generation (and increasingly energy storage) capacity is undertaken by many competitive market agents. In these contexts, bulk power system operators (variously referred to as transmission system operators, independent system operators, or regional transmission organizations) still commonly engage in transmission expansion planning exercises. Systems operators rely on generator interconnection requests from market agents along with

[12]See Poncelet (2018) for a review of energy system optimization models and their representation of power systems.

their own forecasts of generation investment and demand growth to develop inputs to the transmission planning process. Individual market agents may also employ capacity planning and production cost models to explore the value and risk exposure of possible generation or storage investments in competitive markets.

In addition, while electricity markets are increasingly trusted to coordinate efficient and reliable operation of the power system, the trend over recent decades has been towards an active role for policy and regulatory intervention in shaping the evolution of the electricity sector and, in particular, investment in new generation capacity. Markets are effective tools for efficiently allocating scarce resources, and electricity markets are no exception. But markets for the production and sale of electrical energy alone should not be expected to address the wide range of public policy considerations impacted by the electricity sector, including the central role of the power sector in mitigating the worst effects of climate change. Policy makers throughout the world have therefore implemented a range of interventions in electricity markets, from efforts to internalize the social costs of electricity market transactions to direct subsidies or mandates to encourage investment in preferred resources – including distributed resources. In addition, while debate continues about the ability of short-term electricity markets (or "energy-only" markets) to induce adequate capacity investment and deliver long-term security of supply (Joskow and Tirole, 2007; Joskow, 2008; Hogan, 2013), most jurisdictions have chosen to establish capacity remuneration mechanisms or capacity markets of various forms. These markets typically endow the system operator with a greater role in long-term capacity planning, as the design of these markets, forecast of future firm capacity needs, and other decisions inevitably shape competitive investment in new capacity.

Capacity planning models therefore also play an increasingly important role in 'indicative planning' (Pérez-Arriaga and Linares, 2008), whereby policy makers, regulators, and system operators adopt a centralized planning perspective to inform the design of policies, regulations, and supplemental markets to shape electricity markets towards desired ends. Indicative planning is a normative, rather than descriptive process, concerned with how the power sector *should* evolve (from the planner's perspective) in order to achieve desired pol-

icy, regulatory, or security of supply objectives. In particular, by adopting a social welfare maximizing perspective, electricity system planning models can help identify economically efficient outcomes useful for extracting policy guidance. More than just prospective analysis, indicative planning outcomes frequently shape tangible policy and regulatory actions. For example, planning models may be used to evaluate the potential costs and benefits of market interventions such as subsidies, competitive procurements or tenders for low-carbon energy sources, renewable portfolio standards and other mandates, or carbon pricing policies. System operators may also rely on capacity planning models to inform the design of capacity markets. In addition, planning models are frequently used to develop high profile roadmaps published by various policy making bodies (see e.g., European Commission (2012); The White House (2016)), which signal to market participants the likely direction of future policy making efforts.

Finally, power system planning models can play a key role in techno-economic assessment of the potential value and role of novel or emerging technologies (see e.g., Pudjianto et al. (2014); de Sisternes et al. (2016); Heuberger et al. (2017b)). By providing a combination of realistic technical constraints within a system-wide economic optimization context, planning models can help identify the value of a new technology in various contexts, the sensitivity of this value to key uncertainties and competing technologies, and the likely scale of adoption if a technology achieves different cost or performance levels. These insights can be important for guiding research and development efforts, informing early-stage investment in technology companies, or developing technology policy and public research funding objectives.

Whether employed in integrated resource planning for vertically-integrated utilities, indicative planning to shape public policy and regulation, or techno-economic assessment to evaluate the potential of emerging technologies, capacity planning tools therefore play an important role in supporting decision making in the electricity sector. It is thus important for the capabilities of capacity planning models to keep pace with the rapidly changing nature of electricity systems, including newly available technologies and an ever-evolving policy landscape. Indeed, the last decade has seen renewed academic interest in expanding the ca-

pabilities of capacity planning tools. The following section reviews recent developments in the capacity planning literature.

1.2.2 Recent Developments in Capacity Planning Models

Formalized mathematical tools for determining the least-cost mix of electricity generating capacity date back to at least the 1950s, including both the graphical 'load duration curve' or 'screening curve' method (Kirchmayer et al., 1955; Hicks, 1959) and the first applications of linear programming to the electricity capacity expansion problem (Masse and Gibrat, 1957). Both approaches sought to solve the same optimization problem: namely, to find the least-cost combination of thermal generators, including the sum of investment and operating costs, given differences in fixed and variable costs for each resource and the profile of annual demand. The core tradeoff was between generators with higher fixed costs and lower variable costs (such as coal or nuclear plants) economically suited for high utilization rates and therefore best used to serve the 'base load' (or the lowest level below which demand does not fall throughout the year), plants with relatively balanced fixed and variable costs (such as natural gas steam turbines or combined cycle power plants) suited for intermediate utilization rates, and plants with high variable costs and low fixed costs (oil-fired generators or gas combustion turbines) best employed only occasionally to meet the highest or 'peak' levels of electricity demand throughout the year. All of these resources could be dispatched as needed and demand followed relatively predictable patters throughout the days, weeks, and seasons. As such, these planning models disregarded the chronological sequence of demand and any operational constraints on power plants (as these had little impact on the least-cost investment decisions) in order to find the least cost resource suited to different utilization rates driven by the different levels of demand experienced throughout the year. Forced outage rates for each resource type could be used to determine necessary capacity reserve margins.

With improvements in computing capability in the 1970s, '80s, and '90s, capacity planning models steadily evolved to take initial account of operational constraints on thermal gen-

erating units (e.g., minimum loading, ramp rates), hydro reservoir management, the impact of generation investment decisions on transmission costs, and the potential for demand-side management or energy efficiency to reduce peak demands. As the size of thermal generating units steadily increased, planning models began to employ mixed integer linear programming approaches to capture the discrete nature of large-scale thermal power plant investment decisions. Methods used during this period also focused greater attention on risk and uncertainty in investment planning. For reviews of generation expansion planning methods during each of these decades, see Anderson (1972); Nakamura (1984); Hobbs (1995).

Despite steady improvement in detail and methods, even state-of-the-art capacity planning tools as of the end of the 2000s either employed a chronologically non-sequential load duration curve approach to production costing or an extremely simplified representation of operational constraints of thermal power plants, typically modeled over only a handful of time steps or 'blocks' used to represent an entire year (for a review, see Palmintier (2013)). To address these shortcomings, utility planners and policy analysts might 'soft-link' generation capacity planning models with more detailed unit commitment and economic dispatch models to consider the impacts of generation investment decisions on transmission costs or operational flexibility.[13] Most commercially available tools for utility integrated resource planning and energy systems models used in widely cited policy analysis (including U.S. EIA (2009, 2017); Loulou et al. (2016); U.S. EPA (2018); Young et al. (2018); Short et al. (2011); EPRI (2015)) continue to reflect this state of play to this day.

By around 2010, the steady increase in wind and solar energy penetration in many regions and a growing recognition of the central role of power sector decarbonization in global climate change mitigation efforts spurred substantial research into the integration of high shares of variable renewable energy sources into power systems (e.g., GE Energy (2010); EnerNex (2011); MIT Energy Initiative (2011); Denholm and Hand (2011)). These studies all emphasized the impact of substantial wind and solar energy penetration on the

[13]The best of these soft-linking approaches iterate between the models towards some degree of convergence, while others simply check and verify the feasibility (but not optimality) of the initial capacity planning solution.

operational flexibility requirements for power systems, including increased ramp rates, more frequent cycling of thermal generators, more frequent operation of thermal plants at partial load (with associated reductions in efficiency), increased operating reserve requirements, and potential curtailment of excess renewable energy. In addition, studies identified the need for long-distance transmission expansion both to reach higher quality renewable resource areas further from load centers and to aggregate and smooth variability in wind and solar production across wider geographic areas.

With widespread awareness of the impact of variable renewable energy resources on the *operational* flexibility required of power systems, it also become clear that continuing to ignore chronologically variability in electricity demand and wind and solar energy production profiles or treat operational flexibility characteristics of power plants in a highly abstract way could substantially bias the results of *planning* models (Lannoye et al., 2011; Haydt et al., 2011; de Sisternes and Webster, 2013; Palmintier, 2013). Co-optimizing generation expansion, renewable energy siting, and transmission expansion also becomes increasingly important in systems with high shares of location-dependent renewable energy sources (Short et al., 2011; Nelson et al., 2012; Mai et al., 2013). This resulted in a proliferation of recent academic research aimed at enhancing the capabilities of electricity capacity planning methods to better incorporate the impacts of variable renewable energy sources. Three general areas of research were pursued.

First, a set of models were developed with much greater geographic resolution and representation of renewable energy siting options and transmission network constraints and expansion costs, including: Short et al. (2011); Nelson et al. (2012); Haller et al. (2012); Mai et al. (2013); Hirth (2013); Frew (2014); Pudjianto et al. (2014); Mileva et al. (2016); MacDonald et al. (2016); Frew et al. (2016); Hirth (2017); Young et al. (2018); Brown et al. (2018b,a); Clack (2018). Most of these models abstract the detailed transmission system into a smaller number of 'zones.' Transmission power flows between zones are then modeled as point to point 'pipeline flows' (transport models) with simple capacity constraints rather than more detailed power flow equations capturing Kirchhoff's laws used in specialized trans-

mission planning models. Short et al. (2011), Mai et al. (2013) and Pudjianto et al. (2014) are exceptions. Short et al. (2011) can be configured to model either pipeline flows or a more complex approximation of DC power flows using a fixed 'power transfer distribution factor' meant to capture relative impedances of lines and associated limits on parallel flows. Pudjianto et al. (2014) employs a five zone model of Great Britain with linearized DC power flow constraints, while Mai et al. (2013) presents a hybrid model of the Western Interconnection region of North America, in which a high-resolution, 1,406 node transmission system model with linearized DC power flow constraints is used to study two balancing areas in detail and neighboring balancing areas represented as zones with pipeline flow constraints. However, it is worth noting that Mai et al. (2015) later tests the impact of network detail on capacity planning results and concludes that modeling DC power flows has "dramatic adverse effects on computation time but can be largely inconsequential to model investment outcomes." In addition, these models consider transmission capacity expansion decisions to be continuous, abstracting from the more discrete nature of potential expansion options to avoid the computational burden of additional discrete binary variables.

Multi-zonal models with greater geographic and network resolution are capable of exploring important tradeoffs between siting wind or solar plants in areas with greater resource potential that may be further from demand centers and require additional transmission expansion costs versus locations with inferior wind or solar resource quality but greater proximity to demand or existing transmission lines. They also better capture the impact of transmission congestions on localized renewable energy curtailment. Finally, they can begin to capture the value of demand-side flexibility or generation or storage located close to demand centers in reducing transmission network expansion that may otherwise be needed to serve peak demand. However, to accommodate greater geographic and network resolution, these models typically consider limited operational constraints for thermal power plants. They are also usually forced to reduce the number of time periods modeled or abstract from chronological variability entirely and adopt a non-sequential load-duration curve approach, or both (see Fig. 1-12-1-13). These abstractions can limit the ability of these models to

fully capture the impacts of correlated chronological variability in wind, solar, and demand profiles and impacts of variable renewables on power system flexibility requirements. Models lacking sufficient chronologically-ordered time steps may also be unable to accurately reflect the use of energy storage and associated inter-temporal constraints. These shortcomings may bias model results.[14]

A second set of modeling efforts worked to incorporate detailed, hourly operating constraints, including discrete unit commitment (on/off) decisions for thermal generators. In particular, de Sisternes (2014) and Palmintier (2013) (both at MIT) and Koltsaklis and Georgiadis (2015) each pursued parallel efforts to incorporate unit commitment decisions and detailed flexibility constraints into a single long-term capacity planning and production cost model.

de Sisternes (2014) relied on reducing time dimensionality by sampling four representative weeks to match the annual *net* load duration curve, or load less available wind and solar energy output in each hour, for a given exogenously determined installed wind and solar capacity (de Sisternes and Webster, 2013).[15] This reduction in dimensionality permits the model to include plant-by-plant binary investment and hourly unit commitment constraints for each thermal generator eligible for construction. The use of seven consecutive days in each of the four representative weeks also preserves chronological variability of wind, solar, and demand and associated flexibility requirements. de Sisternes et al. (2016) (to which this author contributed) later extended this approach to select representative weeks while allowing endogenous wind and solar investment decisions within the optimization model.[16]

[14]The most recent models in this field overcome these limitations by combining a full year of time series with time coupling constraints and a linear relaxation of unit commitment constraints for thermal generators, including Jenkins and Sepulveda (2017), Clack (2018), and a forthcoming update to the SWITCH model first introduced in Nelson et al. (2012)

[15]Four weeks are selected from all possible four week combinations in the full year in order to minimize root mean square error between the net load duration curve for the full year and the net load duration curve given by the four week sample with each hour representing $\frac{8760}{24\times7}$ hours.

[16]This method considers multiple discrete combinations of variable renewable energy capacity from across a range of possible capacity outcomes the model may select. For each possible combination of four weeks in the full year, the root mean square error between the net load duration curve for the full year and the net load duration curve given by the four week sample with each hour representing $\frac{8760}{24\times7}$ hours is calculated for *each* possible combination of variable renewable energy capacity considered. It is possible to also consider errors in the distribution of ramping events in the sample week and full year as well, to ensure the full

Koltsaklis and Georgiadis (2015) also model binary investment and unit commitment decisions in an integrated capacity expansion and production cost model. In contrast to de Sisternes (2014) and Palmintier2013, their model is a multi-period and mulit-zonal expansion model, which optimizes investments across a five-zone representation of Greece's power system over the 17 years from 2014-2030. The model is also unique in featuring very detailed unit commitment constraints for thermal power plants (coal, lignite, gas), including three different start-up options (hot, warm, and cold starts, depending on how long a unit has been offline), an initial part-loaded 'soak' period after a unit comes online, and a final 'desynchronization' period as a unit's output coasts down towards shutdown. However, these expanded features come at the expense of modeling only one representative day per month in each year. No explanation is offered as to how these days are selected or why modeling 12 discontinuous single day periods provides an accurate abstraction of the full chronological variability of wind, solar, and demand and corresponding impacts on operations and investment decisions.

Palmintier (2013) and Palmintier and Webster (2014) took a different approach to dimensionality reduction, and instead of reducing the time domain, implemented an integer clustering approach to represent thermal generating units. For brownfield incremental expansion problems, existing thermal units are clustered by characteristic features (e.g., age or heat rate) into a limited number of clusters or 'stacks' of similar generators (Fig. 1-11). One additional cluster is created for each new build option as well. (Small, modular technologies like solar, wind, and batteries are treated as continuous decisions). This approach substantially reduces dimensionality by scaling the number of discrete capacity investment and unit commitment decisions and all associated constraints by the number of *clusters* rather than the number of individual units. The resulting substantial improvements in computational performance come at the cost of minimal error resulting from two abstractions inherent to this method (Palmintier and Webster, 2014, 2016): first, all plants within a cluster must

range of hour-to-hour flexibility needs is captured in the sample weeks. The four weeks that minimize the maximum error across all of these possible capacity combinations is then selected. Given that this approach is based on minimizing the maximum likely error, we refer to this method as the "robust week selection method." See de Sisternes et al. (2016) at p. 371 for more.

be treated as identical, with the same capacity, operating characteristics (ramp rate, minimum output, heat rate, etc.); and second, in each time step, all committed units within a cluster must be assumed to operate at the same average output level (e.g., if four units are operating at 80 percent of their combined output, this is represented as each unit operating at 80 percent load rather than say three units at 100 percent and one at minimum load). The former error only applies to clusters of existing generating capacity (in 'brownfield' or incremental expansion models), as new build (or 'greenfield') capacity options are typically already considered identical.

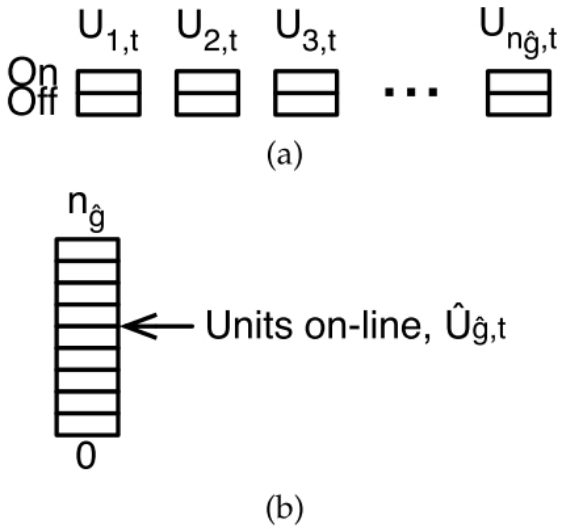

Figure 1-11: Conceptual representation of traditional and clustered unit commitment for a single type of unit in a single time period
In the binary formulation used in most unit commitment models and in de Sisternes (2014) (a), each unit has a separate binary commitment variable, $U_{g,t}$. In the integer clustering method introduced by Palmintier (2013) (b), the entire cluster of $n_{\hat{g}}$ units has only a single integer commitment variable, $\hat{U}_{\hat{g},t}$ Graphic from Palmintier (2013).

The initial implementations of both of these methods for capturing discrete unit commitment and operating constraints in capacity planning models came at the cost of ignoring transmission network constraints and geographic resolution. Both models were applied at the scale of a single system operator region (Texas ERCOT) with copperplate transmission assumptions within the region. These methods therefore capture detailed operating constraints and long, consecutive periods of hourly chronological variability in demand, wind,

and solar profiles, but at the cost of very course geographic resolution. In addition, both authors implemented static planning models for a single future planning year, rather than multi-staged expansion models.

Due to its combination of computational tractability and minimal abstraction error, Palmintier's integer clustering approach to unit commitment has since been incorporated into several recent models, which take advantage of improved computational performance to add other features, including: greater geographic and network detail (Pudjianto et al., 2014; Jenkins and Sepulveda, 2017; Lara et al., 2018; Clack, 2018); multi-stage incremental planning decisions (Heuberger et al., 2017a,b; Abdin and Zio, 2018; Lara et al., 2018); endogenous technical change (Heuberger et al., 2017a); extensive sensitivity analysis (Sepulveda, 2016; Sepulveda et al., 2018); or representing the relationship between electricity and other energy sectors such as heating (Sepulveda, 2016). Additionally, Jenkins and Sepulveda (2017), Heuberger et al. (2017a), and Clack (2018) offer the option to relax the integer unit commitment decisions to continuous variables, which incurs modest additional error from this abstraction[17] but significantly improves computational performance.

Finally, the third branch of research has focused on developing data science and optimization-based methods to select representative time periods, including: de Sisternes and Webster (2013); Nahmmacher et al. (2016); Merrick (2016); de Sisternes et al. (2016); Blanford et al. (2016); Poncelet et al. (2016, 2017); Poncelet (2018); Mallapragada et al. (2018). These efforts move beyond heuristic approaches typically employed until recently (e.g., rules of thumb such as one on peak, intermediate, and off-peak period per season). Instead, these papers use techniques including clustering and regression to identify a set of representative hours, days, or weeks that attempt to minimize abstraction error while reducing time dimensionality. These methods can then allow greater computational effort to be expended in other dimensions, including methods for enhanced network and operational detail described above.

[17]This approach retains the full unit commitment constraint set but relaxes the integer commitment decisions to continuous decisions, such that any portion of a unit may be committed. In effect, the feasible region becomes the convex hull of the original integer unit commitment formulation. This approach is discussed further in Chapter 3.

Table 1.2: Dimensionality of various approaches to representing generation and storage units and time steps in capacity expansion planning models with unit commitment constraints

Number of...							
Thermal unit clusters	Discrete thermal units	Modular resources	Time Steps	Discrete decision variables	Reduction	Continuous decision variables	Reduction
Full year, binary unit commitment constraints							
	300	5	8760	5,256,300		10,687,205	
Four representative weeks, binary unit commitment constraints							
	300	5	672	403,500	-92.3%	819,845	-92.3%
Full year, integer clustered unit commitment constraints							
5		5	8760	87,605	-98.3%	175,205	-98.4%
Four representative weeks, integer clustered unit commitment constraints							
5		5	672	6,725	-99.9%	13,445	-99.9%
Full year, linear relaxation of clustered unit commitment constraints							
5		5	8760	0	-100%	438,010	-95.9%
Four representative weeks, linear relaxation of clustered unit commitment constraints							
5		5	672	0	-100%	33,610	-99.7%

This example assumes: one investment decision per year and two unit commitment decisions (start up, shut down) per hour for each discrete thermal unit or thermal unit cluster; four operational decisions per time period for all units or clusters (contributions of capacity to power, regulation, and operating reserves up and down); and one investment decision per year for each modular resource type (e.g. solar PV, wind). Note the full model may feature additional decision variables and auxiliary variables beyond the main generator-related variables considered here, but these generally scale proportionately.

Table 1.2 provides an example of how various approaches to representing unit commitment decisions and time domain can dramatically affect the number of decision variables and the corresponding dimensionality of the capacity planning problem. Given that capacity planning continues to push the limits of computational capabilities, judicious use of abstractions or 'dimensionality reduction methods' that offer substantially improved computational performance while retaining sufficient accuracy for outcomes of interest is likely to be foundational for further expansion of the capabilities of capacity planning tools.

Figure 1-12: Review of recent electricity system capacity planning models (part 1 of 2)

References	Model	Zones	Network	Line Losses	Time Representation (per planning year)	Planning Horizon	Representation of Generators	Operational Detail	Scope
Abdin and Zio (2018)	unnamed	1	Copper plate	n/a	4 representative weeks selected to minimize error in load duration curve	Every year for 10 years	Integer (Linear for wind, solar, storage)	Hourly, commitment decisions using integer clustering method, minimum stable output and ramp constraints, minimum up and down times after cycling, regulation and reserve requirements.	France
Brown et al. (2018a, 2018b)	PyPSA	30	Pipeline flow / transport model	None	Hourly full year (8760 hours)	Single year	Linear	No time-coupling generator ramp constraints or unit commitment decisions (no large thermal units modelled); inter-temporal storage constraints	Europe
Clack (2018)	WIS:dom	One demand zone per county; resource deployment at 3 km grid resolution	Pipeline flow / transport model	Linear	Hourly full year (8760 time steps) or five minute full year (105,120 time steps)	Single year with myopic multi-stage decisions over multi-year planning horizon	Configurable as linear or integer (Linear for wind, solar, storage)	Typically a linear relaxation of unit commitment decision, minimum stable output and ramp constraints, minimum up and down times after cycling, and both operating and planning reserve requirements. Above constraints may be formulated as discrete unit commitment decisions in smaller dimensionality problems	U.S. Eastern Interconnection, U.S. Western Interconnection, Texas (ERCOT), or various subregions
de Sisternes (2013), de Sisternes et al. (2016)	IMRES	1	Copper plate	n/a	4 representative weeks selected to minimize error in net load duration curve	Single year	Binary (Linear for wind, solar, storage)	Hourly, plant-by-plant unit commitment decisions, minimum stable output and ramp constraints, minimum up and down times after cycling, regulation and reserve requirements.	Texas (ERCOT)
Frew (2013), Frew et al. (2016)	POWER	10	Pipeline flow / transport model	Linear	14 representative days	Single year	Linear	Chronological ramp rate and storage constraints within days. Minimum output constraints for dispatchable generators. Regulation and reserve requirements.	Continental United States
Haller et al. (2012)	LIMES-EU+	20 regions	Pipeline flow / transport model	Linear	49 time slices: four slices per day, three characteristic days per season, four season per year, plus peak net demand hour	Every 5 years from 2010-2050	Linear	No chronological operational constraints	European Union & MENA (Middle East & North Africa)
Heuberger (2017a, 2017b)	ESO-XEL	1	Copper plate	n/a	Two configurations: Hourly full year (8760 hours) with linear relaxation of integer unit commitment constraints; 11-21 representative 24 hour periods per year with integer unit commitment constraints	Every 5 years from 2015-2050	Configurable as linear or integer (Linear for wind, solar, storage)	Hourly, commitment decisions using integer clustering method, minimum stable output and ramp constraints, minimum up and down times after cycling, regulation and reserve requirements. Alternatively, can be configured with the above constraints and linear relaxation of commitment decisions.	United Kingdom
Hirth (2013, 2017)	EMMA	7 countries	Pipeline flow / transport model	None	Hourly full year (8760 hours)	Single year	Linear	No chronological operational constraints. Minimum output constraints for thermal units. System reserve requirements.	Northwestern Europe
Koltsaklis and Georgiadis (2015)	unnamed	5 main zones. Imports from/exports to 5 neighboring regions also exogenously specified with bid/offer prices	Pipeline flow / transport model	Linear	12 representative days per year (one per month)	Every year from 2014-2030	Binary (Linear for wind, solar)	Hourly, plant-by-plant unit commitment decisions, multiple start-up types (hot, warm, cold), soak and desynchronization phases at start/end of commitment period, minimum stable output and ramp constraints, minimum up and down times after cycling, regulation and reserve requirements.	Greece
Lara et al. (2018)	unnamed	5	Pipeline flow / transport model	Linear	1-12 representative 24 hour periods selected via k-means clustering per year	Every year for 30 years; uses a decomposition method to decompose annual sub-problems and speed computational performance	Integer (Linear for wind, solar, storage)	Hourly, commitment decisions using integer clustering method, minimum stable output and ramp constraints, minimum up and down times after cycling, regulation and reserve requirements.	Texas (ERCOT)
Mai et al. (2013); Mai et al. (2015)	RPM	1,406 nodes within focus balancing areas; 34 additional balancing areas modeled as zones	Configurable: copper plate, pipeline flow / transport model, or linear DC power flow	Linear	Peak day + 1-4 consecutive days per three periods representative of the full year	Every 5 years from 2010-2030	Generally linear (configurable for integer unit commitment)	Generally hourly ramp constraints and minimum output constraints on dispatchable generation with regulation and spinning up reserve requirements. May be configured to model integer unit commitment for select thermal units.	Western Interconnection (WECC)

Figure 1-13: Review of recent electricity system capacity planning models (part 2 of 2)

References	Model	Zones	Network	Line Losses	Time Representation (per planning year)	Planning Horizon	Representation of Generators	Operational Detail	Scope
McDonald et al. (2016)	NEWS	Up to 256 load nodes; 13-km resolution grid for wind, solar siting	Pipeline flow / transport model	Linear	Hourly full year (8760 hours)	Single year	Linear	Hourly ramp constraints on dispatchable generation; Planning reserve margin requirement.	Continental United States
Nelson et al. (2012), Mileva et al. (2016)	SWITCH 1.0	50 load zones with 1,527 sites for wind/solar siting	Transmission interconnects each balancing area with pipeline flow. "Spur line" costs are modeled from each wind/solar zone but power flows not modeled	Linear	576 hours (2 days per month, 6 hours per day) in Nelson (2012); 600 hours in Mileva et al. (2016) (same as above plus peak day)	Every 4 years from 2014-2030	Linear	Linear relaxation of hourly dispatch and unit commitment constraints within each sample day. Feasibility verified by subsequent hourly unit commitment and economic dispatch version of model across 1-2 year period.	Western Interconnection (WECC)
Palmintier (2013), Palmintier & Webster (2014, 2016)	Advanced Power	1	Copper plate	n/a	Hourly full year (8760 hours)	Single year	Integer (Linear for wind, solar, storage)	Hourly, commitment decisions using integer clustering method, minimum stable output and ramp constraints, minimum up and down times after cycling, regulation and reserve requirements.	Texas (ERCOT)
Pudjianto et al. (2014)	Whole Systems Model	5 main zones with 10 representative distribution network zones in each, plus 2 neighboring region zones	Linear DC power flow	None	Hourly full year (8760 hours)	Single year	Integer (Linear for wind, solar, storage)	Hourly, commitment decisions using integer clustering method, minimum stable output and ramp constraints, minimum up and down times after cycling, regulation and reserve requirements.	United Kingdom
Short et al. (2011)	ReEDS	365 regions for wind/solar deployment and 134 balancing areas (demand zones and non wind/solar technology siting)	Transmission interconnects each balancing area with pipeline flow OR approximated DC flow with fixed "power transfer distribution factors." "Spur line" costs are modeled for each wind/solar but power flows not modeled	Linear	17 representative time slices (four per season plus peak hour)	Every 2 years from 2006-2050	Linear	No chronological operational constraints. Minimum output constraints for thermal units. Regulation and reserve requirements. (Often soft-linked with production cost model without iteration)	Continental United States
U.S. EIA (2017)	NEMS Electricity Market Module	22	Pipeline flow / transport model	Linear	9 seasonal time slices (peak, intermediate, off-peak for three seasons: summer, winter, spring/fall)	Every year for 30 years	Linear	No chronological operational constraints	North America
U.S. EPA (2018)	IPM	67	Pipeline flow / transport model	Linear	24 step representation of load duration curve for each of four seasons	Eight 'model run years' representing 2021-2050 planning horizon	Linear	No chronological operational constraints	North America
Young et al. (2017)	US-REGEN	15	Pipeline flow / transport model	Linear	109 step representation of load duration curve in each region. 89 hours selected to represent extremes in wind, solar and demand combinations across each zone; 20 hours sampled from intermediate values. Hours weighted to minimize error in LDC.	Every 3 years from 2015-2030 and every 5 years from 2030-2050	Linear	No chronological operational constraints (soft-linked with 8760 hour resolution unit commitment model with no iteration)	Continental United States
Jenkins & Sepulveda (2017), this thesis	**GENX**	**Configurable with as many transmission and distribution network zones as specified**	**Configurable as copper plate, pipeline flow or linear DC power flow**	**Quadratic (segment-wise approx.)**	**Configurable: hourly full year (8760) or representative days/weeks**	**Single year or single year with myopic multi-stage decisions over multi-year planning horizon**	**Configurable as linear or integer (Linear for wind, solar, storage)**	**Hourly, commitment decisions using integer clustering method, minimum stable output and ramp constraints, minimum up and down times after cycling, regulation and reserve requirements. Alternatively, can be configured with the above constraints and linear relaxation of commitment decisions or as hourly economic dispatch model with ramp constraints and minimum plant output constraints but no unit commitment decisions.**	**As specified by inputs. To date: employed to model Texas ERCOT; ISO-New England; Continental Europe**

1.2.3 Limitations of Current Approaches

As befits a rapidly changing sector, researchers have devoted considerable effort in recent years to improving electricity system capacity planning methods. However, one critical area remains deficient: methods to accurately model the impact of distributed energy resources on capacity planning decisions. Indeed, only a handful of prior capacity planning models consider DERs in any way.

Both Short et al. (2011) (as applied in Hand et al. (2012)) and U.S. EIA (2017) specify distributed solar PV capacity as an exogenous input to capture the influence of policy or individual decisions on distributed PV adoption. Frew (2014) performs a sensitivity case in which residential PV capacity is endogenously determined with distributed PV costs discounted by 45% to reflect potential locational value from on-peak distribution network loss reductions and avoided network capacity costs, although these factors are not modeled endogenously. As multi-zonal models, all three works consider transmission constraints and associated network expansion decisions as well as model transmission losses as simple linear functions of power flow.[18] To some extent, these models thus capture locational value due to transmission level congestions and losses captured by distributed solar PV located at demand nodes. Short et al. (2011) models distribution network losses as a simple linear function of consumption at each demand zone as well[19], and distributed PV systems are exempt from these losses.

A number of studies (Frew, 2014; Pudjianto et al., 2014; Frew et al., 2016; Sepulveda, 2016; U.S. EIA, 2017; Pudjianto and Strbac, 2017; Sepulveda et al., 2018; Clack, 2018) consider the presence of flexible or price responsive demand and the influence on bulk generation and storage capacity in some manner. In all cases, the available capacity of flexible demand is determined exogenously, while operational decisions are endogenous. Sepulveda (2016) and Sepulveda et al. (2018) apply single-zone models and, as such, do not consider any locational

[18]Short et al. (2011) assumes transmission line losses are constant 1 percent per 100 miles while Frew (2014) applies 5 percent losses on all long-distance intra-regional transmission interconnections, regardless of distance or line loading

[19]Short et al. (2011) simply assumes distribution network losses are 5.3 percent of demand in all demand zones at all times.

value of demand-side flexibility. Frew (2014); Frew et al. (2016); U.S. EIA (2017) and Clack (2018) credit demand reductions with reduced transmission losses based on a linear line loss function, and decreased demand in some periods may help avoid transmission congestions or constraints.

In an important advance in the capacity planning literature, Pudjianto et al. (2014) and Pudjianto and Strbac (2017) consider the potential for distributed energy storage (with endogenously optimized capacity) and flexible or shiftable demand (with exogenous capacity), respectively, to reduce both transmission *and* distribution network capacity expansion costs. To my knowledge, these papers are the only previous works to consider the impact of DERs on distribution network capacity costs in any way. The papers model distribution network costs as a function of the peak net demand in each demand zone (or demand less distributed energy storage discharge and demand reduction from deferring flexible demand). Distribution expansion costs per megawatt of net peak demand are represented as a piecewise linear function parameterized based on offline modeling of network expansion costs in representative distribution feeders. While modeling the impact of distributed storage or flexible demand on distribution network expansion costs is a key step towards incorporating DERs into electricity system capacity planning, Pudjianto et al. (2014) and Pudjianto and Strbac (2017) fall short of fully considering the locational value and economies of unit scale tradeoffs associated with DERs. Their model ignores transmission and distribution lines losses entirely. In addition, they consider only one voltage level and unit size option for distributed battery storage, which fails to capture economies of unit scale tradeoffs with any granularity. Additionally, distributed batteries are the only DER for which capacity investment decisions are endogenous to the optimization model.

1.2.4 A New Approach to System Planning with Distributed Energy Resources

To capture the key economic and technical considerations associated with DERs with sufficient accuracy, electricity resource capacity expansion models must not only build on recent

advancements in the literature, but also be extended further to include four additional features:

- First, capacity planning tools should endogenously model the largest sources of locational value, including non-linear resistive network losses, impacts of network constraints, and network capacity expansion costs, with all three factors modeled for both transmission and distribution networks.

- Second, models should allow siting of DERs at multiple scales and voltage levels in order to capture economic tradeoffs associated with economies of unit scale.

- Third, models should endogenously account for the potential role of more flexible and price-responsive demand in reducing investment and operating costs, including impacts on both generation and network capacity.

- Finally, planning models should include endogenous investment decisions for a wide range of the most salient distributed and conventional resources, in order to capture competition and complementary between each of these resources.

This thesis introduces new methods to incorporate the impact of DERs and demand-side flexibility on transmission and distribution losses and network reinforcement costs into capacity planning models. In Chapter 2, I present a new processes for detailed, offline modeling of different large-scale distribution networks to derive polynomial equations that parsimoniously capture non-linear distribution network losses and reinforcement costs across an entire distribution network (e.g., a collection of medium-voltage primary feeders and low-voltage secondary feeders downstream from a primary substation). Each distribution network is home to several thousand network customers or connection points with an aggregate peak consumption on the order of 20 to 100 MW. This process involves three components:

1. Using AC power flow simulations, I derive an equation for losses in each distribution network as a function of changes in electricity demand and generation within each distribution network voltage level (Section 2.2).

2. Similarly, I present a method for using an AC optimal power flow model to find the minimum amount of reduction in net demand reduction – achieved either by curtailing consumption or by supplying demand locally with distributed generation or storage – necessary to accommodate a given increment in coincident peak demand growth within each distribution network (Section 2.3).

3. Finally, using a detailed distribution network planning model, I derive an equation for network expansion costs as a function of coincident peak demand less the portion of demand growth accommodated by demand reduction/self generation as per step 2 above (Section 2.4).

In Chapter 3, I describe a multi-zonal capacity expansion model with detailed operating constraints (originally detailed in Jenkins and Sepulveda (2017)), which builds on and extends state-of-the-art techniques from the recent literature. Fig 1-14 provides a visual schematic of the multi-zonal model. Eligible resources include conventional thermal power plants (gas-fired combined cycle and open cycle turbines, nuclear power stations) at transmission voltages, energy storage and renewable resources (wind, solar PV) at both transmission and distribution voltages, gas-fired distributed generation (fuel cells, microturbines), and two classes of demand response resources: curtailable or price-responsive demand and flexible or schedulable demand.

Several transmission voltage zones present opportunities for siting bulk-scale generation and storage resources. Each zone can be parameterized with a different solar and wind energy profile to capture diversity in variable renewable resource quality and variability and transmission extension costs. Power flows between each zone are represented with a pipeline flow or transport model, and transmission network capacity expansion decisions are endogenous. Constraints on transmission flows between zones can capture the most relevant or frequent transmission congestions in a given regional power system. In addition, transmission losses between each zone are modeled as a quadratic function of power flows ($losses = (\frac{power}{voltage})^2 \times resistance$) linearized via a segment-wise interpolation.

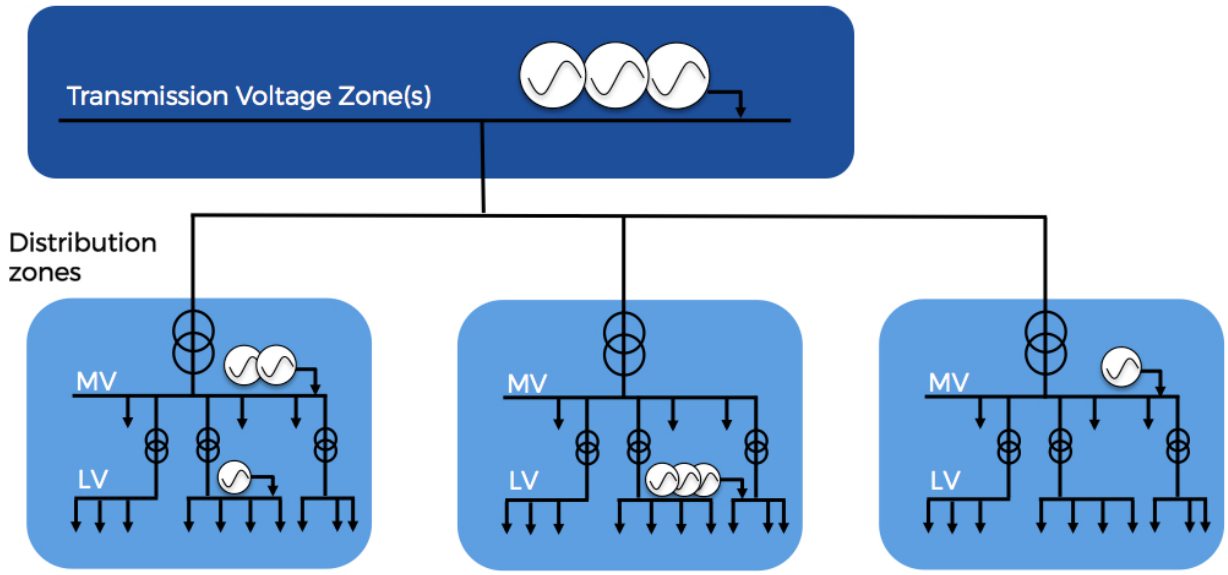

Figure 1-14: Visual schematic of multi-zonal electricity system planning model
The modeling framework features multiple transmission and distribution network zones, constrained power flows between zones, and siting of different scales of generation and storage resources at each voltage level

Multiple distribution network zones can be specified within each transmission zone, with each zone representative of a common network topology in that region (e.g., sparse rural networks, dense and symmetric urban networks, asymmetric semi-urban networks). Each distribution zone itself features two voltage levels: a medium voltage (MV) network zone, representing all primary distribution feeders (typically 4 to 33 or 35 kV), where larger commercial and industrial consumers are located and DERs ranging from 100s of kW to several MW in scale may be sited; and a low-voltage zone representing all secondary distribution feeders (240 to 400 V), where small commercial and residential customers are located and smaller DERs ranging from a few kW to a few 100 kW in scale may be sited. Different installed costs can be specified for DERs located at each distribution network voltage level, capturing economies of unit scale for relevant resources, such as solar PV and battery energy storage. Finally, non-linear losses and network expansion costs for each distribution zone are modeled using the polynomial equations generated via the methods introduced in Chapter 2.

The model simultaneously optimizes the mix of electricity generation, storage, demand-side resource, and electricity network investments and operational decisions to maximize

social welfare in a future planning year. To do so, the model's objective function seeks to meet electricity demand in the planning year while minimizing the costs of electricity supply and maximizing utility of consumption[20] all subject to a variety of power system operational constraints and specified policy constraints, such as CO_2 emissions limits. The model's objective function is to minimize the:

1. Sum of investment and fixed operation and maintenance (O&M) costs across all generation, storage, and distributed resources and all zones;
2. Sum of transmission and distribution network reinforcement and maintenance costs across all transmission lines and distribution zones;
3. Sum of variable O&M and fuel costs per time interval across all resources and zones;
4. Sum of cost or value of other services provided by DERs (e.g. voltage regulation, back-up power) not exogenously modeled;
5. Sum of cost of unmet demand (for price elastic consumers or involuntary non-served energy) or operating reserves for each hour in each zone.

The optimization problem is subject to:

- Operational constraints on thermal generators, dispatchable renewables, energy storage, deferrable (schedulable) demand, and demand curtailment (price-responsive demand);
- Network power flow constraints between transmission zones;
- Aggregate peak electricity withdrawal (demand) and injection (generation) constraints within each distribution zone;
- Optional frequency regulation and operating reserve requirements for the entire system.

[20] As this is a constrained cost minimization optimization problem, the utility of consumption is represented by including a base level of demand in each hour and a set of price-responsive demand 'segments,' each representing a set of consumers with different willingness to pay for electricity consumption. If the marginal cost of supply rises above the willingness to pay of any segment, demand is reduced by the aggregate consumption of that segment of consumers. In this way, the demand curve for electricity is represented as a segment-wise approximation capturing the varying elasticity of demand in approximate manner. A final segment of inelastic consumers is included as well, and if generation scarcity or binding network constraints prevent sufficient supply at any zone, demand can only be balanced via shedding demand in this segment at a very high cost of non-served energy (e.g., $10,000/MWh)

- Optional policy-related constraints such as maximum CO_2 emissions or minimum energy shares from preferred resources

The model can be formulated either as a mixed-integer linear programming (MILP) problem with integer investment and unit commitment decisions for large thermal generators using the integer clustering technique introduced by Palmintier (2013), or as a linear programming (LP) problem using a linear relaxation or convex hull of the unit commitment constraints set (Palmintier and Webster, 2014). In either case, the model features an hourly resolution and is typically modeled for all hours of a single future planning year (although various time domain reduction methods can be employed if desired to reduce dimensionality).

The resulting electricity system capacity planning model is a general purpose tool that can be applied in various power system contexts to explore what factors drive the economic competitiveness of DERs, understand how distributed and conventional generators compete with one another to supply electricity services, and evaluate the potential costs or benefits of policy or regulatory reforms.

Even as DER adoption and greater demand flexibility further decentralize power sector decisions in response to economic (and behavioral) incentives, the model's 'system planning' perspective retains significant value. Incentives for distributed decision making in the power sector are pervasively shaped by public policy and regulatory choices, as well as the choices of regulated agents such as network utilities (e.g., through rate design, 'non-wires' alternatives programs, rebates, and behavioral incentive programs, etc.). In this context, indicative planning and decision support tools are useful for evaluating 'first-best,' social welfare-maximizing outcomes as a normative guide for policy/regulatory/market design decisions – as well as to evaluate the relative economic costs and tradeoffs of second (or third or fourth) best decisions. Likewise, planning models remain important to regulated utilities, particularly vertically integrated utilities as well as network utilities increasingly tasked with enabling efficient and environmentally friendly system-wide outcomes (as in New York, California, the UK, and other jurisdictions). The current state-of-the-art lacks system-wide planning tools that can serve either capacity, which can hamper decision making. Available

tools are able to consider only portions of the system at a time, which cannot provide a holistic analysis of the impacts of DER adoption across distribution, transmission, generation, and DER segments.

The objective of this thesis is to develop a power system modeling framework that can provide a new lens to identify opportunities for DERs to reduce system-wide costs or facilitate other public objectives, elucidate how DERs affect the value/economics of other resources, and provide clarity on the (potentially significant) economic costs incurred by inefficient rate design, poorly designed incentives for DER adoption, or remuneration of distribution utilities that continues to bias them towards conventional network investments over potentially cost-effective alternatives. These methodological contributions are presented in Chapters 2-3.

Chapter 4 presents several system planning case studies employing this novel modeling framework to demonstrate its capabilities and indicate its potential to support improved decision-making in the power sector.

Finally, Chapter 5 concludes this thesis by discussion the implications of enhanced system planning with DERs for electricity economics, regulation, and policy, summarizing the contributions of this work, and discussing future research directions.

Chapter 2

Modeling Locational Value in Distribution Networks: Distribution Losses and Network Expansion Deferral

Distributed energy resources offer new options for the delivery of electricity services. They compete directly with conventional, large-scale generators to supply electrical energy, operating reserves, firm capacity, and similar services. In addition, siting and operation of DERs in ideal locations may offer an alternative to upgrades to electricity transmission and distribution investments, and in this sense, they compete with network assets as well. As discussed in Section 1.1.3, what sets DERs apart in this competition is their ability to be deployed closer to the point of electricity consumption and in locations inaccessible to more centralized resources. This capability offers the potential to capture greater 'locational value' than their larger counterparts. This locational value is associated with services that change in value depending on the location of provision due to the physical characteristics of electricity networks, including resistive losses, capacity limits of network components, voltage limits at network nodes, and the potential for network failures that may disrupt delivery of electricity services.

The three largest sources of locational value are: the effect of marginal losses in transmis-

sion and distribution networks on the value of electrical energy; the ability to reduce or defer transmission or distribution network capacity upgrades; and improvements in reliability of electricity supply. Other services exhibit locational value, including power quality management and black-start or system restoration capabilities, but these are typically more niche services, and as such are not discussed further herein.

This chapter focuses on the first two sources of locational value: marginal losses and network capacity deferral or substitution.[1] In particular, I introduce and demonstrate novel methods for characterizing changes in losses and network capacity requirements as a function of aggregate electricity demand and generation across large-scale distribution networks.

Each large-scale distribution network represents a collection of on the order of 5 to 10 medium voltage primary distribution feeders (e.g., 20 kV lines), roughly 100 to 200 medium-to-low voltage transformers, and associated low voltage secondary distribution feeders (e.g., 400 V lines), all downstream from a single transmission substation. The networks are each home to several thousand individual network customers (or metered connection points) with aggregate peak consumption on the order of 20 to 100 MW. Based on detailed modeling of these distribution networks, I demonstrate how to derive polynomial equations that parsimoniously and accurately capture the behavior of non-linear distribution network losses and reinforcement costs across the entire distribution network. These methods therefore move beyond feeder-by-feeder engineering analysis to describe the behavior of distribution networks at a larger scale and in a computationally tractable manner suitable for inclusion in wide area electricity system planning models.[2]

[1]Reliability benefits may also be an important source of locational value. I discuss and roughly estimate the approximate magnitude of value from avoided service disruptions in developed power systems like the United States in Section 1.1.3. However, assessing the reliability value of DERs in greater detail is beyond the scope of this current work. At present, I will rely on sensitivity analysis of the value of reliability as an exogenous input to the system planning model described in Chapter 3 and demonstrated in Chapter 4. This sensitivity analysis can help determine the potential impact of additional locational value from avoided service disruptions on planning outcomes and indicate whether further analysis is warranted.

[2]Max Luke assisted in implementing earlier versions of these simulation methods and Claudio Vergara advised on initial development.

These methods involve three types of modeling processes:

1. **AC power flow simulations** to derive a multivariate polynomial equation for losses in each distribution network as a function of changes in aggregate electricity withdrawals and injections within each distribution network voltage level (described in Section 2.2).

2. **AC optimal power flow modeling** to find the minimum amount of reduction in net withdrawals – achieved either by demand reduction or self-generation with distributed generation or storage – necessary to accommodate a given increment in coincident peak demand growth within each distribution network (Section 2.3).

3. **Distribution network expansion modeling** to derive an equation for network expansion costs as a function of coincident peak demand less the portion of demand growth accommodated by demand reduction/self generation as per step 2 above (Section 2.4).

I demonstrate all three modeling processes using three representative European test networks with varying topologies from Prettico et al. (2016), which are introduced in the following section.

2.1 Representative Distribution Networks

In Prettico et al. (2016) (later published in Mateo et al. (2018)), researchers with the Joint Research Centre (JRC) of the European Commission created three large-scale test networks designed to be representative of typical urban, semiurban, and rural distribution networks in Europe. To construct these test networks, Prettico et al. (2016) collected technical and structural data on distribution networks from 79 utilities representing more than 70 percent of the electricity supplied by all European distribution utilities serving over 100,000 customers.[3] The researchers then used this data to calculate indicators describing network structure,

[3]Overall, the 79 distribution utilities distribute more than 2 billion MWh of electricity to over 200 million customers per year, covering a total area of more than 3 million square km. See Prettico et al. (2016); Mateo et al. (2018) for more details on survey methods.

network topology, and distributed generation penetration that characterize the range of networks encountered in Europe. Finally, they used these indicators to design synthetic networks representative of typical urban, semiurban, and rural network topologies using the Reference Network Model, a wide-area distribution network expansion planning model described in Domingo et al. (2011). Table 2.1 describes some of the key characteristics of each network and Figures 2-1 to 2-4 depict the network maps.

Figure 2-1: Representative urban European network map
Low voltage customers are colored by network zone, where each zone corresponds to all low voltage feeders connected to a single 20 kV/0.4 kV medium to low voltage transformer. Note that line branches are depicted as vertices between any two buses. The actual line layout differs so as to adhere to street layouts and other restrictions not depicted here.

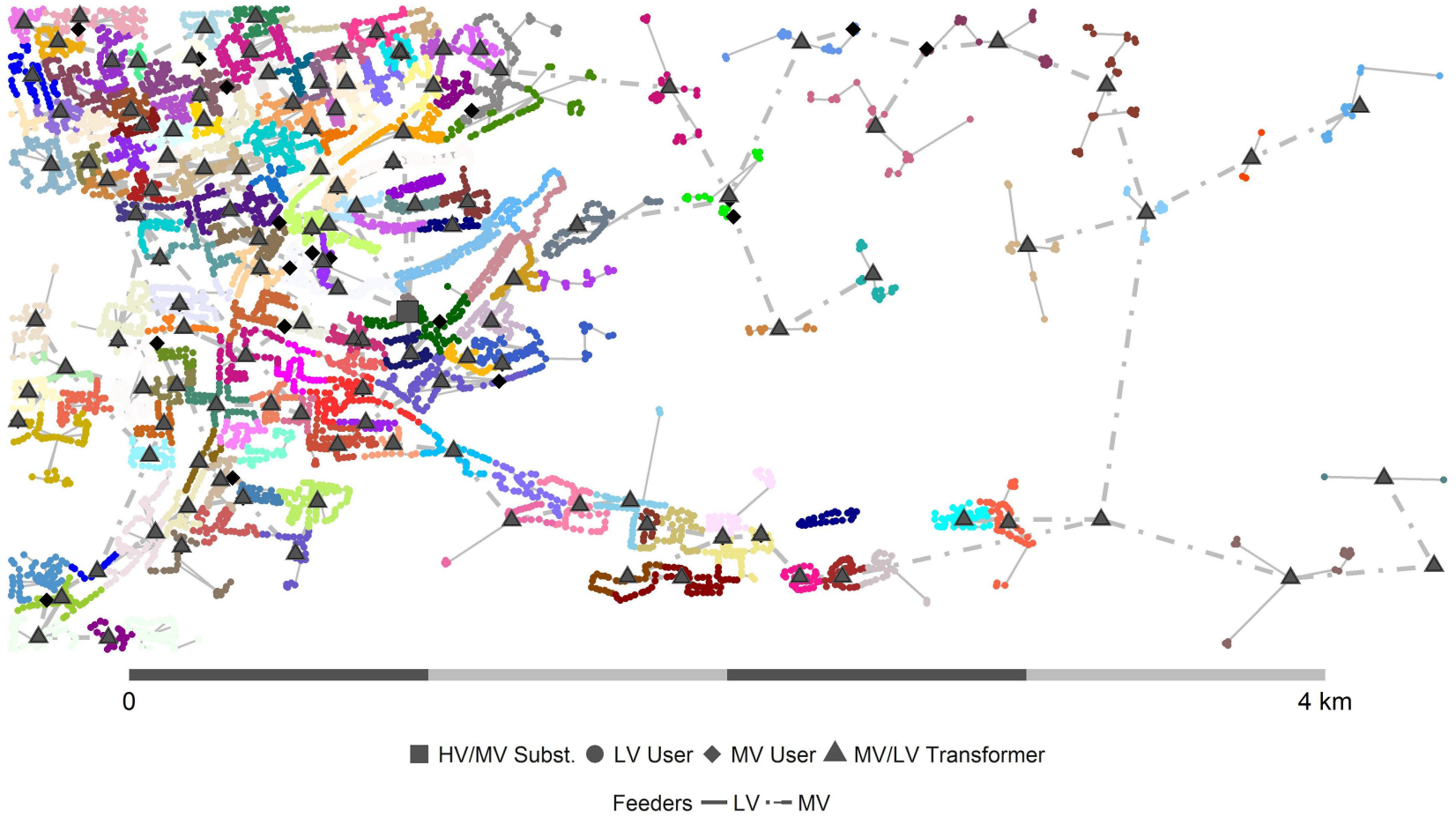

Figure 2-2: Representative semiurban European network map

Low voltage customers are colored by network zone, where each zone corresponds to all low voltage feeders connected to a single 20 kV/0.4 kV medium to low voltage transformer. Note that line branches are depicted as vertices between any two buses. The actual line layout differs so as to adhere to street layouts and other restrictions not depicted here.

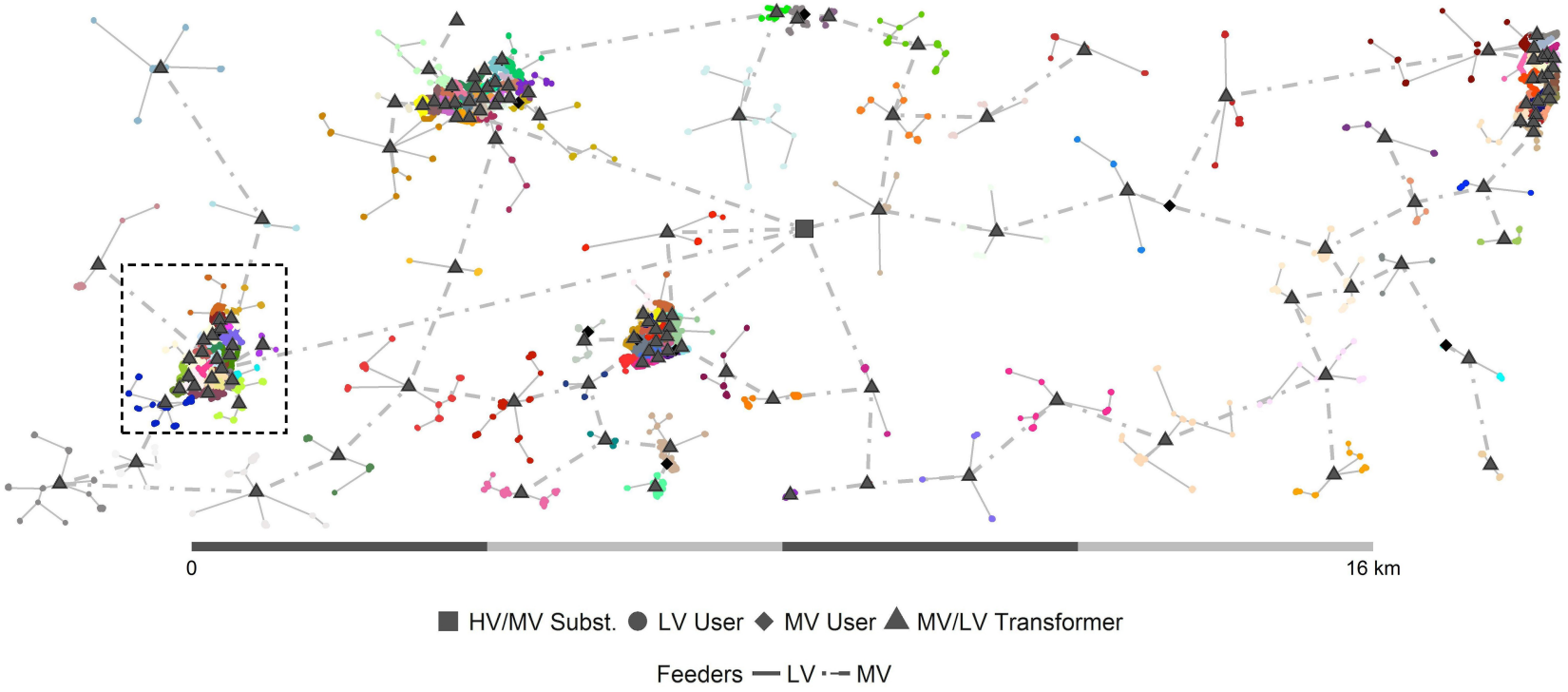

Figure 2-3: Representative rural European network map (full network)

Low voltage customers are colored by network zone, where each zone corresponds to all low voltage feeders connected to a single 20 kV/0.4 kV medium to low voltage transformer. Note that line branches are depicted as vertices between any two buses. The actual line layout differs so as to adhere to street layouts and other restrictions not depicted here. Box indicates area of western village inset in Fig. 2-4.

Figure 2-4: Representative rural European network map (western village inset)
Low voltage customers are colored by network zone, where each zone corresponds to all low voltage feeders connected to a single 20 kV/0.4 kV medium to low voltage transformer. Note that line branches are depicted as vertices between any two buses. The actual line layout differs so as to adhere to street layouts and other restrictions not depicted here. Area represents western village outlined by box in full rural network map (Fig. 2-3).

Table 2.1: Characteristics of representative European distribution networks

Medium-voltage customers	**Urban**	**Semiurban**	**Rural**
Number	38	40	20
Aggregate peak consumption (MW)	5.7	6.0	3.0
Density (kW per km of MV feeders)	183	119	23
Low-voltage customers			
Number	12,735	13,998	7,727
Aggregate peak consumption (MW)	56.8	68.5	25.3
Density (kW per km of LV feeders)	1,054	851	120
Distribution lines			
Medium voltage feeders (20 kV)	5	10	6
-km overhead	0	13.24	111.24
-km underground	31.2	37.16	19.88
Low voltage feeders (0.4 kV)	384	324	181
-km overhead	7.38	67.21	201.97
-km underground	46.49	13.24	9.49
Substations and transformers			
Transmission substations (132/20 kV)			
x 120 MVA	0	1	0
x 80 MVA rating	1	0	1
MV to LV transformers (20/0.4 kV)			
x 1,000 kVA rating	34	38	0
x 630 kVA rating	52	57	0
x 400 kVA rating	40	54	42
x 250 kVA rating	0	8	79
x 100 kVA rating	0	4	29
Total	126	161	150

2.2 Modeling Distribution Losses

DERs can be located within distribution networks and thus offer the ability to supply electrical energy close to demand. In this manner, DERs may reduce power flows across transmission and distribution networks and correspondingly reduce network losses. The marginal effect of DERs on network losses increases their locational value, relative to conventional generators.

The majority of electricity network losses result from resistive losses (also known as 'copper' losses or I^2R losses, after the equation for losses as a function of current and resistance) (Benedict et al., 1992).[4] As current flows through transmission and distribution lines and transformers and encounters electrical resistance, energy is dissipated as heat. Furthermore, as electrical conductors heat up, they become more resistive, causing losses to rise quadratically with current (and thus power) flow across conductors. Marginal resistive losses avoided per unit of power generated in distribution voltages (or per unit of demand reduced) thus rises at double the rate of average resistive losses and can be significant at periods of high network loading.[5] For example, while average resistive losses in the semiurban European test network used herein may be roughly 7 percent when aggregate demand reaches 50 percent of peak, marginal losses are 14 percent. At peak loading, average and marginal losses double to roughly 14 percent and 28 percent, respectively.

Furthermore, the vast majority of total electricity network losses occur within lower voltage distribution networks. As resistive losses are proportionate to $P \times \frac{R}{V^2}$, losses asso-

[4]Energy is also lost to 'core' losses, also known as 'iron' or 'no-load' losses, which may account for 20-35 percent of transmission and distribution losses on average. Core losses arise from eddy current losses, which arise from current magnetically induced in the core of the transformer, and hysteresis losses, which result from energy required to provide the magnetic field in the core as the polarity of the alternative current waveform reverses. Both forms of core losses are relatively constant with respect to current flow through the transformer and instead relate to the maintenance of magnetic fields in the core whenever the transformer is energized (hence the term 'no load' losses, as they are constant with respect to transformer loading). As such, DERs cannot reduce core losses, and the presence of core losses in transmission and distribution systems do not affect locational value. I therefore focus herein on modeling resistive losses only and ignore core losses for the purposes of this analysis.

[5]As losses are proportionate to $I^2 \times R$ or equivalently $P^2 \times \frac{R}{V^2}$ (where I, R, V, and P are current, resistance, voltage, and power respectively), average losses increase proportionate to $P \times \frac{R}{V^2}$ while marginal losses increase proportionate to $2P \times \frac{R}{V^2}$.

ciated with a given power flow are reduced with the square of voltage. Resistive losses in high voltage transmission systems are therefore very low relative to losses in distribution networks. Accurately representing the impact of DERs on distribution network losses is therefore critical to understanding the locational value of DERs in different contexts – as well as representing this value in electricity system planning models.

In this section, I describe a method for using AC power flow simulations to derive the relationship between varying levels of aggregate demand and distributed generation (or power injection from energy storage devices) on resistive losses within a large-scale distribution network. I then demonstrate this method on each of the three European test networks introduced in Section 2.1.

2.2.1 Experimental Method: AC Power Flow Simulations and Resistive Losses

It is possible to use an AC power flow simulation to derive total resistive losses due to power flows across a large-scale distribution network associated with a given distribution of real and reactive power demand and generation across network users. An AC power flow (or load flow) model uses numerical methods to solve for the set of bus voltages and branch flows in an electricity network associated with a steady pattern of power demand and generation (see Zimmerman et al. (2011)).

In an AC power flow model, a single generation or power injection bus (such as the primary transmission substation feeding a distribution network) is considered the reference bus. The voltage angle at the reference bus is given ($\theta_{ref} = 0$) and all other nodal voltage angles are described in reference to this angle. Real and reactive power injection (P_{ref}, Q_{ref}) at the reference bus are considered unknown variables. Real power (P_d) and reactive power (Q_d) consumption at all demand (or withdrawal) buses are specified (hence these buses are referred to as 'PQ' buses) while voltage magnitude (V_d) and angle (θ_d) at these demand buses are variables that must be solved for. Generators (or injection buses) are typically specified with a fixed real power injection (P_g) and voltage magnitude (V_g) (and as such are

termed 'PV' buses) while their voltage angle (θ_g) and reactive power Q_g are unknown and must be solved for. However, distributed generators operating with a fixed power factor can be specified as PQ buses instead.

In a network with n_{pq} PQ and n_{pv} PV buses, we thus have a set of $2n_{pq} + 2n_{pv} + 2$ unknown variables to solve for: voltage angles at all non-reference buses ($\theta_i \ \forall \ d, g$), voltage magnitudes at all PQ buses ($V_i \ \forall \ d$), reactive power at all PV buses ($Q_i \ \forall \ g$), and the real and reactive power injection at the reference bus (P_{ref}, Q_{ref}).

Power balance constraints apply at each bus in the network ($i \in N$) and are decomposed into real and reactive power balance constraints:

$$P_i = \sum_{k=1}^{N} |V_i||V_k|(G_{i,k}\cos(\theta_i - \theta_k) + B_{i,k}\sin(\theta_i - \theta_k)) \tag{2.1}$$

$$Q_i = \sum_{k=1}^{N} |V_i||V_k|(G_{i,k}\sin(\theta_i - \theta_k) + B_{i,k}\cos(\theta_i - \theta_k)) \tag{2.2}$$

where P_i and Q_i are the net real and reactive power injection at bus i and $G_{i,k}$ and $B_{i,k}$ are the real and reactive parts of the bus admittance matrix, which contains a non-zero value describing the admittance of the network branch(es) between all pairs of physically connected buses $(i, k) \in N$. Taking the real and reactive power balance equations for each PQ bus and the real power balance equation for each PV bus yields a system of $2n_{pq} + n_{pv}$ non-linear equations, which makes it possible to solve for each of the $2n_{pq} + n_{pv}$ unknown voltage angle and magnitude values for all non-reference buses. After solving for each voltage variable, the remaining real power balance equation at the reference bus can be used to solve for P_{ref} and the remaining $n_{pv} + 1$ reactive power balance equations can be used to solve for the reactive power Q_g at all PV buses as well as Q_{ref}. Finally, given net power injections and withdrawals at all buses and resistance and reactance for each branch, power flows across network branches and associated resistive losses can also be derived.

In this study, I use the Matpower suite of power flow models (see Zimmerman et al. (2011) and Zimmerman and Murillo-Sánchez (2016)) for the MATLAB scientific programming language to perform AC power flow simulations. For each large-scale European test

network, I perform the same overall experimental method described in Algorithm 1.

First, input files describing each bus and branch in the network are loaded in Matpower case format. Then, each network user connected at low voltage (LV, or 0.4 kV) is assigned to a zone, where a zone is defined as all nodes connected to the set of radial low voltage feeders issuing from a given medium-to-low voltage (20 kV/0.4 kV) transformer. Figures 2-1 to 2-4 visually illustrate the assignment of zones in each network using a different color to denote each LV zone. Next, a series of D individual power flow simulations is performed.[6]

Each simulation corresponds to a pair of random aggregate demand and generation levels independently drawn from a uniform distribution ranging from 0.0 to 1.0 p.u. of the aggregate peak demand in the network. Corresponding demand and generation levels are then assigned to individual network users in the following steps:

1. *Assign users to host generation:* A set of network users is designated to host generation by randomly sampling x nodes (with uniform probability and no replacement) where x is the proportion of aggregate generation to aggregate demand in this simulation or 1.0, whichever is lesser. Thus, in cases where aggregate generation is lower than demand, only a random subset of network users are assumed to host distributed generation. If aggregate generation exceeds aggregate demand, all network users are assumed to host generation.

2. *Assign concentration of demand and generation across LV zones and MV users:* Each low voltage zone and each medium voltage (MV) user are assigned independent 'concentration factors' for both demand and generation levels, indicating how each LV zone or MV user's p.u. demand or generation differs from the network average values. These concentration factors are drawn from a truncated normal distribution with a standard deviation σ specified for each experiment. The normal distribution is truncated such that no LV zone or MV user has an extreme value less than 0 or greater than double the network average values. A σ of 0 corresponds to a uniform distribution of demand

[6]Note that due to the large size and non-linear nature of the power flow problem, not all simulations converge to a solution. I repeat random draws and corresponding simulations until the desired number of successful simulations are reached.

Algorithm 1: Experimental method using AC power flow simulations to calculate resistive losses

Data:

- Matrix of N network nodes (one per electricity user and high and low voltage sides of each transformer) in Matpower 'mpc.bus' format
- Matrix of B network branches (one per line segment and one per transformer) in Matpower 'mpc.branch' format
- Number of individual AC power flow simulations to run, D
- Concentration factor σ, describing the standard deviation of demand or generation in each zone as p.u. of mean demand or generation in each simulation

Result: Matrix of D results for each AC power flow simulation

begin

Load network and branch data;
Group all LV network users into $\mathcal{Z}$ zones, where each user downstream from a given MV-LV transformer is considered a zone;
while *Successful power flow simulations* $< D$ **do**
Generate random p.u. average demand and generation by voltage level $d_v, g_v \sim U(0,1)\ \forall\ v \in \{lv, mv\}$;
Randomly sample network users to create set of users that host generation $\mathcal{G}$ s.t. the proportion of users sampled $= \min(g_v/d_v, 1.0)\ \forall\ v \in \{lv, mv\}$;
foreach $z \in \mathcal{Z}$ **do**
Zonal p.u. demand and generation $d_z = d_{lv} \times c_{d,z}$, $g_z = g_{lv} \times c_{g,z}$, where $c_{d,z}, c_{g,z}$ are random concentration factors i.i.d. $\sim N(1.0, \sigma)$ truncated s.t. $-1.0 < c < 2.0$;
foreach *LV user* $i \in$ *zone* z **do**
User demand $d_i = p_i/(\sum_{j \in z} p_j) \times d_z$ where p is a user's peak demand;
if $i \in \mathcal{G}$ **then** User generation $g_i = p_i/(\sum_{j \in \cap(G,z)} p_j) \times g_z$;
end
end
foreach *MV user* $m \in \mathcal{M}$ **do**
User demand $d_m = p_m \times d_{mv} \times c_{d,m}$, where $c_{d,m}$ is a random demand concentration factor $\sim N(1.0, \sigma)$ truncated s.t. $-1.0 < c < 2.0$;
if $m \in \mathcal{G}$ **then**
User generation $g_m = p_m \times g_{mv} \times c_{g,m}$, where $c_{g,m}$ is a random generation concentration factor $\sim N(1.0, \sigma)$ truncated s.t. $-1.0 < c < 2.0$;
end
end
Run Matpower AC power flow simulation;
Record results: losses, total real & reactive power demand & generation by voltage level; total real & reactive withdrawal & injection by voltage level;
end

end

and generation across the network at the average network value, and as σ increases, the concentration of aggregate demand or generation in specific portions of the network increases. In this manner, demand and generation can be concentrated in specific LV feeders or at specific MV network users to simulate the irregular distribution of demand and generation in real networks.

3. *Assign LV demand and generation by user:* Zonal aggregate demand and generation in each LV zone are then the product of aggregate peak demand for all network users in that zone, the zonal demand or generation concentration factor, and the network average demand or generation values for this simulation. Aggregate demand in each LV zone is assigned to each individual user in proportion to that user's share of the aggregate peak demand in that zone. Aggregate generation in each LV zone is assigned to each individual user in proportion to that user's share of the aggregate peak demand for all users hosting generation in that zone.

4. *Assign MV demand and generation by user:* Demand for each MV network user is the product of that user's peak demand, the user's demand concentration factor, and the network average demand for this simulation. Generation for each MV network user designated to host generation is likewise the product of that user's peak demand, the user's generation concentration factor, and the network average generation for this simulation.

Note that each network user is assumed to have a fixed power factor in these simulations, as specified in the bus input files. Reactive power demand and generation for all network users are therefore proportionate to the real power values assigned via the process above. Finally, a Matpower AC power flow simulation is run and the results are recorded for each of the D individual simulations for processing.

2.2.2 Deriving the Functional Relationship Between Losses, Demand, and Generation

Using the experimental method described above, I perform experiments for each of the three European distribution networks (urban, semiurban, and rural) and using three different values for the standard deviation of demand and generation concentration within networks ($\sigma = 0.0, 0.2, \& \ 0.4$). In each experiment, I produce 10,000 individual AC power flow simulation results ($D = 10,000$) with independently varying combinations of demand and generation in each voltage level, as per Algorithm 1.

Figures 2-5 and 2-6 depict the relationship between distribution network losses and aggregate demand and distributed generation levels across both low and medium voltage portions of the network. Each point represents results of an individual AC power flow simulation. The location of each point in the horizontal (x,y) coordinate plane corresponds to demand and generation in LV feeders, while the location on the vertical (z) axis indicates the level of aggregate resistive losses across the entire network. Additionally, the color of each point reflects the net of (demand − generation) in MV feeders; brighter colors indicate greater net demand and darker colors indicate greater net generation. In this way, these figures depict all four independent variables and their relationship to the outcome variable (losses) in each experiment. Fig. 2-5 presents results for each network for experiments using a concentration factor, $\sigma = 0.2$, while Fig. 2-6 illustrates the effect of changes in the concentration of demand and generation (e.g., changes in σ) in the semiurban network.[7] Visual inspection of these figures illustrates several important relationships.

1. Losses rise quadratically in proportion to |demand − generation| in low voltages: By examining the location of each point, one can see a clear non-linear relationship between LV net (demand − generation) and total network losses. Indeed, increases in the magnitude of either net demand or net generation result in quadratic increases in total network losses. As net demand increases, more power must be imported to the distribution network to satisfy local demand, increasing power flows across lines and transformers and driving quadratic re-

[7]Effects of changing concentration factor are similar for other networks, and figures are omitted for brevity.

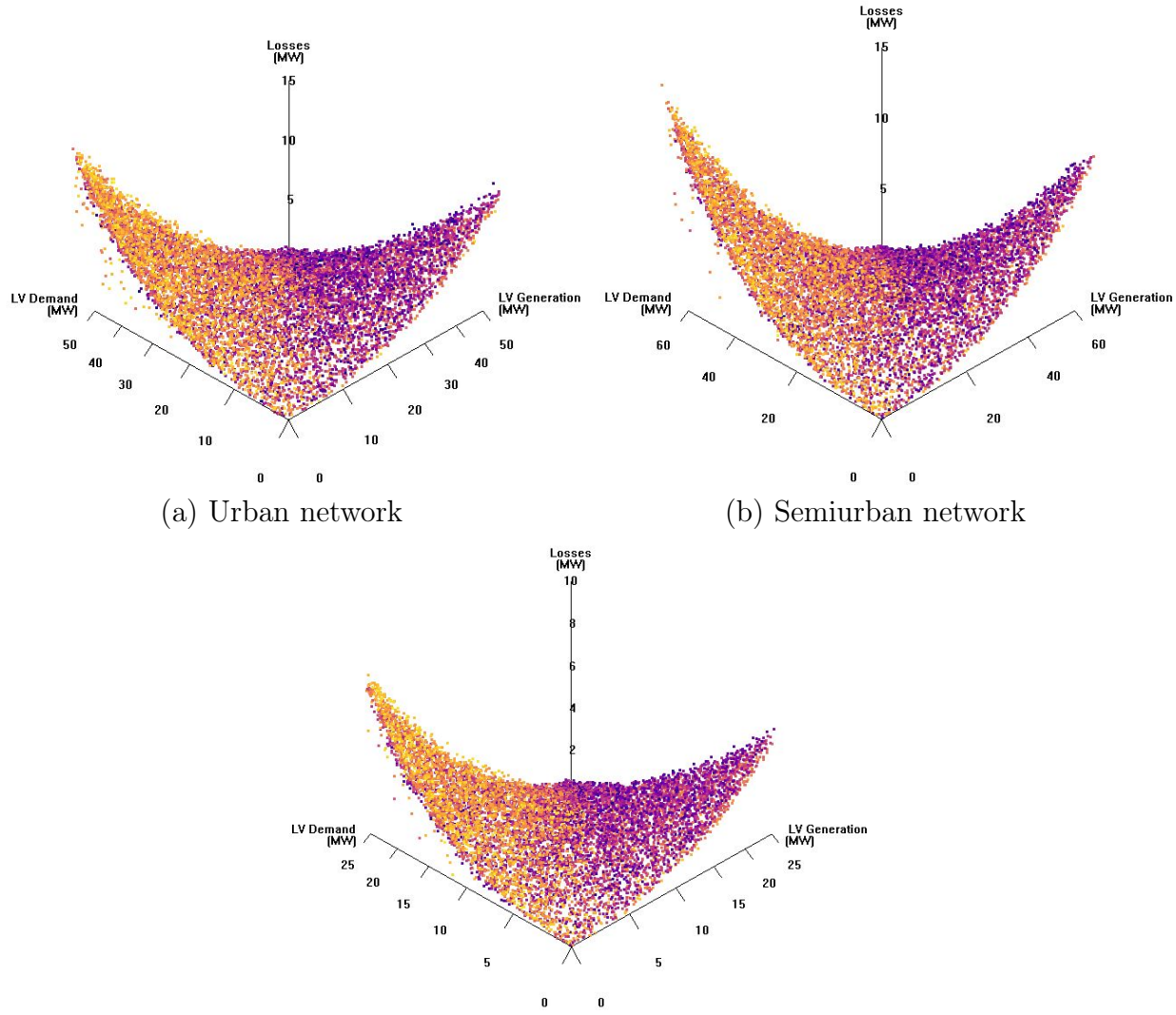

(a) Urban network

(b) Semiurban network

(c) Rural network

Figure 2-5: Resistive losses by network as a function of demand & generation with $\sigma = 0.2$
Location of points in (x,y) coordinates indicate demand and generation in low voltage (0.4 kV) feeders and color of points indicate net (demand − generation) in medium voltage (20 kV) feeders (brighter colors = higher net demand; darker colors = net generation). $D = 10,000$.

sistive losses. Similarly, as distributed generation (or power injections) within the low voltage portion of a distribution network begins to outstrip local demand, power flows reverse and are exported from low voltage, to satisfy demand in medium voltage, other low voltage feeders in the network, or even upstream to higher voltage levels. Reverse power flows associated with net generation in low voltage therefore drive quadratic resistive losses as well.[8] Finally, all else equal, losses fall as $|\text{demand} - \text{generation}| \to 0$. When local demand is satisfied primarily by behind the meter generation – or at least by distributed generation located not far away in the low voltage network – very little power flows across the distribution network. Thus, even cases with very high LV demand may produce very little network losses if LV generation supplies most or all of this demand.

2. Losses are less sensitive to changes in medium voltage demand and generation, although net (demand − generation) in MV has an interactive effect with LV (demand − generation) Examining the color of each point in Fig. 2-5, which correspond to net (demand − generation) in the MV feeders, reveals two additional insights.

First, variation in MV demand has a far smaller impact on losses than variation in low voltages.[9] There are two intuitive reasons. LV demand in each of the test networks is approximately an order of magnitude larger than in MV (see Table 2.1). Any percent change in MV demand therefore corresponds to an order of magnitude smaller change in absolute power consumption than an equivalent percent change in LV demand. In addition, with an order of magnitude greater voltage (20 kV in MV vs 0.4 kV in LV), losses per MVA-km of power flow are dramatically smaller. Recall that resistive losses scale inversely to the square of voltage. The fifty-fold increase in voltage between LV and MV thus results in a 2,500-fold decrease in losses per MVA of power flow across an equal distance of conductor.

Second, Fig. 2-5 reveals an interactive effect between net (demand − generation) in each

[8]Note that as these experiments are primarily concerned with the effect of demand and generation on network losses, power flow simulations are performed without constraining voltage angles to typical tolerance bounds (e.g. +/- 5 percent off nominal for most consumption buses). Voltage violations increase significantly as net generation reaches extreme levels, which may make these outcomes physically impossible without additional voltage regulation or reconfiguration of network components.

[9]Note that these experiments independently vary demand and generation in LV and MV across an equivalent range, from 0 to 100 percent of peak demand in each voltage level

voltage level. In cases with positive net demand in LV, an increase in net demand in MV drives greater losses, while an increase in net generation drives lower losses. The converse is apparent when aggregate LV demand and generation result in positive net generation; greater net demand in MV decreases losses in these cases, while greater net generation increases losses. The explanation for this interactive effect is also intuitive. When net demand in LV is high, flows across MV lines are already significant as these lines transfer power from the primary substation to customers in lower voltages. Adding additional net demand from MV customers further increases power flows across MV lines, driving up quadratic losses. At the same time, net generation in MV can supply LV customers in lieu of power imported from the primary substation, reducing power flows and losses in MV lines. Conversely, if net generation in LV is high, then higher net demand in MV consumes more of the power exported from LV and reduces power flows to the primary substation, while greater net generation in MV only adds to power flows across MV to the substation.

Third, if demand or generation are clustered within the network, then losses also increase in proportion to total LV (demand + generation): As Fig. 2-6 illustrates, increasing the concentration factor σ has the effect of tilting to parabolic surface formed by the points such that losses increase as the sum of both demand and generation in LV increases. This is perhaps most readily apparent by examining the lowest points where (demand − generation) = 0 in each sub-figure. At $\sigma = 0$, all points where (demand − generation) = 0 lie flat along the vertical axis origin; that is, any combination of demand and generation such that (demand − generation) = 0 results in virtually no losses.[10] However, as σ increases to 0.2 and 0.4, losses along the (demand − generation) = 0 axis increase as (demand + generation) increases. In cases where $\sigma > 0$, any given aggregate demand or generation will become distributed unevenly and clustered at individual LV feeders (and MV customers). As such, it becomes possible for demand in one area to be supplied by generation in another part of the network, even if net (demand − generation) = 0. This results in power flows and corresponding losses that increase as the sum of total demand and generation increases. In other words, when demand and generation are highly concentrated in specific pockets of the network, power

[10]Positive net demand in MV can still drive very small but non-zero losses.

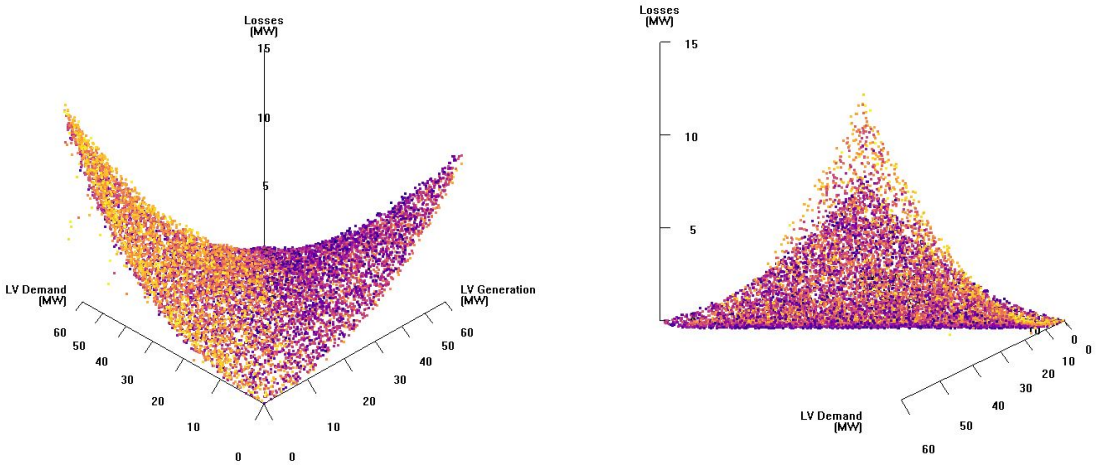

(a) $\sigma = 0.0$

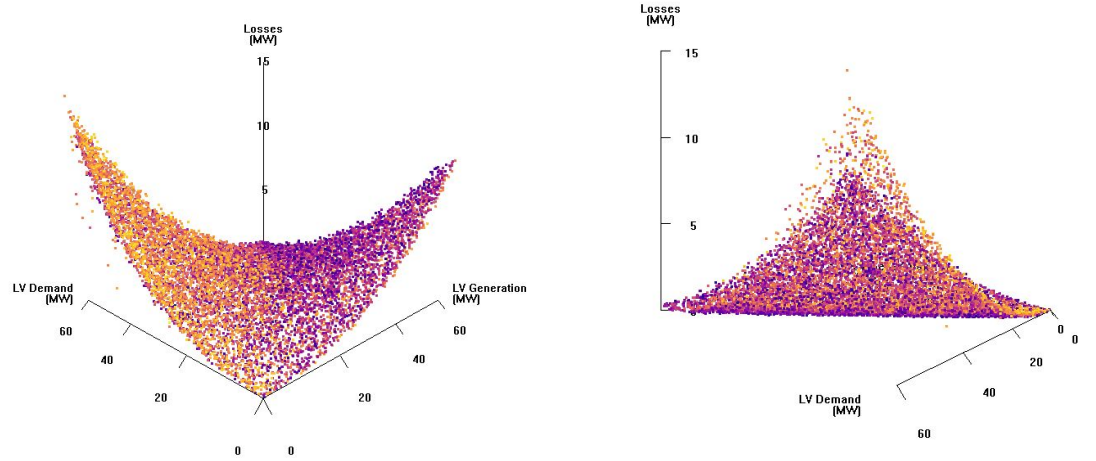

(a) $\sigma = 0.2$

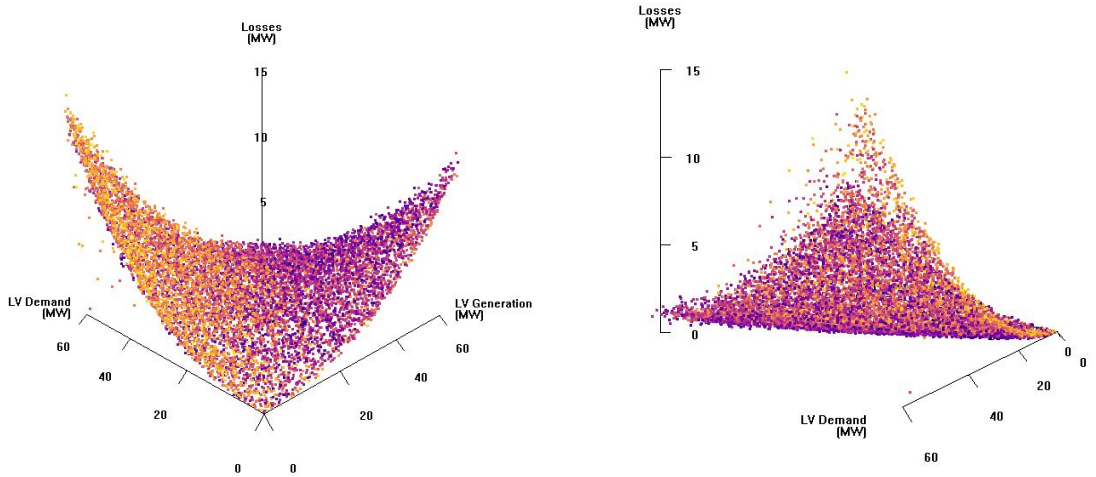

(a) $\sigma = 0.4$

Figure 2-6: Network losses by demand concentration factor σ as a function of demand & generation for the semiurban network
See note with Fig. 2-5 for explanation.

flows and resistive losses become larger as (demand + generation) $\rightarrow$ peak network capacity; losses become smaller when (demand + generation) $\rightarrow 0$.[11]

...

These insights indicate that aggregate distribution network losses can be represented as a multi-variate function of LV demand (D_{lv}), LV generation (G_{lv}), MV demand (D_{mv}), and MV generation (G_{mv}). Specifically, a linear regression function of the form:

$$\hat{\ell} = \hat{\alpha}(D_{lv} - G_{lv})^2 + \hat{\beta}(D_{lv} + G_{lv}) + \hat{\gamma}(D_{lv} - G_{lv})(D_{mv} - G_{mv}) \tag{2.3}$$

can accurately represent the behavior of losses across an entire large-scale distribution network.

Table 2.2 presents the predictive ability of several candidate regression models, using the rural network with $\sigma = 0.4$. This is the most difficult experiment for the regression to predict, due to the asymmetric and sparse nature of the rural network. Consistent with the visual exploration of the results above, the greatest portion of variation in losses is explained by the $(D_{lv} - G_{lv})^2$ term. Model 1, which contains only this term, predicts about 96 percent of the variation in losses in the rural network. Adding the interaction between variation in LV and MV, $(D_{lv} - G_{lv})(D_{mv} - G_{mv})$, (Model 2) improves the model by an additional increment, and the estimated coefficient for this term is statistically significant. Model 2 explains about 97 percent of variation in this experiment and residual standard error falls, indicating a closer fit between the model and actual losses. The effect of increased total demand and generation in LV, $(D_{lv} + G_{lv})$, added in Model 3, is also statistically significant for all experiments with $\sigma >= 0.2$, and improves the predictive power of the model in these cases (with higher R^2 and lower residual standard error). Model 3, which corresponds to the full regression model described in Eq. 2.3, predicts approximately 98 percent or more of the variation in losses across each network experiment, providing an accurate estimate of the effect of demand and generation on losses in each distribution network. Table 2.3 shows results of the full regression model (Model 3 above) for all experiments.

[11] It is likely that this effect is actually quadratic, but as we will see, it can be closely approximated by a

Table 2.2: Regression models - rural network with $\sigma = 0.4$

	Dependent variable:					
	Losses in MW (ℓ)					
	(1)	(2)	(3)	(4)	(5)	(6)
$(D_{lv} - G_{lv})^2$	0.008***	0.008***	0.007***	0.007***	0.007***	
	(0.00002)	(0.00001)	(0.00002)	(0.00002)	(0.00002)	
$(D_{lv} + G_{lv})$			0.006***	0.006***	0.005***	0.038***
			(0.0001)	(0.0001)	(0.0002)	(0.0004)
$(D_{lv} - G_{lv})(D_{mv} - G_{mv})$		0.012***	0.012***			
		(0.0002)	(0.0002)			
$(D_{mv} - G_{mv})$				0.059***		0.159***
				(0.002)		(0.008)
$(D_{mv} - G_{mv})^2$					0.023***	
					(0.001)	
$(D_{lv} - G_{lv})$						0.035***
						(0.001)
Adjusted R^2	0.957	0.970	0.977	0.966	0.964	0.560
Residual Std. Error	0.315	0.263	0.232	0.281	0.287	1.007
Degrees of Freedom	9999	9998	9997	9997	9997	9997
Note:	*p<0.1; **p<0.05; ***p<0.01					

Table 2.3: Regression results for estimated losses by network and demand concentration factor σ - Model 3 with LV-MV interaction term

Coefficients per MW								
Network	σ	$(D_{lv} - G_{lv})^2$	$(D_{lv} - G_{lv}) \times (D_{mv} - G_{mv})$	$(D_{lv} + G_{lv})$	Adj. R^2	Max Error	Mean Error	Residual Std. Error
Urban	0	0.0024***	0.0036***	0.0000	0.992	5.54	0.12	0.22
		(<0.0001)	(<0.0001)	(<0.0001)				
Urban	0.2	0.0025***	0.0036***	0.0014***	0.991	4.11	0.14	0.24
		(<0.0001)	(<0.0001)	(0.0001)				
Urban	0.4	0.0025***	0.0037***	0.0059***	0.987	8.28	0.19	0.31
		(<0.0001)	(<0.0001)	(0.0001)				
Rural	0	0.0068***	0.0109***	-0.0005	0.982	3.40	0.10	0.18
		(<0.0001)	(0.0001)	(0.0001)				
Rural	0.2	0.0068***	0.0112***	0.0011***	0.980	1.27	0.12	0.20
		(<0.0001)	(0.0001)	(0.0001)				
Rural	0.4	0.0070***	0.0121***	0.0062***	0.977	2.42	0.15	0.23
		(<0.0001)	(0.0002)	(0.0001)				
Semiurban	0	0.0019***	0.0026***	-0.0001	0.991	6.32	0.14	0.26
		(<0.0001)	(<0.0001)	(<0.0001)				
Semiurban	0.2	0.0019***	0.0027***	0.0016***	0.991	3.50	0.16	0.27
		(<0.0001)	(<0.0001)	(<0.0001)				
Semiurban	0.4	0.0019***	0.0029***	0.0063***	0.987	6.53	0.24	0.35
		(<0.0001)	(<0.0001)	(0.0001)				
Coefficients p.u. of Base Network Capacity								
Network	σ	$(D_{lv} - G_{lv})^2$	$(D_{lv} - G_{lv}) \times (D_{mv} - G_{mv})$	$(D_{lv} + G_{lv})$	Adj. R^2	Max Error	Mean Error	Residual Std. Error
Urban	0	0.1389***	0.0204***	0.0000	0.992	0.10	0.002	0.004
		(0.0002)	(0.0002)	(<0.0001)				
Urban	0.2	0.1399***	0.0206***	0.0014***	0.991	0.07	0.002	0.004
		(0.0002)	(0.0002)	(0.0001)				
Urban	0.4	0.1406***	0.0212***	0.0059***	0.987	0.15	0.003	0.005
		(0.0002)	(0.0003)	(0.0001)				
Rural	0	0.1714***	0.0328***	-0.0005	0.982	0.13	0.004	0.007
		(0.0003)	(0.0004)	(0.0001)				
Rural	0.2	0.1724***	0.0337***	0.0011***	0.980	0.05	0.005	0.008
		(0.0004)	(0.0004)	(0.0001)				
Rural	0.4	0.1763***	0.0362***	0.0062***	0.977	0.10	0.006	0.009
		(0.0004)	(0.0005)	(0.0001)				
Semiurban	0	0.1308***	0.0154***	-0.0001	0.991	0.09	0.002	0.004
		(0.0002)	(0.0002)	(<0.0001)				
Semiurban	0.2	0.1312***	0.0160***	0.0016***	0.991	0.05	0.002	0.004
		(0.0002)	(0.0002)	(<0.0001)				
Semiurban	0.4	0.1332***	0.0174***	0.0063***	0.987	0.10	0.003	0.005
		(0.0002)	(0.0003)	(0.0001)				

Note: *p<0.1; **p<0.05; ***p<0.01

Models 4 and 5 present two alternative functional forms for the effect of demand and generation in the MV portion of the network. As Table 2.2 indicates, both models are inferior to Model 3 which employs the interactive term between each voltage level.

However, representing interaction terms in a linear programming optimization modeling framework (as discussed Chapter 3) involves a computationally intensive piecewise linearization of the terms. Model 4 therefore includes a linear parameter term for net demand in MV, $(D_{mv} - G_{mv})$, in place of the interaction term. Figure 2-7 visually depicts the difference in the regression fits created by Models 3 and 4. Each surface shown depicts the predicted effect of variation in LV demand and generation conditional on a discrete combination of MV demand and generation. As the two sub-figures illustrate, the interactive term effectively rotates the LV conditional regression plane around the $(D_{lv} - G_{lv}) = 0$ axis, while the linear term simply shifts the LV conditional regression plane up and down. Model 3 accurately captures the interaction between power flows in LV and MV with minimal error across the entire range of variation in LV demand and generation. The linear term in Model 4, in contrast, begins to produce greater errors for extreme values of net LV demand or net LV generation. Model 4 performs well however across the bulk of the range of variation in LV demand and generation (e.g., more intermediate values of net demand or net generation).

Indeed, across all network experiments, Model 4 explains at least 96.6 percent of variation in losses with only slightly higher mean errors than Model 3. Table 2.4 presents regression results for this model. Fig. 2-8 illustrates the small increase in the residual errors from Model 4 as compared to Model 3. The difference in predicted losses is also very small between the two models (see Fig. 2-9). Model 4 also performs better (greater R^2 and smaller residual errors) than Model 5 with a quadratic net MV (demand − generation) term. I therefore consider Model 4 to be a suitable alternative for use in a linear programming context.

Unfortunately, as Table 2.2 indicates (and as visual inspection of the results quickly confirms), replacing the quadratic LV term, $(D_{lv} - G_{lv})^2$, with a linear term, $(D_{lv} - G_{lv})$, as in Model 6, severely degrades the predictive ability of the model and is not a suitable

linear function.

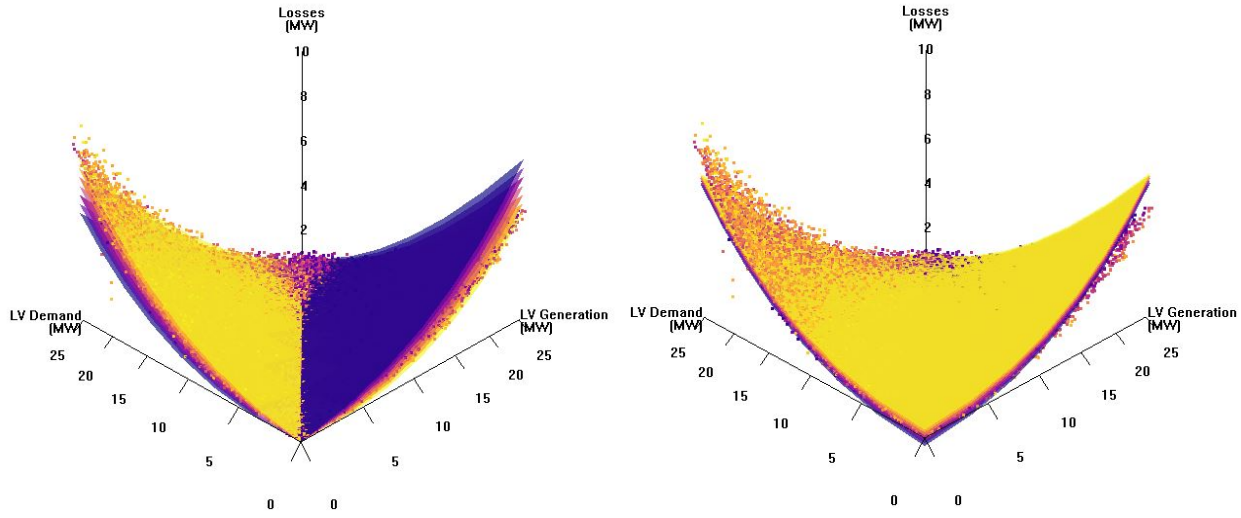

(a) Model 3 with interaction term

(b) Model 4 with linear term

Figure 2-7: Comparison of predicted losses for two alternative regression models for the rural network with $\sigma = 0.4$

Location of points in horizontal (x,y) coordinates indicate demand and generation in low voltage (0.4 kV) feeders and color of points indicate net (demand − generation) in medium voltage (20 kV) feeders (brighter colors = higher net demand; darker colors = net generation). Surfaces represent predicted losses as a function of variation in LV demand and generation conditional on a discrete combination of MV demand and generation.[12] Coloring of each surface indicates net demand using the same color scheme as the points. $D = 10,000$.

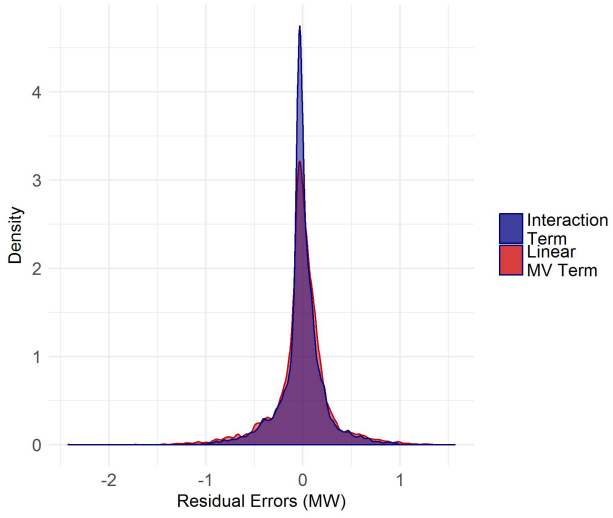

Figure 2-8: Comparison of residual errors for Models 3 and 4 for rural network with $\sigma = 0.4$

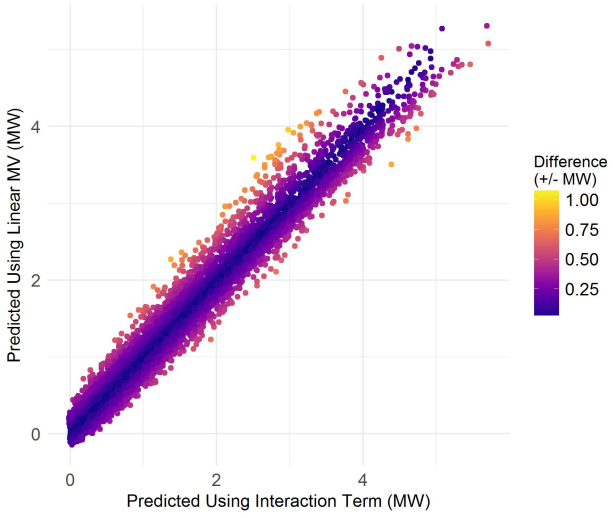

Figure 2-9: Comparison of predicted losses for Models 3 and 4 for rural network with $\sigma = 0.4$

alternative. This LV quadratic term is essential, and it must therefore be approximated in a linear programming context with an accurate piecewise linearization.

Table 2.4: Regression results for estimated losses by network and concentration factor σ - Model 4 with linear MV term

Coefficients per MW								
Network	σ	$(D_{lv} - G_{lv})^2$	$(D_{mv} - G_{mv})$	$(D_{lv} + G_{lv})$	Adj. R^2	Max Error	Mean Error	Residual Std. Error
Urban	0	0.0025***	0.0353***	0.0000	0.985	5.10	0.18	0.30
		(<0.0001)	(0.0012)	(<0.0001)				
Urban	0.2	0.0025***	0.0366***	0.0015***	0.985	3.79	0.19	0.32
		(<0.0001)	(0.0013)	(0.0001)				
Urban	0.4	0.0025***	0.0347***	0.0059***	0.981	7.49	0.24	0.38
		(<0.0001)	(0.0015)	(0.0001)				
Rural	0	0.0070***	0.0562***	-0.0004	0.971	3.40	2.99	0.23
		(<0.0001)	(0.0018)	(0.0001)				
Rural	0.2	0.0070***	0.0561***	0.0013***	0.970	1.33	0.15	0.25
		(<0.0001)	(0.0019)	(0.0001)				
Rural	0.4	0.0072***	0.0590***	0.0063***	0.966	2.04	0.18	0.28
		(<0.0001)	(0.0021)	(0.0001)				
Semiurban	0	0.0020***	0.0346***	0.0000	0.987	5.81	0.18	0.31
		(<0.0001)	(0.0012)	(<0.0001)				
Semiurban	0.2	0.0020***	0.0348***	0.0017***	0.983	3.26	0.20	0.32
		(<0.0001)	(0.0012)	(<0.0001)				
Semiurban	0.4	0.0025***	0.0337***	0.0063***	0.983	6.66	0.27	0.41
		(<0.0001)	(0.0016)	(0.0001)				
Coefficients p.u. of Network Peak Capacity								
Network	σ	$(D_{lv} - G_{lv})^2$	$(D_{mv} - G_{mv})$	$(D_{lv} + G_{lv})$	Adj. R^2	Max Error	Mean Error	Residual Std. Error
Urban	0	0.1428***	0.0035***	0.0000	0.985	0.09	0.003	0.005
		(0.0002)	(0.0001)	(0.0001)				
Urban	0.2	0.1441***	0.0037***	0.0015***	0.985	0.07	0.003	0.006
		(0.0002)	(0.0001)	(0.0001)				
Urban	0.4	0.1443***	0.0035***	0.0059***	0.981	0.13	0.004	0.007
		(0.0003)	(0.0002)	(0.0001)				
Rural	0	0.1777***	0.0067***	-0.0004	0.971	0.12	0.004	0.009
		(0.0004)	(0.0002)	(0.0001)				
Rural	0.2	0.1782***	0.0066***	0.0013***	0.970	0.05	0.006	0.010
		(0.0004)	(0.0002)	(0.0001)				
Rural	0.4	0.1832***	0.0070***	0.0063***	0.966	0.08	0.007	0.011
		(0.0005)	(0.0003)	(0.0001)				
Semiurban	0	0.1337***	0.0030***	0.0000	0.987	0.08	0.003	0.005
		(0.0002)	(0.0001)	(0.0001)				
Semiurban	0.2	0.1339***	0.0031***	0.0017***	0.987	0.05	0.003	0.005
		(0.0002)	(0.0001)	(0.0001)				
Semiurban	0.4	0.1365***	0.0033***	0.0063***	0.983	0.10	0.004	0.006
		(0.0003)	(0.0001)	(0.0001)				
Note:				*p<0.1; **p<0.05; ***p<0.01				

2.3 Modeling Distribution Network Expansion and Deferral: 'Non-Wires Alternatives'

Traditionally, distribution network utilities have planned and dimensioned distribution networks to accommodate any potential aggregate or coincident demand that might occur over the next several years (Eurelectric, 2013). In particular, distribution networks have been designed to ensure power flows during periods of highest aggregate consumption (or 'coincident peak' periods) do not exceed physical and engineering constraints, including thermal limits of transformers and conductors designed to prevent damage and premature failure of these costly assets, or node voltage constraints established by relevant standards designed to prevent damage to or ensure efficient operation of electrical devices – e.g., the ANSI C84.1 standard for North America (National Electrical Manufacturers Association, 2011), which requires service voltages to remain within ±5 percent of nominal, and the European Standard EN 50160 (CEER, 2016), which requires voltage to remain within ±10 of nominal. Many distribution assets, including transformers and distribution circuits, are long-lived, capital intensive assets that exhibit economies of scale. As such, distribution network investments are planned in anticipation of future peak demands, and the planning horizon may extend five to ten years into the future. Furthermore, unlike system operators at the transmission level, distribution utilities have historically had only limited operational recourse to manage distribution network constraints.[13] Thermal and voltage limits may be exceeded for brief periods, but prolonged violations will result in damage to or even failure of network components or end users' property. Facing such conditions, utilities would typically be forced to resort to shedding load by disconnecting circuits until the problem is resolved, a costly and disruptive course of action that utilities generally seek to avoid at nearly any cost. For all of these reasons,[14] distribution network components are commonly sized not only to meet an

[13]Conventional options include changing settings on transformer tap changers to adjust voltage, reconfiguring any meshed portions of networks the network by opening or closing circuits to change power flows, or operating shunt capacitors and voltage regulators to provide reactive power compensation or voltage support.

[14]Widely employed cost of service-based remuneration of distribution utilities also establishes incentives for the companies to invest heavily in capital assets, including distribution network components, whenever such investments can be approved by the regulator. For more, see Jenkins and Pérez-Arriaga (2017)

expectation of possible future peak demand, but also to provide some additional 'headroom' or 'network capacity margin' to ensure some margin of error above anticipated peaks.[15]

These practices ensure reliable electricity supply during coincident peak demand periods, but also result in poorly utilized network assets. Electricity demand reaches peak levels only rarely throughout the year, which means that the vast majority of the time, distribution networks are operating at a fraction of their rated capacity. As an example, Fig. 2-10 shows the load duration curve – or rank-ordered levels of demand from highest to lowest – for a 4.16 kV distribution feeder in Buffalo, New York for January 1, 2015 to March 18, 2018.[16] This feeder is one of the more heavily loaded in the entire New York service territory of National Grid and is expected to require an upgrade to meet peak demand growth within the next 10 years. Yet as Fig. 2-10 illustrates, demand reaches high levels in an exceedingly few hours of the year: demand on the feeder exceeds 90 percent of its rated capacity only 12 hours over this three-plus year period, or 0.04 percent of hours. Indeed, demand exceeds 75 percent of the line's thermal capacity only 1.1 percent of the hours over this period.

Thus, if distribution network utilities could reliably depend on a reduction in demand – or the ability to supply that demand with local generation or storage – when needed during only a handful of peak demand hours, it would be possible to defer or even permanently avoid physical network upgrades. Depending on the cost of procuring available demand reduction or distributed generation or storage in the correct portion of the network, distribution utilities may be able to cost-effectively substitute the operation of DERs for network upgrades, lowering the cost of distribution networks and thus the delivered cost of electricity.

Increasingly, distribution utilities must also plan their networks to accommodate growing penetrations of distributed generation (DG), chiefly rooftop solar and, in some regions, larger wind and solar farms connected to distribution networks at medium voltage. High levels of DG on distribution circuits can cause power flows to reverse and increase voltage along a feeder, potentially violating voltage constraints or causing congestions due to thermal limits,

[15] In this way, network capacity margin can be considered analogous to the generation reserve margins.

[16] This data corresponds to feeder ID 36 01 2869 connected to the Buffalo Substation 028 and was accessed via the National Grid System Data Portal for New York state, see National Grid (2018)

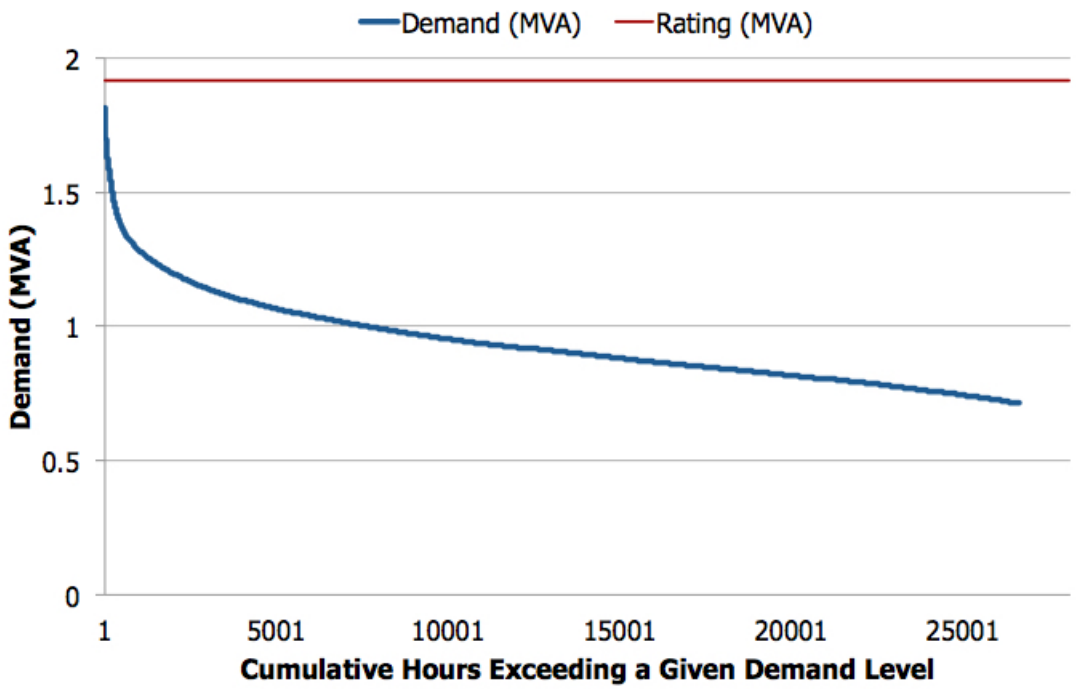

Figure 2-10: Load duration curve for example 4.16 kV feeder in Buffalo, New York, January 1, 2015 to March 18, 2018

among other challenges for integrating DG (see Eurelectric (2013); Horowitz et al. (2018)). The so-called 'hosting capacity' of distribution networks may also be increased without new network investment by operating DERs at the right times and the right locations to curtail real power output, provide reactive power compensation (e.g., via 'smart' inverters), or absorb and store local generation in order to avoid network constraints.

The growth of DERs and the potential for the use of 'distribution management systems' or 'active network management' strategies has been driving increased academic and industry research into effective DER control strategies (Zhao et al., 2014; Li et al., 2017; Vallés Rodríguez, 2017; Robertson et al., 2017) and pricing mechanisms (Caramanis et al., 2016). Regulatory pressure has also been increasing for distribution utilities to plan their networks in a more integrated fashion that thoroughly explores 'non-wires alternatives' to network upgrades, such as incentivizing or contracting with demand response or DERs (Zibelman et al., 2014, 2015; California Public Utility Commission, 2015).

In this section, I present a new method to simulate the optimal quantity of net demand reduction – achieved either by reducing consumption or by supplying power locally with DG or storage – needed to accommodate a given increment of aggregate peak demand across a large-scale distribution network. Specifically, I use a series of AC optimal power flow simulations to find the minimal reduction in aggregate demand required to render all power flows feasible during the period of highest aggregate consumption, including respecting all node voltage limits and branch thermal ratings. I demonstrate this method on each of the three European test networks introduced in Section 2.1 under a variety of conditions. I then derive the functional relationship between aggregate peak demand growth and net demand reduction required to accommodate that level of growth without network upgrades.

Note that my focus here is on understanding these aggregate relationships at the network-wide level, rather than a more common feeder-level engineering analysis. The goal is to derive a parsimonious functional form to describe the high level potential for optimal siting and operation of DERs to meet peak demand in lieu of network upgrades. This function will be useful in the system-wide planning model described in Chapter 3. This method can also provide insight on the potential locational value of DERs at an aggregate level, including the overall size of the potential market opportunity for 'non-wires' alternatives to network upgrades and the marginal changes in that opportunity as demand growth increases and/or DERs saturate the opportunity. Implementing any non-wires alternatives to network upgrades would require additional engineering study and effective strategies to procure and control necessary flexibility from DERs at a level of reliability comparable to network assets. Those challenges are important, but beyond the scope of this work.

2.3.1 Experimental Method: AC Optimal Power Flow Simulations with Increasing Peak Demand

An AC optimal power flow (AC OPF) model is a non-linear optimization problem in which energy supply costs are minimized subject to the full set of AC power flow constraints (including demand balance, node voltage magnitude, branch current rating limits, and voltage

angle difference limits across branches) as well as constraints on the capabilities of available generation (or storage) and mechanical equipment such as transformer tap changers. The AC OPF problem was first formulated in the 1960s by J.L. Carpentier at Electricite de France (Carpentier, 1962), and yet it remains a challenging optimization problem given its nonlinear nature and the large size of realistic problems. For sequential reviews of the development of AC OPF solution methods, see: Carpentier (1979); Huneault and Galiana (1991); and Cain et al. (2012). The AC OPF problem – and its various decompositions, simplifications, and linearizations – features prominently in power system planning and operations, including transmission network expansion planning, power system dispatch, and distribution network planning and operations.

In this case, I employ the AC OPF modeling framework provided by the Matpower suite (Zimmerman et al., 2011; Zimmerman and Murillo-Sánchez, 2016) to model large-scale distribution networks and find the minimum amount of reduction in net demand – modeled as either demand curtailment or self generation – necessary to keep all power flows feasible despite growth in aggregate peak demand above the network's designed capacity. Each distribution network is modeled independently from the rest of the system (e.g., upstream transmission or generation) with the primary substation as the main source of power for customers in the network. Customers can curtail demand (or generate their own power) at a marginal cost set to be much greater than the cost of imported power at the substation. This ensures that the least cost OPF solution only involves demand reduction or self generation when network constraints prevent import of power from the substation. Formulated in this manner, the AC OPF problem identifies the minimum quantity of net demand reduction required to avoid violating network constraints while satisfying all remaining demand.

I perform these simulations with steadily increasing coincident peak demand and under different assumptions about the distribution of demand across the network and the marginal cost of reducing net demand as part of the AC OPF dispatch solution. The model is solved for a single static period representing the expected future coincident peak demand, or the 'planning peak,' to which network assets are to be sized.

Algorithm 2 describes the experimental method in detail. Just as with the power flow experiments used to model losses in Section 2.2, the process begins with loading input files describing each bus and branch in the network in Matpower case format and assigning each network user connected at low voltage (LV, or 0.4 kV) to a zone, where a zone is defined as all nodes connected to the set of radial low voltage feeders issuing from a given medium-to-low voltage (20 kV/0.4 kV) transformer. See Figures 2-1 to 2-4 for a depiction of the zones in each of the three European test networks.

Each simulation corresponds to a set of incremental increases in mean coincident peak demand across the network. For each increase in demand, the following steps are performed:

1. *Assign concentration of coincident peak demand across LV zones and MV users:* Each low voltage zone and each medium voltage (MV) user are assigned independent 'concentration factors' for their increase in demand during the coincident peak, indicating how each LV zone or MV user's p.u. change in demand differs from the increase in the network-wide mean coincident peak demand for the current simulation. These concentration factors are drawn from a truncated normal distribution with a standard deviation σ specified for each experiment. The distribution is truncated such that no LV zone or MV user has an extreme value less than -1, meaning that demand in that zone cannot decrease by more than the mean increase in coincident peak demand for that simulation. A σ of 0 corresponds to a uniform distribution of demand across the network at the mean coincident peak increase, and as σ increases, the concentration of aggregate demand growth in specific portions of the network increases. In this manner, demand can be concentrated in specific LV feeders or at specific MV network users to simulate the irregular distribution of demand in real networks.

2. *Assign LV demand by user:* Zonal aggregate peak demand in each LV zone is then the product of aggregate peak demand for all network users in that zone times 1 + the product of the zonal concentration factor and the increase in mean coincident peak demand for this simulation. Aggregate demand in each LV zone is assigned to each individual user in proportion to that user's share of the aggregate peak demand in that

Algorithm 2: Experimental method using AC optimal power flow simulations to determine the minimum quantity of net demand reduction required to accommodate increased coincident peak demand without network upgrade

Data:

- Matrix of N network nodes (one per electricity user and high and low voltage sides of each transformer) in Matpower 'mpc.bus' format
- Matrix of B network branches (one per line segment and one per transformer) in Matpower 'mpc.branch' format
- Set of incremental increases in coincident peak demand $\mathcal{D}$ (p.u. of network rated capacity) to perform AC OPF simulations
- Concentration factor σ, describing the standard deviation of demand in each zone as p.u. of mean coincident peak demand $d \in \mathcal{D}$
- Binary variable x indicating whether marginal cost of net demand reduction is constant or stepwise increasing

Result: Matrix of results for each AC OPF simulation

begin

Load network and branch data;
Group all LV network users into $\mathcal{Z}$ zones, where each user downstream from a given MV-LV transformer is considered a zone;
foreach $d \in \mathcal{D}$ **do**
foreach $z \in \mathcal{Z}$ **do**
Zonal p.u. demand $d_z = 1 + d \times c_z$ where c_z are random concentration factors i.i.d. $\sim N(1.0, \sigma)$ truncated s.t. $c \geq -1$;
foreach *LV user* $i \in$ *zone* z **do**
User demand $d_i = p_i / (\sum_{j \in z} p_j) \times d_z$ where p is a user's peak demand
end
end
foreach *MV user* $m \in \mathcal{M}$ **do**
User demand $d_m = p_m \times (1 + d \times c_m)$, where c_m is a random demand concentration factor $\sim N(1.0, \sigma)$ truncated s.t. $c \geq -1$
end
if $x = 1$ **then**
Randomly assign p.u. share of demand falling on each of three segments of piecewise marginal cost function for each user $\in \mathcal{G}$
end
Run Matpower AC OPF simulation;
Record results: success/failure of OPF solution; total real & reactive power demand by voltage level; total net real & reactive demand reduction by voltage level; network losses;
end

end

zone.

3. *Assign MV demand by user:* Demand for each MV network user is the product of that user's peak demand times 1 + the product of the user's concentration factor and the mean increase in coincident peak demand for this simulation.

4. *Assign segments of stepwise increasing marginal cost for active users:* If the marginal cost of net demand reduction for active network users is to be modeled as a stepwise increasing marginal cost ($x = 1$), then for each user, their total demand is segmented into three segments, with the break points between segments randomly determined for each user to create heterogeneity. Else, the marginal cost of net demand reduction is treated as constant and equal for all network users.

A Matpower AC optimal power flow simulation is then run to find the minimum amount of aggregate net demand reduction required to render the OPF feasible at least cost.[17] As the AC OPF problem is nonlinear and solution methods use various heuristic approaches, there is no guarantee that the OPF model will find a stable, feasible solution within a pre-specified limit on the number of solution iterations permitted, nor that the solution found will be a global rather than local optima. Therefore, I perform each AC OPF simulation several times from different starting positions[18] and record results for the best solution found for processing. If no solution is found, the case is recorded as a failed solution.

Note that this same experimental method can be used to identify the minimum quantity of aggregate curtailment (or storage) of variable distributed generation sources such as wind

[17]Note that in these experiments, active network users are assumed to reduce net demand at a fixed power factor equal to their consumption power factor, as specified in the bus input files – e.g., they are modeled as 'PQ' nodes with a constant power factor. Modeling active users as 'PQ' nodes is consistent with simulating net demand reductions achieved by demand curtailment or distributed generation operating at a fixed power factor, as is common in most cases today. Section 2.3.7 discusses the possible implications of instead modeling active users as 'PV' nodes, as would be appropriate where active users hosts a distributed generator or storage device with a smart inverter capable of reactive power compensation.

[18]For each experiment, I specify the number of starting points to use, $n \in [1 : N]$, s.t. for $n = 1$, reduction in net real power demand is set to zero for all active network users; for $n = 2$, reduction in net real power demand is set to 1.0 p.u. of user's demand for all active network users; and for $n > 2$, reduction in net real power demand is set to random value $\sim U(0, 1.0)$ for all active network users. Reactive power for each user is then determined based on the user's consumption power factor $\forall\ n$.

or solar PV required to make network power flows feasible during periods of coincident peak injections and reverse power flows. For any specified initial distribution of generation and demand across network users, the AC OPF method will seek the least cost set of curtailments required to satisfy all network constraints. In this manner, one could explore the potential for active network strategies to accommodate greater penetration of DG without network upgrades at the scale of an entire distribution network area.

However, in this thesis, I focus only on the potential for avoidance of distribution upgrades driven by increases in coincident peak consumption. Due to the tradeoffs between economies of unit scale and locational value described in Chapter 1.1, DERs such as solar PV or wind turbines capable of deployment at multiple scales would only occur in a least-cost system context in cases where locational value is positive and exceeds incremental unit costs relative to larger scale wind or solar systems. In cases where distributed wind or solar penetration is high enough to *cause* rather than defer distribution network upgrades, any positive locational value is all but certainly exhausted or even negative. In other words, while DERs could avoid network upgrades caused by large shares of variable distributed wind or solar injections, this amounts to amelioration of the costs posed by high shares of variable DG, not a positive locational value that would justify DER deployment in a least-cost system planning context. However, in future work, I intend to explore the potential cost of policy and regulatory incentives that drive penetration of distributed wind or solar well above levels consistent with a least-cost system outcome. In this context, I will also determine the minimum generation curtailment that could reduce network costs associated with such high DG penetration levels.

The following sections summarize results for different experimental set-ups using the method outlined in Algorithm 2 above. I perform each experiment for all three European test networks described in Section 2.1.

2.3.2 Experiment: the Effect of Demand Concentration

Experimental setup: In this experiment, I explore the impacts of changes in the concentration of demand within each distribution network. For each network – urban, semiurban, and rural

– I perform three individual experiments using the following parameters and the general method in Algorithm 2:

- $\mathcal{D} = [0.00 : 0.01 : 0.20]$. Coincident peak demand, d, increases from 0 to 0.2 p.u. (20 percent) above the base network capacity[19] in increments of 0.01 p.u. (one percent).

- $\sigma = \{0, 0.2, 0.4\}$. I increase the standard deviation of demand growth across each LV zone and MV customer, σ, from 0.0 to 0.2 and 0.4. As incremental demand growth in each simulation is randomly distributed from a normal distribution $\sim N(1.0, \sigma)$, approximately 68 percent of LV zones and MV customers will experience incremental demand growth within a range of up to σ p.u. above or below the mean incremental growth level $d \in \mathcal{D}$; an additional 27 percent of zones/MV customers see incremental demand growth $\pm\ \sigma$ to 2σ p.u. above or below the mean; and 4.7 percent of vary between $\pm\ 2\sigma$ to 3σ around d. At $\sigma = 0$, demand is thus evenly distributed across the network with every feeder and zone increasing by the mean coincident peak demand increase d. For any $\sigma > 0$, a portion of zones/MV customers begin to experience demand growth a good deal above or below the mean level. This creates 'pockets' where demand grows rapidly, and other areas where growth proceeds at a lower pace, as is to be expected in real-world systems. Since the distribution of demand is randomized in each simulation, for each case with $\sigma > 0$, I perform four different iterations of the experiment, to generate a range of possible outcomes.

- $x = 0$. The marginal cost of net demand reduction is constant and uniform across all active users ($x = 0$). This setup can be considered consistent with a case where the same DER with constant marginal cost of production (such as a fuel cell or energy storage device) is

[19]Base network capacity is defined as the total coincident peak demand that can be accommodated by a given network without either network reinforcements or net demand reductions required to render power flows feasible across all network components. Note that the Urban and Semiurban networks are apparently built with some 'headroom' and do not experience significant net demand reductions until peak demand reaches 10 percent above the values specified in Prettico et al. (2016). I therefore reset the base network capacity in these two networks to 1.1 times the values specified in Table 2.1 for purposes of all experiments in Section 2.3

available for installation by any customer in the network and is required to operate at a fixed power factor. Less restrictive assumptions are explored in subsequent experiments.

Results: Fig. 2-11 depicts the overall results by network for this experiment with increasing concentration factors σ (labeled 'Sigma' on the figure). Each point corresponds to results from an individual AC OPF solution.[20] A regression function approximating each set of results is also presented, plotted as a dashed line, with the regression coefficients and results describing the predictive ability of the function also printed. Coefficients are in percent of original coincident peak demand, $d = 0$, for each network. Examining these results yields several initial insights.

1. *Across all networks, the total net demand reduction, y, required to accommodate an increase in coincident peak demand, d, is non-linear and increasing and can be closely approximated with a linear regression function of the form:*

$$\hat{y}(d) = \hat{\alpha}d + \hat{\beta}d^2 \tag{2.4}$$

   As Fig. 2-11 illustrates, this function explains nearly 100 percent of the variance in results across all cases. Mean and maximum prediction errors tend to increase modestly as σ increases, but this regression function remains quite accurate across all demand concentration factors.

2. *Across low to moderate demand growth, a one percent increases in coincident peak demand across a large-scale distribution network can be accommodated with a less than one percent increase in total net demand reduction.* Given the functional form described above, the marginal reduction in net demand required to accommodate a marginal increment in coincident peak demand takes the form $\hat{\alpha} + 2\hat{\beta}d$. At levels of coincident peak demand growth $d < \frac{1-\hat{\alpha}}{2\hat{\beta}}$, it is technically possible for a marginal increase in demand of x to be accommodated by marginal reductions in net demand less than x. In other words, across this range of demand growth, there are potential opportunities for

[20] A small number of simulations that failed to converge are discarded.

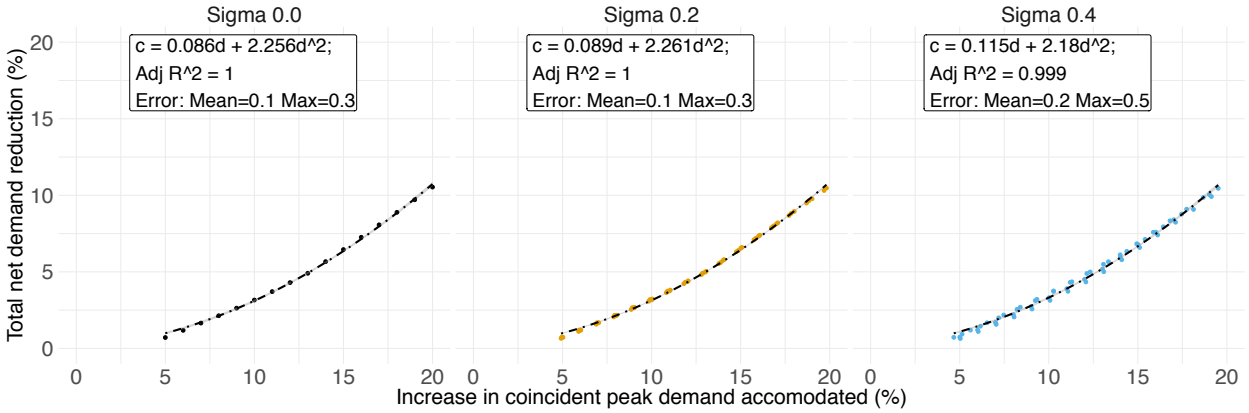

(a) Rural network

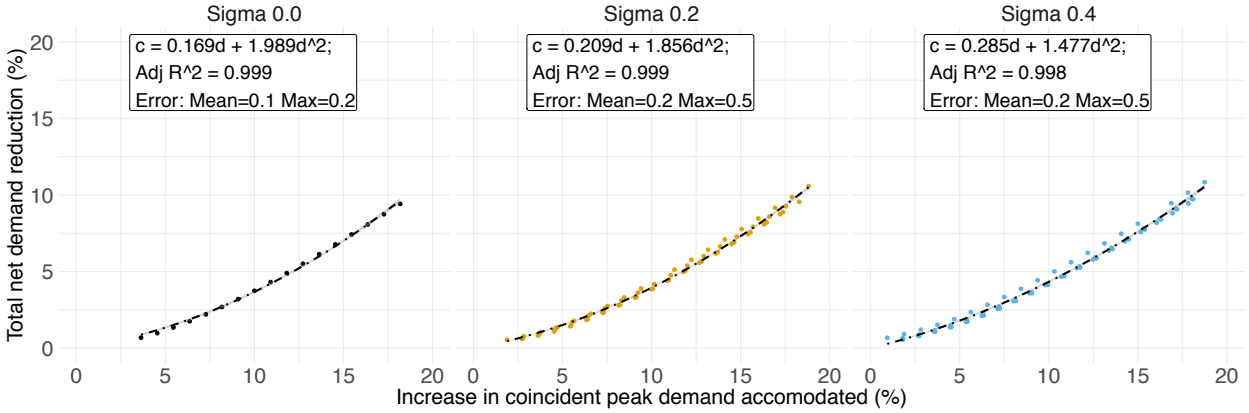

(b) Semiurban network

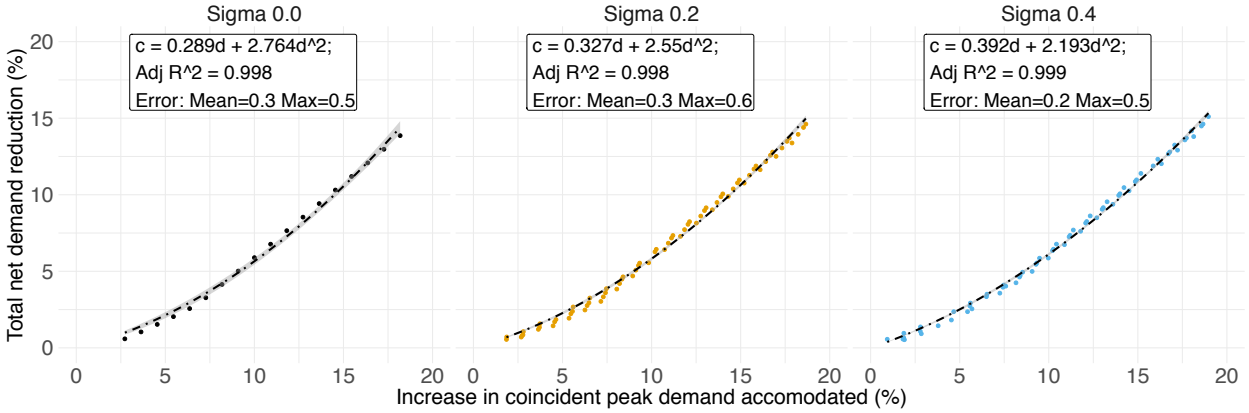

(c) Urban network

Figure 2-11: Aggregate reduction in net demand required to accommodate up to 20 percent coincident peak demand growth by network and demand concentration factor σ
All values are in percent of base network capacity.

one MW of optimally sited flexible demand and DERs to accommodate proportionately more than one MW of peak demand without requiring investments in distribution network upgrades. Beyond this point, any marginal increase in coincident peak demand must be either entirely supplied locally with DG or storage or left unsatisfied (e.g., curtailed).

Based on the regression results presented in Fig. 2-11 and with $\sigma = 0$, Fig. 2-12 shows the marginal rate of net demand reduction required as coincident peak demand increases. This can be considered the marginal rate of substitution between net demand reduction and network upgrades per unit of coincident peak demand growth. As can be seen in Fig. 2-12, the predicted crossover point where an increase in peak demand begins to require a proportionate decrease in net demand is 12.9 percent for the urban network. It is even higher for the semiurban and rural networks, which do not reach a marginal rate of demand reduction >1.0 until 20.9 and 20.3 percent demand growth, respectively (at the highest end of the range of demand growth modeled here). As is common in European networks, the high density of demand in urban networks typically results in higher equipment loading factors, particularly MV cables and transformers (Eurelectric, 2013). Semiurban and rural networks are sparser, with lower load density and longer lines and typically have lower loading factors. The three test networks employed in these experiments match these general characteristics (see Table 2.1). As such, demand growth in the urban network results in more congestion than its sparser counterparts. Further experiments with a larger number of networks would be needed to confirm that this results holds generally across denser/sparser network topologies.

3. *Net demand reduction is primarily driven by thermal constraints on branches and MV-LV transformers.* Fig. 2-13 depicts the location and magnitude of reductions in real power demand required to keep network power flows feasible at 5, 10, 15 and 20 percent growth in coincident peak demand. Distribution lines and transformers or substations at their maximum MVA rating are depicted in red. As this figure illustrates, net demand reductions are driven primarily by branch and transformer thermal ratings,

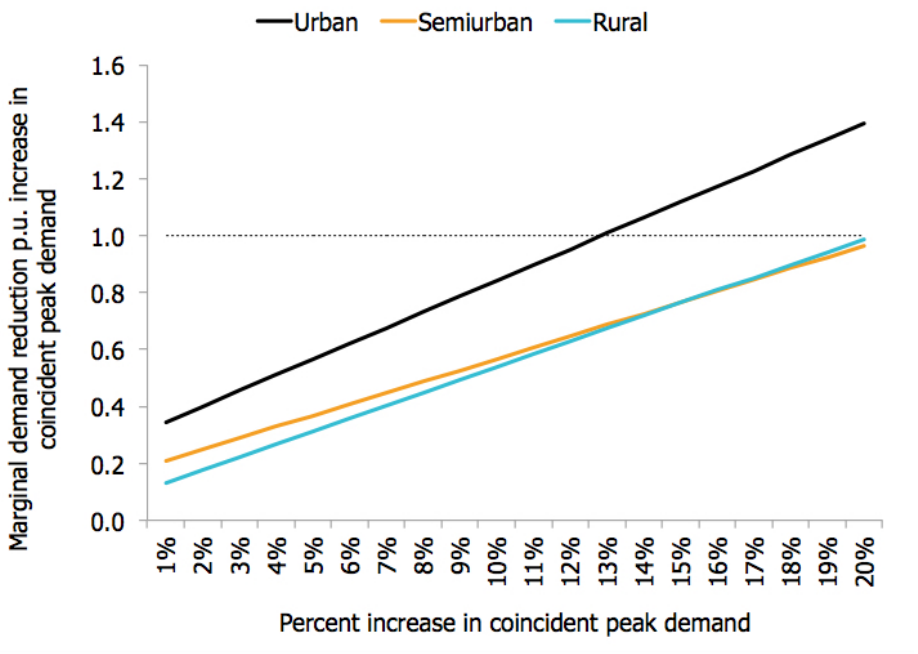

Figure 2-12: Marginal rate of net demand reduction required per unit increase in peak demand as a function of coincident peak demand growth with $\sigma = 0$

rather than node voltage limits.[21]

4. *With constant and equal marginal costs of net demand reduction across all users, the ideal location for demand reduction is at the end of LV feeders at locations experiencing the greatest marginal losses.* As coincident peak demand grows and various network components reach their maximum thermal rating, congestion prevents further import of power to serve downstream customers. The OPF solution then begins to reduce demand at the end of LV feeders in order to meet node demand balance constraints

[21] These networks are built to comply with a ±10 percent limit on voltage magnitude deviations from the nominal, as per European standards. See 2.3.3 for more on the impact of voltage limits. Note also that the minor role played by voltage limits in these cases stands in contrast to studies examining network constraint violations caused by increased DG penetration, such as solar PV (see e.g, Schmalensee et al. (2015); Horowitz et al. (2018)). In these cases, injections increase voltages in ways that voltage regulation devices such as tap changers were not originally configured to handle. Thus, voltage violations are the most common drivers of network upgrades to increase 'hosting capacity' for distributed solar PV or wind. In contrast, existing voltage protections are designed to accommodate peak demand and appear to provide sufficient flexibility to maintain node voltages above the minimum limit at nearly all nodes. A handful of nodes are at voltage limits in some results, but this is much less common than congestions due to branch or transformer thermal ratings.

without violating the thermal ratings of congested lines or transformers. Customers at the end of LV feeders are curtailed first because the effect of a kW of demand reduction at these locations on congested components upstream is magnified by the effect of marginal network losses. As network components are under heavy loading during these simulations, marginal losses are quite high. Using the results of the network losses experiments summarized in Table 2.3, marginal losses when demand reaches maximum network capacity are on the order of 32 percent, 29 percent, and 41 percent in the urban, semiurban, and rural networks, respectively.

Recall that all customers in this experiment are 'active' customers capable of reducing net demand at the same constant marginal cost. Thus, as demand grows higher, the OPF solution effectively finds the user downstream from any network constraint with the largest marginal losses. This user's net demand is reduced until constraints are satisfied or their net demand falls to zero (100 percent of their demand is supplied by local generation or curtailed). Net demand reduction then proceeds to the user with the next highest marginal losses, and so on, until all constraints are satisfied. Net demand reductions thus spread up each feeder as demand growth increases, progressively moving from users at the ends of feeders to those closer to the upstream congested line or transformer. This dynamic is best illustrated by Fig. 2-14, which zooms in on a single 'zone' or set of all LV feeders connected to a single MV-LV transformer. As coincident peak demand rises, the progressive increase in the number of network components at their maximum thermal rating and the decrease in the marginal losses incurred by the next set of users available for net demand reduction are responsible for the increasing marginal demand reduction required per marginal growth in demand seen in Figures 2-11 and 2-12.

5. *Increasing the concentration of demand in particular parts of the network has only a modest impact on the level of net demand reductions required for a given growth in network-wide coincident peak demand.* Finally, as Fig. 2-11 shows, increasing the demand concentration factor σ has a small and ambiguous effect on the total reduction in

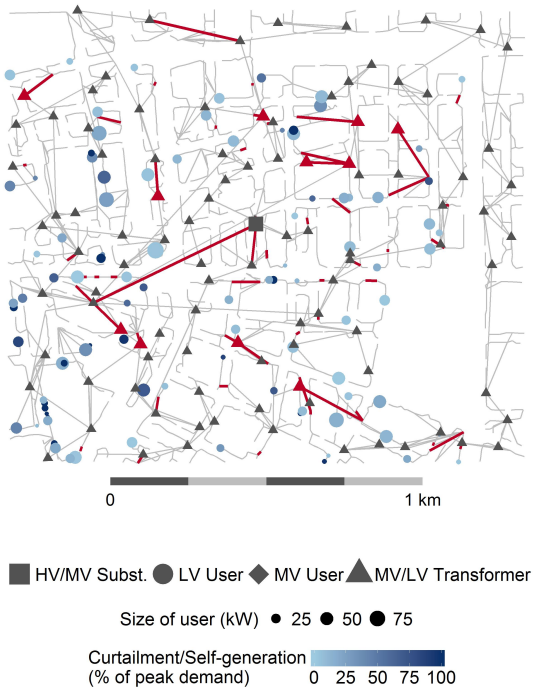

(a) 5 percent peak demand growth

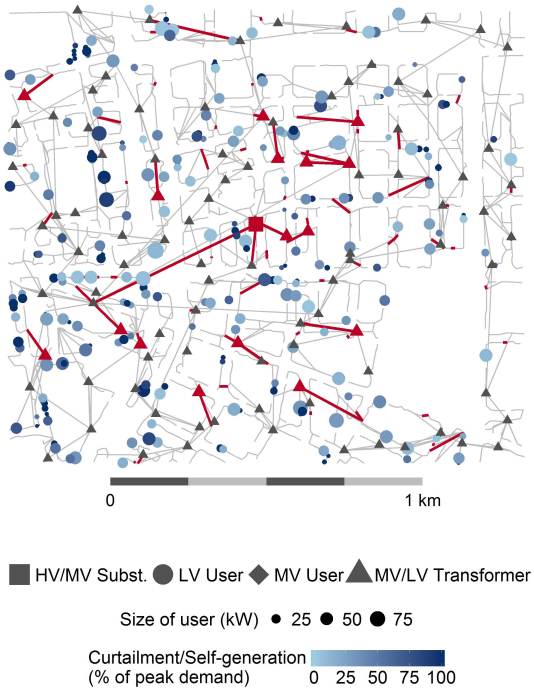

(b) 10 percent peak demand growth

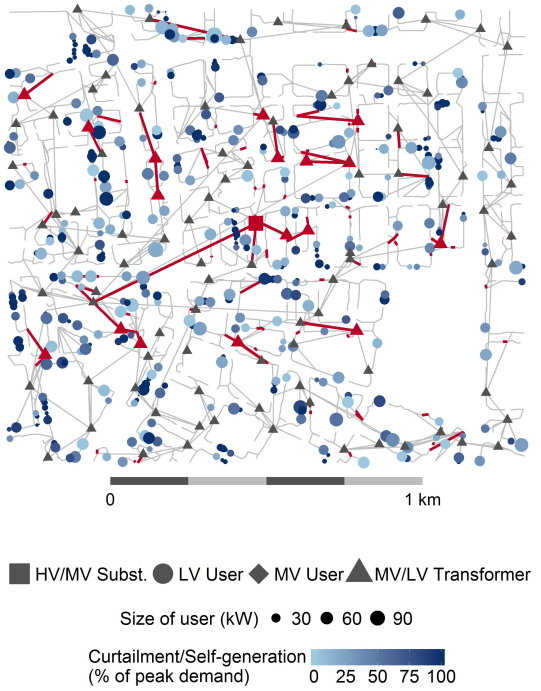

(a) 15 percent peak demand growth

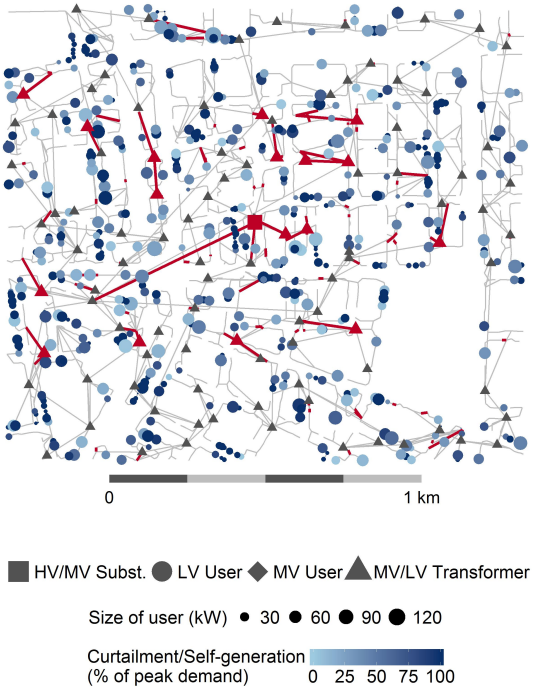

(b) 20 percent peak demand growth

Figure 2-13: Location and magnitude of net real power demand reductions required to accommodate up to 20 percent coincident peak demand growth in the urban European network with $\sigma = 0$

Red branches and transformers indicate components at thermal MVA rating.

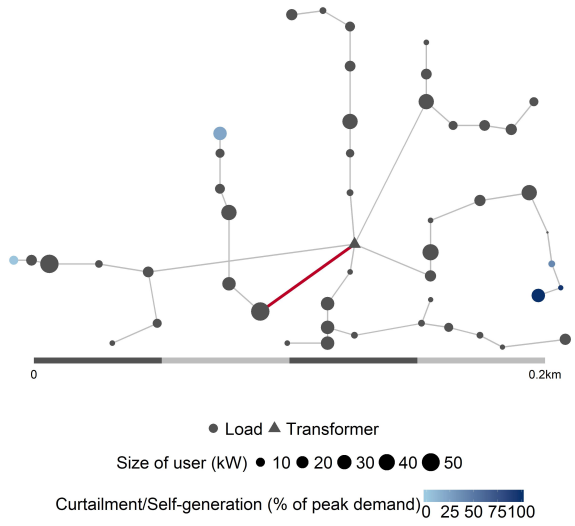

(a) 5 percent peak demand growth

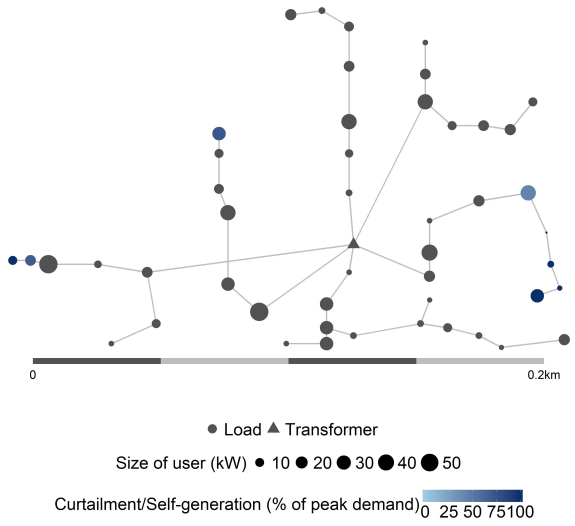

(b) 10 percent peak demand growth

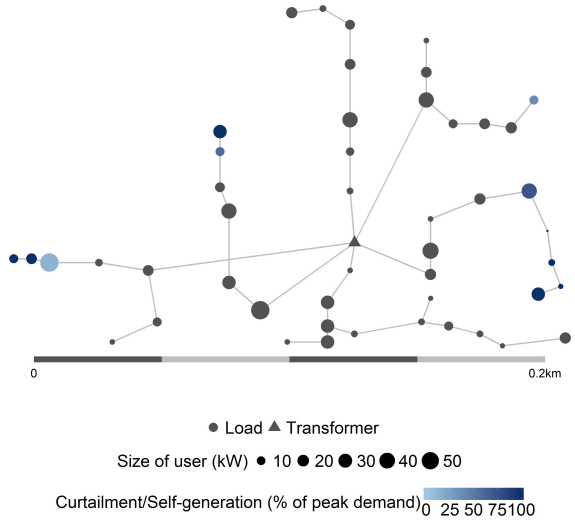

(a) 15 percent peak demand growth

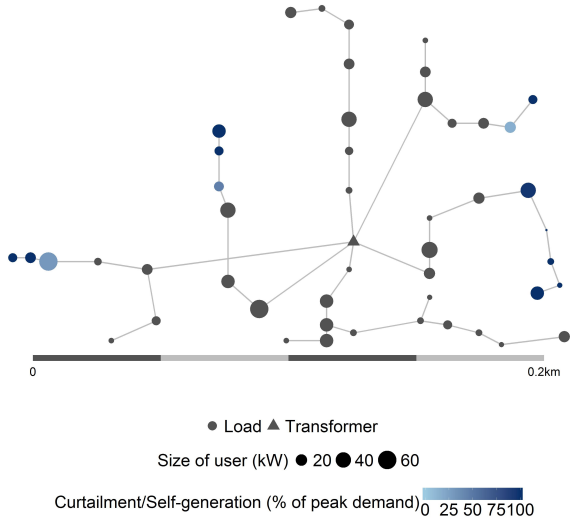

(b) 20 percent peak demand growth

Figure 2-14: Location and magnitude of net real power demand reductions required to accommodate up to 20 percent coincident peak demand growth within a single LV network zone in the urban European network with $\sigma = 0$

Red branches and transformers indicate components at thermal MVA rating.

net demand required. Some iterations results in slightly higher total demand reduction than in the $\sigma = 0$ cases for an equivalent level of peak demand growth, while others require less demand reduction. The total variance across iterations is fairly narrow, but increases as coincident peak demand grows and as σ increases.

Individual network components are discrete investment decisions exhibiting economies of scale. Even in an optimally-planned distribution network, some parts of the network will therefore have more 'headroom' than others at $d = 0$. In practice, these differences will also be compounded by errors in network planning, such as network investments built for load growth that did not materialize as quickly as forecasted. This heterogeneity in available power flow capacity across different parts of the network means that if demand is concentrated in areas with less headroom than average, net demand reductions will be larger to accommodate a given increase in average coincident peak demand across the network. The converse is true to when demand is concentrated in areas with more headroom than average.

In a realistic planning context, if the distribution of demand growth within a network is known or can be predicted with confidence, it can be input at the beginning of the AC OPF simulation process described herein. A single function relating net demand reduction and coincident demand growth can be generated for this specific distribution of demand, as the curves for each individual iteration in this experiment follow the same clear form: $\hat{y} = \hat{\alpha}d + \hat{\beta}d^2$. However, if there is uncertainty about where demand growth will concentrate within a network, these results indicate that it is possible to run multiple cases with different possible allocations of demand across the network and produce a regression function that predicts the range of possible outcomes with reasonably high accuracy. Thus, unless there is substantial heterogeneity in base network capacity or demand growth patterns far beyond the variation considered in this experiment, the effect of demand concentration on the amount of net demand reduction required to accommodate coincident peak demand growth appears to be a second order effect.

2.3.3 Experiment: the Effect of Node Voltage Limits

Experimental setup: This experiment mimics the set-up of the previous experiment in Section 2.3.2, but differs by modeling each network with tighter voltage constraints. The representative European test networks used herein were designed to comply with European Standard EN 50160, which specifies that service voltages (at each network user's point of connection to the network) should remain within ±10 percent of the nominal voltage with the exception of brief excursions. This standard was implemented in 28 European countries as of 2016 (CEER, 2016). However, North American distribution networks are designed for tighter voltage tolerances of ±5 percent of nominal voltage, as per ANSI Standard C84.1. The two standards are summarized and compared in Table 2.5. This experiment therefore adjusts the Matpower input parameters for all network user nodes to apply a voltage magnitude constraint of ±5 percent p.u. to explore the impacts of tighter voltage limits on required net demand reductions as coincident peak demand increases.

Results: Fig. 2-15 presents results for this experiment for each network and each demand concentration value σ, while Fig 2-16 compares the best fit regressions for comparable cases at ±10 percent and ±5 percent voltage constraints to illustrate the impact of tighter voltage limits as compared to results from Section 2.3.2. These figures illustrate the following finding:

1. *Voltage constraints have little effect on reduction in net demand required to accommodate a given increase in coincident peak demand, with the exception of sparse rural networks.* As Fig. 2-16 clearly shows, tightening the voltage limit to ±5 percent has virtually no effect on the mean regression fits for the urban and semiurban networks across all σ values modeled. This is consistent with the finding in Section 2.3.2 that the thermal MVA ratings of distribution lines and transformers are the primary cause of constraints requiring net demand reductions as coincident peak demand grows.

   However, for the rural network, the tighter voltage limits consistently increase the total net demand reduction required for a given level of coincident demand growth. This indicates that limits on customer service voltages do sometimes bind in the rural

Table 2.5: Comparison of continuous supply voltage standards for distribution networks in Europe and North America

European Standard EN 50160 on Voltage Characteristics of Public Distribution Systems

Voltage level	Continuous supply voltage standard
Low voltage (LV)	95 percent of the 10 minute mean r.m.s values for 1 week within ± 10 percent of nominal voltage; 100 percent of the 10 minute mean r.m.s values for 1 week within > -15 & < +10 percent of nominal voltage
Medium voltage (MV)	99 percent of the 10 minute mean r.m.s values for 1 week within ± 10 percent of reference voltage; 100 percent of the 10 minute mean r.m.s values for 1 week within ± 15 percent of reference voltage

American National Standard ANSI C84.1 for Electric Power Systems and Equipment Voltage Ratings (60 Hertz)

Voltage level	Continuous supply voltage standard
Service voltages ranging from 120 to 660 V	Service voltages remain within 'Range A' limits of ±5 percent of nominal with exception of infrequent excursions. Excursions of voltage into 'Range B' limits of > -9.33 & < +5.83 percent of nominal shall be limited in extent, frequency, and duration.
Service voltages >660 V	Service voltages remain within 'Range A' limits of > -2.5 & < +5.0 percent of nominal with exception of infrequent excursions. Excursions of voltage into 'Range B' limits of > -5.0 & < +5.83 percent of nominal shall be limited in extent, frequency, and duration.

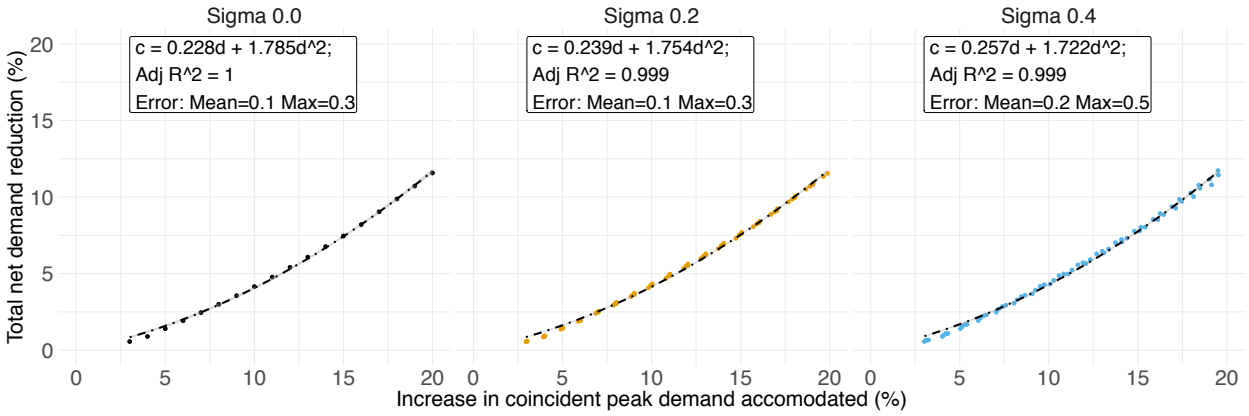

(a) Rural network

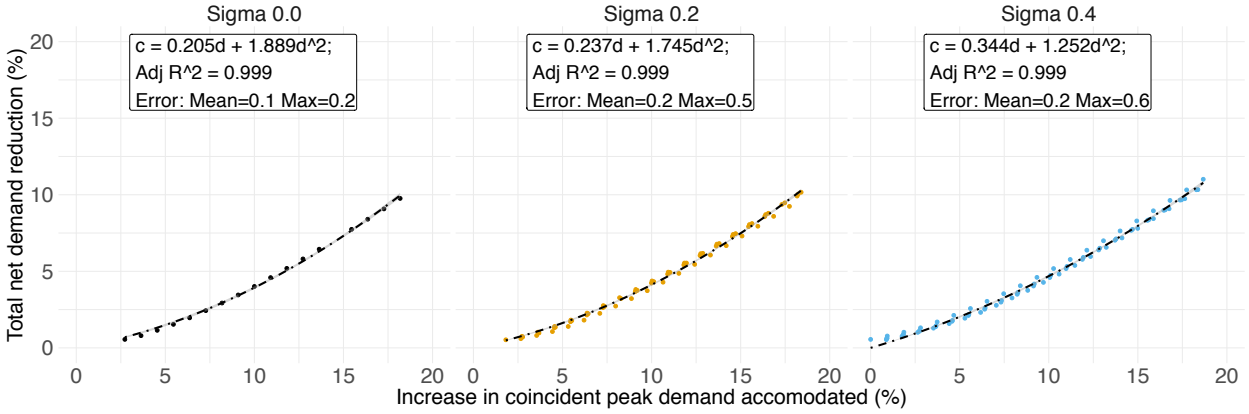

(b) Semiurban network

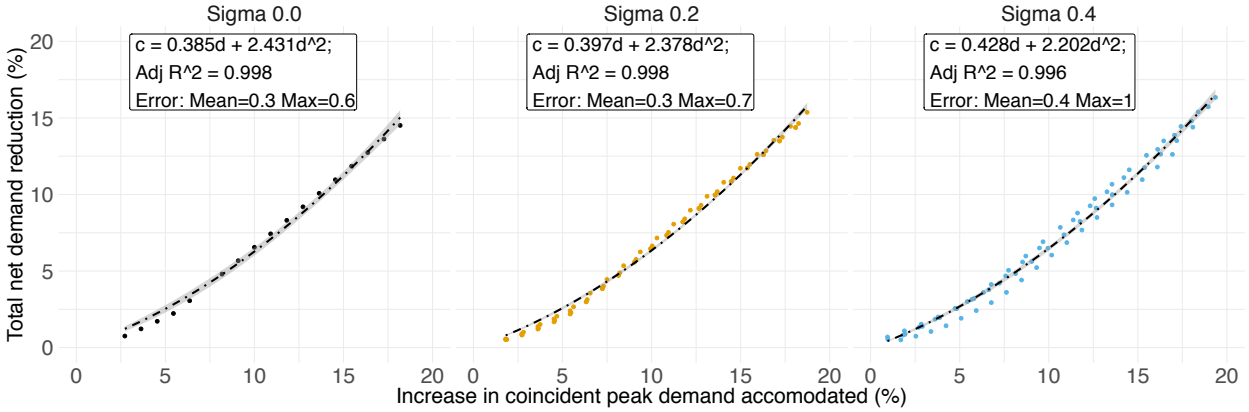

(c) Urban network

Figure 2-15: Aggregate reduction in net demand required to accommodate up to 20 percent coincident peak demand growth by network and demand concentration factor σ with voltage limit of ± 5 percent

All values are in percent of base network capacity.

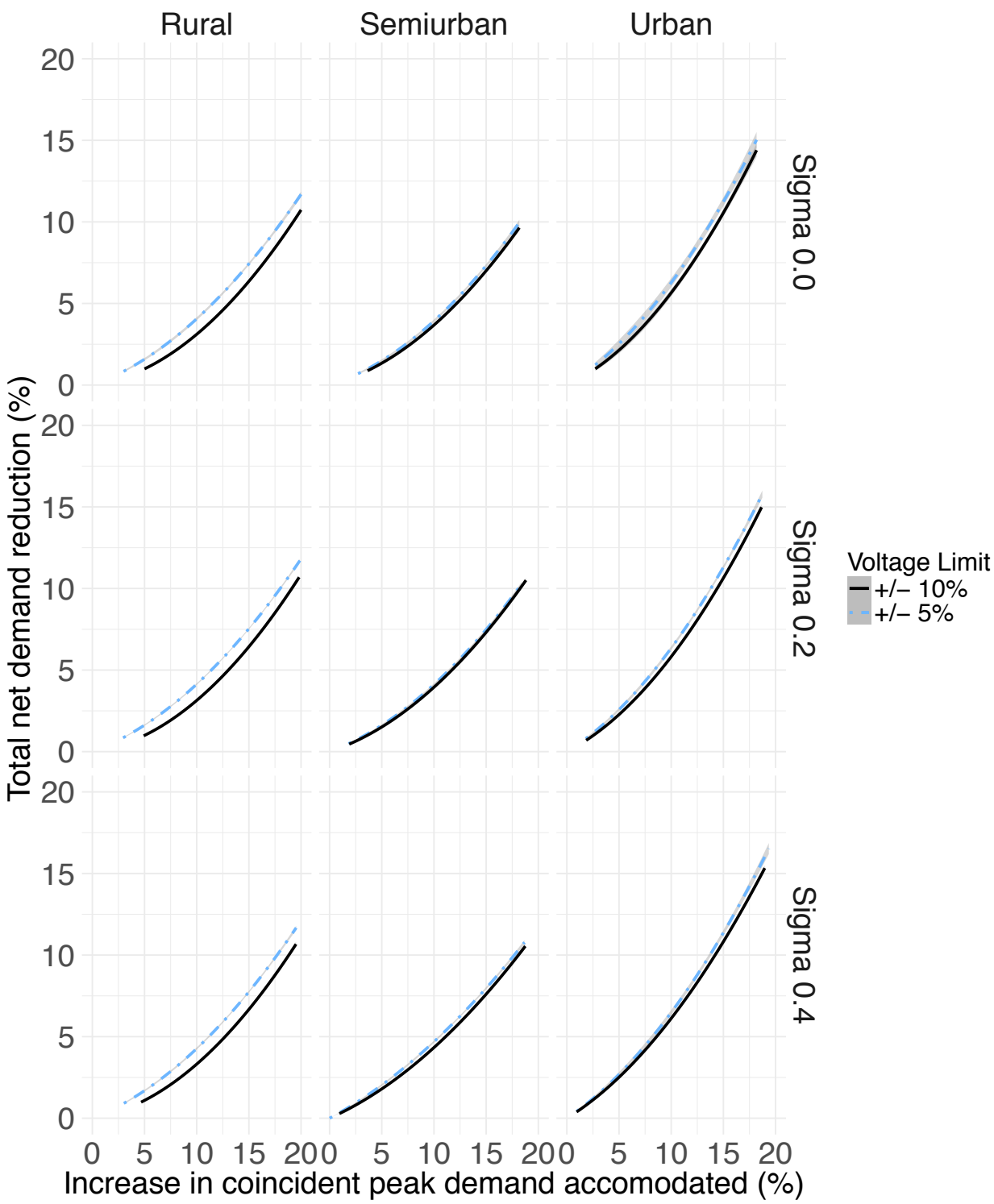

Figure 2-16: Comparison of reduction in net demand required to accommodate up to 20 percent coincident peak demand growth at ±5 percent and ±10 percent voltage limits
All values are in percent of base network capacity.

network and create additional constraints (above and beyond those caused by thermal limits) requiring greater net demand reduction. Rural networks are sparse and generally feature longer circuits and may experience greater voltage drops along feeders due to load than more compact networks. This appears to be the case amongst these three networks.

However, note that while these AC OPF simulations include the ability to adjust voltage tap changers at transformers, I do not model other voltage regulation devices that may be more commonly employed in rural networks. To the extent that these devices provide sufficient additional flexibility not considered in these experiments, voltage constraints may have no significant effect on the quantity of net demand reduction required in rural networks as well. If future work confirms this finding, then it will not be necessary to consider variations in voltage standards between regions when considering the drivers of net demand reduction necessary to accommodate growth in various network topologies. In any case, I use a ± 5 percent voltage limit in all subsequent experiments to represent any effect of more conservative voltage constraints.

2.3.4 Experiment: the Effect of Non-linear Marginal Costs

Experimental setup: In this experiment, I explore the impacts of non-linear marginal costs of net demand reduction on the total demand reduction required to accommodate a given increase in coincident peak demand. For each network – urban, semiurban, and rural – I perform three individual experiments using the following parameters and the general method in Algorithm 2:

- $\mathcal{D} = [0.00 : 0.01 : 0.20]$. Coincident peak demand, d, increases from 0 to 0.2 p.u. (20 percent) above the base network capacity in increments of 0.01 p.u. (one percent).
- $\sigma = \{0, 0.4\}$. I model the standard deviation of demand growth across each LV zone and MV customer, σ, at values of 0.0 and 0.4 only in this experiment. See Section 2.3.2 for more on the interpretation of σ.

- $x = 1$. The marginal cost of net demand reduction in this experiment increases as a stepwise linear function with three segments spanning [0,1] p.u. of each user's peak demand. Two break points b_1, b_2 define the length of each segment such that $S_1 = [0, b_1], S_2 = [b_1, b_2]$ and $S_3 = [b_2, 1]$. The values are determined as follows: b_1 for each active network user is randomly distributed as $\sim U(0, 1)$. Then, once b_1 is determined, b_2 is randomly distributed for each active user $\sim U(b_1, 1)$. The first segment is set to well above the marginal cost of imported energy from the primary substation, while the second and third segments are set at a marginal cost of 5x and 10x the cost of the first segment, respectively. This process creates heterogeneity in each user's marginal cost function. This setup can be considered consistent with a case where net demand reductions are achieved by curtailing real power consumption (with a fixed power factor), such as in a demand response program or the response of elastic demand to real time or critical peak pricing tariffs. In such cases, each user's willingness to curtail demand will differ, and it will no doubt steadily increase as a greater share of their power demand goes unsatisfied. That is, a user may be willing to curtail a little bit of their consumption by turning off non-critical devices or deferring demand to a later period. But this willingness will be limited, and users will require higher prices or greater compensation to curtail more essential uses of electricity.

- As the distribution of marginal cost segments and the distribution of demand concentration for cases with $\sigma = 0.4$ are randomized, I perform four iterations of this experiment with each network at each σ value to create some variation in results.

- Note that this experiment is performed with the more restrictive ± 5 percent voltage constraints.

Results: Fig. 2-17 presents results for this experiment by network and σ and Fig 2-18 compares the mean regression fit for cases with nonlinear marginal costs of demand reduction in this experiment with the comparable cases using constant marginal costs in 2.3.2. This experiment produces the following findings:

1. *Whether active users have a constant or increasing marginal cost of net demand reduction does not significantly affect the total net demand reduction required for a given increase in coincident peak demand.* As Fig 2-18 clearly shows, the regression fits for the two experiments with differing marginal costs of demand reduction are virtually identical. It therefore appears that one can consider reductions in net demand achieved via demand curtailment (which is characterized by increasing marginal costs for each active user) and self-generation with DG or storage (which, for most technologies, has approximately constant marginal cost) as direct substitutes in terms of their impact per kW of net demand reduction on network constraints, provided both resources are appropriately sited in the network. In other words, at a network-wide scale, one can consider a kW of total net demand reduction achieved either by demand curtailment or distributed generation as equivalent for purposes of accommodating coincident peak demand growth without network upgrades.

2. *In cases where each active user exhibits increasing marginal cost of net demand reduction, more active users are called on to accommodate increases in coincident peak demand.* As users have increasing marginal costs of curtailment in this experiment, the AC OPF solution involves more active users each curtailing at lower p.u. shares of demand. The solution now logically proceeds by exhausting demand reduction from the lowest cost segment of each active user in locations with high marginal losses, before proceeding up the feeder to the next set of users and activating their lowest cost segments and so forth. The result is a larger number of active users participating in the final OPF solution for any given level of peak demand growth, even though the total volume of net demand reduction remains nearly identical. This can be clearly seen in Fig. 2-19, which presents the location and magnitude of net demand reduction across the urban network and within a specific LV zone for a 15 percent increase in coincident peak demand ($\sigma = 0$) and contrasts the results from comparable experiments with increasing and constant marginal costs.

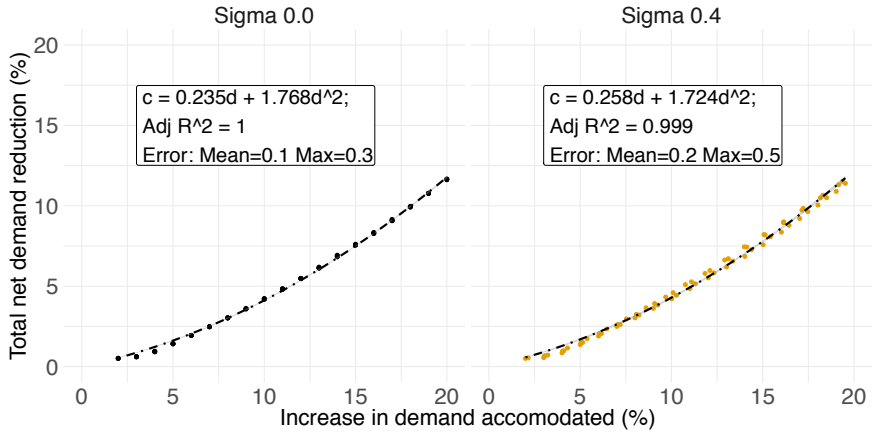

(a) Rural network

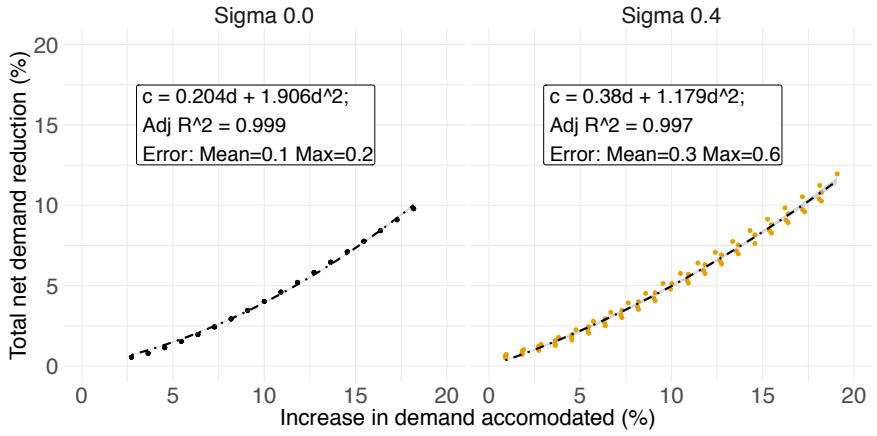

(b) Semiurban network

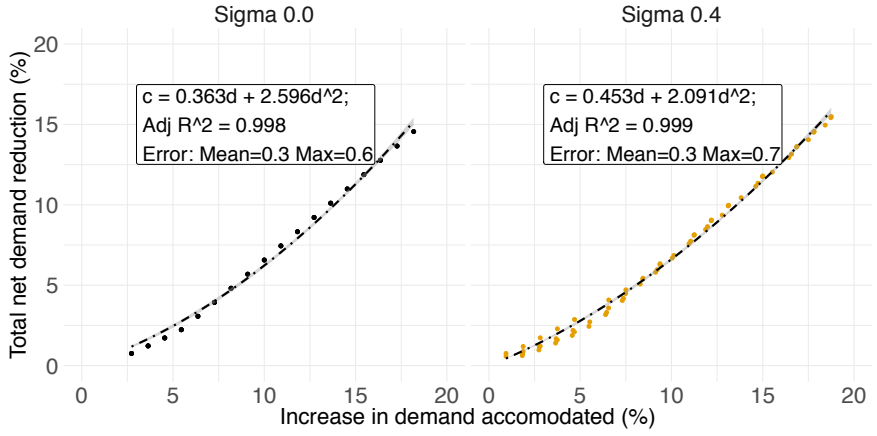

(c) Urban network

Figure 2-17: Aggregate reduction in net demand required to accommodate up to 20 percent coincident peak demand growth by network and demand concentration factor σ with nonlinear and heterogenous marginal cost of demand reduction
All values are in percent of base network capacity.

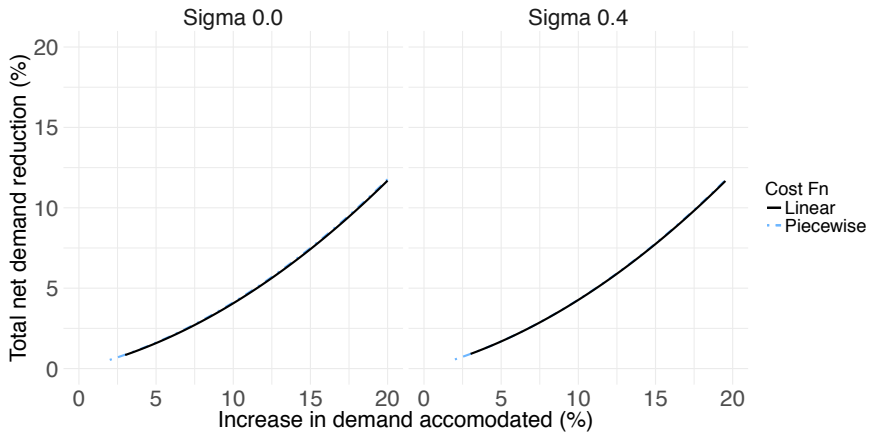

(a) Rural network

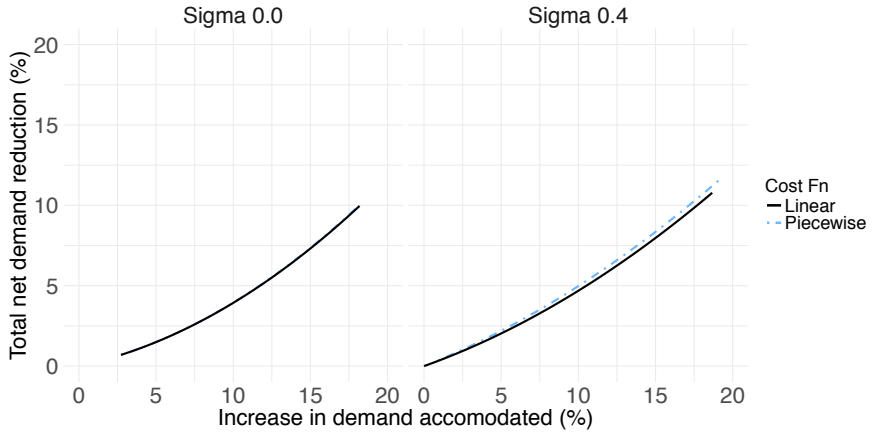

(b) Semiurban network

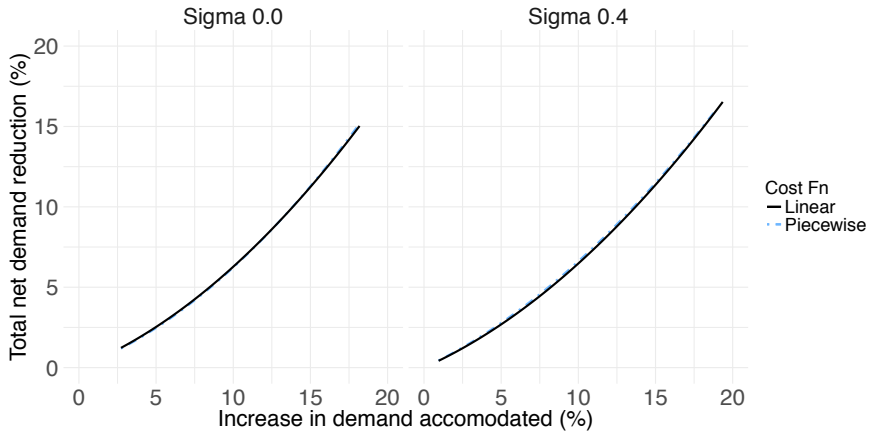

(c) Urban network

Figure 2-18: Comparison of reduction in net demand required to accommodate up to 20 percent coincident peak demand growth with constant/uniform ("linear") and nonlinear/heterogenous ("piecewise") marginal costs of demand reduction
All values are in percent of base network capacity.

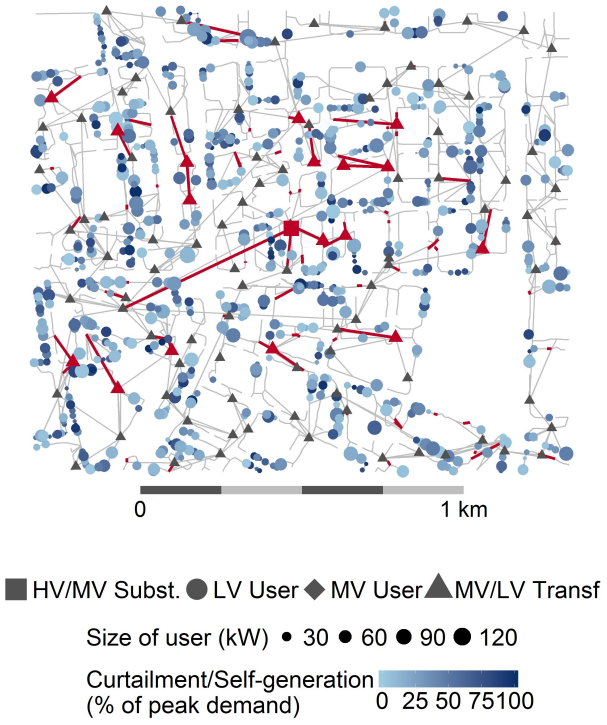

(a) Increasing marginal costs

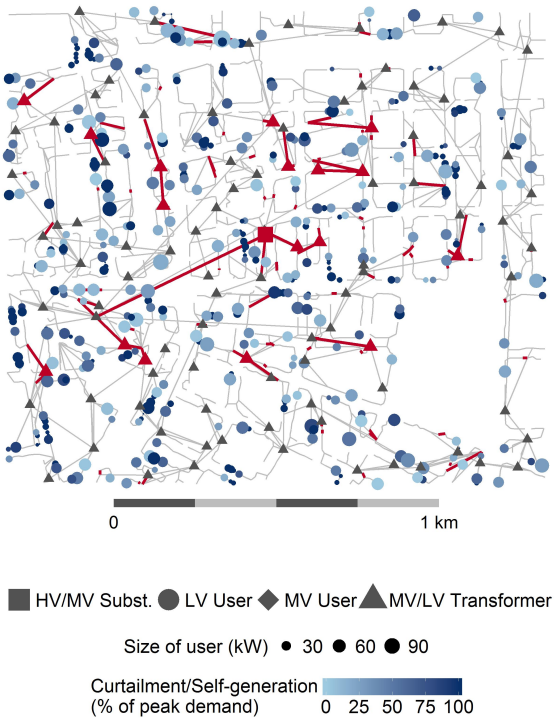

(b) Constant marginal costs

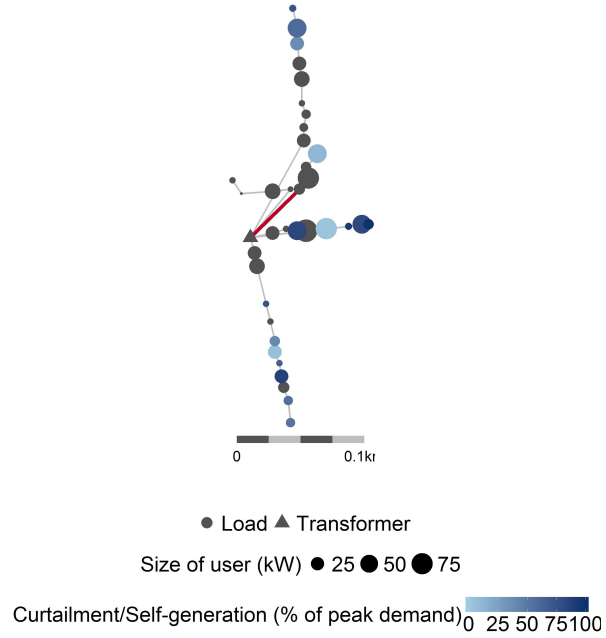

(c) Increasing marginal costs

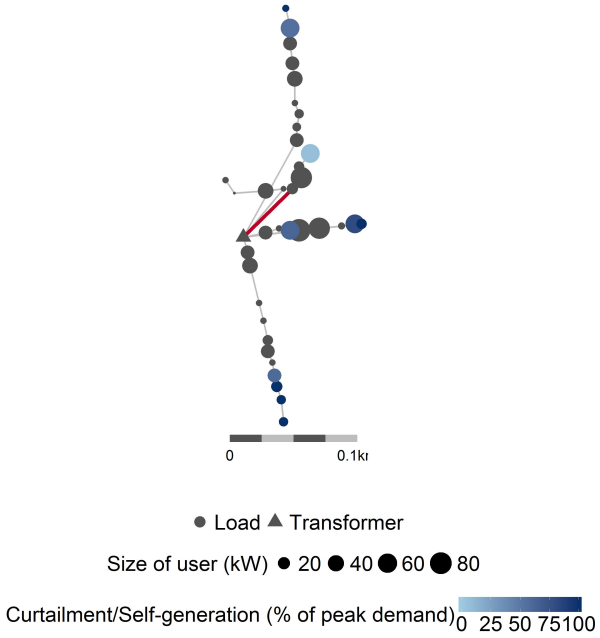

(d) Constant marginal costs

Figure 2-19: Comparison of location and magnitude of net real power demand reductions required to accommodate 15 percent coincident peak demand growth across the urban network and within a specific LV zone with $\sigma = 0$

Red branches and transformers indicate components at thermal MVA rating.

2.3.5 Experiment: the Role of Medium Voltage Demand

Experimental setup: In previous experiments, demand in both LV and MV was incremented in parallel, with each simulation modeling the same percent growth in both distribution voltage levels. Additionally, net demand reductions in these experiments exclusively occur within low voltage, as LV users at locations with high marginal losses deliver the greatest effect on upstream network constraints per unit of demand reduction and are thus preferentially selected as part of the AC OPF solution when the objective function seeks to minimize total net demand reduction (see Section 2.3.2).

However, it is clear that changes in coincident peak demand in medium and low voltages have different effects on network constraints. Power must flow through MV feeders to reach MV-LV transformers and LV feeders serving electricity demand connected at low voltage. Thus, changes in LV demand can contribute to congestions in network components in both low and medium voltage levels. In contrast, growth in MV demand can only contribute to congestions in MV feeders and the upstream primary substation. Thus, we should expect increases in coincident peak demand at low and medium voltages to have different impacts on total net demand reductions required to accommodate a given level of total coincident peak demand.

As a corollary, we should also expect net demand reductions in MV to be able to contribute only to relieving congestions in MV feeders or at the primary substation, while demand reductions in LV can help relieve congestions in either voltage level (provided the congestions occur 'upstream' from the point of demand reduction). As such, net demand reductions in MV should only be able to contribute a portion of the total net demand reductions required to accommodate a given increment in coincident peak demand growth, namely those reductions in demand necessary to relieve congestions in medium voltage or above. That is, net demand reductions in LV can fully substitute for reductions in MV (as proven in the prior experiments), while the converse should not be the true.

In this experiment, I therefore vary coincident peak demand in LV and MV independently to explore and isolate the impact of changes in each voltage level on net demand reductions

required to render power flows feasible. For each of the three European test networks, I perform two experiments using the following parameters:

- $\mathcal{D}_{lv} = [0.00 : 0.02 : 0.20]$; $\mathcal{D}_{mv} = [-0.25 : 0.05 : 0.25]$. Coincident peak demand in low voltage, d_{lv}, increases from 0 to 0.2 p.u. of initial LV peak demand (20 percent) in increments of 0.02 p.u. (two percent). Furthermore, for each $d_{lv} \in \mathcal{D}_{lv}$, I also vary coincident peak demand in medium voltage, d_{mv} from 0.75 to 1.25 p.u. ($\pm$ 25 percent) of initial peak MV demand in increments of 0.05 (5 percent) to identify the impact of independent changes in MV demand on required net demand reductions.

- $\sigma = 0$. I model the standard deviation of demand growth across each LV zone and MV customer, σ, at a value of 0.0 only in this experiment. As we will see below, changes in MV demand have small effects on net demand reductions, so I model a uniform distribution of demand ($\sigma = 0$) in order to avoid any 'noise' in the results from randomization of demand concentration within voltage levels that may mask the effects of changes in coincident peak demand in medium voltage.

- $x = 0$. The marginal cost of net demand reduction is constant and uniform across all active users. This setup can be considered consistent with a case where the same DER with constant marginal cost of production (such as a fuel cell or energy storage device) is available for installation by any customer in the network and is required to operate at a fixed power factor. As Section 2.3.4 found above, modeling marginal costs as linear or nonlinear and increasing has little effect on the total net demand reduction required, so I use the simpler setup in this experiment.

- In the first experiment performed for each network, the marginal cost of net demand reductions at MV and LV are equal, allowing the model to choose the ideal combination of MV and LV users to minimize total net demand reductions (as in all prior experiments). In the second experiment, however, I decrease the marginal cost of net demand reduction in MV to half the cost of demand reductions in LV. At 50 percent lower cost, the AC

OPF solution should prefer reductions in MV whenever possible.[22] Any net demand reductions in LV that result should therefore be necessary to relieve congestions at MV-LV transformers or LV feeders which upstream MV demand cannot affect. In this way, I isolate the maximum potential contribution of net demand reductions in MV to accommodating coincident peak demand growth in each network.

- Note that this experiment is performed with ±5 percent voltage constraints.

Results: Fig. 2-20 presents results for each network for the first experiment, in which net demand reductions at both voltage levels have equal costs. The panel of the figure also displays estimated coefficients for a linear regression of the form:

$$\hat{y}(d_{lv}, d_{mv}) = \hat{\alpha} d_{lv} + \hat{\beta} d_{lv}^2 + \hat{\gamma} d_{mv} \tag{2.5}$$

where y is total net demand reduction required and d_{lv} and d_{mv} are changes in coincident peak demand in low and medium voltages, respectively. Variation in MV demand is depicted in Fig. 2-20 by the color of each point, with lighter colors indicating higher coincident peak demand in MV and darker colors lower MV demand.

In addition, Fig. 2-21 depicts the same results in three dimensional form, with variation of points on the horizontal plane corresponding to changes in peak coincident demand in LV and MV and the color of each point corresponding to the total demand across both voltage levels. These 3D figures also include a surface corresponding to predictions from the regression function in Eq. 2.5. Note that LV demand is considerably larger than MV demand (approximately 10 times greater in each network). While MV demand varies from ± 25 percent in relative terms, this amounts to changes of only roughly ± 2 to 2.5 percent relative to each network's total capacity. Thus, each figure depicts all values as percent shares of maximum network capacity in order to use an equivalent base unit.

[22]This discount more than offsets the increased effect of each unit of LV demand reductions due to marginal losses downstream from MV. Using the results of the network losses experiments summarized in Table 2.3, marginal losses when demand reaches maximum network capacity are on the order of 32 percent, 29 percent, and 41 percent in the urban, semiurban, and rural networks, respectively, inclusive of losses that occur at MV.

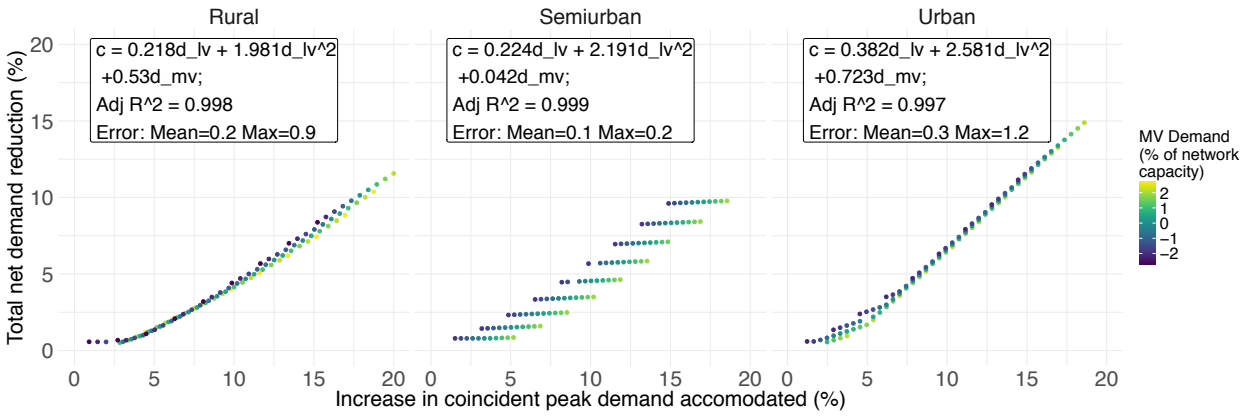

Figure 2-20: Aggregate reduction in net demand required to accommodate up to 20 percent coincident peak demand growth in LV and ± 25 percent variation in MV coincident peak demand (depicted by color) by network with $\sigma = 0$ and linear marginal costs of curtailment. All values are in percent of base network capacity.

As Figures 2-20 and 2-21 illustrate, the effect of changes in MV demand on net demand reductions is quite different across networks. In the semiurban network, variation in MV demand has little effect on net demand reductions. Changes in MV demand contribute little to net demand reductions because binding constraints in this network are nearly all found at MV-LV transformers or within LV feeders 'downstream' from MV network users, as depicted in Fig. 2-22. In this semiurban network, the base network design from Prettico et al. (2016) has sufficient 'headroom' at the primary substation and within MV feeders to accommodate an up to 25 percent increase in demand in MV (or a 2.0 percent increase in total network demand) with a net demand reduction of less than one tenth of one percent. While this implies that demand growth in MV can be accommodated without significant network upgrades in the semiurban network, as we will see below, this also means that reductions in net demand by MV customers contribute only minimally to network deferral, which reduces the potential locational value of DERs that might be sited in the MV portion of this network.

In contrast, variation in MV demand has a significant effect in the rural and urban networks. In both networks, beyond an initial level of total network demand growth (about 2 percent in the rural network and 5 percent in the urban network), changes in MV demand

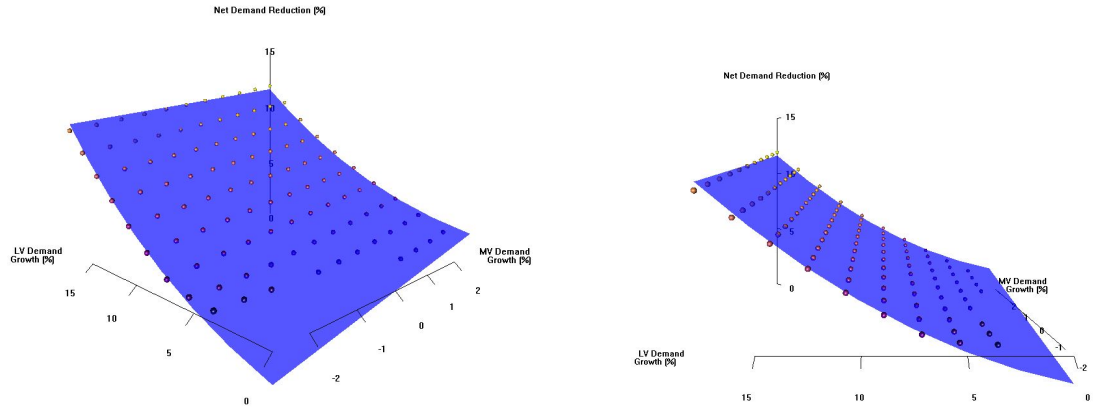

(a) Rural

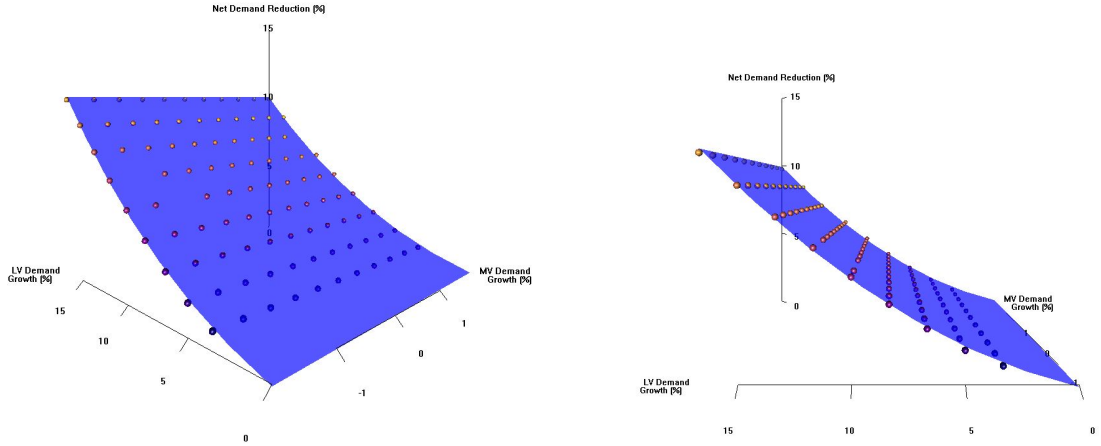

(b) Semiurban

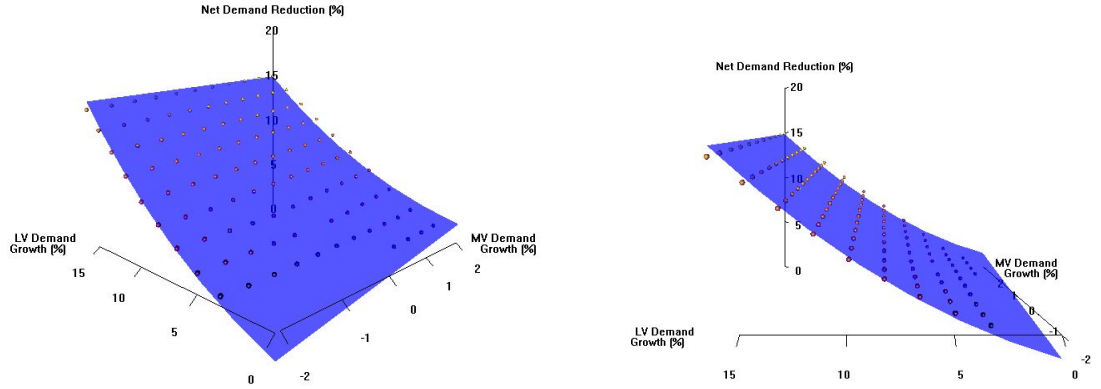

(c) Urban

Figure 2-21: 3D plot of aggregate reduction in net demand (vertical axis) required to accommodate up to 20 percent coincident peak demand growth in LV and ± 25 percent variation in MV coincident peak demand (horizontal axes) by network with $\sigma = 0$ and linear marginal costs of curtailment.

The color of each point corresponds to total coincident peak demand across both voltage levels. Darker colors are lower peak demand and lighter colors signify higher peak demand. Surface corresponds to predictions using the regression function in Eq. 2.5. All values are in percent of base network capacity.

have a direct and approximately linear effect on net demand reductions. In the rural network, several of the MV feeders connecting to the primary substation become congested as peak demand grows, while in the urban network, the primary substation as well as a couple of MV feeder segments become congested (Fig. 2-23). Thus, increases in demand in MV drive upgrades in these networks.

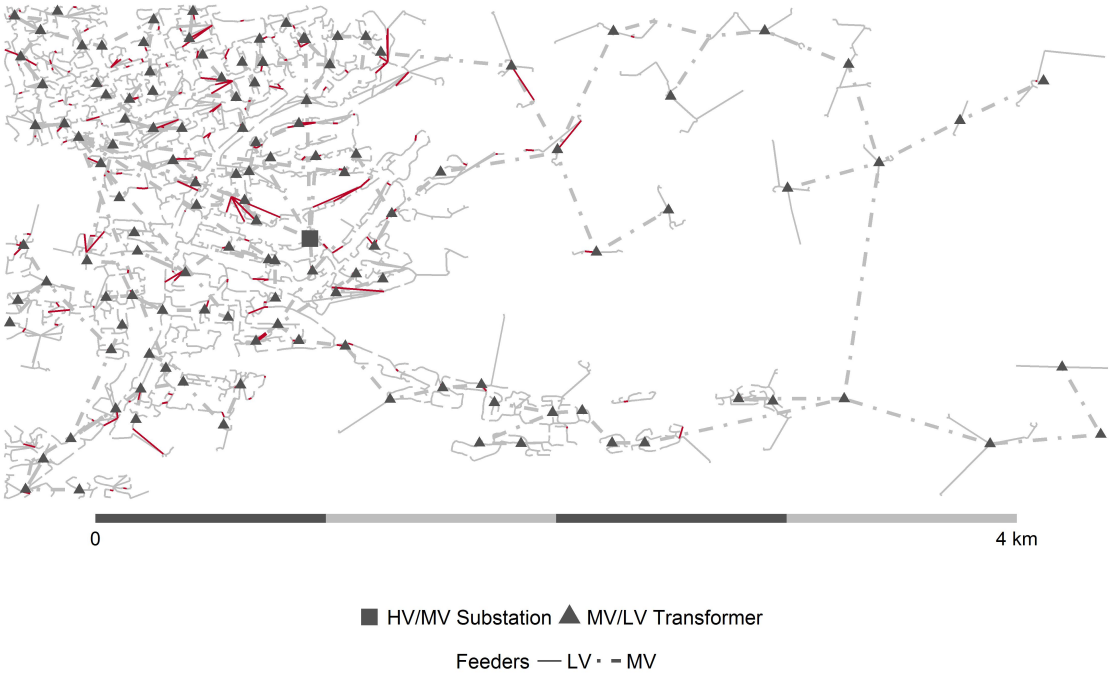

Figure 2-22: Location of network congestions (in red) in the semiurban European network

As discussed in the introduction to this experiment, reductions in net demand by MV users can only contribute to relieving congestions in MV feeders and at the primary substation. Net demand reductions by MV users therefore cannot fully substitute for net demand reductions in LV. In the second set of experiments here, I thus reduce the cost of net demand reduction at MV users (relative to LV users) such that the OPF solution will exhaust opportunities to reduce demand in MV whenever possible and turn to LV demand reduction only to reduce congestions 'downstream' of MV users. This experiment is designed to provide an estimate of the maximum share of total net demand reductions that can come from MV users in order to accommodate net demand growth in each network.

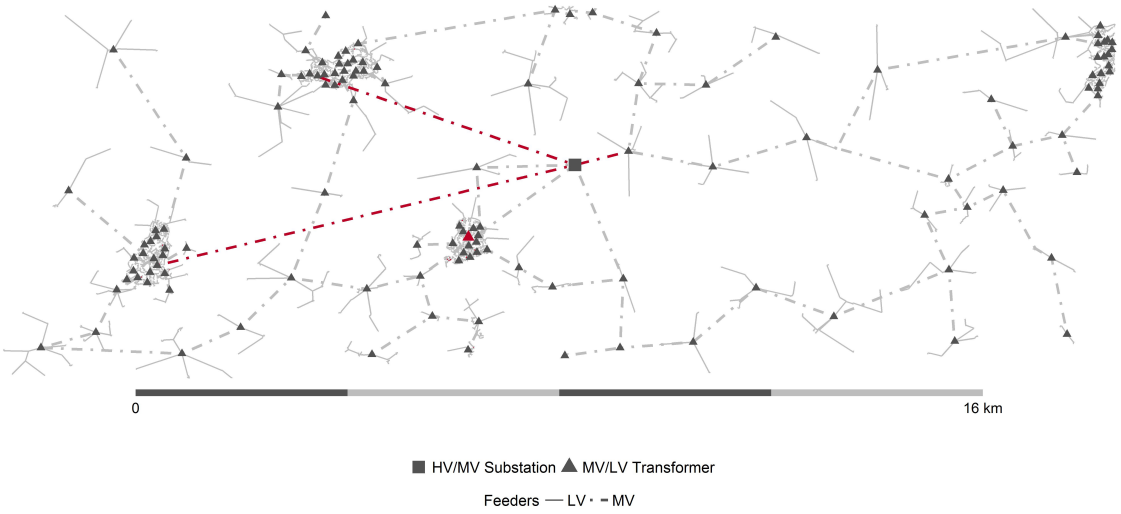

(a) Rural network

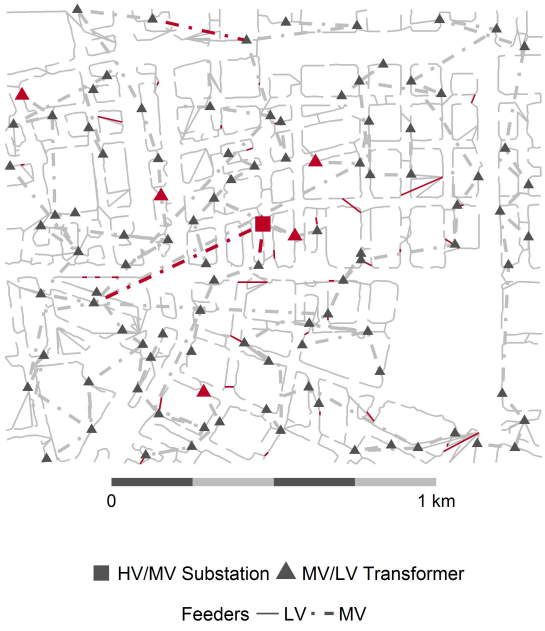

(b) Urban network

Figure 2-23: Location of network congestions (in red) in the rural and urban European networks

Fig. 2-24 shows the breakdown of net demand reductions in each portion of the network in these experiments. As expected, net demand reductions from MV users only contribute a portion of the total net demand reduction in each case. Consistent with the location of congestions in the semiurban network (within MV-LV substations and LV feeders, see Fig. 2-22), MV users do not contribute much to overall net demand reductions in this network. MV net demand reductions do however contribute a substantial share of overall reductions in the other two networks, where these reductions help relieve congestions in MV feeders or at the primary substation.

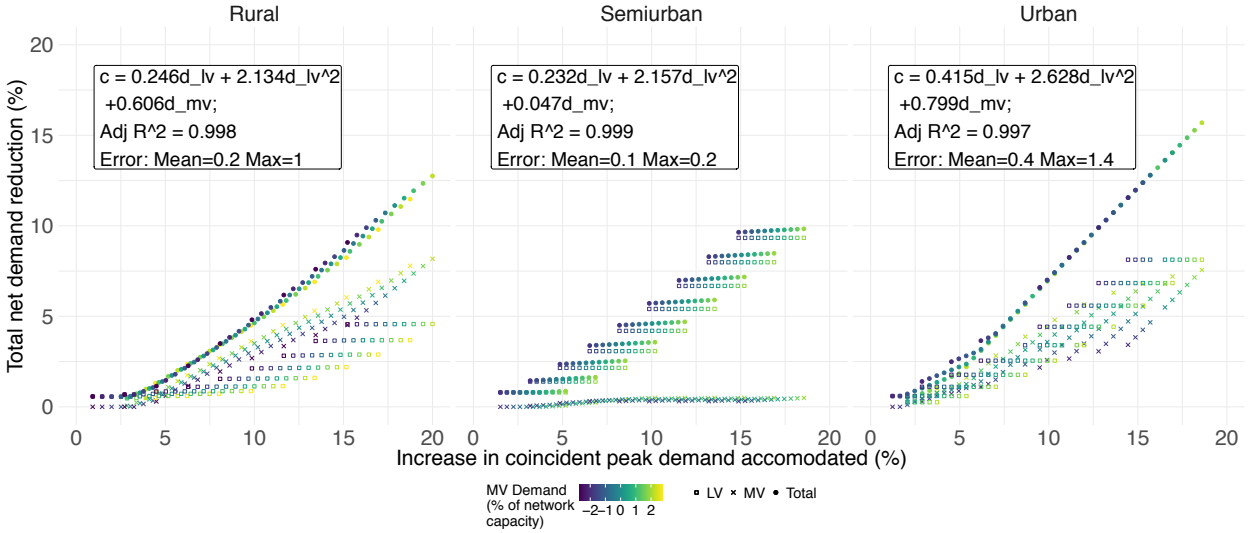

Figure 2-24: Aggregate reduction in net demand (total and by voltage level) required to accommodate up to 20 percent coincident peak demand growth in LV and ± 25 percent variation in MV coincident peak demand.
Variation in coincident peak demand in medium voltage depicted by color. Results presented by network with $\sigma = 0$ and linear marginal costs of curtailment. All values are in percent of base network capacity.

This pair of experiments establishes the following mathematical relationships between observed variables and estimated parameters...

- Total net demand reductions y can be made up of net demand reductions contributed by both MV users, y_{mv}, and LV users, y_{lv}.
- Total net demand reductions, y, is driven by peak coincident demand growth in both MV, d_{mv}, and LV, d_{lv}, and this relationship can be closely approximated by regression function

in Eq. 2.5 such that:

$$\hat{y}(d_{lv}, d_{mv}) = \hat{y}(d_{lv}) + \hat{y}(d_{mv}) = \hat{\alpha} d_{lv} + \hat{\beta} d_{lv}^2 + \hat{\gamma} d_{mv}. \tag{2.6}$$

- The portion of total net demand reductions driven by coincident peak demand in MV, $y(d_{mv})$, can thus be approximated as:

$$\hat{y}(d_{mv}) = \hat{\gamma} d_{mv} \tag{2.7}$$

and the portion of total net demand reductions driven by coincident peak demand in LV, $x(d_{lv})$ is approximately equal to:

$$\hat{y}(d_{lv}) = \hat{\alpha} d_{lv} + \hat{\beta} d_{lv}^2 \tag{2.8}$$

- As coincident peak demand growth in MV can *only* contribute to congestions at the MV voltage level or the primary substation, reductions in net demand by MV users, y_{mv}, can help relieve up to 100 percent of the net demand reductions driven by MV demand growth, $y(d_{mv})$. Thus:

$$y_{mv}(d_{mv}) \leq \overline{y_{mv}}(d_{mv}) \approx \hat{y}(d_{mv}) = \hat{\gamma} d_{mv} \tag{2.9}$$

- In the second experiment, the cost of MV net demand reduction is discounted relative to reductions in LV such that the AC OPF solution will exhaust any possible MV reductions. In the case of this experiment, Eq. 2.10 thus holds with equality and:

$$y_{mv}(d_{mv})^* = \hat{\gamma} d_{mv} \tag{2.10}$$

- As demand in both MV and LV contribute to power flows and congestions at the primary substation and MV feeders, net demand reductions in MV, y_{mv}, can also be driven by

coincident peak demand growth in *either* MV or LV. Thus:

$$y_{mv}(d_{lv}, d_{mv}) = y_{mv}(d_{mv}) + y_{mv}(d_{lv}) \tag{2.11}$$

- In the case of the second experiment where MV net demand reductions are exhausted where possible, Eq. 2.10 can be substituted into Eq. 2.11 to yield:

$$y_{mv}(d_{lv}, d_{mv}) = y_{mv}(d_{mv})^{*} + y_{mv}(d_{lv}) = \hat{\gamma} d_{mv} + y_{mv}(d_{lv}) \tag{2.12}$$

$$y_{mv}(d_{lv}) = y_{mv}(d_{lv}, d_{mv}) - \hat{\gamma} d_{mv} \tag{2.13}$$

- Coincident peak demand growth in LV can contribute to congestions at *either* the LV voltage level (e.g., at LV feeders or MV-LV substations) and the MV level (e.g., at 'upstream' MV feeders or the primary substation). Therefore, net demand reductions by MV users can at most contribute a portion of the total net demand reductions driven by LV peak demand growth, $y(d_{lv})$, namely the portion associated with congestions in MV feeders and the primary substation, denoted $\overline{y_{mv}}(d_{lv})$. Thus:

$$y(d_{lv}) = y_{mv}(d_{lv}) + y_{lv}(d_{lv}) \tag{2.14}$$

$$y_{mv}(d_{lv}) <= \overline{y_{mv}}(d_{lv}) < y(d_{lv}) \tag{2.15}$$

- Substituting in Eq. 2.13 and knowing that MV net demand reductions are exhausted where possible in the second experiment, 2.15 holds with equality and:

$$y_{mv}(d_{lv})^{*} = \overline{y_{mv}}(d_{lv}) = y_{mv} - \hat{\gamma} d_{mv} \tag{2.16}$$

- Finally, using Eq. 2.8, 2.14, & 2.16, the maximum contribution of net demand reductions by MV users as a share of the total set of net demand reductions driven by LV coincident

peak demand growth, ϕ, can be expressed as:

$$\phi(d_{lv}, d_{mv}) = \frac{y_{mv}(d_{lv})}{y(d_{lv})} = \frac{\overline{y_{mv}}(d_{lv})}{y(d_{lv})} = \frac{y_{mv} - \hat{\gamma} d_{mv}}{\hat{\alpha} d_{lv} + \hat{\beta} d_{lv}^2} \tag{2.17}$$

$$\overline{y_{mv}}(d_{lv}) = \phi(d_{lv}, d_{mv}) y(d_{lv}) = \phi(d_{lv}, d_{mv})(\hat{\alpha} d_{lv} + \hat{\beta} d_{lv}^2) = y_{mv} - \hat{\gamma} d_{mv} \tag{2.18}$$

The results of the second set of experiments, as presented in Fig. 2-24, yield known values for all terms in Eq. 2.17 above. Fig. 2-25 depicts ϕ by network for all combinations of coincident peak demand growth simulated in the second set of experiments. After an initial level of coincident peak demand growth (about 5 percent) across each network, ϕ becomes fairly consistent. This share of net demand reductions from MV users tends to decrease as total coincident peak demand increases, and increase as demand in MV increases.

Based on these results, ϕ can be roughly approximated by taking the mean of all values with total net demand reductions above a *de minimis* level (e.g., 2 percent here).[23] This approximate share of net demand reduction caused by LV demand growth contributed by MV users, $\hat{\phi}$, is depicted with the dashed line in Fig. 2-25 and the value is printed for each network. Net demand reductions by MV users contribute up to approximately 64 percent of net demand reductions caused by LV peak demand in the rural network, roughly 47 percent in the urban network, and only about 8 percent in the semiurban network.

Using these results, the maximum potential contribution of net demand reductions in MV to accommodate coincident peak demand growth in each network can therefore be approximated by:

$$\widehat{\overline{y_{mv}}}(d_{lv}, d_{mv}) = \hat{\phi}(\hat{\alpha} d_{lv} + \hat{\beta} d_{lv}^2) + \hat{\gamma} d_{mv} \tag{2.19}$$

Fig. 2-26 compares this estimated maximum net demand reductions from MV users, $\widehat{\overline{y_{mv}}}$, with the actual net demand reductions from the second set of experiments above. As can be seen, this approximation provides a reasonable estimate of the upper bound on the ability

[23] Below this *de minimis* level, very small changes in LV or MV demand reduction significantly affect the share of total demand reductions from MV users; this effect diminishes as the total net demand reduction reaches more meaningful levels.

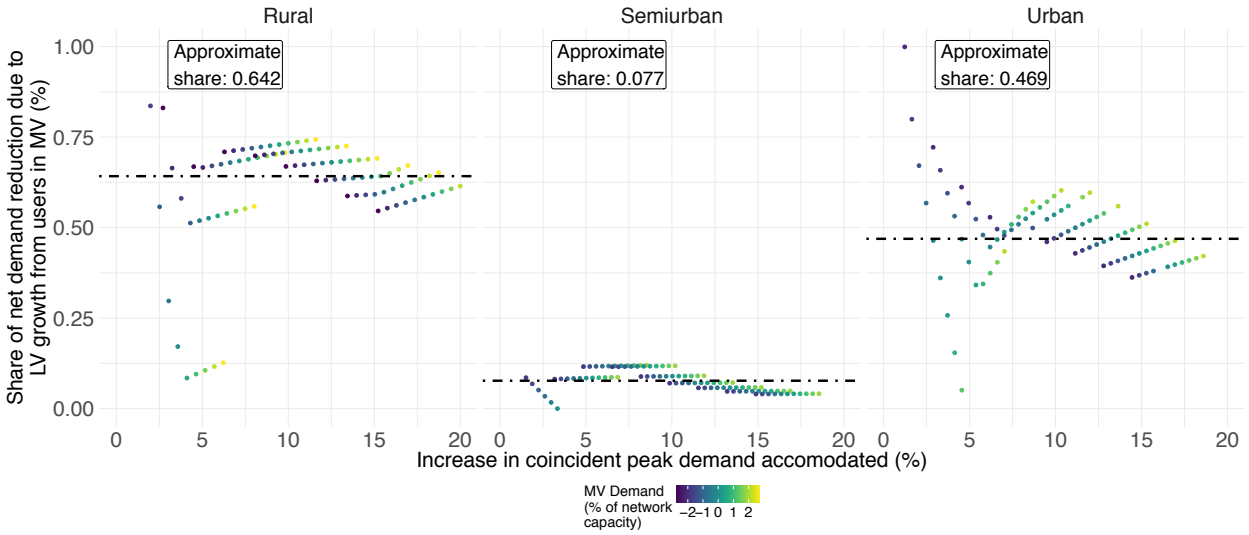

Figure 2-25: Share of net demand reduction due to coincident peak demand growth in LV provided by users in medium voltage, ϕ

Variation in coincident peak demand in medium voltage depicted by color. Results presented by network with $\sigma = 0$ and linear marginal costs of curtailment. All values are in percent of base network capacity.

of net reductions in MV to help accommodate for increases in coincident peak demand across each network. This estimate, $\widehat{\overline{y_{mv}}}$, can therefore be used to constrain the maximum contribution of DERs in MV to network deferral in the system-wide planning model described in Chapter 3.

One final step remains to approximate the potential for net demand reductions in MV to substitute for reductions in LV: accounting for the effect of losses. As prior experiments have demonstrated, the effect of reductions in LV net demand on congestions upstream in MV is magnified by marginal losses. Thus, if net demand reductions occur in MV rather than LV, it should require slightly greater total reduction in net demand to accommodate the same quantity of coincident peak demand. Fig. 2-27 compares the estimated total net demand reduction required per unit of coincident peak demand growth using the regression estimates from the first experiment, $\hat{y}_1$ (see Fig. 2-20 with net demand reduction in LV only) with the estimates from the second experiment, $\hat{y}_2$ (see Fig. 2-24 with net demand reductions in both MV and LV). As expected, $\hat{y}_2$ is slightly higher than $\hat{y}_1$ in both the rural and urban networks, where reductions by MV users contribute a substantial share of overall

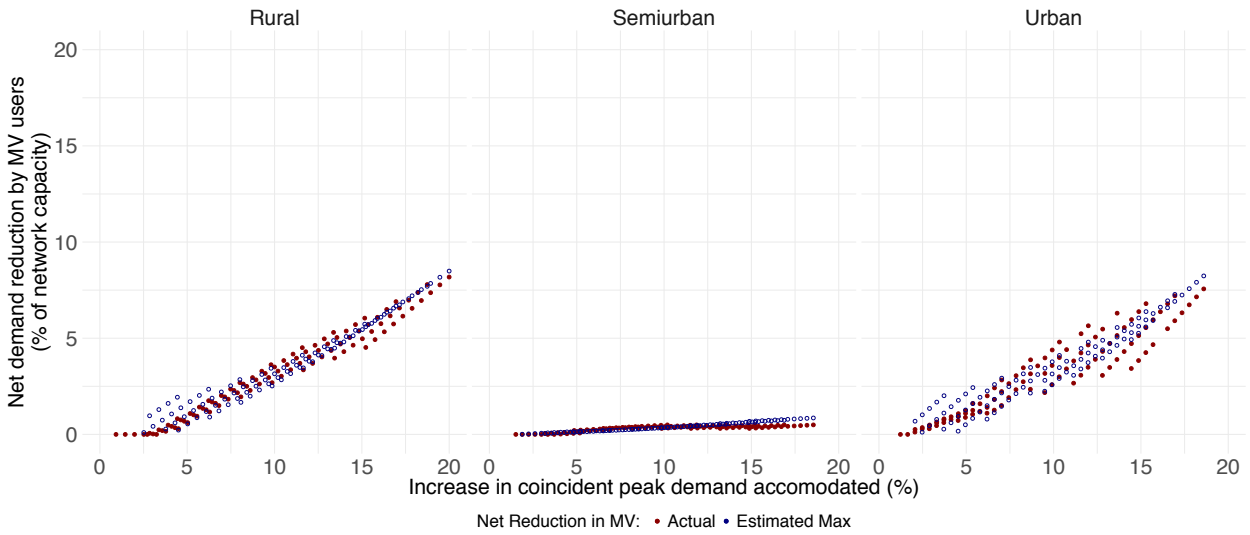

Figure 2-26: Estimated and actual maximum net demand reductions by MV users to accommodate up to 20 percent increase in coincident peak demand
Results presented by network with $\sigma = 0$ and linear marginal costs of curtailment. All values are in percent of base network capacity.

net demand reductions. Results for the semiurban network are nearly identical, consistent with the very small contribution of net demand reductions in MV in this network (see Fig. 2-24).

I thus calculate the effect of each unit of MV net demand reduction on the total net demand reduction required per unit of coincident peak demand growth with the following equation:

$$\delta(d_{lv}, d_{mv}) = \frac{\hat{y}_2(d_{lv}, d_{mv}) - \hat{y}_1(d_{lv}, d_{mv})}{y_{mv,2}(d_{lv}, d_{mv})} \tag{2.20}$$

where $y_{mv,2}$ is the sum of net demand reductions in MV in the second experiment. This estimate is presented in Fig. 2-28 for the rural and urban networks. Unfortunately, the difference in total reductions in the semiurban network is too small to be meaningful, given the very small contribution of reductions in MV demand in this network. However, as this figure illustrates, the increase in total net demand reduction required per unit of net demand reductions in MV is fairly consistent across all values of coincident peak demand growth for both the rural and urban networks. I thus approximate $\hat{\delta}$ for each network by taking the

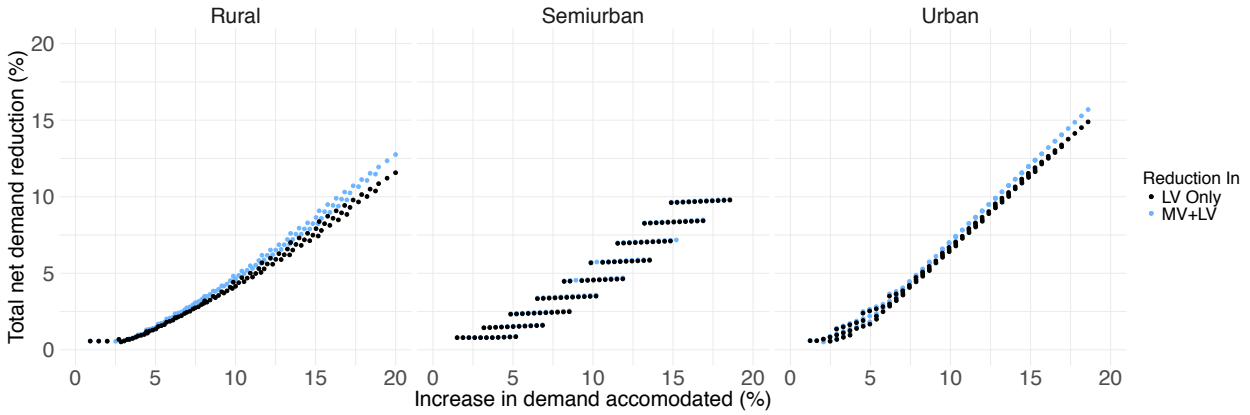

Figure 2-27: Comparison of estimated total reduction in net demand required to accommodate up to 20 percent coincident peak demand growth in LV and ± 25 percent variation in MV coincident peak demand with and without net demand reductions in medium voltage.
Results presented by network with $\sigma = 0$ and linear marginal costs of curtailment. All values are in percent of base network capacity.

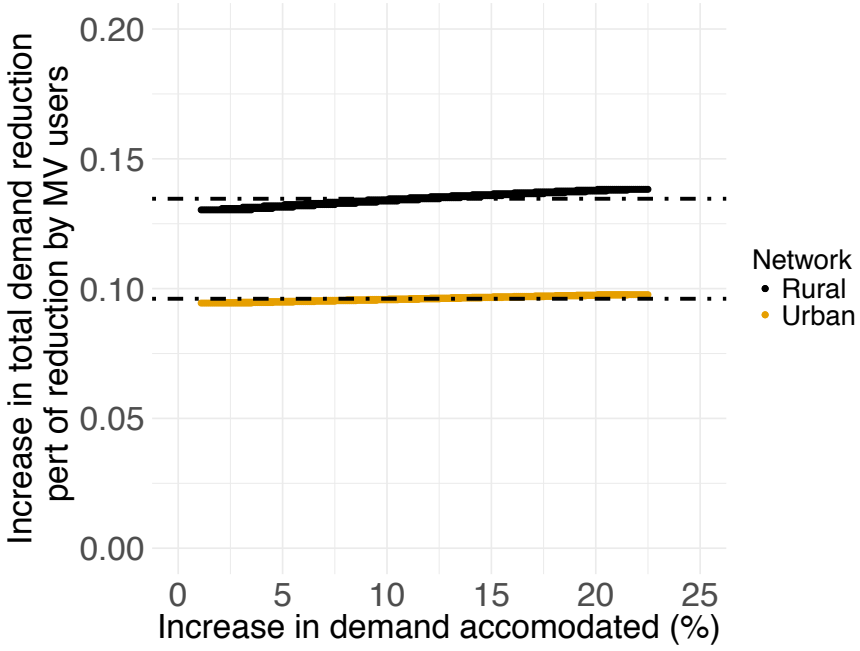

Figure 2-28: Estimated increase in total reduction in net demand required per unit of net demand reductions in MV as a function of coincident peak demand growth.
Results presented by network with $\sigma = 0$ and linear marginal costs of curtailment.

mean of δ across all values of peak demand growth. In the urban network, net demand reductions increase by 0.096 units per unit of net demand reduction in MV and increase by 0.135 units per unit of MV reduction in the rural network. Both values are approximately one-third of the estimated marginal losses at maximum network capacity in each network (32 percent in the urban network and 41 percent in the rural network as per Table 2.3). Assuming the same ratio between marginal network losses and $\hat{\delta}$ holds for the the semiurban network as well, I estimate that $\hat{\delta}$ is somewhere between 0.087 to 0.095 units per unit of net demand reduction in MV.

Additionally, by rearranging 2.20 and substituting in 2.5, I can relate the results of the first and second experiments, $\hat{y}_1, \hat{y}_2$ as follows:

$$\hat{y}_2(d_{lv}, d_{mv}) = \delta y_{mv,2}(d_{lv}, d_{mv}) + \hat{y}_1(d_{lv}, d_{mv}) = \\ \hat{\alpha}_1 d_{lv} + \hat{\beta}_1 d_{lv}^2 + \hat{\gamma}_1 d_{mv} + \delta y_{mv,2}(d_{lv}, d_{mv}) \tag{2.21}$$

Assuming (1) that this relationship holds for any $y = y_{lv} + y_{mv}$ where $0 \leq y_{mv} \leq \overline{y_{mv}}$; and (2) δ is approximately constant across all values of d_{lv}, d_{mv} and thus accurately estimated by $\hat{\delta}$ (as illustrated in Fig. 2-28); then I propose estimating total net demand reduction as:

$$\hat{y}(d_{lv}, d_{mv}) = y_{lv}(d_{lv}) + y_{mv}(d_{lv}, d_{mv}) = \\ \hat{\alpha}_1 d_{lv} + \hat{\beta}_1 d_{lv}^2 + \hat{\gamma}_1 d_{mv} + \hat{\delta} y_{mv}(d_{lv}, d_{mv}) \tag{2.22}$$

Or:

$$y_{lv}(d_{lv}) + (1 - \hat{\delta}) y_{mv}(d_{lv}, d_{mv}) = \hat{\alpha}_1 d_{lv} + \hat{\beta}_1 d_{lv}^2 + \hat{\gamma}_1 d_{mv} \tag{2.23}$$

The value $(1 - \hat{\delta})$ can thus be thought of as a 'conversion rate' or 'discount rate' between net demand reductions in MV and LV. That is, every unit of net demand reduction in MV can substitute for $(1 - \hat{\delta})$ units of net demand reductions in LV due to the magnifying effect of average network losses between locations in LV and MV.

2.3.6 Summary of Findings: the Ability of Net Demand Reductions to Accommodate Coincident Peak Demand Growth in Distribution Networks

Summarizing the results of experiments in Sections 2.3.2 to 2.3.5, I make the following findings:

1. The total reduction in net demand required to accommodate a given increase in coincident peak demand across an entire large-area distribution network can be closely approximated with a function form

$$y(d) = \alpha d + \beta d^2 + \epsilon$$

   This function can be estimated by linear regression analysis of the results of AC OPF simulations configured to identify the minimum net demand reduction required to render network power flows feasible despite demand growth. This estimated regression explains nearly 100 percent of variation observed in the experiments herein with minimal mean error of ± 0.1 to 0.4 percent of base network capacity and maximum errors of no more than ± 0.5 percent of base network capacity.[24] (*Section 2.3.2*)

2. This functional form is robust to variations in the concentration of demand growth across LV feeders and MV customers. Regression results closely estimate the total net demand reduction required across experiments where the magnitude of demand growth varies across LV feeder and MV customers with a standard deviation of up to 40 percent of the mean coincident peak demand growth for the network as a whole. (*Section 2.3.2*)

3. Net demand reductions are driven primarily by thermal MVA ratings at transformers or feeders, rather than node voltage limits. (*Section 2.3.2*)

[24] Base network capacity is defined as the total coincident peak demand that can be accommodated by a given network without either network reinforcements or net demand reductions required to render power flows feasible across all network components.

4. Applying more restrictive node voltage constraints of ± 5 percent of nominal voltage as per North American standards for distribution networks (versus ± 10 percent in European standards) does not affect the total reduction in net demand required to accommodate a given increase in coincident peak demand *except* in the rural network. In the case of this sparse network with longer feeders that allow greater voltage drops, voltage limits do drive a small portion of overall net demand reductions under this tighter voltage constraint, requiring approximately 1 percentage point greater net demand reduction per percent growth in coincident peak demand. However, this increase may be mitigated by additional voltage regulation equipment not modeled in this experiment. (*Section 2.3.3*)

5. The total net demand reduction required for a given increase in coincident peak demand is not significantly different if active users have a constant or increasing marginal cost of net demand reduction. However, if the marginal cost of net demand reduction is increasing in quantity for each user (as one would expect if reductions are achieved via demand curtailment rather than local generation or storage), then the total number of active users providing net demand reductions increases. In other words, smaller reductions per user are spread out across more users to achieve the same total net demand reduction across the network. (*Section 2.3.4*)

6. Increases in coincident peak demand from customers in medium voltage and low voltage have different effects on network congestions and thus on total net demand reductions. Demand in MV may only cause congestions in MV feeders or at the primary substation. LV demand can cause congestions in LV feeders, at MV-LV transformers, as well as upstream in MV feeders or the primary substation. Total net demand reductions required to accommodate a given increase in coincident peak demand at LV and MV can be closely approximated by a function of the form:

$$y(d_{lv}, d_{mv}) = y(d_{lv}) + y(d_{mv}) = \alpha d_{lv} + \beta d_{lv}^2 + \gamma d_{mv} + \epsilon$$

This function can also be estimated by linear regression analysis of the results of AC OPF simulations that independently vary demand in both voltage levels and are configured to minimize net demand reduction required to render network power flows feasible despite demand growth. The estimated regression explains nearly 100 percent of variation in observed results and predicts outcomes with minimal mean error of $\pm$ 0.1 to 0.4 percent of base network capacity and a maximum error of no more than 1.4 percent across experiments. (*Section 2.3.5*)

7. Net demand reductions by MV users can only help relieve network constraints in MV feeders or the primary substation, whereas reductions by LV users can help relieve any 'upstream' congestion regardless of voltage level. MV net demand reductions are therefore only partial substitutes for LV net demand reductions, whereas LV net demand reductions can satisfy up to 100 percent of network constraints. The maximum contribution of MV net demand reduction to congestion relief is related to the share of congestions caused by MV demand and the portion of congestions caused by LV demand that occur in MV feeders or at the primary substation. Thus, MV net demand reductions can contribute up to 100 percent of demand reductions driven by MV demand and only a share of reductions driven by LV demand. The maximum contribution of net demand reduction in MV can be expressed as:

$$\overline{y_{mv}}(d_{lv}, d_{mv}) = \phi(d_{lv}, d_{mv})y(d_{lv}) + y(d_{mv}) = \phi(d_{lv}, d_{mv})(\alpha d_{lv} + \beta d_{lv}^2) + \gamma d_{mv} + \epsilon$$

(*Section 2.3.5*)

8. The share of net demand reductions driven by LV demand growth that can be met by MV users, ϕ, can be identified by performing AC OPF simulations configured to preferentially reduce net demand in MV wherever feasible. Using these results, ϕ can be expressed as:

$$\phi(d_{lv}, d_{mv}) = \frac{y_{mv}(d_{lv})}{y(d_{lv})} = \frac{y_{mv}(d_{lv}, d_{mv}) - y(d_{mv})}{y(d_{lv})} = \frac{y_{mv}(d_{lv}, d_{mv}) - \hat{\gamma} d_{mv}}{\hat{\alpha} d_{lv} + \hat{\beta} d_{lv}^2}$$

Furthermore, taking the mean of ϕ for all cases with more than *de minimis* net demand reductions produces an estimate $\hat{\phi}$ of the maximum share of net demand reductions driven by LV customers that can be contributed by MV users. (*Section 2.3.5*)

9. The maximum contribution of MV active users to total net demand reductions can be approximated by

$$\widehat{\overline{y_{mv}}}(d_{lv}, d_{mv}) = \hat{\phi}(\hat{\alpha} d_{lv} + \hat{\beta} d_{lv}^2) + \hat{\gamma} d_{mv}$$

This estimated parameter can be used to constrain the ability of DERs or demand response in medium voltage levels to reduce the need for network upgrades. (*Section 2.3.5*)

10. As the effect of net demand reductions in LV on 'upstream' constraints is magnified by network losses, net demand reductions in LV have a greater effect on constraints in MV than net demand reductions by MV users. By comparing simulation results in cases where all net demand is satisfied by LV users with those where the maximum potential contribution of MV users is exhausted, one can calculate the effective conversion rate between MV and LV net demand reductions:

$$\delta(d_{lv}, d_{mv}) = \frac{\hat{y}_2(d_{lv}, d_{mv}) - \hat{y}_1(d_{lv}, d_{mv})}{y_{mv,2}(d_{lv}, d_{mv})}$$

where $\hat{y}_1$ is the estimated total net demand reduction if all reductions occur in low voltage; $\hat{y}_2$ is the estimated total net demand reduction if MV net demand reductions are exhausted where possible; and $y_{mv,2}$ is the level of net demand reduction in MV in this case. It turns out that δ is roughly constant across all values of peak coincident demand and thus can be approximated with a constant estimate $\hat{\delta}$ without meaningful loss of accuracy. (*Section 2.3.5*)

11. Finally, putting all results together, total net demand reductions as a function of coincident peak demand growth in LV and MV can be expressed for any feasible combination

of net demand reductions by LV and MV users as:

$$y(d_{lv}, d_{mv}) = y_{lv} + (1 - \hat{\delta})y_{mv} = \hat{\alpha_1} d_{lv} + \hat{\beta}_1 d_{lv}^2 + \hat{\gamma}_1 d_{mv}$$
$$\text{s.t. } y_{mv} \leq \widehat{\overline{y_{mv}}} = \hat{\phi}(\hat{\alpha} d_{lv} + \hat{\beta} d_{lv}^2) + \hat{\gamma} d_{mv} \tag{2.24}$$

(*Section 2.3.5*)

Table 2.6 summarizes the key parameters estimated from these experiments for the three representative European networks.

Table 2.6: Summary of estimated parameters defining net demand reductions required to accommodate coincident peak demand growth by network

	Coefficients per MW		
Parameter	Rural	Semiurban	Urban
$\hat{\alpha}$	0.218	0.224	0.382
$\hat{\beta}$	0.070	0.027	0.038
$\hat{\gamma}$	0.530	0.042	0.723

	Coefficients p.u. of Base Network Capacity		
Parameter	Rural	Semiurban	Urban
$\hat{\alpha}$	0.218	0.224	0.382
$\hat{\beta}$	1.981	2.191	2.581
$\hat{\gamma}$	0.530	0.042	0.723

	MV Contribution Parameters		
Parameter	Rural	Semiurban	Urban
$\hat{\phi}$	0.642	0.077	0.469
$\hat{\delta}$	0.135	0.087-0.095	0.096

2.3.7 Limitations and Future Work

The experiments herein indicate that the network deferral value of DERs within any large-scale distribution network – or the ability to accommodate coincident peak demand growth d without network upgrades by reducing net demand in LV and MV voltage levels y – can be estimated fairly accurately using a parsimonious equality of the form:

$$y_{lv} + (1 - \delta)y_{mv} = \alpha d_{lv} + \beta d_{lv}^2 + \gamma d_{mv}$$

where parameters are estimated via a series of AC optimal power flow simulation experiments described in Section 2.3.5. However, these experiments make three assumptions that could be relaxed and explored in future work.

1. I assume that all network customer nodes in each distribution system are 'active users' and thus available to site and operate distributed generation or storage or to reduce demand in response to network congestions.

2. I assume that all 'active' network users respond as needed to ensure feasible power flows across the distribution network.

3. I assume that all 'active' network users reduce real and reactive power demand with a fixed power factor.

The first two assumptions imply that all network users act rationally, respond to appropriate price signals, incentives, and/or dispatch signals to contribute to net demand reductions and do so reliably without fail. These assumptions are consistent with the somewhat idealized least-cost system-wide planning framework for which these experiments are developed (discussed in Chapter 3). In reality, incentivizing participation of myriad distributed actors in the optimal dispatch and management of distribution network constraints will involve transaction costs and face behavioral economics barriers that will no doubt result in less than full participation of all network users. Additionally, it is unlikely that network users will respond with perfect reliability, making this dispatch problem stochastic in nature and

thus requiring either robust optimization methods or conservative heuristics such as reserve commitments to ensure power flows remain reliable in all contexts. As such, relaxing either or both of these first two assumptions would likely make the results presented in this section a somewhat optimistic upper bound estimate on the potential value of DERs for network capacity deferral.

For example, if users at ideal locations at the ends of LV feeders with the greatest marginal losses cannot be curtailed, other network users 'upstream' must be called upon instead. Each kW of demand reduction at these sites will have somewhat lower effect on congestions per unit due to lower marginal losses at these users' locations. This dynamic can be seen in the experiments in Section 2.3.5 where customers in MV were preferentially curtailed where feasible, requiring greater total net demand reduction than in comparable experiments with demand reduction exclusively in LV. If these results are considered as an extreme case – e.g., where the location of net demand reduction is forced all the way from LV to MV rather than simply to a less than ideal location in LV – then suboptimal siting may increase total required net demand reduction by on the order of 8 to 14 percent at maximum.

Similarly, let us assume that a distribution system operator knows it requires 500 kW of collective net demand reduction below a given MV-LV transformer in order to relieve congestions at peak loading but believes active users will only respond with 90 percent reliability. In this case, the distribution system operator will need a reserve margin of 55.6 kW of additional active users on call to ensure an adequate response. Thus, the system planning context presented in this thesis could be extended by adding a reserve requirement for DER capacity in each distribution network zone or by de-rating the available distributed generation, storage, or demand response capacity at peak periods by an expected reliability rate (similar to the 'forced outage rates' used in generation reserve planning) when considering the effective substitution of DERs for distribution network capacity.

Finally, the third assumption – that active users' operate with fixed power factors – implies that net demand reductions are achieved either with curtailment of real power consumption or with distributed generation or storage operating at a fixed power factor. This

assumption is consistent with most interconnection standards to date, which require DG and storage devices to operate at fixed power factors. However, many DERs are actually capable of providing reactive power compensation. AC-DC inverters associated with solar PV, electrochemical batteries, wind turbines, and fuel cells can all technically use a portion of their capacity to supply or consume VARs. So-called 'smart inverters' capable of receiving remote dispatch signals or adjusting power factor based on a local control strategy are becoming increasingly common (for more, see e.g., Braun (2007); Ntakou and Caramanis (2015); Ding et al. (2016)). These devices could be used to improve the power factor of co-located demand by providing capacitance locally to compensate for any inductive loads. This improvement in power factor could in turn reduce apparent power flows across the distribution network associated with the user's demand, allowing additional demand growth to be accommodated before network constraints become binding.

Table 2.7 illustrates the additional congestion relief that might result from reactive power (Q) compensation that brings a user's power factor (PF) up to unity given different initial power factors. All values are in per unit of the user's real power consumption (P) and I assume 30 percent marginal distribution losses at peak network loading at the user's location for this example. As this table illustrates, reactive power compensation with smart inverters could reduce apparent power (S) withdrawal at the user's location by up to 11 percent for user's with power factors above 0.9 (common for most residential and commercial customers). The second row (highlighted in Table 2.7) represents the fixed power factor of 0.958 assumed for all network users in the experiments above, which would correspond to a 4 percent decline in apparent power draw if corrected to unity power factor. Furthermore, reductions in apparent power withdrawals at the user's location are compounded by the high marginal losses experienced during peak network loading. As a result, power factor correction for a LV user with a power factor of 0.958 would reduce apparent power flows at the primary transmission substation by 5.7 percent of the user's real power demand, assuming 30 percent marginal losses. The impact on power flows across other components would lie somewhere between the apparent power reductions at the substation and the user's location.

Table 2.7: Approximate reduction in apparent power flows possible via reactive power compensation (or power factor correction) for users with different power factors

	User's power consumption				Approx. marginal losses	Total reduction in S at	
	PF	P	Q	S	at primary substation	substation w/1.0 PF	
	1.00	1.00	0.00	1.00	0.000	0.000	
→	0.958	1.00	0.30	1.04	0.013	0.057	←
	0.95	1.00	0.33	1.05	0.016	0.068	
	0.90	1.00	0.48	1.11	0.033	0.144	
	0.85	1.00	0.62	1.18	0.053	0.229	
	0.80	1.00	0.75	1.25	0.075	0.325	
	0.75	1.00	0.88	1.33	0.100	0.433	
	0.70	1.00	1.02	1.43	0.129	0.557	

Reduction in apparent power flow at substation assumes 30 percent marginal losses at network user's location. Results for a power factor of 0.958 are highlighted as this is the power factor used for all network users in the AC OPF experiments above.

Future research could therefore model net demand reduction via distributed generators with variable power factor (PV nodes rather than PQ nodes). This would presumably increase the network deferral value of any DERs by on the order of 5-10 percent for typical power factors in the range of 0.95 to 0.9.

In combination then, the three restrictive assumptions used herein may counteract one another in terms of directional bias, but further research could be fruitful and would be needed to confirm the magnitude of each effect.

2.4 Modeling Distribution Network Expansion and Deferral: Network Expansion

The traditional approach to accommodating an increase in coincident peak demand is to make new investments in network assets that ensure expected power flows remain feasible during peak demand periods. In this section, I present an experimental method for estimating the total cost of distribution network reinforcements or upgrades required to accommodate a given margin of coincident peak demand growth. Paralleling the net demand reduction and network expansion deferral experiments in Section 2.3 above, this method proceeds by independently varying coincident peak demand in both low and medium voltage levels (LV and MV). However, in lieu of an optimal power flow simulation to identify necessary net demand reductions, this experiment uses the Reference Network Model (RNM), a distribution network planning model detailed in Domingo et al. (2011), to estimate the least cost set of network investments required to accommodate a given increase in peak demand. I then use linear regression to estimate a function that predicts network expansion costs as a function of coincident peak demand in LV and MV.

2.4.1 Experimental Method: RNM Network Expansion Experiments with Increased Peak Demand

The Reference Network Model (Domingo et al., 2011; Domingo, 2018) is a distribution planning model which emulates the engineering design process of an efficient electric distribution company by specifying the placement and layout of all major distribution network components connecting one or more primary transmission interconnection substations with all power injection or consumption points (i.e., demand and DERs). The model designs the high, medium and low voltage networks, planning both substations and feeders (conductors). In designing the network layout, the model considers geographical constraints such as the street map, the topography of the area, and forbidden rights of way such as nature reserves or water bodies.

The RNM takes as input the location and power injection/withdrawal profile of all network users as well as a catalog containing cost and performance characteristics and probability of component failure for available distribution network assets and equipment (i.e., various cables, overhead lines, distribution transformers, substation components, and protection devices), and the cost and time burden of maintenance actions. Given these inputs, the RNM constructs a network to serve all network users while minimizing total network costs (including capital expenditures, operational expenditures, and a specified penalty for resistive losses) and meeting three specified quality of service constraints: (1) maximum system average interruption duration index (SAIDI); (2) maximum system average interruption frequency index (SAIFI); and (3) maximum acceptable voltage range at every node. The RNM can be run in a 'greenfield' mode, designing the full network from scratch, or in a 'brownfield' or network expansion mode taking as inputs the existing network layout and location of the utility's existing network users and specifying the layout of network reinforcements and extensions necessary to serve projected changes in network use over the planning period.

The ability of the RNM to construct networks representative of European distribution network planning practices has been well vetted[25] and the model has been used in various research purposes to date (see Domingo (2018)). In addition, the RNM was used to originally construct the three European networks used for each of the experiments in this thesis (see Prettico et al. (2016)). Thus, I employ the same model to estimate the cost of expanding each of these three networks to accommodate coincident peak demand growth.

These simulations employ the experimental design summarized by Algorithm 3:

[25]A version of the model designed to build synthetic networks representative of U.S. utility planning practices has also recently been developed as part of the SMART-DS project, a joint project of the National Renewable Energy Laboratory, MIT Energy Initiative, IIT-Comillas, and GE Grid Solutions with support from ARPA-E. See Krishnan et al. (2017)

Algorithm 3: Experimental method using Reference Network Model simulations to determine cost of distribution network expansion necessary to accommodate increased coincident peak demand

Data:

- Existing distribution network data in RNM 'brownfield' input format, including set of all network users $\mathcal{N}$ and all network branches $\mathcal{B}$
- RNM distribution network asset catalog
- Set of incremental increases in coincident peak demand in LV and MV $(d_{lv}, d_{mv}) \in \mathcal{D}$ (p.u. of base coincident peak demand in each voltage level) to perform RNM simulations

Result: Matrix of results for each RNM simulation

begin
  Load network data;
  foreach $(d_{lv}, d_{mv}) \in \mathcal{D}$ **do**
    foreach *LV user* i **do**
      User demand $d_i = p_i \times d_{lv}$ where p is a user's base demand
    end
    foreach *MV user* m **do**
      User demand $d_m = p_m \times d_{mv}$ where p is a user's base demand
    end
  end
  Run RNM network expansion simulation;
  Record results: success/failure of RNM solution; total net present value of network reinforcements and total network maintenance costs; break down of network reinforcement costs by type of substation, transformer, and voltage level;
end

2.4.2 Experiment: Drivers of Distribution Network Expansion Costs

This section presents results from an experiment using the method described in Algorithm 3 to identify the effect of coincident peak demand growth in both medium and low voltage levels (20 kV and 0.4 kV respectively) of a large-area distribution network. I perform the experiment for each of the three representative European networks used throughout this chapter. I increase coincident peak demand in LV from 1.0 to 1.2 times the base network capacity[26] for LV demand in each network with demand increased in increments of 0.02 p.u. I also independently vary coincident peak demand in MV from 1.0 to 1.25 times the base network capacity for MV demand in increments of 0.05 p.u. This range mirrors the variation in LV and MV demand explored in the net demand reduction experiments in Section 2.3.5 to allow comparison between network reinforcement and net demand reduction (or 'non-wires') strategies. This results in 66 individual combinations of LV and MV demand growth levels. Incremental network costs for each experiment are the sum of new reinforcements/upgrades to LV and MV circuits, LV-MV transformers, the primary substation, various protection devices in each level, as well as the RNM's estimate of preventative and restorative maintenance expenditures for each component. Capital and maintenance expenditures are converted to net present value terms integrated over 40 years at 5 percent discount rate.

Figure 2-29 presents the relationship between total incremental network costs across all components as a function of coincident peak demand growth for each network. Variations in LV demand drive the majority of network reinforcements, just as they did for net demand reductions required to accommodate coincident peak demand growth in Section 2.3.5. This is in part a function of the order of magnitude larger total demand from customers in LV as compared to MV customers in each of these networks, as well as the fact that LV demand can drive reinforcements or upgrades in both LV components as well as MV circuits and at the primary substation. In contrast, coincident peak demand of MV customers only contributes to costs in MV circuits or at the primary substation.

[26]Base network capacity is defined as the total coincident peak demand that can be accommodated by a given network without either network reinforcements or net demand reductions required to render power flows feasible across all network components.

In addition, there is a sharp discontinuity in total incremental costs for the urban network at about 3 percent increase in total coincident peak demand (Fig. 2-29). Fig. 2-30 breaks down total incremental network costs into components, including upgrades to LV circuits, MV-LV transformers, MV circuits, and the primary substation in each network. As this figure illustrates, the jump in cost in the urban network is driven by an upgrade at the primary substation. Substation components exhibit economies of unit scale and involve large, discrete component investments (such as transformers). Like utility planners, the RNM anticipates future demand growth beyond the current planning window when deciding how large to size components when making discrete investment decisions.[27] As such, it sizes the substation upgrade to capture economies of unit scale and provide 'headroom' for anticipated demand growth. This results in a discontinuous change in total incremental costs as this 'lumpy' investment is made.

Incremental network costs for other cost components also exhibit smaller discontinuities, reflecting discrete investment decisions made by the network expansion model. After the primary substation, the next largest discrete increase in cost is associated with MV circuit upgrades, as exhibited in the rural network results at around 8 percent coincident peak demand growth (Fig. 2-30). However, as unit sizes are smaller relative to total network demand growth, changes in incremental network costs (excluding the primary substation) are more gradual and can be considered approximately linear. Fig. 2-30 includes a linear regression fit for incremental costs excluding primary substation upgrades as a function of coincident peak demand growth.

[27] As run here, the model is configured to consider 10 years of additional demand growth at 1 percent per year when considering the sizing of network components.

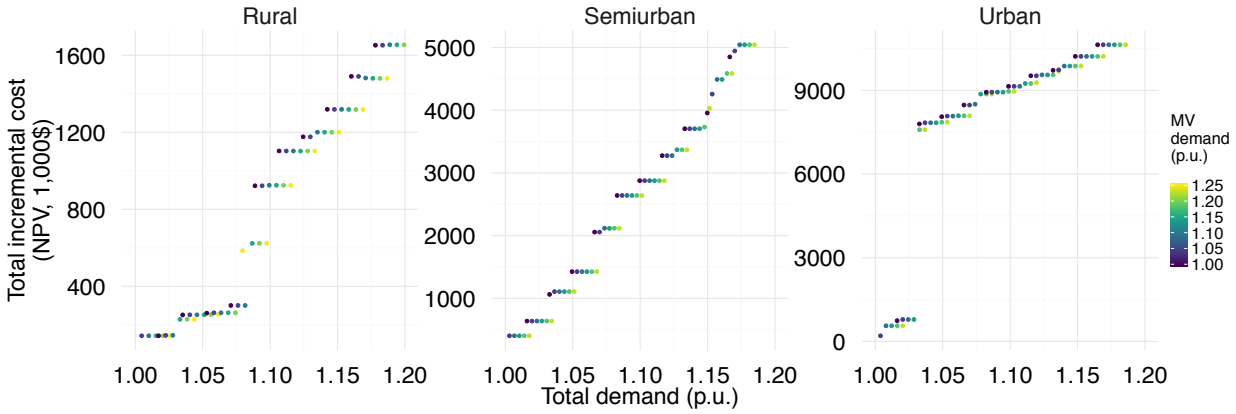

Figure 2-29: Total distribution network expansion cost required to accommodate coincident peak demand growth of up to 20 percent in LV and up to 25 percent in MV

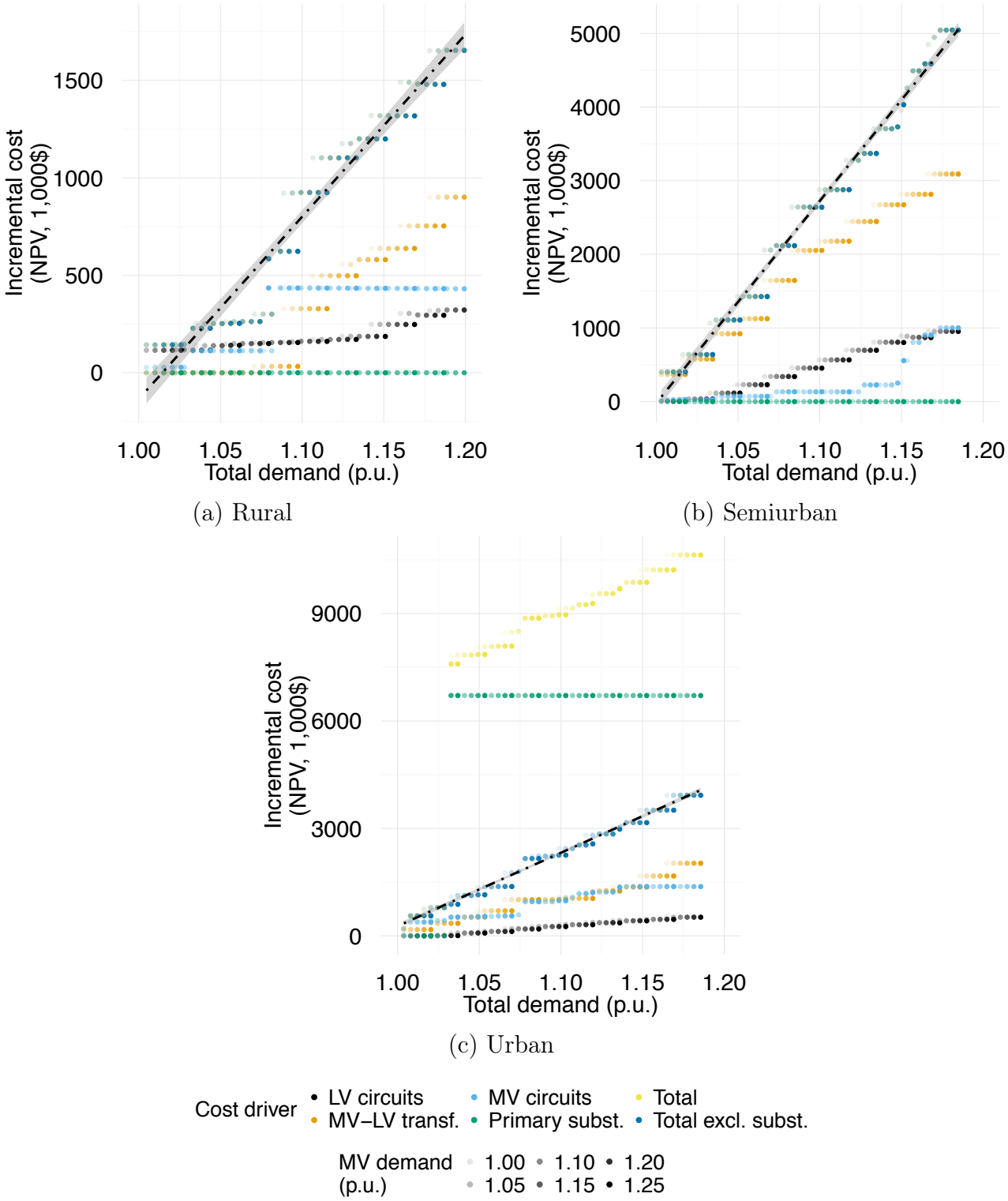

(a) Rural

(b) Semiurban

(c) Urban

Figure 2-30: Distribution network expansion cost by cost component required to accommodate coincident peak demand growth of up to 20 percent in LV and up to 25 percent in MV

This simple regression fit in Fig. 2-30 can be further improved by regressing total incremental costs on independent variations in LV and MV demand growth (D_{lv}, D_{mv}) as in:

$$\hat{y}(D_{lv}, D_{mv}) = \hat{\alpha} D_{lv} + \hat{\beta} D_{mv} \tag{2.25}$$

As Table 2.8 illustrates, this function provides a strong fit for both the rural and semiurban networks, where no substation upgrades occur across the range of demand growth explored in this experiment. However, we see that this function provides a poor approximation of total network costs in the urban network, as the linear regression terms fail to capture the discrete increase in cost associated with the substation upgrade. In cases where networks may require a large, discrete substation upgrade if demand grows sufficiently during the next planning window, a binary variable can be included in the regression function, such that the variable is equal to 0 if coincident peak demand is below the level sufficient to trigger a substation upgrade, S, and 1 if above this level (see the final column in Table 2.8), as in:

$$\hat{y}(D_{lv}, D_{mv}) = \hat{\alpha} D_{lv} + \hat{\beta} D_{mv} + \hat{\gamma}(D_{lv} + D_{mv} \overset{?}{>} S) \tag{2.26}$$

Network expansion costs for a large-scale distribution network can therefore be approximated via regression on results from Reference Network Model simulations performed as per Algorithm 3. Future work could further explore sensitivity of results to variation in demand concentration, as per the net demand reduction experiments in Section 2.3.2. However, this serves as sufficient proof of concept for this stage of work. Chapter 3 will demonstrate how results from each of the experimental methods introduced in this chapter can be used to parameterize a system-wide planning model capable of incorporating distributed energy resources at multiple unit scales and associated impacts on distribution network-level losses and reinforcement costs.

Table 2.8: Regression coefficient estimates for total incremental network costs as a function of variation in LV and MV coincident peak demand by network

	Coefficients 1000$ per MW			
Variable	Rural	Semiurban	Urban (excl. substation term)	Urban (incl. substation term)
D_{lv}	329.6***	335.6***	713.5***	300.9***
	(9.43)	(4.07)	(66.27)	(4.28)
D_{mv}	93.8	74.8**	592.3	102.1***
	(58.88)	(34.39)	(488.89)	(25.05)
$D_{lv} + D_{mv} > S$				−6,723.1***
				(43.11)
Constant	−8,661.8***	−25,603.3***	−44,885.1***	−12,329.7***
	(329.44)	(419.49)	(5,665.22)	(355.67)
Observations	66	66	66	66
Adjusted R^2	0.949	0.991	0.640	0.999
Residual Std. Error	122.5	143.2	1,933.2	98.3
Deg. of Freedom	63	63	63	62
	Coefficients 1000$ p.u. of Base Network Capacity			
Variable	Rural	Semiurban	Urban (excl. substation term)	Urban (incl. substation term)
D_{lv}	8,338.4***	25,286.9***	44,577.3***	18,796.4***
	(238.64)	(306.66)	(4,140.23)	(267.61)
D_{mv}	281.5	493.8**	3,713.5	640.1***
	(176.63)	(226.98)	(3,065.36)	(157.05)
$D_{lv} + D_{mv} > S$				−6,723.1***
				(43.11)
Constant	−8,661.8***	−25,603.3***	−44,885.1***	−12,329.7***
	(329.44)	(419.49)	(5,665.22)	(355.67)
Observations	66	66	66	66
R^2	0.951	0.991	0.651	0.999
Adjusted R^2	0.949	0.991	0.640	0.999
Residual Std. Error	122.5	143.2	1,933.2	98.3
Deg. of Freedom	63	63	63	62
Note:			*p<0.1; **p<0.05; ***p<0.01	

Chapter 3

Electricity Resource Expansion Planning with Distributed Energy Resources: the GenX Modeling Framework

3.1 Overview

This chapter describes the 'GenX' electricity resource expansion planning model, a highly configurable optimization modeling framework designed to incorporate a wide range of state-of-the-art methods to provide improved decision support capabilities for a changing electricity landscape (Jenkins and Sepulveda, 2017).[1] See Section 1.2 for a review of recent developments in the electricity resource capacity planning literature and a discussion of the role of planning models in utility integrated resource planning, techno-economic assessment of emerging technologies, and indicative planning to inform policy and regulatory decisions.

GenX is a constrained optimization model that determines the mix of electricity generation, storage, and demand-side resource investments and operational decisions to maximize

[1]The overall GenX modeling framework was developed and implemented with Nestor Sepulveda and has been employed by the co-developers in a growing body of research. Specific capabilities developed for this thesis include the multi-zonal modeling framework and representation of distribution networks and distributed energy resources. This chapter includes material originally published in Jenkins and Sepulveda (2017).

social welfare in a future planning year. To do so, the model's objective function seeks to meet electricity demand in the planning year while minimizing the costs of electricity supply and maximizing utility of consumption all subject to a variety of power system operational constraints and specified policy constraints, such as CO_2 emissions limits. As GenX is implemented as a constrained cost minimization problem, the utility of consumption is represented by including a base level of demand in each hour and a set of price-responsive demand 'segments,' each representing a set of consumers with different willingness to pay for electricity consumption. If the marginal cost of supply rises above the willingness to pay of any segment, demand is reduced by the aggregate consumption of that segment of consumers. In this way, the demand curve for electricity is represented as a segment-wise approximation capturing the varying elasticity of demand in an approximate manner. A final segment of inelastic consumers is included as well, and if generation scarcity or binding network constraints prevent sufficient supply at any zone, demand can only be balanced via shedding demand in this segment at a very high cost of non-served energy (e.g., \$10,000/MWh).

The GenX model formulation allows for the simultaneous co-optimization of seven interlinked power system decision layers:

1. Capacity expansion planning (e.g., investment and retirement decisions for a full range of centralized and distributed generation, storage, and demand-side resources);
2. Hourly dispatch of generation, storage, and demand-side resources;
3. Unit commitment decisions and operational constraints for thermal generators;
4. Commitment of generation, storage, and demand-side capacity to meet system operating reserves requirements;
5. Transmission network power flows (including losses) and network expansion decisions;
6. Distribution network power flows, losses, and network reinforcement decisions; and
7. Interactions between electricity and heat markets.

With appropriate configuration of the model, GenX thus allows the user to tractably consider several interlinking decision layers in a single, monolithic optimization problem

that would otherwise have been necessary to solve in different separated stages or models. However, depending on the dimensionality of the problem, it may not be possible to model all seven decision layers at the highest possible resolution of detail. As such, the GenX model is designed to be highly configurable, allowing the user to specify the level of detail or abstraction along each of these seven layers or to omit one or more layers from consideration entirely. In particular, the appropriate level of model resolution with regards to (1) chronological variability of load and renewable energy availability, (2) operational constraints of thermal generators and system flexibility requirements, and (3) transmission and distribution network representation varies for a given planning problem or research question. The model can therefore be configured as desired with different degrees of resolution possible on each of these three key dimensions using a variety of state-of-the-art techniques. Fig. 3-1 depicts the range of configurations currently possible along the three key dimensions of chronological detail, operational detail, and network detail.

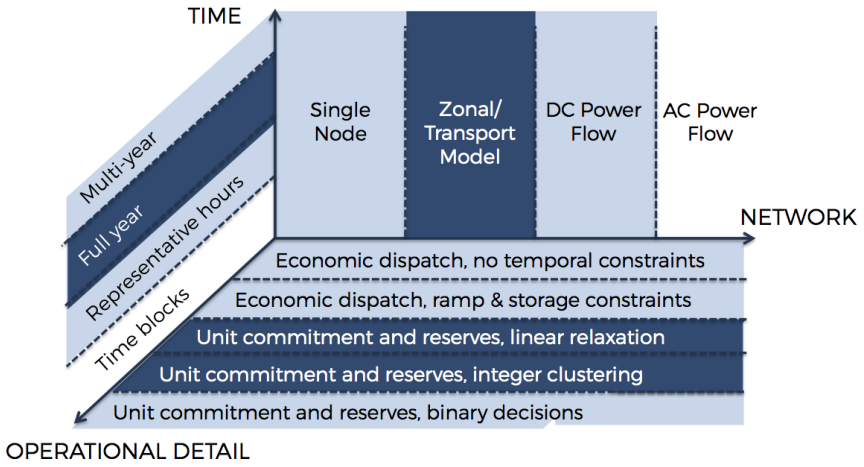

Figure 3-1: Range of configurations currently implemented in the GenX model along three key dimensions of model resolution
Dark blue areas represent the level of detail along each key dimension used for the research in this thesis. The full range of configurations possible in the GenX model are highlighted in light blue. See Jenkins and Sepulveda (2017) for additional detail on these options.

The full capabilities of the GenX model are described in Jenkins and Sepulveda (2017). This chapter describes the model as specifically configured to incorporate transmission and distribution network losses, congestions, and reinforcements and distributed energy resources.

The remainder of this section provides a high level overview of the model, while the following sections present the mathematical formulation.

The model is usually configured to consider a full year of operating decisions at an hourly interval to represent some future planning year. In this sense, the current formulation is *static* because its objective is not to determine when investments should take place over time, but rather to produce a snapshot of the minimum-cost generation capacity mix under some pre-specified future conditions. However, the current implementation of the model can be run in sequence (with outputs from one planning year used as inputs for another subsequent planning year) to represent a step-wise or myopic expansion of the network.[2] In addition, to improve computational tractability, the model can consider a reduced number of representative hours within the future planning year, selected using an appropriate time domain reduction technique (e.g., de Sisternes and Webster (2013); de Sisternes (2014); Poncelet et al. (2016); Nahmmacher et al. (2016); Blanford et al. (2016); Merrick (2016)).

As configured for use in this thesis, the model includes unit commitment (e.g., start-up and shut-down) decisions and associated constraints for thermal generators (Morales-Espana et al., 2013). Depending on the scale of the problem, these decisions can be modeled as discrete decisions using an efficient clustering of similar or identical units (as per Palmintier (2013); Palmintier and Webster (2014)); or by using a linear relaxation (or convex hull) of the integer unit commitment constraints set. In general, I employ the latter configuration herein, as it provides an ideal combination of computational performance and accuracy while allowing sufficient network detail to capture the key tradeoffs associated with DERs – the key focus of this thesis.

The model can also be configured to consider commitment of capacity to supply frequency regulation and operating reserves needed by system operators to robustly resolve short-term uncertainty in load and renewable energy forecasts and power plant or transmission network failures. Alternatively, reserve commitments can be ignored to reduce computational burden.

In this work, transmission networks are represented at a zonal level with transport con-

[2] A version of the model allowing simultaneous co-optimization of sequential planning decisions is currently under development.

straints on power flows between zones (as per, e.g., Nelson et al. (2012); Mai et al. (2013); Hirth (2017)). Power flows between zones are constrained with a maximum transfer capacity, and network capacity expansion decisions (to increase this transfer capacity) are included as continuous decisions.[3] Transmission losses between zones are represented with a segment-wise linear approximation of quadratic losses as a function of power flows between zones (as per Zhang et al. (2013); Fitiwi et al. (2016)). The number of segments in the linear approximation is specified as desired. In this multi-zonal configuration, GenX can therefore consider siting generators in different locations, including balancing tradeoffs between access to different renewable resource quality, siting restrictions, and impacts on transmission network congestions, power flows, and losses, each of which are important to considering the locational value of DERs and other resources.

Finally, this thesis introduces a novel method for representing distribution networks using a zonal approximation (see Sections 3.3.8–3.3.9), with each zone representative of a different distribution network topology (see Fig. 3-2). Electricity demand in each distribution zone is split between medium and low voltage levels. Resource capacity investment and operational decisions are indexed across both zone and voltage level in the system. This allows the model to select the optimal location and scale of capacity investments and operations across each location, including considering distributed energy resources (DERs, such as distributed solar PV, energy storage, fuel cells, etc.) in different distribution zones and voltage levels.

Losses due to power flows within each distribution network zone can be represented as a segment-wise linear approximation of a polynomial function of power injections and withdrawals within each zone. This function is parameterized based on detailed offline AC power flow simulations for the representative networks, as described in Chapter 2, Section 2.2.

Additionally, distribution network reinforcement costs modeled as a function of peak

[3]This is an abstraction of the more discrete transmission expansion decisions encountered in reality, which are typically the focus of more detailed transmission planning models that could be used in conjunction with this planning tool if greater focus on transmission investments is important. Binary decision variables for network expansion can also be easily implemented in this modeling framework, but computational performance may suffer.

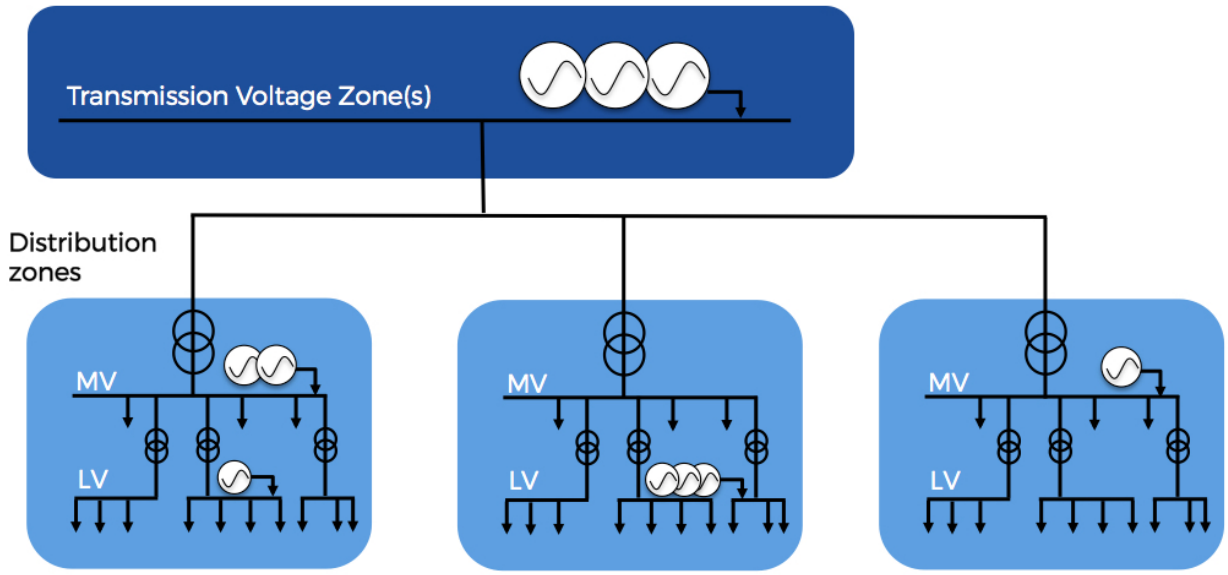

Figure 3-2: Visual schematic of multi-zonal electricity system planning model
The modeling framework features multiple transmission and distribution network zones, constrained power flows between zones, and siting of different scales of generation and storage resources at each voltage level.

power injections (generation) or withdrawals (demand) within each distribution voltage level and network zone. Total network capacity reinforcements required are a function of peak injections or withdrawals within each distribution zone, less any network capacity margin that can be secured via dispatch of DERs or demand response within that zone. The effective network margin gained per unit of net demand reduction is represented as a segment-wise linear approximation of a polynomial function for each representative distribution network zone parameterized based on the offline optimal power flow simulation method presented in Chapter 2, Section 2.3. Distribution network expansion costs are likewise parameterized using a distribution network planning model as per the methods in Chapter 2, Section 2.4.

Finally, power flows between transmission and distribution voltage zones can be constrained to represent primary substation capacity constraints. Substation upgrade decisions and associated costs can also be factored in here in a similar manner as transmission expan-

sion decisions.[4]

With the methodological contributions developed in this thesis, the GenX model can thus be configured to evaluate the role and value of DERs in a system-wide electricity resource capacity planning framework (see Chapter 4). This includes balancing important tradeoffs between economies of unit scale at different voltage levels on the one hand and the differential impacts or benefits of locating DERs at different zones or voltage levels on the other hand.

The high level structure of the GenX model is presented in Table 3.1, with reference to each block of equations implementing the various components of the configurable model. GenX is implemented using Julia Language (Bezanson et al., 2017) with the model formulation specified using JuMP (Dunning et al., 2017), a package for mathematical programming embedded in Julia. JuMP supports a number of open-source and commercial solvers for a variety of problem classes, including linear programming and mixed-integer programming. Gurobi (Gurobi Optimization Inc., 2016) is employed as the solver for both LP and MILP problems in the present work.

The remainder of this chapter is structured as follows. First, Section 3.2 introduces the nomenclature used to describe the formulation of the model. Section 3.3 then presents the full mathematical formulation of this mixed integer linear programming (MILP) or linear programming (LP) problem, including the decision variables, objective function, and constraints and provides descriptions of each key set of equations.

[4]Like transmission expansion, this decision variable is currently implemented as a continuous decision, a clear abstraction given the discontinuous substation upgrade costs exhibited by some networks in Section 2.4. Options for incorporating discrete substation upgrade decisions will be explored in the future, but are currently excluded due to computational constraints.

Table 3.1: General structure of GenX model and reference to equations

Minimize Investment costs + Operational costs - DER Revenues (3.1);	
Subject to:	
Resource investment and retirement constraints	(3.2–3.3)
Demand balance constraint	(3.4)
Transmission network power flow constraints	(3.5–3.7)
Transmission network loss constraints	(3.8–3.17)
Distribution network loss constraints	(3.19–3.29)
Distribution network power withdrawal and injection constraints	(3.30–3.39)
Unit commitment constraints	(3.40–3.49)
Economic dispatch constraints for other thermal generators	(3.50–3.53)
Variable renewable energy resources operational constraints	(3.54–3.55)
Storage resources operational constraints	(3.56–3.62)
Flexible demand management constraints	(3.63–3.65)
Demand response constraint	(3.66)
Operating reserves constraints	(3.67–3.93)
CO_2 emissions constraint	(3.94)
Minimum renewable energy mandate constraint	(3.95)

3.2 Nomenclature

3.2.1 Model Indices and Sets

Table 3.2: Model indices and sets

Notation	Description
$t, e \in \mathcal{T}$	where t denotes an hour and $\mathcal{T}$ is the set of hours in the data series (e is an alternate index).
$z, d \in \mathcal{Z}$	where z denotes a zone and $\mathcal{Z}$ is the set of zones in the network (d is an alternate index).
$v \in \mathcal{VL}$	where v denotes a voltage level and $\mathcal{VL}$ is the set of voltage levels at which resources can be installed.
$l \in \mathcal{L}$	where l denotes a line or path and $\mathcal{L}$ is the set of transmission lines/paths in the network.
$y, x \in \mathcal{G}$	where y denotes a technology and $\mathcal{G}$ is the set of available technologies (x is an alternate index).
$s \in \mathcal{S}$	where s denotes a segment and $\mathcal{S}$ is the set of consumers segments for price-responsive demand curtailment.
$m \in \mathcal{M}$	where m denotes a segment used in segment-wise linear approximation of quadratic terms in loss functions and $\mathcal{M}$ is the set of segments $[0 : M]$
$n \in \mathcal{N}$	where n denotes a segment used in segment-wise linear approximation of the quadratic term in the distribution network margin function and $\mathcal{N}$ is the set of segments $[0 : N]$
$\mathcal{H} \subset \mathcal{G}$	where $\mathcal{H}$ is the subset of thermal resources.
$\mathcal{RE} \subset \mathcal{G}$	where $\mathcal{RE}$ is the subset of variable renewable energy resources.
$\mathcal{O} \subset \mathcal{G}$	where $\mathcal{O}$ is the subset of storage resources.
$\mathcal{DR} \subset \mathcal{G}$	where $\mathcal{DR}$ is the subset of flexible demand management resources.
$\mathcal{UC} \subset \mathcal{H}$	where $\mathcal{UC}$ is the subset of thermal resources subject to unit commitment constraints.
$\mathcal{D} \subset \mathcal{RE}$	where $\mathcal{D}$ is the subset of dispatchable[5]renewable resources.
$\mathcal{ND} \subset \mathcal{RE}$	where $\mathcal{ND}$ is the subset of non-dispatchable renewable resources.
$\mathcal{E} \subset \mathcal{L}$	Subset of transmission lines eligible for reinforcement
$\mathcal{R} \subset \mathcal{Z}$	Subset of transmission zones
$\mathcal{V} \subset \mathcal{Z}$	Subset of distribution zones
$\mathcal{PW} \subset \mathcal{T}$	Subset of hours in which coincident peak withdrawal may occur
$\mathcal{PI} \subset \mathcal{T}$	Subset of hours in which coincident peak injection may occur

[5]Dispatchable renewable energy resources allow generation curtailment. Non-dispatchable renewable energy resources are must-run resources that cannot be curtailed.

3.2.2 Decision Variables

Table 3.3: Decision variables

Notation	Description
$\Omega_{y,z,v} \in \mathbb{R}_+$ or $\mathbb{Z}_+$	Installed capacity of technology [MW or discrete units].
$\Delta_{y,z,v} \in \mathbb{R}_+$ or $\mathbb{Z}_+$	Retired capacity of technology [MW or discrete units].
$\Theta_{y,t,z,v} \in \mathbb{R}_+$	Energy injected into the grid (or flexible demand deferred) [MWh].
$\Pi_{y,t,z,v} \in \mathbb{R}_+$	Energy withdrawn from grid (or deferred demand satisfied) [MWh].
$\Gamma_{y,t,z} \in \mathbb{R}_+$	Stored energy level [MWh].
$\upsilon_{y,t,z} \in \mathbb{Z}_+$	Commitment state of generator cluster.
$\chi_{y,t,z} \in \mathbb{Z}_+$	Startup events of generator cluster.
$\zeta_{y,t,z} \in \mathbb{Z}_+$	Shutdown events of generator cluster.
$\Lambda_{s,t,z} \in \mathbb{R}_+$	Non-served energy/curtailed demand from the price-responsive demand [MWh].
$\ell_{l,t} \in \mathbb{R}$	Transmission losses [MWh].
$\Phi_{l,t} \in \mathbb{R}$	Transmission power flow [MWh].
$\Phi^+_{l,t}, \Phi^-_{l,t} \in \mathbb{R}_+$	Power flow absolute value auxiliary variables
$\gamma_l \in \mathbb{R}_+$	Expansion of transmission power flow capacity [MW].
$\S^+_{m,l,t}, \S^-_{m,l,t} \in \mathbb{R}_+$	Segment of segment-wise linear approximation of quadratic transmission losses term [MW] in positive (+) and negative (-) domains.
$\beta^+_{m,l,t}, \beta^-_{m,l,t} \in \{0,1\}$	Activation variable for segment of segment-wise linear approximation of quadratic transmission losses term in positive (+) and negative (-) domains.
$\ell_{z,t} \in \mathbb{R}+$	Losses within distribution zone [MWh].

Continued on next page

Table 3.3—continued from previous page

Notation	Description
$\S^{+}_{m,z,t}, \S^{-}_{m,z,t} \in \mathbb{R}_{+}$	Segment for segment-wise linear approximation of quadratic term in distribution losses function [MW] in the positive (+) and negative (-) domains.
$\beta^{+}_{m,z,t}, \beta^{-}_{m,z,t} \in \{0,1\}$	Activation variable for segment of segment-wise linear approximation of quadratic term in distribution losses function in positive (+) and negative (-) domains.
$\lambda^{W}_{z} \in \mathbb{R}+$	New power withdrawal network capacity added to distribution zone [MW].
$\lambda^{I}_{z} \in \mathbb{R}+$	New power injection network capacity added to distribution zone [MW].
$\phi^{W}_{z,t} \in \mathbb{R}+$	Power withdrawal margin gained via optimal dispatch of distributed resources [MW].
$\phi^{I}_{z,t} \in \mathbb{R}+$	Power injection margin gained via optimal dispatch of distributed resources [MW].
$\delta^{mv}_{z,t}$	Auxiliary variable for net demand reduction in medium voltage used to provide additional power withdrawal margin [MW]
$\S^{\phi,W}_{m,z,t} \in \mathbb{R}+$	Segment for segment-wise linear approximation of quadratic term in network withdrawal margin gained from optimal dispatch of distributed resources.
$\rho^{+}_{y,z,t} \in \mathbb{R}_{+}$	Reserves contribution up [MW].
$\rho^{-}_{y,z,t} \in \mathbb{R}_{+}$	Reserves contribution down [MW].
$\theta^{+}_{y,z,t} \in \mathbb{R}_{+}$	Frequency regulation contribution up [MW].
$\theta^{-}_{y,z,t} \in \mathbb{R}_{+}$	Frequency regulation contribution down [MW].
$\rho^{+C}_{y,z,t} \in \mathbb{R}_{+}$	Reserves contribution up [MW] from storage technology during charging process.

Continued on next page

Table 3.3—continued from previous page

Notation	Description
$\rho_{y,z,t}^{-C} \in \mathbb{R}_+$	Reserves contribution down [MW] from storage technology during charging process.
$\theta_{y,z,t}^{+C} \in \mathbb{R}_+$	Frequency regulation contribution up [MW] from storage technology during charging process.
$\theta_{y,z,t}^{-C} \in \mathbb{R}_+$	Frequency regulation contribution down [MW] from storage technology during charging process.
$\rho_{y,z,t}^{+D} \in \mathbb{R}_+$	Reserves contribution up [MW] from storage technology during discharging process.
$\rho_{y,z,t}^{-D} \in \mathbb{R}_+$	Reserves contribution down [MW] from storage technology during discharging process.
$\theta_{y,z,t}^{+D} \in \mathbb{R}_+$	Frequency regulation contribution up [MW] from storage technology during discharging process.
$\theta_{y,z,t}^{-D} \in \mathbb{R}_+$	Frequency regulation contribution down [MW] from storage technology during discharging process.
$\rho_t^{+,unmet} \in \mathbb{R}_+$	Unmet reserves up [MW].
$\rho_t^{-,unmet} \in \mathbb{R}_+$	Unmet reserves down [MW].

3.2.3 Parameters

Table 3.4: Model parameters

Notation	Description
$D_{t,z}$	Electricity demand [MWh].
$SHARE_z^{mv}$	Share of electricity demand located at medium distribution voltage [%].
$CNSE_s$	Cost of non-served energy/demand curtailment for price-responsive demand segment [$/MWh].
NSE_s	Size of price-responsive demand segment as a fraction of the hourly zonal demand [%].
$\overline{CAP}_{y,z,v}$	Maximum new capacity of technology [MW].
$\underline{CAP}_{y,z,v}$	Minimum new capacity of technology [MW].
$CAP^0_{y,z,v}$	Existing installed capacity of technology [MW].
$U_{y,z,v}$	Unit size of technology [MW].
$CINV_{y,z,v}$	Investment cost (annual amortization of total construction cost) for technology [$/MW-yr].
$CFOM_{y,z,v}$	Fixed O&M cost of technology [$/MW-yr].
$CVOM_{y,z,v}$	Variable O&M cost of technology [$/MWh].
$CFUEL_{y,z,v}$	Fuel cost of technology [$/MWh].
$CSTART_{y,z}$	Startup cost of technology [$/startup].
$RDER_{y,z,v}$	Revenue earned by distributed energy resources for services not endogenously modeled [$/MW-yr].
$CO2_{y,z,v}$	CO_2 emissions per unit energy produced [tons/MWh].
$PMIN_{y,z,v}$	Minimum stable power output per unit of installed capacity [%].
$DISCH_{y,z,v}$	Storage self discharge rate per hour per unit of installed capacity [%].
$EFF^{up}_{y,z,v}$	Single-trip efficiency of storage charging/demand deferral [%].
$EFF^{down}_{y,z,v}$	Single-trip efficiency of storage discharging/demand satisfaction [%].
$P2E^{stor}_{y,z,v}$	Storage power to energy ratio [MW/MWh].

Continued on next page

Table 3.4—continued from previous page

Notation	Description [units]
$FLEX_{y,z,v}$	Maximum percentage of hourly demand that can be shifted or deferred by flexible demand technology [%].
$SHIFT_{y,z,v}$	Time periods over which demand can be shifted or deferred using flexible demand technology before demand must be satisfied [hours].
$RUP_{y,z,v}$	Maximum ramp-up rate per time step [% of capacity/hr].
$RDN_{y,z,v}$	Maximum ramp-down rate per time step [% of capacity/hr].
$MINUP_{y,z,v}$	Minimum uptime for thermal generator before new shutdown [hours].
$MINDN_{y,z,v}$	Minimum downtime or thermal generator before new restart [hours].
$\overline{P}_{y,t,z,v}$	Maximum available generation per unit of installed capacity [%].
$MAP_{l,z}$	Topology of the network: $MAP_{l,z} = 1$ for zone z of origin, -1 for zone z of destination, 0 otherwise.
$TCAP_l$	Transmission line/path capacity [MW].
$VOLT_l$	Transmission line/path voltage [kV].
OHM_l	Transmission line/path resistance [Ohms].
$\overline{TCAP}_l$	Maximum power flow capacity reinforcement [MW]
$CTCAP_l$	Transmission power flow reinforcement cost (annual amortization of total construction cost plus annual O&M cost) [$/MW-yr].
$CDCAP_z^{lv}$	Distribution network reinforcement costs driven by low-voltage network users (annual amortization of total construction cost plus annual O&M cost) [$/MW-yr].
$CDCAP_z^{mv}$	Distribution network reinforcement costs driven by medium-voltage network users (annual amortization of total construction cost plus annual O&M cost) [$/MW-yr].
$\overline{I}_z$	Maximum aggregate power injection possible in distribution [MW]
$\overline{W}_z$	Maximum aggregate power withdrawal possible in distribution [MW]

Continued on next page

Table 3.4—continued from previous page

Notation	Description [units]
$\overline{DCAP}_z^W$	Maximum distribution network withdrawal capacity reinforcement [MW]
$\overline{DCAP}_z^I$	Maximum distribution network injection capacity reinforcement [MW]
$\overline{MARGIN}_z^W$	Maximum network withdrawal margin that can be gained by DER dispatch [MW]
$\overline{MARGIN}_z^I$	Maximum network injection margin that can be gained by DER dispatch [MW]
$LVCOEF_z^W$	Linear term coefficient for net demand reductions in low voltage required to deliver network withdrawal margin [per MW]
$LVCOEF2_z^W$	Quadratic term coefficient for net demand reductions in low voltage required to deliver network withdrawal margin [per MW]
$MVCOEF_z^W$	Linear term coefficient for net demand reductions in medium voltage required to deliver network withdrawal margin [per MW]
$\overline{MV}_z^W$	Maximum contribution of medium voltage net demand reductions to network withdrawal margin required to accommodate low voltage demand [%]
$DISCOUNT_z$	Discount factor applied to contributions of medium voltage net demand reductions to network withdrawal margin required to accommodate low voltage demand [%]
$LVQUAD_z$	Within zone distribution loss coefficient for quadratic term of polynomial function for losses due to net withdrawals in low voltage [per MW]
$MVNET_z$	Within zone distribution loss coefficient for linear term of polynomial function for losses due to net withdrawals in medium voltage [per MW]
$LVTOT_z$	Within zone distribution loss coefficient for linear term of polynomial function for losses due to total withdrawals and injections in low voltage [per MW]

Continued on next page

Table 3.4—continued from previous page

Notation	Description [units]
M	Number of segments to use in piecewise linear approximation of quadratic terms in transmission and distribution losses functions
N	Number of segments to use in piecewise linear approximation of quadratic term in distribution network margin function
$\overline{RSV^+}_{y,z,v}$	Max. contribution of capacity to reserves up [p.u.]
$\overline{RSV^-}_{y,z,v}$	Max. contribution of capacity to reserves down [p.u.]
$\overline{REG^+}_{y,z,v}$	Max. contribution to frequency regulation up [p.u.]
$\overline{REG^-}_{y,z,v}$	Max. contribution to frequency regulation down [p.u.]
$R^+(D)$	Reserves requirement up as a function of hourly load [%].
$R^+(RE)$	Reserves requirement up as a function of hourly variable renewable resource availability[%].
$R^-(D)$	Reserves requirement down as a function of hourly load [%].
$R^-(RE)$	Reserves requirement down as a function of hourly variable renewable resource availability[%].
$F(D)$	Frequency regulation requirement as a function of hourly load [%].
$F(RE)$	Frequency regulation requirement as a function of hourly variable renewable resource availability[%].
$CRSV$	Penalty for unmet reserve requirement [$/MW].
$MINRE$	Minimum penetration of qualifying renewable energy resources required [%].
$\overline{CO2}$	Maximum CO_2 emissions constraint [tons/MWh].

3.3 Model Formulation and Description

This section describes the different indices and sets used in the formulation, followed by mathematical formulation and textual description of each of the expressions and constraints

that make up the model under the configuration used in this thesis. For a full description of alternative configurations, see Jenkins and Sepulveda (2017).

3.3.1 Indices and Sets

Six indices are used in this model: y, x represent technologies $\in \mathcal{G}$; t, e represent hours $\in \mathcal{T}$; z represents a zone $\in \mathcal{Z}$; v represents a voltage level $\in \mathcal{VL}$; l represents a transmission line $\in \mathcal{L}$; and s represents a consumers' segment $\in \mathcal{S}$.

$\mathcal{G}$ denotes the set of resources that can be built/deployed, containing all the different thermal technologies (nuclear, coal, combined cycle gas turbines (CCGTs), open cycle gas turbines (OCGTs), denoted $\mathcal{H} \subset \mathcal{G}$), disptachable (e.g., curtailable) variable renewable energy technologies (wind, solar photovoltaic, solar thermal, denoted $\mathcal{D} \subset \mathcal{G}$), non-dispatchable renewables (such as behind the meter distributed solar PV, denoted $\mathcal{ND} \subset \mathcal{G}$), different storage technologies ($\mathcal{O} \subset \mathcal{G}$), as well as flexible demand management technologies ($\mathcal{DR} \subset \mathcal{G}$). The subset $\mathcal{RE} \subset \mathcal{G}$, denotes the subset of renewable energy resources that qualify to fulfill a minimum renewable energy generation requirement or mandate (e.g., a renewable portfolio standard requirement), if any is modeled.

$\mathcal{T}$ denotes the set of hours modeled in the simulation (e.g., 8760 hours in a full year, or some reduced set of representative hours).

$\mathcal{Z}$ denotes the number of zones simulated in the analysis. There will be one zone for each area of the transmission system at which bulk generation and storage can be installed ($\mathcal{R} \subset \mathcal{Z}$) and one zone for each distribution network zone ($\mathcal{V} \subset \mathcal{Z}$) where demand is located and distributed energy resource can be installed.

$\mathcal{VL}$ is the set of voltage levels at which resources can be installed, {Trans., MV, LV}, where Trans. corresponds to transmission voltage levels (above 35 kV), MV corresponds to medium distribution voltages (e.g., 4-35 kV), and LV corresponds to low voltage distribution (240-400 V).

$\mathcal{L}$ denotes the number of transmission lines or paths simulated in the analysis. Primary substations connecting distribution zones to the transmission zones in which they are

embedded are also modeled as lines in $\mathcal{L}$ (albeit without any losses, as transformer losses are included in within-zone distribution losses). In addition, $\mathcal{E} \subset \mathcal{L}$ denotes the subset of transmission lines or substations eligible for reinforcements.

Finally, $\mathcal{S}$ denotes multiple blocks or segments of curtailable demand, in order to represent price responsive demand curtailment or a piecewise approximation of increasing willingness to pay for electricity at different price levels.

3.3.2 Decision Variables

The GenX model can operate in either a 'greenfield' or 'brownfield' mode for each technology independently. That is, it can solve starting from an existing brownfield capacity mix, $CAP^0_{y,z,v}$, while making decisions about building new capacity, $\Omega_{y,z,v}$, and retiring existing capacity, $\Delta_{y,z,v}$. Otherwise, GenX solves a greenfield expansion problem assuming no existing capacity, making decisions about new capacity, $\Omega_{y,z,v}$, from scratch. Maximum and minimum installed capacity constraints ($\overline{CAP}$, $\underline{CAP}$), can be specified for each resource (see Eq. 3.2) to reflect constraints on the siting of resources or to force adoption of a specific technology.

Capacity additions for all units of specific technology y belonging to the set $\mathcal{UC}$ are treated as integer decisions to add a discrete number of units each with a fixed capacity $U_{y,z,v}$. For example, the model could decide to install 5 combined cycle gas turbine units each with a capacity of 250 MW, yielding a total capacity for the cluster of CCGTs in that zone of 1,250 MW. For all other technologies $\notin \mathcal{UC}$, the investment decision variables take continuous positive values i.e., the model could decide to install, for example, 10.5 MW of capacity for solar, wind, or thermal generators that do not belong to the set $\mathcal{UC}$.

For any given technology y in zone z at voltage level v, it is possible to generate/inject $\Theta_{y,t,z,v}$ MWh at each hour t. For flexible demand management resources, $y \in \mathcal{DR}$, $\Theta_{y,t,z,v}$ represents MWh of flexible demand that are deferred in hour t. The maximum amount of generation/injection will be limited by the net capacity installed—equal to $U_{y,z,v} \times (CAP^0_{y,z,v} + \Omega_{y,z,v} - \Delta_{y,z,v})$, or total existing capacity plus installed additions less retirements—as well as a set of different operational constraints that are applied depending on the type (subset) of the

specific technology (e.g., ramping constraints for thermal units, state of charge constraints for storage). At the same time, for energy storage devices belonging to $\mathcal{O}$, $\Pi_{y,t,z,v}$ MWh of energy can be withdrawn and stored at each hour t. The total energy stored, $\Gamma_{y,t,z,v}$, at time t will depend on the amount of energy discharged, $\Theta_{y,t,z,v}$, the amount of energy charged, $\Pi_{y,t,z,v}$, and the storage energy level at time $t-1$. Similarly, $\Pi_{y,t,z,v}$ for all $y \in \mathcal{DR}$ represents any flexible demand previously deferred that is satisfied in hour h, thus adding to total demand in that period. For non-storage technologies, $\Pi_{y,t,z,v}$ and $\Gamma_{y,t,z,v}$ are eliminated from the problem.

For generators $y \in \mathcal{UC}$, generating units are combined into clusters of similar or identical units using the integer clustering method developed by Palmintier (2013). This replaces the large set of binary commitment decisions and associated constraints (which scale with the number of individual generating units) with a smaller set of integer commitment states and constraints (which instead scale with the number of clusters y of alike units). In traditional binary unit commitment, each unit is either on or off. With clustering, the integer commitment state $\upsilon_{y,t,z}$[6] varies from zero to the number of units in the cluster, $(CAP^0_{y,z,v} + \Omega_{y,z,v} - \Delta_{y,z,v})$, with the commitment variable representing the number of individual units in the cluster committed at any given time. In any given time period t, a number of units in each cluster may start-up, $\chi_{y,t,z}$, or shut-down, $\zeta_{y,t,z}$, which will change $\upsilon_{y,t,z}$. In this way, clustering still captures integer commitment decisions and associated relations at the individual plant level, subject to the simplifying assumption that all clustered units have identical parameters (e.g., capacity size, ramp rates, heat rate) and that all committed units in a given time step t are operating at the same power output per unit (see Palmintier (2013); Palmintier and Webster (2014, 2016) for detailed discussion of this method). All of the other generator variables—such as power output level—and constraints are then aggregated for the entire cluster.

For every hour, the system must resolve how much energy to inject/withdraw in each

[6]Note that as only large thermal units are subject to unit commitment constraints, these commitment-related variables and parameters are not indexed across voltage levels. All thermal units are installed at transmission voltage.

zone z given the hourly demand $D_{t,z}$ and the variable costs of the different electricity resource options. Consumers present different preferences about their willingness to pay for electricity at different prices; i.e., if the hourly marginal cost of electricity supply goes above a consumer's marginal value of consumption, that consumer is better off not consuming and will thus curtail demand. For this purpose, the model can decide how much demand not to serve $\Lambda_{s,t,z}$ at time t in zone z with different costs $CNSE_s$ for each segment of demand s. Each segment is represented by a per unit portion NSE_s of the hourly demand in each zone z that is willing to pay no more to consume energy than the specified price $CNSE_s$. Multiple segments can therefore be specified to create a segment-wise approximation of the demand curve for electricity.

When more than one zone is modeled, energy can flow, $\Phi_{l,t}$, through the line l at time t connecting zones according to the network map, $MAP_{l,z}$. Different lines present different characteristics like maximum capacity, $TCAP_l$, voltage, $VOLT_l$, and electrical resistance, OHM_l. The power flow variable, $\Phi_{l,t}$, for any line connecting nodes i and j can be either positive or negative, representing flows from i to j (positive values) or from j to i (negative values) at any given time. If the model is configured to allow network expansion, then $\forall l \in \mathcal{E}$, maximum transmission capacity can be increased by investing in transmission reinforcements, γ_l, at a cost of $CTCAP_l$. Reinforcements are limited by the maximum reinforcement capacity, $\overline{TCAP_l}$ of each line and the current version of the model considers reinforcements to be continuous variables.[7] For lines that are not eligible for reinforcements ($\forall l \notin \mathcal{E}$), $\overline{TCAP_l}$ is set to zero and the model accordingly eliminates $TCAP$ from the problem during presolve for each of these lines. Additionally, transmission power flows cause losses $\ell_{l,t}$ which are modeled as a segment-wise approximation of a quadratic function of $\Phi_{l,t}$. The variables $\S^+_{m,l,t}, \S^-_{m,l,t}$ correspond to each segment of the approximation. As $\Phi_{l,t}$ can take on both positive and negative values, M segments are created covering both the positive and negative real domains for $\Phi_{l,t}$ (see Section 3.3.7). In addition, if integer unit commitment decisions are used (e.g., unless $\mathcal{UC} = \varnothing$), additional auxiliary variables—$\Phi^+_{l,t}, \Phi^-_{l,t}, \beta^+_{m,l,t}, \beta^-_{m,l,t}$—are used by

[7]Binary transmission expansion variables will be added in the future but are computationally expensive, so are excluded in the current implementation.

the model to ensure that no 'phantom losses' exist i.e., fake losses created to avoid cycling by thermal units and save on startup costs (see Fitiwi et al. (2016)).

GenX also models distribution network losses and constraints on coincident peak injections and withdrawals within each distribution zone. These capabilities (and the methods to parameterize these equations) are key contribution of this thesis.

Losses from power flows within a distribution zone, $\ell_{z,t}$, are a polynomial function of power withdrawals and injections in each distribution voltage level, as per Section 2.2. For these purposes, demand in each zone, D_t, z, is assigned to either low or medium voltage (LV or MV) based on the parameter $SHARE_z^{mv}$. Accurately representing distribution network losses entails a segment-wise linear approximation of a polynomial with a quadratic term for net LV withdrawals in each zone. To do so, GenX employs a set of auxiliary variables $\S_{m,z,t}^{+}$ and $\S_{m,z,t}^{-}$. If integer unit commitment decisions are included in the model, additional binary variables, $\beta_{m,z,t}^{+}, \beta_{m,z,t}^{-}$, are also created to ensure that each segment of the approximation fills in order, preventing phantom losses (as in the representation of transmission losses).

Aggregate withdrawals and injections are constrained in each distribution zone based on the parameters $\overline{I}_z, \overline{W}_z$. Additional distribution network capacity can be added to accommodate withdrawals (λ_z^W) or injections (λ_z^I) at different costs to accommodate demand in each voltage level ($CDCAP_z^{lv}, CDCAP_z^{mv}$), as discussed in Chapter 2 Section 2.4. In addition, GenX models the network withdrawal margin gained by optimal dispatch of DERs or demand flexibility/curtailment, $\phi_{z,t}^W$, as per Section 2.3.[8] The auxiliary variables $\S_{m,z,t}^{\phi,W}$ represent the segments used to approximate the quadratic term in the function for network withdrawal margins gained.

Finally GenX can also model two classes of operating reserves required by system operators to maintain supply-demand balance at all nodes within tolerances in the case of unexpected generator or transmission line failures or errors in demand or renewable energy

[8]The model does not currently include a similar contribution of optimal dispatch to injection margins (e.g. targeted curtailment of DERs). This will be developed in the future pending implementation of the experimental process in Section 2.3 for coincident peak injections. Currently, DER dispatch (curtailment of DG or storage discharging or increase in storage charging) during periods of coincident peak injection contribute to network margins linearly by directly reduction the net injection peak.

forecasts within the hourly time step considered in the model. In this way, GenX allows a robust treatment of important stochastic processes not explicitly modeled. Frequency regulation (or primary reserves) requirements are symmetric (e.g., equal in both upward and downward directions) and are determined as a linear function of the hourly demand and the hourly generation from VRE resources, $F(D)$ and $F(RE)$, respectively. Different technologies can contribute some portion of their capacity to frequency regulation, up to a maximum, $\overline{REG}^{+}_{y,z,v}$ and $\overline{REG}^{-}_{y,z,v}$ for regulation up and down respectively. Regulation provided by the different resources at each hour, $\theta^{+}_{y,z,t}$ and $\theta^{-}_{y,z,t}$, must fulfill the total primary reserve requirements at each hour in both upwards and downwards direction. Primary reserve requirements are considered a hard constraint, and primary reserve shortfalls are not permitted.

In addition, secondary reserves (a.k.a, spinning reserves, contingency reserves, or balancing energy) requirements can be specified asymmetrically (with different requirements for upwards and downward directions) as a linear function of demand, $R^{+}(D)$ and $R^{-}(D)$, and VRE generation, $R^{+}(RE)$ and $R^{-}(RE)$, for each hour. Different technologies can commit capacity to secondary reserves up to a maximum, $\overline{RSV}^{+}_{y,z,v}$ and $\overline{RSV}^{-}_{y,z,v}$, for regulation up and down respectively. In addition, secondary reserve shortfalls, $\rho^{+,unmet}_{t}$ and $\rho^{-,unmet}_{t}$, are permitted with a penalty for shortfalls imposed at the cost $CRSV$ per MW-hr. Secondary reserves provided by the different resources at each hour, $\rho^{+}_{y,z,t}$ and $\rho^{-}_{y,z,t}$, minus unmet secondary reserves, $\rho^{+,unmet}_{t}$ and $\rho^{-,unmet}_{t}$, must fulfill the total secondary reserve requirements at each hour in each direction.

As storage can provide regulation in both directions while either charging or discharging (subject to energy and power capacity constraints) the variables $\theta^{+C}_{y,z,t}, \theta^{+D}_{y,z,t}$ and $\theta^{-C}_{y,z,t}, \theta^{-D}_{y,z,t}$, represent the contribution of storage resources to upwards and downwards regulation while either charging or discharging. Likewise, $\rho^{+C}_{y,z,t}, \rho^{+D}_{y,z,t}$, and down, $\rho^{-C}_{y,z,t}, \rho^{-D}_{y,z,t}$, represent storage contributions to secondary reserves in each direction while either charging and discharging.

3.3.3 Objective Function

The Objective Function of the model (see Eq. 3.1) minimizes over 8 components:

$$
\begin{aligned}
\min \Bigg\{ & \sum_{z\in\mathcal{Z}} \sum_{v\in\mathcal{VL}} \sum_{y\in\mathcal{G}} \Bigg((CINV_{y,z,v} \times U_{y,z,v} \times \Omega_{y,z,v}) + \\
& \qquad (CFOM_{y,z,v} \times U_{y,z,v} \times (CAP^{0}_{y,z,v} + \Omega_{y,z,v} - \Delta_{y,z,v})) \Bigg) \\
& + \sum_{z\in\mathcal{Z}} \sum_{v\in\mathcal{VL}} \sum_{y\in\mathcal{G}} \sum_{t\in\mathcal{T}} \Bigg(((CVOM_{y,z,v} + CFUEL_{y,z,v}) \times \Theta_{y,t,z,v}) + (CVOM_{y,z,v} \times \Pi_{y,t,z,v}) \Bigg) \\
& \quad + \sum_{z\in\mathcal{Z}} \sum_{t\in\mathcal{T}} \sum_{s\in\mathcal{S}} \Bigg(CNSE_{s} \times \Lambda_{s,t,z} \Bigg) \\
& \quad + \sum_{z\in\mathcal{Z}} \sum_{y\in\mathcal{G}} \sum_{t\in\mathcal{T}} \Bigg(CSTART_{y,z} \times \chi_{y,t,z} \Bigg) \\
& \qquad + \sum_{t\in\mathcal{T}} \Bigg(CRSV(\rho^{+,unmet}_{t} + \rho^{-,unmet}_{t}) \Bigg) \\
& \qquad + \sum_{l\in\mathcal{L}} \Bigg(CTCAP_{l} \times \gamma_{l} \Bigg) \\
& \qquad + \sum_{z\in\mathcal{V}} \Bigg(CDCAP^{lv}_{z} \times (\lambda^{W}_{z} + \lambda^{I}_{z}) \times (1 - S^{mv}_{z}) + \\
& \qquad\qquad (CDCAP^{mv}_{z} \times (\lambda^{W}_{z} + \lambda^{I}_{z}) \times S^{mv}_{z} \Bigg) \\
& - \sum_{z\in\mathcal{V}} \sum_{v\in\{LV,MV\}} \sum_{y\in\mathcal{G}} \Bigg(RDER_{y,z,v} \times (CAP^{0}_{y,z,v} + \Omega_{y,z,v} - \Delta_{y,z,v})) \Bigg) \Bigg\}
\end{aligned}
\tag{3.1}
$$

The first component represents the minimization of fixed cost across all zones, voltage levels, and technologies. Total fixed costs reflect the sum of the annualized capital cost, $CINV_{y,z,v}$, times the total new capacity added (if any), plus the fixed O&M cost, $CFOM_{y,z,v}$, times the net installed capacity (e.g., existing capacity less retirements plus additions).

The second term represents the minimization of variable costs across all zones, voltage levels, technologies, and hours. Variable costs include the sum of fuel cost, $CFUEL_{y,z,v}$, plus variable O&M cost, $CVOM_{y,z,v}$, times the hourly energy injection, $\Theta_{y,t,z,v}$ for each technology, as well as the variable cost, $CVOM_{y,z,v}$, times the energy withdrawn or stored

by storage resources, $\Pi_{y,t,z,v}$.

The third term minimizes the cost of non-served demand ($CNSE_s$) across all different consumer segments s, equal to the marginal value of consumption (or cost of non-served energy) times the amount of non-served energy, $\Lambda_{s,t,z}$, for each segment in each zone during each hour. As this model is a constrained cost minimization problem, the utility of consumption enters the objective function here reflecting the foregone welfare associated with decreases in demand below the base level of demand in each hour represented by $D_{z,t}$. Each segment of price-responsive demand represents a set of consumers with different willingness to pay for electricity consumption representing their marginal utility of consumption. If the marginal cost of supply rises above the willingness to pay of any segment, demand is reduced by the aggregate consumption of that segment of consumers, and their foregone utility enters the objective function as the sum of $CNSE_s \times \Lambda_{s,t,z}$ for each zone and time period. Note that the final segment of demand always represents inelastic consumers and the cost of involuntarily shedding demand at a very high cost of non-served energy (e.g., \$10,000/MWh). At least this one segment must be included in the model.

The fourth term corresponds to the startup costs incurred by technologies to which unit commitment decisions apply (e.g., $\forall\ y \in \mathcal{UC}$), equal to the cost of start-up $CSTART_{y,z,v}$, times the number of startup events, $\chi_{y,t,v}$, for each cluster of units.

The fifth term correspond to the cost for the system of any unmet secondary reserve requirements, equal to the sum across all hours of the cost of unmet reserves, $CRSV$, times the sum of unmet secondary up and down reserves, $\rho_t^{+,unmet} + \rho_t^{-,unmet}$.

The next two terms correspond to the network reinforcement or construction costs, for both transmission lines and distribution zones. Transmission reinforcement costs are equal to the sum across all lines of the product between the transmission reinforcement/construction cost, $CTCAP_l$, times the additional transmission capacity variable, γ_l. Distribution network reinforcement costs are likewise equal to the sum across all distribution zones ($z \in \mathcal{V}$) of the product between the distribution reinforcement/construction cost, $CDCAP_l$, times the sum of additional distribution withdrawal (λ_z^W) and injection (λ_z^I) capacity reinforcements

added.

The final component of the objective function reflects revenues $RDER_{y,z,v}$ earned by distributed energy resources (DERs; e.g., resources installed at voltage levels $v \in \{LV, MV\}$) for services that are not captured endogenously in this model. This parameter could reflect the value of reliability (e.g., backup power supply) provided by DERs, the extra 'premium' value individuals are willing to pay to produce their own energy or own their own storage systems, use of a device's inverters for conservation voltage reduction, or other potential revenue streams. This is a crude measure to allow adjustments to the effective cost of DERs to account for potential sources of value that fall outside of the model.

In summary, Eq. 3.1 can be understood as the maximization of social welfare represented in a cost minimization context as the minimization of costs associated with eight sets of different decisions: (1) where and how to invest in (or retire) capacity, (2) how to dispatch that capacity, (3) which consumer segments to serve or curtail, (4) how to cycle and commit thermal units subject to unit commitment decisions, (5) how to provide operating reserves, (6) where and how to invest in additional transmission network capacity to increase power transfer capacity between zones, (7) where and how to investment in reinforcements of distribution network capacity to accommodate increases in coincident peak withdrawals or injections within each distribution network, and (8) what additional revenues can be earned by DERs. Note however that each of these components are considered jointly and the optimization is performed over the whole problem at once as a monolithic co-optimization problem.

3.3.4 Resource Investment Decision Constraints

Eq. 3.2 and 3.3 constrain resource investment and retirement decisions. Maximum and minimum capacity constraints can be placed on each zone and voltage level to signify constraints on siting or to force the model to select certain technologies. Eq. 3.3 simply ensures retirements cannot exceed existing installed capacity in cases where the model is run in a 'brownfield' expansion mode. Large thermal units may be given a discrete unit size,

$U_{y,z,v} > 1$, in which case $\Omega_{y,z,v}, \Delta_{y,z,v} \in \mathbb{Z}^+$, making these discrete decision variables. (These units also typically belong to the set $\mathcal{UC}$ subject to unit commitment constraints.) For other small, modular technologies that can be added in small increments, $U_{y,z,v} = 1$ and $\Omega_{y,z,v}, \Delta_{y,z,v} \in \mathbb{R}^+$, making investment and retirement decisions continuous variables.

$$\frac{\underline{CAP}_{y,z,v}}{U_{y,z,v}} \leq \Omega_{y,z,v} \leq \frac{\overline{CAP}_{y,z,v}}{U_{y,z,v}}, \qquad \forall y \in \mathcal{G}, \forall z \in \mathcal{Z}, \forall v \in \mathcal{VL} \tag{3.2}$$

$$\Delta_{y,z,v} \leq \frac{CAP^0_{y,z,v}}{U_{y,z,v}}, \qquad \forall y \in \mathcal{G}, \forall z \in \mathcal{Z}, \forall v \in \mathcal{VL} \tag{3.3}$$

3.3.5 Demand Balance Constraint

The demand balance constraint (Eq. 3.4) ensures that electricity demand is met at every hour in each zone. As shown in the constraint, electricity demand, $D_{t,z}$, at each hour and for each zone must be strictly equal to the sum of generation, $\Theta_{y,t,z}$, from thermal technologies ($\mathcal{H}$), dispatchable renewables ($\mathcal{D}$), and non-dispatchable renewables ($\mathcal{ND}$). At the same time, energy storage devices ($\mathcal{O}$) can discharge energy, $\Theta_{y,t,z}$ to help satisfy demand, and when these devices are charging, $\Pi_{y,t,z}$, they increase demand. For the case of shiftable demand ($y \in \mathcal{DR}$), delaying demand, $\Theta_{y,t,z}$, decreases demand in that time period and any previously deferred demand satisfied in the time period, $\Pi_{y,t,z}$, increases demand. Price-responsive demand curtailment, $\Lambda_{s,t,z}$, can also contribute to the demand balance by reducing demand when marginal costs are high. Finally, power flows into or out of a zone are considered in the demand balance equation for each zone. Power flows leaving their reference zone are positive and power flows entering the zone will have a negative value. Thus, subtracting $\Phi_{l,t}$ from the available supply in the zone ensures the appropriate effect on the demand balance. At the same time, one-half of transmission losses across a transmission line linking two zones $\ell_{l,t}$ are attributed to each connected zone. In addition, if the zone is a distribution zone ($z \in \mathcal{V}$), then distribution losses reflecting power flows within each distribution zone, $\ell_{z,t}$, are also applied.

$$
\begin{aligned}
D_{t,z} = & \sum_{y \in \mathcal{H}} \Theta_{y,t,z} + \sum_{y \in \mathcal{D}} \Theta_{y,t,z} + \sum_{y \in \mathcal{ND}} \Theta_{y,t,z} \\
& + \sum_{y \in \mathcal{O}, \mathcal{DR}} (\Theta_{y,t,z} - \Pi_{y,t,z}) \\
& + \sum_{s \in \mathcal{S}} \Lambda_{s,t,z} - \sum_{l \in \mathcal{L}} (MAP_{l,z} \times \Phi_{l,t}) - \frac{1}{2} \sum_{l \in \mathcal{L}} (\mid MAP_{l,z} \mid \times \ell_{l,t}) - \ell_{z,t} \\
& \forall z \in \mathcal{Z}, \forall t \in \mathcal{T}
\end{aligned} \tag{3.4}
$$

Note that if the model is solved as a linear program (e.g., without integer unit commitment constraints), the dual variable of the demand balance constraint can be interpreted as the hourly marginal price of electricity at each zone z. In addition, if unit commitment and discrete capacity expansion decisions are considered, GenX is programmed to allow the user to optionally output hourly prices by solving the model a second time with all integer decisions fixed to equal outcomes of the initial MILP solution, using the dual variable of the demand balance constraint in this second LP solution as the hourly price.

3.3.6 Transmission Capacity and Network Expansion Between Zones

The model represents transmission paths or lines with a simplified 'transport flow' or 'pipeline' model, neglecting limits on parallel flows or voltage angle differences imposed in reality. Instead, Eq. 3.5 places a simple capacity limit on the maximum power flow, $\Phi_{l,t}$, on each line to be less than or equal to the line's maximum power transfer capacity, $TCAP_l$. Because $\Phi_{l,t}$ can take on positive and negative values, indicating the direction of power flow across the line, this variable is bound by $\pm TCAP_l$. For lines eligible for expansion (each $l \in \mathcal{E}$), Eq. 3.5 is replaced by Eq. 3.6, reflecting that power flows must be less than the initial line transfer capacity plus any transmission capacity added on that line, γ_l. The additional transmission capacity is further constrained by a maximum allowed reinforcement, $\overline{TCAP_l}$, for each line, as is shown in Eq. 3.7.

$$-TCAP_l \leq \Phi_{l,t} \leq TCAP_l, \qquad \forall l \in (\mathcal{L} \setminus \mathcal{E}), \forall t \in \mathcal{T} \qquad (3.5)$$

$$-(TCAP_l + \gamma_l) \leq \Phi_{l,t} \leq (TCAP_l + \gamma_l), \qquad \forall l \in \mathcal{E}, \forall t \in \mathcal{T} \qquad (3.6)$$

$$\gamma_l \leq \overline{TCAP}_l, \qquad \forall l \in \mathcal{E}, \forall t \in \mathcal{T} \qquad (3.7)$$

3.3.7 Transmission Losses

Transmission losses, $\ell_{l,t}$ are modeled as a quadratic function of power flows across a line using a segment-wise linear approximation with total number of segments equal to the size of the set $\mathcal{M}$. In order to do this, the absolute value of the line flow variable is represented by the sum of stepwise flow variables ($\S^+_{m,l,t}, \S^-_{m,l,t}$), associated with each partition of line losses computed using the corresponding linear expressions. The model always includes constraints Eq. 3.8–Eq. 3.11. Eq. 3.12–3.17 are added if the model includes integer unit commitment decisions. In these cases, increasing demand by increasing losses incurs additional supply costs but may avoid greater costs associated with discrete start-up decisions in some circumstances. The least-cost solution may therefore involve 'phantom losses' that are not associated with actual power flows (see Fitiwi et al. (2016)). These phantom losses are prevented by Eq. 3.12–3.17, although at the cost of additional computational burden (due to inclusion of additional binary variables). If the model is fully linear (e.g., $\mathcal{UC} = \emptyset$), Eq. 3.12–3.17 are automatically omitted to reduce dimensionality.

Eq. 3.8 provides the expression of linearized losses, which are computed as the accumulated sum of losses for each linear stepwise segment of the approximated quadratic function, including both positive domain ($\S^+_{m,l,t}$) and negative domain ($\S^-_{m,l,t}$) segments; Eq. 3.9 ensures that the stepwise variables do not exceed the maximum size per segment. The slope and maximum size for each segment are calculated as per the method in Zhang et al. (2013).

$$\ell_{l,t} = \frac{OHM_l/10^6}{(VOLT_l/10^3)^2}\Bigg(\sum_{m\in\mathcal{M}}(slope^+_{m,l} \times \S^+_{m,l,t} + slope^-_{m,l} \times \S^-_{m,l,t})\Bigg), \qquad \forall l \in \mathcal{L}, \forall t \in \mathcal{T}$$

Where:

$$slope^+_{m,l} = \frac{2 + 4 \times \sqrt{2} \times (m-1)}{1 + \sqrt{2} \times (2 \times M - 1)}(TCAP_l + \overline{TCAP_l}) \qquad \forall m \in [1\colon M], l \in \mathcal{L}$$

$$slope^-_{m,l} = \frac{2 + 4 \times \sqrt{2} \times (m-1)}{1 + \sqrt{2} \times (2 \times M - 1)}(TCAP_l + \overline{TCAP_l}) \qquad \forall m \in [1\colon M], l \in \mathcal{L}$$

(3.8)

$$\S^+_{m,l,t}, \S^-_{m,l,t} \leq \overline{length}_{m,l} \qquad \forall m \in [1:M], l \in \mathcal{L}, t \in \mathcal{T}$$

Where:

$$\overline{length}_{m,l} = \begin{cases} \frac{(1+\sqrt{2})}{1+\sqrt{2}\times(2\times M-1)}(TCAP_l + \overline{TCAP_l}) & \text{if m=1} \\ \\ \frac{2\times\sqrt{2}}{1+\sqrt{2}\times(2\times M-1)}(TCAP_l + \overline{TCAP_l}) & \text{if m} > 1 \end{cases}, \tag{3.9}$$

Eq. 3.10 and Eq. 3.11 ensure that the sum of auxiliary segment variables ($m \geq 1$) minus the 'zero' segment (which allows values to go into the negative domain) from both positive and negative domains must total the actual power flow across the line.

$$\sum_{m\in[1:M]}(\S^+_{m,l,t}) - \S^+_{0,l,t} = \Phi_{l,t}, \qquad \forall l \in \mathcal{L}, \forall t \in \mathcal{T} \tag{3.10}$$

$$\sum_{m\in[1:M]}(\S^-_{m,l,t}) - \S^-_{0,l,t} = -\Phi_{l,t}, \qquad \forall l \in \mathcal{L}, \forall t \in \mathcal{T} \tag{3.11}$$

Eq. 3.12–3.15 ensure that auxiliary segments variables do not exceed the maximum value per segment and that they are filled in order; i.e., one segment cannot be non-zero unless the prior segment is at its maximum value. Eq. 3.16 and Eq. 3.17 are binary constraints to deal with absolute value of power flow on each line. If the flow is positive, $\S^+_{0,l,t}$ must be

zero; if flow is negative, $§^{+}_{0,l,t}$ must be positive and takes on value of the full negative flow, forcing all $§^{+}_{m,l,t}$ other segments ($m \geq 1$) to be zero. Conversely, if the flow is negative, $§^{-}_{0,l,t}$ must be zero; if flow is positive, $§^{-}_{0,l,t}$ must be positive and takes on value of the full positive flow, forcing all other segments $§^{-}_{m,l,t}$ where $m \geq 1$ to be zero. Requiring segments to fill in sequential order and binary variables to ensure variables reflect the actual direction of power flows are both necessary to eliminate phantom losses from the solution, which can occur when unit commitment decisions are employed for some generators.

$$§^{+}_{m,l,t} \leq \overline{length}_{m,l} \times \beta^{+}_{m,l,t}, \qquad \forall m \in [1:M], \forall l \in \mathcal{L}, \forall t \in \mathcal{T} \tag{3.12}$$

$$§^{-}_{m,l,t} \leq \overline{length}_{m,l} \times \beta^{-}_{m,l,t}, \qquad \forall m \in [1:M], \forall l \in \mathcal{L}, \forall t \in \mathcal{T} \tag{3.13}$$

$$§^{+}_{m,l,t} \geq \beta^{+}_{m+1,l,t} \times \overline{length}_{m,l}, \qquad \forall m \in [1:M], \forall l \in \mathcal{L}, \forall t \in \mathcal{T} \tag{3.14}$$

$$§^{-}_{m,l,t} \geq \beta^{-}_{m+1,l,t} \times \overline{length}_{m,l}, \qquad \forall m \in [1:M], \forall l \in \mathcal{L}, \forall t \in \mathcal{T} \tag{3.15}$$

$$§^{+}_{0,l,t} \leq TCAP_{l} \times (1 - \beta^{+}_{1,l,t}), \qquad \forall l \in \mathcal{L}, \forall t \in \mathcal{T} \tag{3.16}$$

$$§^{-}_{0,l,t} \leq TCAP_{l} \times (1 - \beta^{-}_{1,l,t}), \qquad \forall l \in \mathcal{L}, \forall t \in \mathcal{T} \tag{3.17}$$

3.3.8 Distribution Network Losses

This thesis develops a new method for representing distribution networks using a zonal approximation, with each zone $z \in \mathcal{V}$ representative of a different distribution network topology. Each distribution zone is home to two voltage levels, medium and low voltage, with the total demand in the zone $D_{z,t}$ split between voltage levels based on the parameter $SHARE^{mv}_{z}$. In addition, as capacity investment and operational decisions are indexed across each zone and voltage level in the system, distributed energy resources (DERs, such as distributed solar PV, energy storage, fuel cells, etc.) can be made eligible for installation and operation in each distribution zone.

Distribution zone topology is specified just as it is for transmission zones, using the $MAP_{l,z}$ parameters, and power flows between distribution zones and the transmission zone they are embedded in can be constrained using Eq. 3.5–3.7, to represent limits on aggregate transformer capacity at the primary substation between transmission and distribution

voltages.

GenX applies a novel approach to represent aggregate losses from power flows *within* distribution network zones as a segment-wise linear approximation of a polynomial function of both power injections and withdrawals within each zone. Based on detailed offline AC power flow simulations of large-scale realistic distribution networks described in detail in Ch 2 (Section 2.2), within zone distribution losses can be closely approximated as a polynomial function with three terms: (1) a quadratic term for net power withdrawals at low voltage (e.g., aggregate withdrawals less aggregate injections) within each zone; (2) a linear term for aggregate net withdrawal minus injection at the medium voltage level; (3) and a linear term for the sum of both aggregate withdrawal and aggregate injection in medium voltage. That is:

$$\ell_{z,t} = LVQUAD_z(W_{z,t,LV} - I_{z,t,LV})^2 + MVNET(W_{z,t,MV} - I_{z,t,MV}) + LVTOT(W_{z,t,LV} + I_{z,t,LV}) \quad (3.18)$$

GenX thus implements a segment-wise linear approximation of the quadratic term in this function plus the linear terms, to represent within zone losses as per Eq. 3.19. The slopes and constraints on the lengths of each segment used for linear approximation of the quadratic term are calculated as per Eq. 3.19–3.21 to minimize error at any point in the domains $[0 : (\lambda_z^I + \overline{DCAP}_z^I)]$ and $[0 : (\lambda_z^W + \overline{DCAP}_z^W)]$ (e.g., over the realm of all possible injections and withdrawals that may be modeled). This method is based on the segment-wise linear interpolation of quadratic functions in Zhang et al. (2013).

$$\ell_{z,t} = LVQUAD_z \sum_{m=1}^{M} \left(slope^{+}_{m,z} \times \S^{+}_{m,z,t} + slope^{-}_{m,z} \times \S^{-}_{m,z,t} \right)$$
$$+ MVNET(withdraw^{mv}_{z,t} - inject^{mv}_{z,t})$$
$$+ LVTOT(withdraw^{lv}_{z,t} + inject^{lv}_{z,t}) \qquad \forall z \in \mathcal{V}, \forall t \in \mathcal{T}$$

Where:

$$slope^{+}_{m,z} = \frac{2 + 4 \times \sqrt{2} \times (m-1)}{1 + \sqrt{2} \times (2 \times M - 1)} (\overline{W}_z + \overline{DCAP}^{W}_{z}) \qquad \forall m \in [1\colon M], z \in \mathcal{V}$$

$$slope^{-}_{m,z} = \frac{2 + 4 \times \sqrt{2} \times (m-1)}{1 + \sqrt{2} \times (2 \times M - 1)} (\overline{I}_z + \overline{DCAP}^{I}_{z}) \qquad \forall m \in [1\colon M], z \in \mathcal{V}$$

$$withdraw^{lv}_{z,t} = D_{z,t} \times (1 - SHARE^{mv}_{z})$$
$$+ \sum_{y \in \mathcal{O}, \mathcal{DR}, v = LV} (\Pi_{y,t,z,v}) - \sum_{y \in \mathcal{DR}, v = LV} (\Theta_{y,t,z}) - \sum_{s \in S} (\Lambda_{s,z,t}) \qquad \forall z \in \mathcal{Z}, t \in \mathcal{T}$$

$$inject^{lv}_{z,t} = \sum_{y \notin \mathcal{DR}, v = LV} (\Theta_{y,t,z,v}) \qquad \forall z \in \mathcal{Z}, t \in \mathcal{T}$$

$$withdraw^{mv}_{z,t} = D_{z,t} \times SHARE^{mv}_{z}$$
$$+ \sum_{y \in \mathcal{O}, \mathcal{DR}, v = MV} (\Pi_{y,t,z,v}) - \sum_{y \in \mathcal{DR}, v = MV} (\Theta_{y,t,z})$$

$$inject^{mv}_{z,t} = \sum_{y \notin \mathcal{DR}, v = MV} (\Theta_{y,t,z,v}) \qquad \forall z \in \mathcal{Z}, t \in \mathcal{T}$$

(3.19)

$$\S^{+}_{m,z,t}, \leq \overline{length} +_{m,z}, \qquad \forall m \in [1\colon M], z \in \mathcal{Z}, t \in \mathcal{T}$$

Where:

$$\overline{length}^{+}_{m,z} = \begin{cases} \frac{(1+\sqrt{2})}{1+\sqrt{2}\times(2\times M-1)} (\overline{W}_z + \overline{DCAP}^{W}_{z}) & \text{if m=1} \\ \\ \frac{2\times\sqrt{2}}{1+\sqrt{2}\times(2\times M-1)} (\overline{W}_z + \overline{DCAP}^{W}_{z}) & \text{if m} > 1 \end{cases} \tag{3.20}$$

$$\S^{-}_{m,z,t}, \leq \overline{length}^{-}_{m,z}, \qquad \forall m \in [1\colon M], z \in \mathcal{Z}, t \in \mathcal{T}$$

Where:

$$\overline{length}^{-}_{m,z} = \begin{cases} \frac{(1+\sqrt{2})}{1+\sqrt{2}\times(2\times M-1)}(\overline{I}_z + \overline{DCAP}^{I}_{z}) & \text{if m=1} \\ \\ \frac{2\times\sqrt{2}}{1+\sqrt{2}\times(2\times M-1)}(\overline{I}_z + \overline{DCAP}^{I}_{z}) & \text{if m} > 1 \end{cases}, \tag{3.21}$$

Eq. 3.22 and Eq. 3.23 ensure that the sum of auxiliary segment variables ($m \geq 1$) minus the 'zero' segment (which allows values to go into the negative domain) from both positive and negative domains must total the actual net withdrawal in low voltage.

$$\sum_{m\in[1:M]} (\S^{+}_{m,l,t}) - \S^{+}_{0,l,t} = (withdraw^{lv}_{z,t} - inject^{lv}_{z,t}), \qquad \forall z \in \mathcal{V}, \forall t \in \mathcal{T} \tag{3.22}$$

$$\sum_{m\in[1:M]} (\S^{-}_{m,l,t}) - \S^{-}_{0,l,t} = (inject^{lv}_{z,t} - withdraw^{lv}_{z,t}), \qquad \forall z \in \mathcal{V}, \forall t \in \mathcal{T} \tag{3.23}$$

If integer unit commitment decisions are modeled, then Eq. 3.19 allows the solver to produce phantom losses, or losses unrelated to physical power withdrawals or injections in each distribution zone, as discussed in Section 3.3.7. To prevent these phantom losses, Eq 3.24–3.29 are added to the model whenever discrete unit commitment decisions are modeled. Eq. 3.24–3.25 require that each segment in the linear approximation can be nonzero only if the binary auxiliary variable ($\beta^{+}_{m,z,t}$ or $\beta^{-}_{m,z,t}$) for that segment equals 1. Then Eq 3.26–3.27 require that if any segment $m+1$ is nonzero, the proceeding segment m must take on its maximum possible value, where the maximum length per segment ($\overline{length}^{+}_{m,z}$ or $\overline{length}^{-}_{m,z}$) is given by Eq. 3.20–3.21 above. Eq. 3.28–3.29 are binary constraints to deal with the absolute value of net withdrawals. If net withdrawal is positive, $\S^{+}_{0,m,t}$ must be zero; if net withdrawal is negative, $\S^{+}_{0,z,t}$ must be positive and takes on the value of the full net withdrawal, forcing all $\S^{+}_{m,z,t}$ other segments ($m \geq 1$) to be zero. Conversely, if the net with-

drawal is negative, $\S^-_{0,z,t}$ must be zero; if net withdrawal is positive, $\S^-_{0,z,t}$ must be positive and takes on the value of the full net withdrawal, forcing all $\S^-_{m,z,t}$ other segments ($m \geq 1$) to be zero.

$$\S^+_{m,z,t} \leq \overline{length}^+_{m,z} \times \beta^+_{m,z,t} \qquad \forall m \in [1\colon M], z \in \mathcal{V}, t \in \mathcal{T} \qquad (3.24)$$

$$\S^-_{m,z,t} \leq \overline{length}^-_{m,z} \times \beta^-_{m,z,t} \qquad \forall m \in [1\colon M], z \in \mathcal{V}, t \in \mathcal{T} \qquad (3.25)$$

$$\S^+_{m,z,t} \geq \beta^+_{m+1,z,t} \times \overline{length}^+_{m,z} \qquad \forall m \in [1\colon (M-1)], z \in \mathcal{V}, t \in \mathcal{T} \qquad (3.26)$$

$$\S^-_{m,z,t} \geq \beta^-_{m+1,z,t} \times \overline{length}^-_{m,z} \qquad \forall m \in [1\colon (M-1)], z \in \mathcal{V}, t \in \mathcal{T} \qquad (3.27)$$

$$\S^+_{0,z,t} \leq (\overline{W}_z + \overline{DCAP}^W_z) \times (1 - \beta^+_{1,z,t}), \qquad \forall z \in \mathcal{V}, \forall t \in \mathcal{T} \qquad (3.28)$$

$$\S^-_{0,z,t} \leq (\overline{I}_z + \overline{DCAP}^I_z) \times (1 - \beta^-_{1,z,t}), \qquad \forall z \in \mathcal{V}, \forall t \in \mathcal{T} \qquad (3.29)$$

3.3.9 Distribution Network Capacity, Network Reinforcements, and Network Margin Provided by DERs

Total power withdrawals and injections in each distribution zone z are also constrained to represent the aggregate capacity of the network zone to absorb injections ($\overline{I}$) or deliver withdrawals ($\overline{W}$) without violating network operating constraints, such as line or transformer thermal ratings or node voltage limits, as per Eq. 3.30–3.31. This initial capacity can be parameterized using AC optimal power flow simulations with the base network as per Chapter 2, Section 2.3. As coincident peak power withdrawal and injection periods drive network capacity investment requirements, the user can specify a subset of time steps $\mathcal{PW}, \mathcal{PI} \subset \mathcal{T}$ during which aggregate peak withdrawals and injections are likely to occur. The distribution network withdrawal and injection constraints then only apply in these time periods to limit computational burden.

Eq. 3.30–3.31 specify that coincident peak demand (plus storage withdrawals, if any) and net injections in each distribution zone z cannot exceed the sum of the specified initial network capacity plus any network margin gained via investment in network expansion (e.g., reinforcements and upgrades, λ^W_z, λ^I_z). Coincident peak demand or injection can also be

accommodated by additional 'network margin' gained via optimal dispatch of distributed energy resources ($\phi^W_{z,t}, \phi^I_{z,t}$). Additionally, network capacity can only be expanded up to a specified maximum additional capacity for withdrawal and injection, as per 3.32–3.33, to reflect limits on the ability to reinforce or expand networks (if any).

$$D_{z,t} + \sum_{y \in \mathcal{O}, \mathcal{DR}} \Pi_{y,z} \leq \overline{W}_z + \lambda^W_z + \phi^W_{z,t}, \qquad \forall z \in \mathcal{V}, t \in \mathcal{PW} \tag{3.30}$$

$$\sum_{y \notin DR} \Theta_{y.z} \leq \overline{I}_z + \lambda^I_z + \phi^I_{z,t}, \qquad \forall z \in \mathcal{V}, t \in \mathcal{PI} \tag{3.31}$$

$$\lambda^W_z \leq \overline{DCAP}^W_z, \qquad \forall z \in \mathcal{V} \tag{3.32}$$

$$\lambda^I_z \leq \overline{DCAP}^I_z, \qquad \forall z \in \mathcal{V} \tag{3.33}$$

The ability to capture the additional 'network margin' – or ability to accommodate aggregate peak withdrawals or injections without network reinforcement – achieved via optimal dispatch of distributed energy resources (DERs) and demand response, given by the variables $\phi^W_{z,t}, \phi^I_{z,t}$, is a novel feature of GenX introduced in this thesis based on results from the AC optimal power flow simulations performed in Chapter 2, Section 2.3. Where coincident peak demand exceeds network capacity margins, distribution system operators may dispatch (directly or via aggregators or price signals) DERs within a given distribution network zone to inject power (e.g., via distributed generation or storage discharging) or reduce withdrawals (e.g., via demand response or deferral of flexible demand) in targeted locations to render network power flows feasible where they would otherwise violate network operating limits (such as voltage constraints or transformer or circuit thermal limits). Similarly, curtailment of injections by dispatchable DERs or charging by storage devices targeted to the right parts of the distribution network may also relieve network constraints and allow for an increase in overall injections elsewhere, reducing the need for network capacity upgrades (e.g., increasing DER hosting capacity). This additional network margin gained via DER operation thus acts as a substitute for the additional network investments that would otherwise be necessary to accommodate peak withdrawals or injections. In this manner, GenX can model

'non-wires' alternatives or operational strategies to harness optimal dispatch of DERs and demand response to avoid investments in network 'wires' solutions or physical upgrades to distribution networks with Eq. 3.35–3.38.

The total net demand reduction required to deliver this needed network margin is derived from detailed optimal AC power flow modeling of realistic large-scale distribution networks. As demonstrated in Chapter 2, Section 2.3, this additional peak withdrawal margin gained by optimal dispatch of DER injection and demand curtailment can be closely approximated by a polynomial function:

$$\begin{aligned} &lvreduction + (1 - DISCOUNT)mvreduction \\ &\qquad = LVCOEF^W(1 - SHARE^{mv})\phi^W_{z,t} \\ &\qquad + LVCOEF2^W((1 - SHARE^{mv})\phi^W_{z,t})^2 \\ &\qquad + MVCOEF^W \times SHARE^{mv} \times \phi^W_{z,t} \end{aligned} \tag{3.34}$$

This polynomial function is implemented with a segment-wise linear approximation of the quadratic term as per Eq. 3.35–3.37. The slopes and constraints on the lengths of each segment used for linear approximation of the quadratic term are calculated as elsewhere to minimize error at any point in the domains $[0 : \overline{MARGIN}^W_z(1 - SHARE^{mv}_z)]$ where $\overline{MARGIN}^W_z$ is the maximum network margin that can be gained via DER dispatch, as specified via user inputs.

$$lvreduction_{z,t} + (1 - DISCOUNT)\delta^{mv}_{z,t} = LVCOEF^W_z(1 - SHARE^{mv}_z)\phi^W_{z,t}$$
$$+ LVCOEF2^W_z \sum_{n=1}^{N}(slope^{\phi}_{n,z} \times \S^{\phi,W}_{n,z,t})$$
$$+ MVCOEF^W_z \times SHARE^{mv}_z \times \phi^W_{z,t} \qquad \forall z \in \mathcal{V}, t \in \mathcal{PW}$$

Where:

$$lvreduction_{z,t} = \sum_{y \in \mathcal{G}, v=LV}(\Theta_{y,t,z,v}) + \sum_{s \in \mathcal{S}}(\Lambda_{s,z,t}) \qquad \forall z \in \mathcal{V}, t \in \mathcal{PW}$$
$$slope^{\phi}_{n,z} = \frac{2 + 4 \times \sqrt{2} \times (n-1)}{1 + \sqrt{2} \times (2 \times N - 1)} \overline{MARGIN}^W_z (1 - SHARE^{mv}_z) \qquad \forall n \in [1\colon N], z \in \mathcal{V} \tag{3.35}$$

$$\S^{\phi}_{n,z,t} \leq \overline{length}_{n,z} \qquad \forall n \in [1:N], z \in \mathcal{V}, t \in \mathcal{PW}$$

Where:

$$\overline{length}_{n,z} = \begin{cases} \frac{(1+\sqrt{2})}{1+\sqrt{2}\times(2\times N-1)} \overline{MARGIN}^W_z (1 - SHARE^{mv}_z) & \text{if n=1} \\ \\ \frac{2\times\sqrt{2}}{1+\sqrt{2}\times(2\times N-1)} \overline{MARGIN}^W_z (1 - SHARE^{mv}_z) & \text{if n} > 1 \end{cases}, \tag{3.36}$$

$$\sum_{n=1}^{M} \S^{\phi,W}_{n,z,t} = (1 - SHARE^{mv})\phi^W_{z,t} \qquad \forall n \in [1:N], z \in \mathcal{V}, t \in \mathcal{PW} \tag{3.37}$$

In addition, Eq. 3.38 imposes a limit on the maximum share of net demand reductions that can be contributed by DERs or demand in medium voltage. As per discussion in Chapter 2, Section 2.3, net demand reductions in medium voltage cannot help alleviate constraints in low voltage during periods of peak withdrawals and thus cannot fully substitute for reductions in LV. The parameter $\overline{MV}^W_z$ therefore represents the portion of net demand reductions caused by LV demand that occur in MV network components or at the primary substation, and thus can be potentially mitigated by DERs or demand reductions installed at MV.

$$\delta_{z,t}^{mv} \leq \overline{MV}_z^W \Bigg(LVCOEF_z^W (1 - SHARE_z^{mv}) \phi_{z,t}^W + LVCOEF2_z^W \sum_{n=1}^{N} (slope_{n,z}^{\phi} \times \S_{n,z,t}^{\phi,W}) \Bigg) + MVCOEF_z^W \times SHARE_z^{mv} \tag{3.38}$$

Finally, in the current version of the model, network injection margin gained via optimal dispatch of DERs is constrained to equal zero (Eq. 3.39) and thus not considered. At this stage, further research and offline modeling is required to determine an accurate representation for injection margins that may be gained by optimal curtailment of DERs, and whether this gain is nonlinear, as it is for withdrawal margins. Results from this future work will be incorporated into subsequent versions of GenX. In the current version of GenX, dispatchable DERs may still reduce their injections $\Theta_{y,z}$ during aggregate peak injection periods to directly reduce their contributions to required network capacity in the lefthand side of Eq. 3.31. DER curtailments thus have a linear effect on the need for network reinforcement and associated costs in the objection function.

$$\lambda_z^I = 0 \quad \forall z \in \mathcal{V} \tag{3.39}$$

3.3.10 Unit Commitment Constraints and Abstraction Methods

As already mentioned, commitment and cycling (start-up, shut-down) of thermal generators is accounted for using the integer clustering technique developed in Palmintier (2013); Palmintier and Webster (2014). In a typical binary unit commitment formulation, each unit is either on or off (see e.g. Morales-Espana et al. (2013); de Sisternes (2014)). With the clustered unit commitment formulation, generators are clustered by type and zone, and the integer commitment state variable $\upsilon_{y,t,z}$ for each cluster varies from zero to the number of units in the cluster, $(\frac{CAP_{y,z}^0}{U_{y,z}} + \Omega_{y,z} - \Delta_{y,z})$. As shown in Fig. 3-3, this approach replaces the large set of binary commitment decisions and associated constraints, which scale directly with the number of individual units, with a smaller set of integer commitment states and

constraints, one for each cluster. The dimensionality of the problem thus scales with the number of different resources types eligible for investment in each zone and voltage level, rather than the number of discrete units, significantly improving computational efficiency.

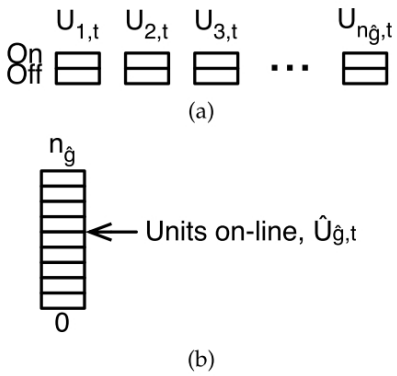

Figure 3-3: Unit commitment approaches (a) binary and (b) integer clustering
Graphic from Palmintier (2013)

This clustered unit commitment formulation entails two simplifying assumptions: (1) that all clustered units have identical parameters (e.g., capacity size, ramp rates, heat rate) and (2) that all committed units in a given time step t are operating at the same power output per unit. As new units are typically considered identical in capacity planning models, the first assumption does not affect results. However, it is relevant for brownfield capacity planning where $CAP^0_{y,z} > 0$. In this case units should be clustered using an appropriate clustering methodology (e.g., k-means) based on one or more parameters. Palmintier (2013) finds that clustering based on plant efficient (heat rate) produces minimal errors across all metrics (objective function, capacity totals, energy shares, CO_2). The second simplifying assumption applies to both new and existing units and results in some degree of unavoidable abstraction error. For example, if a cluster of 10 units are operating at 80% of total committed capacity, it is assumed that all units are operating at 80% of their individual capacity. In reality, one or more units would likely be operating at their minimum stable output level, while the others would be operating at full capacity. However, Palmintier (2013); Palmintier and Webster (2014) demonstrates that this assumption produces very small abstraction errors, generally below 1 percent on each metric compared to a binary unit commitment formulation, while

offering a roughly order of magnitude improvement in solution time.[9]

In addition, it is possible to configure GenX to model a linear relaxation of the discrete unit commitment decisions and related constraints. This is accomplished by replacing the integer unit commitment and capacity addition variables with continuous variables, but subject to the same set of constraints (e.g., Eq. 3.40–3.49). That is, the feasible solution set must be contained in the convex hull formed by the integer commitment decisions and constraints described in this section. The linear relaxation of the unit commitment constraints set offers an additional significant improvement computational tractability (run-times are improved by roughly 60-80% in most cases), but entails a further reduction in accuracy as final solutions ignore the discrete nature of real-world generator construction and unit commitment decisions. By still employing the full set of unit commitment constraints, however, this linear relaxation produces more accurate results than a simple linear economic dispatch formulation that entirely ignores unit commitment decisions. The feasible region for this linear relaxation matches more closely to the set of discrete feasible solutions to the integer unit commitment problem than the simpler set of economic dispatch constraints more typically applied in capacity planning models (i.e., ignoring start-up, shut-down, minimum output, etc. and constraining only ramp rates and maximum output). However, GenX also offers the ability to model thermal generators using simplified economic dispatch constraints, simply by including generators in the set $\mathcal{H}$ but not $\mathcal{UC}$. See Fig. 3-4 for a conceptual depiction of these three approaches.

In practice, I find that this linear relaxation of the unit commitment constraints offers an acceptable level of accuracy and reduces dimensionality sufficiently to permit inclusion of significantly more zones (including distribution network zones) and more resource options (including various DERs). Tables 3.5–3.7 depicts abstraction errors and Fig. 3-5 depicts solve

[9]Note that in a capacity expansion problem, the number of units that may be built (e.g., are eligible for capacity expansion) can significantly exceed the number of units in the final solution. Using a binary unit commitment formulation, decision variables and constraints must be added to the model for all individual units that may possibly be built, vastly increasing the dimensionality relative to a static unit commitment and production cost simulation with fixed capacity. For realistic-size systems, capacity expansion with binary unit commitment decisions is typically not computationally tractable unless the dimensionality is reduced by selecting a significantly smaller set of representative hours, rather than modeling a full year. See de Sisternes (2014).

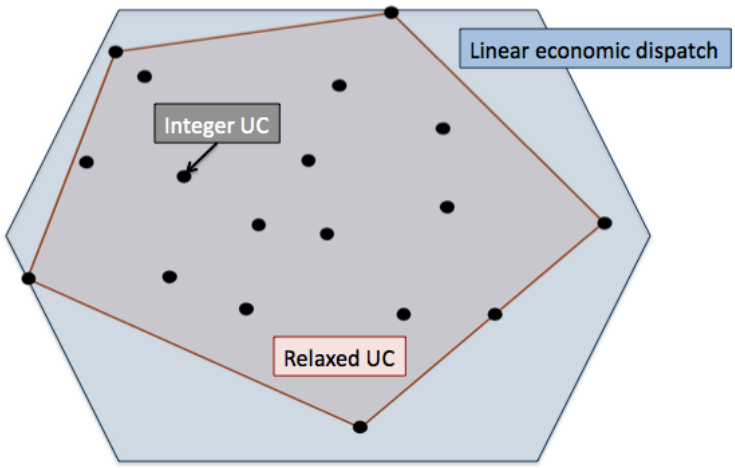

Figure 3-4: Illustrative depiction of feasible regions of discrete unit commitment, linear relaxation of unit commitment, and linear economic dispatch constraints

time for an example case I performed to compare the three approaches depicted in Fig. 3-4. Results of the relaxed unit commitment problem were generally less than 1 percent different from the integer unit commitment formulation results, including on total cost and each individual component of the objective function (maximum error ± 0.7%), installed capacity by individual unit type (maximum error ± 5% of peak system demand and less than 1% for most technologies), and annual energy output of individual technologies (maximum error ± 2.5% of share of annual energy demand supplied and less than 0.3% for most technologies). These results are substantially better than the simpler linear economic dispatch constraint set, which produces much larger errors.

These results align with findings from Palmintier and Webster (2014) who also compares these three approaches in a different set of test cases with >20% variable renewable energy shares. He found that the linear relaxation improves solution time by ≈ 50x with the lowest errors across all metrics, including: cost (≈ 1%), CO_2 (≈ 1%), and capacity and energy for individual technologies (≈ 9% or less difference).[10]

[10]Note that Palmintier reports results in terms of error relative to individual plant results, whereas I normalize all errors relative to the size of the system, so as to avoid treating a small difference in outcomes for a technology with a small installed capacity as more significant than errors for resources with higher installed capacity. Reported errors are thus not directly comparable.

Table 3.5: Comparison of errors due to abstraction of unit commitment constraints: cost

Abstraction error: cost

	Annual Cost (Million $)			Error (as % of total cost)	
Resource	Integer UC	Relaxed UC	Linear	Relaxed UC	Linear
Total cost	$44,229.2	$44,121.8	$44,467.2	-0.2%	0.5%
Fixed cost	$30,162.3	$29,878.5	$28,742.2	-0.6%	-3.2%
Variable cost	$3,779.2	$4,066.9	$5,346.8	0.7%	3.5%
Non-served energy cost	$10,225.0	$10,114.3	$10,378.2	-0.3%	0.3%
Start-up cost	$62.6	$62.3	$-	0.0%	-0.1%
Unmet reserve costs	$0.0	$0.0	$-	0.0%	0.0%
		1% Error =	$442.29	2% Error =	$884.58

Table 3.6: Comparison of errors due to abstraction of unit commitment constraints: capacity

Abstraction error: installed capacity

	Capacity (MW)			Error (as % of peak demand)	
Resource	Integer UC	Relaxed UC	Linear	Relaxed UC	Linear
Open cycle gas	500	466	0	-0.1%	-1.5%
Combined cycle gas	12,800	12,517	14,339	-0.8%	4.5%
Nuclear	5,000	4,870	3,390	-0.4%	-4.7%
Onshore wind	2,428	1,100	957	-3.9%	-4.3%
Solar - 10kW	52,899	53,182	52,616	0.8%	-0.8%
Li-ion storage - 10kW	21,942	21,922	21,576	-0.1%	-1.1%
Total	95,569	94,057	92,877	-4.4%	-7.9%
Peak demand	34,055	1% Error =	341 MW	2% Error =	681 MW

Table 3.7: Comparison of errors due to abstraction of unit commitment constraints: energy

Abstraction error: annual energy generation

	Annual Energy (GWh)			Error (as % of total demand)	
Resource	Integer UC	Relaxed UC	Linear	Relaxed UC	Linear
Open cycle gas	23.1	27.9	-	0.0%	0.0%
Combined cycle gas	48,794.7	52,624.4	70,003.6	2.2%	12.3%
Nuclear	42,428.4	41,469.7	28,150.5	-0.6%	-8.3%
Onshore wind	6,444.6	3,048.6	2,574.7	-2.0%	-2.2%
Solar - 10kW	78,953.6	79,469.2	75,994.1	0.3%	-1.7%
Li-ion storage – 10kW	22,903.8	22,836.1	23,303.6	0.0%	0.2%
Li-ion storage – (charge)	-28,276.3	-28,192.7	-28,769.9	0.0%	0.3%
Total annual demand	172,294.5	1% Error =	1,722.9	2% Error =	3,445.9

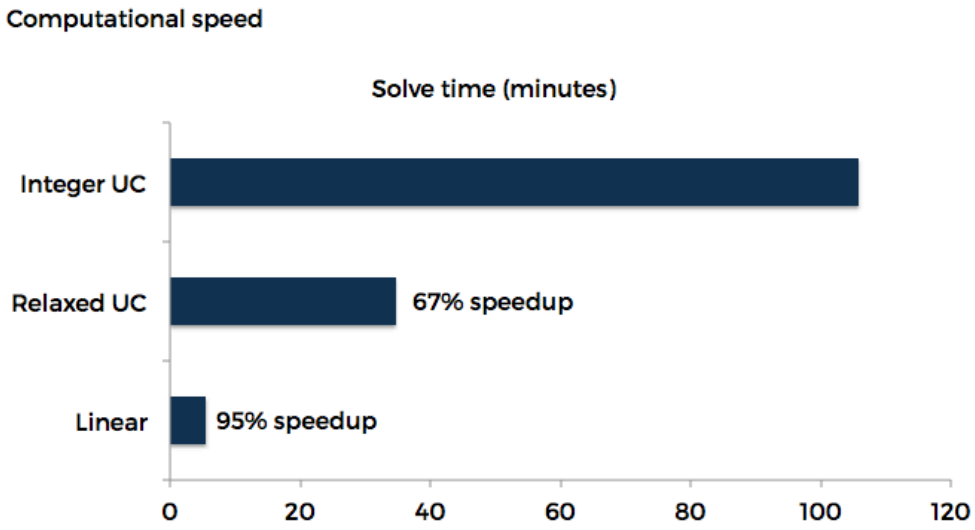

Figure 3-5: Improvement in computational performance for various approaches to abstraction of unit commitment constraints

Unit Commitment Constraints

Eq. 3.40–3.42, constrain the start-up, shut-down, and units committed variables to be less than or equal the total number of installed units in each cluster. Eq. 3.43 sets the relationship between the commitment state of the cluster, startups, and shutdowns across time. Note that as described in the objective function (Eq. 3.1), startup decisions will incur a startup cost $CSTART_{y,z}$ for every individual unit that it is started in cluster y in each time t.

$$\upsilon_{y,t,z} \leq (\frac{CAP^0_{y,z}}{U_{y,z}} + \Omega_{y,z} - \Delta_{y,z}), \qquad \forall y \in \mathcal{UC}, \forall z \in \mathcal{Z}, \forall t \in \mathcal{T} \tag{3.40}$$

$$\chi_{y,t,z} \leq (\frac{CAP^0_{y,z}}{U_{y,z}} + \Omega_{y,z} - \Delta_{y,z}), \qquad \forall y \in \mathcal{UC}, \forall z \in \mathcal{Z}, \forall t \in \mathcal{T} \tag{3.41}$$

$$\zeta_{y,t,z} \leq (\frac{CAP^0_{y,z}}{U_{y,z}} + \Omega_{y,z} - \Delta_{y,z}), \qquad \forall y \in \mathcal{UC}, \forall z \in \mathcal{Z}, \forall t \in \mathcal{T} \tag{3.42}$$

$$\upsilon_{y,t,z} = \upsilon_{y,t-1,z} + \chi_{y,t,z} - \zeta_{y,t,z}, \qquad \forall y \in \mathcal{UC}, \forall z \in \mathcal{Z}, \forall t \in \mathcal{T} \tag{3.43}$$

Eq. 3.45 and 3.44 require that clustered thermal generators' output in any time period does not exceed the installed capacity and does not fall below the minimum stable output of committed generators in the cluster.

$$\Theta_{y,t,z} \geq PMIN_{y,z} \times U_{y,z} \times \upsilon_{y,t,z}, \qquad \forall y \in \mathcal{UC}, \forall z \in \mathcal{Z}, \forall t \in \mathcal{T} \tag{3.44}$$

$$\Theta_{y,t,z} \leq U_{y,z} \times \upsilon_{y,t,z}, \qquad \forall y \in \mathcal{UC}, \forall z \in \mathcal{Z}, \forall t \in \mathcal{T} \tag{3.45}$$

Ramping limits capture constraints on how fast thermal units can adjust their power output in a given time step (e.g., change in power output per hour), reflecting constraints that limit the rate of change in output to avoid related thermal and mechanical stresses on generator equipment. For clusters of thermal generators, the hourly change in output must be constrained to reflect limits on the rate of change in the output of committed (online) generators, as well changes in aggregate output of the cluster reflecting start-up or shut-down of individual units in the cluster within the time step as per Palmintier (2013).

$$\Theta_{y,t-1,z} - \Theta_{y,t,z} \leq DOWN_{y,z} \times U_{y,z} \times (\upsilon_{y,t,z} - \chi_{y,t,z})$$
$$- PMIN_{y,z} \times U_{y,z} \times \chi_{y,t,z}$$
$$+ \max(PMIN_{y,z}, DOWN_{y,z}) \times U_{y,z} \times \zeta_{y,t,z}, \qquad \forall y \in \mathcal{UC}, \forall z \in \mathcal{Z}, \forall t \in \mathcal{T} \quad (3.46)$$

$$\Theta_{y,t,z} - \Theta_{y,t-1,z} \leq UP_{y,z} \times U_{y,z} \times (\upsilon_{y,t,z} - \chi_{y,t,z})$$
$$+ \max(PMIN_{y,z}, UP_{y,z})) \times U_{y,z} \times \chi_{y,t,z}$$
$$- PMIN_{y,z} \times U_{y,z} \times \zeta_{y,t,z}, \qquad \forall y \in \mathcal{UC}, \forall z \in \mathcal{Z}, \forall t \in \mathcal{T} \quad (3.47)$$

Thermal generators subject to unit commitment decisions must also respect minimum 'up time' and 'down time' constraints reflecting limits on the period of time between when a unit starts-up and when it can be shut-down again, and vice versa, which are applied at the cluster level as per Palmintier (2013) in Eq. 3.48 and 3.49:

$$\upsilon_{y,t,z} \geq \sum_{\hat{t}=t-MINUP_{y,z}}^{t} \chi_{y,\hat{t},z}, \qquad \forall y \in \mathcal{UC}, \forall z \in \mathcal{Z}, \forall t \in \mathcal{T} \quad (3.48)$$

$$(\frac{CAP^0_{y,z}}{U_{y,z}} + \Omega_{y,z} - \Delta_{y,z}) - \upsilon_{y,t,z} \geq \sum_{\hat{t}=t-MINDOWN_{y,z}}^{t} \zeta_{y,\hat{t},z}, \qquad \forall y \in \mathcal{UC}, \forall z \in \mathcal{Z}, \forall t \in \mathcal{T} \quad (3.49)$$

3.3.11 Economic Dispatch Constraints

Thermal units for which unit commitment constraints do not apply (e.g., $y \in (\mathcal{H} \setminus \mathcal{UC})$ face a simplified set of economic dispatch constraints given by Eq. 3.50–3.53. For these generators, investment and dispatch decisions are considered continuous variables. In this case, hourly changes in output (ramps down and ramps up) are constrained by Eq. 3.50 and 3.51 to be less than the maximum ramp rates ($DOWN_{y,z}$ and $UP_{y,z}$) in per unit terms times the total installed capacity of technology y. In addition, the total power output for technology y

must always operate between the minimum stable output, $PMIN_{y,z}$, and the total installed capacity of technology y (Eq. 3.52 and 3.53). Note that $PMIN_{y,z}$ may be equal to 0.

$$\Theta_{y,t-1,z} - \Theta_{y,t,z} \leq DOWN_{y,z} \times (CAP^0_{y,z} + \Omega_{y,z} - \Delta_{y,z}), \qquad \forall y \in (\mathcal{H} \setminus \mathcal{UC}), \forall z \in \mathcal{Z}, \forall t \in \mathcal{T} \tag{3.50}$$

$$\Theta_{y,t,z} - \Theta_{y,t-1,z} \leq UP_{y,z} \times (CAP^0_{y,z} + \Omega_{y,z} - \Delta_{y,z}), \qquad \forall y \in (\mathcal{H} \setminus \mathcal{UC}), \forall z \in \mathcal{Z}, \forall t \in \mathcal{T} \tag{3.51}$$

$$\Theta_{y,t,z} \geq PMIN_{y,z} \times (CAP^0_{y,z} + \Omega_{y,z} - \Delta_{y,z}), \qquad \forall y \in (\mathcal{H} \setminus \mathcal{UC}), \forall t \in \mathcal{T}, \forall z \in \mathcal{Z} \tag{3.52}$$

$$\Theta_{y,t,z} \leq (CAP^0_{y,z} + \Omega_{y,z} - \Delta_{y,z}), \qquad \forall y \in (\mathcal{H} \setminus \mathcal{UC}), \forall t \in \mathcal{T}, \forall z \in \mathcal{Z} \tag{3.53}$$

3.3.12 Variable Renewable Energy Resources

Power output from variable renewable energy (VRE) resources, including wind and solar energy and run-of-river hydroelectric power, are treated as a function of each technology's hourly capacity factor (or availability factor), in per unit terms, and the total capacity deployed. As the available solar insolation, wind speed, or streamflow for a given VRE resource varies over time, the capacity factor ($\overline{P}_{y,t,z,v}$) reflects the maximum possible power output in time t, expressed in per unit terms, and is specified exogenously for each resource type y, zone z, and voltage level, v. For dispatchable VRE resources ($y \in \mathcal{D}$), power output can be curtailed if desired, and thus hourly power output $\Theta_{y,t,z}$ must be less than or equal to the the hourly capacity factor times the installed capacity of that resource, as depicted in Eq. 3.54. This adds the possibility of introducing VRE curtailment as an extra degree of freedom to guarantee that generation exactly meets hourly demand. On the other hand, Eq. 3.55 shows that for non-dispatchable renewable resources ($y \in \mathcal{ND}$, e.g., generally distributed VRE generators that do not receive dispatch signals), output must exactly equal

the available capacity factor times the installed capacity, not allowing for curtailment.

$$\Theta_{y,t,z,v} \leq \overline{P}_{y,t,z,v} \times (CAP^{0}_{y,z,v} + \Omega_{y,z,v} - \Delta_{y,z,v}), \qquad \forall y \in \mathcal{D}, \forall t \in \mathcal{T}, \forall z \in \mathcal{Z}, \forall v \in \mathcal{VL} \tag{3.54}$$

$$\Theta_{y,t,z,v} = \overline{P}_{y,t,z,v} \times (CAP^{0}_{y,z,v} + \Omega_{y,z,v} - \Delta_{y,z,v}), \qquad \forall y \in \mathcal{ND}, \forall t \in \mathcal{T}, \forall z \in \mathcal{Z}, \forall v \in \mathcal{VL} \tag{3.55}$$

VRE resources are indexed across both zone and voltage level. Different unit scales can therefore be specified for available installations at each voltage level, including distributed solar (or wind) installed at distribution voltages.

3.3.13 Energy Storage Technologies

Different storage technologies, including pumped-hydro storage, mechanical storage devices, or electro-chemical storage batteries of various types (e.g., $y \in \mathcal{O}$) are all parametrized by their 'single-trip' charging and discharging efficiencies ($EFF^{up}_{y,z,v}$ and $EFF^{down}_{y,z,v}$), self-discharge rate (per hour, $DISCH_{y,z,v}$), and a fixed power to energy ratio, $P2E^{stor}_{y,z,v}$. This ratio captures the energy storage capacity (MWh) per unit of power charging/discharging capacity (MW), and can be considered the inverse of the numbers of hours it would take to fully discharge a full state of charge for a given power capacity of technology y. Note that in GenX, rated power capacity is treated as the AC injection and withdrawal capacity at the interface with the grid. Charging and discharging efficiencies are thus applied 'up-stream' of the injection/withdrawal interface, and reflect factors such as single-trip AC-DC inverter losses (if relevant), other balance of system losses, and charge/discharge conversion losses. Storage devices are then governed by a set of constraints which track the state of charge or stored energy level over time steps and constrain the state of charge and the charging and discharging power rates based on installed capacity.

Finally, note that since storage investment decisions are modeled as continuous, storage capacity represents the aggregated capacity of a number of similar storage units. Thus, charging and discharging are not mutually exclusive in any give time step (e.g., some storage

units may be charging and some discharging, if needed). However, the total power devoted to charging and discharging combined in any given time step t must remain less than or equal to the total installed capacity as shown in Eq. 3.62.

$$\Gamma_{y,t,z} = \Gamma_{y,t-1,z} - \left(\frac{\Theta_{y,t,z}}{EFF^{down}_{y,z,v}}\right) + (EFF^{up}_{y,z,v} \times \Pi_{y,t,z}) - (DISCH_{y,z,v} \times \Gamma_{y,t,z}), \qquad \forall y \in \mathcal{O}, \forall t \in \mathcal{T}, \forall z \in \mathcal{Z}, \forall v \in \mathcal{VL} \tag{3.56}$$

$$\Gamma_{y,t,z} \leq \frac{1}{P2E^{stor}_{y,z,v}} \times (\overline{\Delta_{y,z,v}} + \Omega_{y,z,v} - \Delta_{y,z,v}), \qquad \forall y \in \mathcal{O}, \forall t \in \mathcal{T}, \forall z \in \mathcal{Z}, \forall v \in \mathcal{VL} \tag{3.57}$$

$$\Pi_{y,t,z} \leq \left(\frac{1}{EFF^{up}_{y,z,v}}\right) \times (\overline{\Delta_{y,z,v}} + \Omega_{y,z,v} - \Delta_{y,z,v}), \qquad \forall y \in \mathcal{O}, \forall t \in \mathcal{T}, \forall z \in \mathcal{Z}, \forall v \in \mathcal{VL} \tag{3.58}$$

$$\Pi_{y,t,z} \leq \frac{1}{P2E^{stor}_{y,z,v}} \times (\overline{\Delta_{y,z,v}} + \Omega_{y,z,v} - \Delta_{y,z,v}) - \Gamma_{y,t,z}, \qquad \forall y \in \mathcal{O}, \forall t \in \mathcal{T}, \forall z \in \mathcal{Z}, \forall v \in \mathcal{VL} \tag{3.59}$$

$$\Theta_{y,t,z} \leq EFF^{down}_{y,z,v} \times (\overline{\Delta_{y,z,v}} + \Omega_{y,z,v} - \Delta_{y,z,v}), \qquad \forall y \in \mathcal{O}, \forall t \in \mathcal{T}, \forall z \in \mathcal{Z}, \forall v \in \mathcal{VL} \tag{3.60}$$

$$\Theta_{y,t,z} \leq \Gamma_{y,t,z}, \qquad \forall y \in \mathcal{O}, \forall t \in \mathcal{T}, \forall z \in \mathcal{Z} \tag{3.61}$$

$$\left(\frac{\Theta_{y,t,z}}{EFF^{down}_{y,z,v}}\right) + (EFF^{up}_{y,z,v} \times \Pi_{y,t,z}) \leq (\overline{\Delta_{y,z,v}} + \Omega_{y,z,v} - \Delta_{y,z,v}), \qquad \forall y \in \mathcal{O}, \forall t \in \mathcal{T}, \forall z \in \mathcal{Z}, \forall v \in \mathcal{VL} \tag{3.62}$$

Storage resources are also indexed across both zone and voltage level. Different unit scales can therefore be specified for available installations at each voltage level, including distributed storage installed at each distribution voltage level.

3.3.14 Demand Flexibility and Price-Responsive Demand

GenX includes two different forms of demand-side flexibility. First, flexible demand management technologies represent demand which may be shifted or deferred in time (i.e., some thermal loads, electric vehicle charging, water pumping, etc.). As implemented, flexible demand is characterized by the maximum percentage of demand at hour t that can be shifted, $FLEX_{y,z,v}$, and the maximum time before this demand must be satisfied, $SHIFT_{y,z,v}$. Multiple segments of deferrable or shiftable demand can be specified for each zone and voltage level by setting different values of $FLEX_{y,z,v}$ and $SHIFT_{y,z,v}$ for each segment. Note that the portion of load that can be shifted with a flexible demand management technology is specified exogenously, and as such, there is no investment decision variable for flexible demand in the current model. Operational decisions are endogenous and subject to constraints Eq. 3.63–3.65. The amount of deferred demand remaining to be served, $\Gamma_{y,t,z}$, depends on the amount in the previous hour $t-1$, minus the served energy during hour t, $\Pi y,t,z$, plus the demand that has been deferred during the current hour, $\Theta_{y,t,z}$ (see Eq. 3.63). At any given hour, the maximum amount of demand that can be shifted or deferred, $\Theta_{y,t,z}$, correspond to a fraction, $FLEX_{y,z,v}$, of the demand in that time period, $D_{t,z}$ (see Eq. 3.64). Shifted demand must then be served within a fixed period of time, as shown in Eq. 3.65. This is done by forcing the sum of demand satisfied in the following $SHIFT_{y,z,v}$ hours (e.g., $t+1$ to $t+SHIFT$) to be greater than or equal to the level of energy deferred at that time.

$$\Gamma_{y,t,z} = \Gamma_{y,t-1,z} - \Pi_{y,t,z} + \Theta_{y,t,z}, \qquad \forall y \in \mathcal{DR}, \forall t \in \mathcal{T}, \forall z \in \mathcal{Z}, \forall v \in \mathcal{VL} \tag{3.63}$$

$$\Theta_{y,t,z} \leq FLEX_{y,z,v} \times D_{t,z}, \qquad \forall y \in \mathcal{DR}, \forall t \in \mathcal{T}, \forall z \in \mathcal{Z}, \forall v \in \mathcal{VL} \tag{3.64}$$

$$\sum_{\hat{t}=t+1}^{t+SHIFT_{y,z,v}} \Pi_{y,\hat{t},z} \geq \Gamma_{y,t,z}, \qquad \forall y \in \mathcal{DR}, \forall t \in \mathcal{T}, \forall z \in \mathcal{Z}, \forall v \in \mathcal{VL} \tag{3.65}$$

GenX also includes demand response or price-responsive demand curtailment. Different segments, s, of the hourly demand represent aggregations of consumers with different marginal value of electricity consumption, given by $CNSE_s$. Thus, for a penalty or price equal to or greater than $CNSE_s$, consumers in segment s would be willing to curtail their

demand in a given time period t. In each time step, the amount of curtailed demand or non-served energy for each consumer segment, $\Lambda_{s,t,z}$, must be less than or equal to the fraction of demand, NSE_s, that belongs to segment s times the hourly demand $D_{t,z}$ (see Eq. 3.66). Note that at this stage, all demand response within distribution zones is assumed to occur at low voltage, as LV demand curtailments yield the greatest benefits in terms of marginal loss reduction and network capacity margin (see Chapter 2).

$$\Lambda_{s,t,z} \leq NSE_s \times D_{t,z}, \qquad \forall s \in \mathcal{S}, \forall t \in \mathcal{T}, \forall z \in \mathcal{Z} \tag{3.66}$$

3.3.15 Operating Reserves

GenX may be configured to model requirements for two types of operating reserves: frequency regulation or primary reserves; and secondary reserves, also known as balancing energy, spinning reserves, or contingency reserves. Reserve requirements and technical definitions vary across system operators, so there is no universal definition of reserve categories. Requirements for the two reserve categories and constraints on the ability of different resources to provide each reserve class can be parameterized to reflect different practices.

As GenX is currently written, the primary reserve or frequency regulation requirement is intended to represent system operator requirements for automatic inertial response to deviations in frequency out of the nominal operating range (i.e., 60 Hz in the United States, 50 Hz in Europe, etc.), typically achieved via the governor response of online generators with rotational mass (e.g., thermal generators, hydro generators, kinetic storage devices). It is also technically possible for inverter-connected devices (e.g., solar PV, electrochemical storage, fuel cells) and wind turbines to provide synthetic inertial response, although this is not common practice in most systems today. GenX is flexible to allow the user to specify the fraction of a given resource's capacity that can be committed to frequency regulation/primary reserves, including asynchronous generators capable of providing synthetic inertia, if desired.

Secondary or spinning reserve requirements are intended to represent online (or certain quick start) generators capable of automatically and rapidly responding to system operator

dispatch signals in case of a significant frequency imbalance or contingency (e.g., generator or transmission outage), typically within a 5-30 minute response time. The user can also specify the portion of capacity that can be committed to secondary reserves for each resource type, as desired.

Note that GenX does not currently include requirements for tertiary or replacement reserves (e.g., offline generators capable of starting up to replace secondary reserves after a contingency).

Operating Reserve Requirements

Eq. 3.67 and Eq. 3.68 require that in every hour the sum of primary reserves/frequency regulation provided across all technologies and zones must be greater than or equal to the system's reserve requirement. The hourly requirements for frequency regulation reserve are symmetric—equal in magnitude for regulation up and down—and are determined as a fraction of the total hourly demand $F(D)$ and the total hourly generation from VRE resources $F(RE)$. This requirement thus represents regulation required to respond rapidly to forecast errors in demand or VRE output.

$$\sum_{y\in\mathcal{G}}\sum_{z\in\mathcal{Z}}\theta^{+}_{y,z,t} \geq F(D)\sum_{z\in\mathcal{Z}}D_{t,z} + F(RE)\sum_{z\in\mathcal{Z}}\sum_{y\in(\mathcal{RE})}(\Omega_{y,z,v}\times PMAX_{y,t,z,v}), \qquad \forall t\in\mathcal{T} \quad (3.67)$$

$$\sum_{y\in\mathcal{G}}\sum_{z\in\mathcal{Z}}\theta^{-}_{y,z,t} \geq F(D)\sum_{z\in\mathcal{Z}}D_{t,z} + F(RE)\sum_{z\in\mathcal{Z}}\sum_{y\in(\mathcal{RE})}(\Omega_{y,z}\times PMAX_{y,t,z}), \qquad \forall t\in\mathcal{T} \quad (3.68)$$

Secondary reserves requirements can be specified asymmetrically in the upward and downward directions as a function of demand, $R^{+}(D)$ and $R^{-}(D)$, and VRE generation, $R^{+}(RE)$ and $R^{-}(RE)$, for each hour. As shown in Eq. 3.69, the total secondary reserves up provided across all technologies and zones must be greater than or equal to the system requirement, unless the unmet reserve variable, $\rho^{+,unmet}_{t}$, takes a value different from zero, which entails a cost of $CRSV$ for each MW of unmet reserves. This penalty, $CRSV$, should represent the increased probability of incurring costs of non-served energy as secondary reserves are depleted and can be used to approximate a (linear) operating reserve demand curve (Hogan,

2013).

As Eq. 3.69 illustrates, secondary reserve requirements up not only depend on demand and VRE generation, but also on a contingency requirement, $contingency_t$, that changes depending on the model configuration, and is intended to represent the secondary reserves required to ramp up quickly in case of unanticipated generator or transmission line outages. As shown in Eq. 3.69 the contingency requirement can take one of four values:

- (Configuration 1) the capacity of the largest single generator that *could* be deployed in the system;
- (Configuration 2) the capacity of either the largest generator that *could* be deployed in the system or the largest transmission capacity in the system, whichever is greater;
- (Configuration 3) the capacity of either the largest generator that *has* been deployed in the system or the largest transmission capacity in the system, whichever is greater; or
- (Configuration 4) the capacity of the largest generator that has been *committed* in the specific hour in the system or the largest transmission capacity in the system, whichever is greater.

The latter options for specifying contingency requirements based on actual generator investment or commitment decisions are more dynamic and realistic, but they entail greater computational burden due to the requirement for auxiliary variables and constraints required to track the largest generator built or committed. Implementing the *max* function for Configuration 3 adds a number of auxiliary constraints equal to the number of resource types eligible for construction, while Configuration 4 adds a number of auxiliary constraints equal to the number of resource types eligible for construction times the number of time steps modeled. Configuration 1 and 2 add only a single constraint and are thus simpler and more computationally efficient options.

$$\sum_{y\in\mathcal{G}}\sum_{z\in\mathcal{Z}}\rho^{+}_{y,z,t}+\rho^{+,unmet}_{t}\geq$$
$$R^{+}(D)\sum_{z\in\mathcal{Z}}D_{t,z}+R^{+}(RE)\sum_{z\in\mathcal{Z}}\sum_{y\in(\mathcal{RE})}(\Omega_{y,z}\times PMAX_{y,t,z})+contingency_{t},\qquad\forall t\in\mathcal{T}$$

Where:

$$contingency_{t}=\begin{cases}\max(U_{y,z}) & \text{if cont. 1}\\ \max(\max(U_{y,z}),\max(TCAP_{l})) & \text{if cont. 2}\\ \max(\max(U_{y,z}),\max(TCAP_{l})) & \forall y\mid\Omega_{y,z}\neq 0\text{ if cont. 3}\\ \max(\max(U_{y,z}),\max(TCAP_{l})) & \forall y\mid\upsilon_{y,t,z}\neq 0\text{ if cont. 4}\end{cases},\qquad\forall t\in\mathcal{T}$$

(3.69)

Secondary reserves in the downward direction are a function solely of forecasted demand ($R^{-}(D)$) and VRE output (($R^{-}(RE)$). Total secondary reserves down provided across all technologies and zones must be greater than or equal to the system requirement, unless the unmet reserve variable, $\rho^{-,unmet}_{t}$, takes a value different from zero, incurring a cost of $CRSV$ for each MW of unmet reserves.

$$\sum_{y\in\mathcal{G}}\sum_{z\in\mathcal{Z}}\rho^{-}_{y,z,t}+\rho^{-,unmet}_{t}\geq$$
$$R^{-}(D)\sum_{z\in\mathcal{Z}}D_{t,z}+R^{-}(RE)\sum_{z\in\mathcal{Z}}\sum_{y\in(\mathcal{RE})}(\Omega_{y,z}\times PMAX_{y,t,z}),\qquad\forall t\in\mathcal{T}\qquad(3.70)$$

Constraints on Contribution of Capacity to Reserves

If reserve requirements are modeled, an additional set of constraints is added for each resource type capable of providing reserves, as follows.

$$\theta^{+}_{y,z,t} \leq \overline{REG}^{+}_{y,z}(U_{y,z} \times \upsilon_{y,t,z}), \qquad \forall y \in (\mathcal{UC} \cap \mathcal{H}), \forall t \in \mathcal{T}, \forall z \in \mathcal{Z} \quad (3.71)$$

$$\theta^{-}_{y,z,t} \leq \overline{REG}^{-}_{y,z}(U_{y,z} \times \upsilon_{y,t,z}), \qquad \forall y \in (\mathcal{UC} \cap \mathcal{H}), \forall t \in \mathcal{T}, \forall z \in \mathcal{Z} \quad (3.72)$$

$$\rho^{+}_{y,z,t} \leq \overline{RSV}^{+}_{y,z}(U_{y,z} \times \upsilon_{y,t,z}), \qquad \forall y \in (\mathcal{UC} \cap \mathcal{H}), \forall t \in \mathcal{T}, \forall z \in \mathcal{Z} \quad (3.73)$$

$$\rho^{-}_{y,z,t} \leq \overline{RSV}^{-}_{y,z}(U_{y,z} \times \upsilon_{y,t,z}), \qquad \forall y \in (\mathcal{UC} \cap \mathcal{H}), \forall t \in \mathcal{T}, \forall z \in \mathcal{Z} \quad (3.74)$$

$$\theta^{+}_{y,z,t} \leq REG^{+}_{y,z} \times PMAX_{y,t,z}(CAP^{0}_{y,z} + \Omega_{y,z} - \Delta_{y,z}), \qquad \forall y \notin (\mathcal{UC} \cup \mathcal{ND} \cup \mathcal{DR}), \forall t \in \mathcal{T}, \forall z \in \mathcal{Z} \quad (3.75)$$

$$\theta^{-}_{y,z,t} \leq REG^{-}_{y,z} \times PMAX_{y,t,z}(CAP^{0}_{y,z} + \Omega_{y,z} - \Delta_{y,z}), \qquad \forall y \notin (\mathcal{UC} \cup \mathcal{ND} \cup \mathcal{DR}), \forall t \in \mathcal{T}, \forall z \in \mathcal{Z} \quad (3.76)$$

$$\rho^{+}_{y,z,t} \leq RSV^{+}_{y,z} \times PMAX_{y,t,z}(CAP^{0}_{y,z} + \Omega_{y,z} - \Delta_{y,z}), \qquad \forall y \notin (\mathcal{UC} \cup \mathcal{ND} \cup \mathcal{DR}), \forall t \in \mathcal{T}, \forall z \in \mathcal{Z} \quad (3.77)$$

$$\rho^{-}_{y,z,t} \leq RSV^{-}_{y,z} \times PMAX_{y,t,z}(CAP^{0}_{y,z} + \Omega_{y,z} - \Delta_{y,z}), \qquad \forall y \notin (\mathcal{UC} \cup \mathcal{ND} \cup \mathcal{DR}), \forall t \in \mathcal{T}, \forall z \in \mathcal{Z} \quad (3.78)$$

Finally, storage technologies can provide reserves when both charging and discharging by adjusting the amount of power injection or withdrawal according to system operator dispatch. The total amount of primary reserves and secondary reserves provided by storage

technologies thus equals the sum provided by each process, charging (C) and discharging (D) (see Eq. 3.79 to Eq. 3.82).

$$\theta^{+}_{y,z,t} = \theta^{+D}_{y,z,t} + \theta^{+C}_{y,z,t}, \qquad \forall y \in \mathcal{O}, \forall t \in \mathcal{T}, \forall z \in \mathcal{Z} \tag{3.79}$$

$$\theta^{-}_{y,z,t} = \theta^{-D}_{y,z,t} + \theta^{-C}_{y,z,t}, \qquad \forall y \in \mathcal{O}, \forall t \in \mathcal{T}, \forall z \in \mathcal{Z} \tag{3.80}$$

$$\rho^{+}_{y,z,t} = \rho^{+D}_{y,z,t} + \rho^{+C}_{y,z,t}, \qquad \forall y \in \mathcal{O}, \forall t \in \mathcal{T}, \forall z \in \mathcal{Z} \tag{3.81}$$

$$\rho^{-}_{y,z,t} = \rho^{-D}_{y,z,t} + \rho^{-C}_{y,z,t}, \qquad \forall y \in \mathcal{O}, \forall t \in \mathcal{T}, \forall z \in \mathcal{Z} \tag{3.82}$$

Alternative Operating Constraints Applied if Reserves are Modeled

If reserves are modeled, the minimum and maximum power output constraints for each resource type capable of providing reserves are also replaced by alternate operating constraints as follows:

$$\Theta_{y,t,z} - \theta^{-}_{y,z,t} - \rho^{-}_{y,z,t} \geq PMIN_{y,z} \times \Omega^{size}_{y,z} \times \upsilon_{y,t,z}, \qquad \forall y \in \mathcal{UC}, \forall z \in \mathcal{Z}, \forall t \in \mathcal{T} \tag{3.83}$$

$$\Theta_{y,t,z} + \theta^{+}_{y,z,t} + \rho^{+}_{y,z,t} \leq \Omega^{size}_{y,z} \times \upsilon_{y,t,z}, \qquad \forall y \in \mathcal{UC}, \forall z \in \mathcal{Z}, \forall t \in \mathcal{T} \tag{3.84}$$

$$\Theta_{y,t,z} - \theta^{-}_{y,z,t} - \rho^{-}_{y,z,t} \geq PMIN_{y,z}(CAP^{0}_{y,z} + \Omega_{y,z} - \Delta_{y,z}), \qquad \forall y \in (\mathcal{H} \setminus \mathcal{UC}), \forall t \in \mathcal{T}, \forall z \in \mathcal{Z} \tag{3.85}$$

$$\Theta_{y,t,z} + \theta^{+}_{y,z,t} + \rho^{+}_{y,z,t} \leq (CAP^{0}_{y,z} + \Omega_{y,z} - \Delta_{y,z}), \qquad \forall y \in (\mathcal{H} \setminus \mathcal{UC}), \forall t \in \mathcal{T}, \forall z \in \mathcal{Z} \tag{3.86}$$

$$\Pi_{y,t,z} + \theta^{-C}_{y,z,t} + \rho^{-C}_{y,z,t} \leq \frac{(CAP^0_{y,z} + \Omega_{y,z} - \Delta_{y,z})}{EFF^{up}_{y,z}}, \qquad \forall y \in \mathcal{O}, \forall t \in \mathcal{T}, \forall z \in \mathcal{Z} \tag{3.87}$$

$$\Pi_{y,t,z} + \theta^{-C}_{y,z,t} + \rho^{-C}_{y,z,t} \leq \frac{(CAP^0_{y,z} + \Omega_{y,z} - \Delta_{y,z})}{P2E_{y,z}} - \Gamma_{y,t,z}, \qquad \forall y \in \mathcal{O}, \forall t \in \mathcal{T}, \forall z \in \mathcal{Z} \tag{3.88}$$

$$\Pi_{y,t,z} - \theta^{+C}_{y,z,t} - \rho^{+C}_{y,z,t} \geq 0, \qquad \forall y \in \mathcal{O}, \forall t \in \mathcal{T}, \forall z \in \mathcal{Z} \tag{3.89}$$

$$\Theta_{y,t,z} + \theta^{+D}_{y,z,t} + \rho^{+D}_{y,z,t} \leq EFF^{down}_{y,z} \times (CAP^0_{y,z} + \Omega_{y,z} - \Delta_{y,z}), \qquad \forall y \in \mathcal{O}, \forall t \in \mathcal{T}, \forall z \in \mathcal{Z} \tag{3.90}$$

$$\Theta_{y,t,z} + \theta^{+D}_{y,z,t} + \rho^{+D}_{y,z,t} \leq \Gamma_{y,t,z}, \qquad \forall y \in \mathcal{O}, \forall t \in \mathcal{T}, \forall z \in \mathcal{Z} \tag{3.91}$$

$$\Theta_{y,t,z} - \theta^{-D}_{y,z,t} + \rho^{-D}_{y,z,t} \geq 0, \qquad \forall y \in \mathcal{O}, \forall t \in \mathcal{T}, \forall z \in \mathcal{Z} \tag{3.92}$$

$$\left(\frac{\Theta_{y,t,z} + \theta^{+D}_{y,z,t} + \rho^{+D}_{y,z,t}}{EFF^{down}_{y,z}}\right) + \left(EFF^{up}_{y,z}(\Pi_{y,t,z} + \theta^{-C}_{y,z,t} + \rho^{-C}_{y,z,t})\right) \leq (CAP^0_{y,z} + \Omega_{y,z} - \Delta_{y,z}), \qquad \forall y \in \mathcal{O}, \forall t \in \mathcal{T}, \forall z \in \mathcal{Z} \tag{3.93}$$

3.3.16 Policy Constraints: CO_2 Emissions Limits and Renewable Energy Requirements

For every technology y, the parameter $CO2_{y,z,v}$ reflects the carbon emissions rate in tCO_2/MWh associated with operation.[11] A constraint or cap on total system-wide CO_2 emissions inten-

[11]The model implementation uses a parameter to specify a CO_2 content per MMBtu for each fuel, and each generator has a designated fuel type (which determines both CO_2 content and fuel price); then the heat rate of each unit times the CO_2 content is the plant's CO_2 emissions rate. Ultimately, the solver will treat this resulting emissions rate as a single parameter.

sity in tCO_2/MWh, $\overline{CO2}$, can be established as shown in Eq. 3.94:

$$\sum_{z\in\mathcal{Z}}\sum_{y\in\mathcal{G}}\sum_{t\in\mathcal{T}}(CO2_{y,z}\times(\Theta_{y,t,z}+\Pi_{y,t,z}))\leq\sum_{z\in\mathcal{Z}}\sum_{t\in\mathcal{T}}(\overline{CO2}_{z}\times D_{t,z}), \tag{3.94}$$

Note that if the model is fully linear (e.g., $\mathcal{UC}=\emptyset$ or a linear relaxation of the unit commitment constraints is employed), the dual variable of the emissions constraints can be interpreted as the marginal CO_2 price per ton associated with the emissions limit.

The model can also include a renewable electricity mandate, renewable portfolio standard policy, or other constraint requiring a minimum share of energy from qualifying renewable energy resources as in Eq. :

$$\sum_{z\in\mathcal{Z}}\sum_{y\in\mathcal{RE}}\sum_{t\in\mathcal{T}}\Theta_{y,t,z}\geq MINRE\times\sum_{z\in\mathcal{Z}}\sum_{t\in\mathcal{T}}D_{t,z}, \tag{3.95}$$

Chapter 4

A System Planning Case Study

In this chapter, I demonstrate the application of the GenX whole system electricity resource planning model described in Chapter 3. I build a fictional but realistic power system region, 'Enerlandia,' with most inputs based on data from the New York Independent System Operator (NYISO). I then demonstrate how to apply the parameters from detailed distribution network experiments performed in Chapter 2 in order to represent distribution networks and distributed energy resources in a capacity planning framework. Indicative results are presented, illustrating the value of the new capabilities offered by this methodology and providing initial insight on the value and role of DERs and price-responsive demand in power systems.

4.1 Welcome to Enerlandia

To demonstrate the uses of the GenX model for whole system electricity resource planning, I constructed 'Enerlandia,' a fictional power system modeled loosely on the NYISO region. A diagram of the power system region is presented in Fig. 4-1. The region has five key transmission zones, with power flows within each zone unconstrained and power flows between zones subject to transmission constraints. Transmission path constraints and nominal voltages are taken from summer cross-state thermal transfer limits of the major transmission

paths in the NYISO system from NYISO (2016b).[1] Table 4.1 specifies other key transmission network parameters used by GenX.[2]

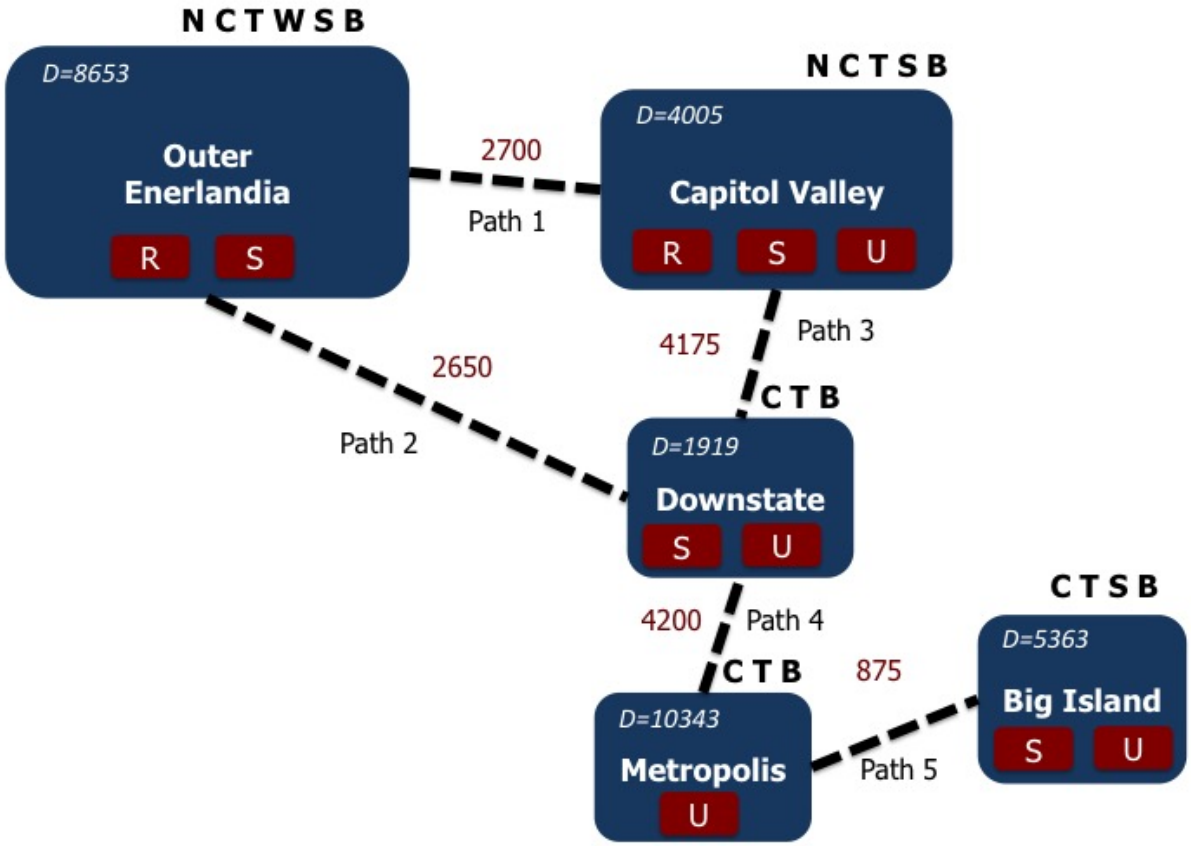

Figure 4-1: Diagram of the Enerlandia power system region
Dark blue areas are transmission zones with peak demand within the region in the upper left corner. Red areas indicate the types of representative distribution systems within each transmission zone (R=rural, S=semiurban, U=urban). The set of bulk generation resources available is printed above each zone (N=nuclear, C=CCGT, T=CT, W=wind, S=solar PV, B=Li-ion battery). Dashed lines indicate transmission corridors with power flow capacity limits in red lettering.

Demand for each region also comes from NYISO and represents 2016 hourly demand

[1]Path 1 corresponds to Central East, Line 2 to the remainder of the Total East transfer capacity (e.g., Total East less the Central East path), Path 3 corresponds to UPNY-ConEd, Path 4 to Sprain Brook-Dunwoodie South, and Path 5 to ConEd-LIPA.

[2]Line resistance was selected to yield 2.2 percent losses at 100% line loading for Paths 1-3 and 1% for Paths 4-5. Transmission expansion costs based on per mile costs from a 2014 WECC report on transmission component costs (Pletka et al., 2014) and approximate distances for each corresponding path in New York state with investment costs converted to an annuity at 8% weighted average cost of capital over 40 year asset life.

Table 4.1: Summary of key parameters for transmission network

Transmission Path	Maximum Capacity Expansion [MW] ($\overline{TCAP_l}$)	Expansion Cost [$ per MW-yr] ($CTCAP_l$)	Line Voltage [kV] ($VOLT_l$)	Line Resistance [Ohms] (OHM_l)
Path 1	1350	4348.3	345	0.9698
Path 2	1325	5316.4	345	0.9881
Path 3	2088	4419.0	345	0.6272
Path 4	2100	1757.1	345	0.2834
Path 5	438	4600.3	230	0.6046

from one or more corresponding zones in the NYISO system.[3] Wind and solar profiles for each zone are created by Renewables.ninja (Pfenninger and Staffell, 2018, 2016; Staffell and Pfenninger, 2016) using 2016 weather time series and several locations throughout the corresponding New York regions. Utility-scale solar PV systems installed at transmission voltage levels are modeled as single-axis tracking systems, while distributed PV installed at distribution voltage levels is modeled as roof-mounted fixed tilt systems (facing south and tilted at 35°).

Demand within each transmission zone is split across one or more representative distribution network zones with a share of demand assigned to both medium voltage (20 kV feeders) and low voltage (0.4 kV feeders), as summarized in Table 4.2. Each distribution network is either rural, semiurban, or urban in topology, with parameters based on the European distribution test networks created in Prettico et al. (2016) and described in detail in Chapter 2 Section 2.1. For simplicity, each network of a given typology (rural, semiurban, urban) is assumed to have identical parameters to all others of the same typology, with the exception of coincident peak withdrawal and injection capacities. Network withdrawal capacity is set at different p.u. shares of peak demand, with some networks lacking sufficient existing capacity to accommodate total peak demand within the distribution zone, representing various degrees of projected peak demand growth.[4] Table 4.3 summarizes the key distribution network

[3]Outer Enerlandia corresponds to NYISO Zones A-E, Capitol Valley to Zones F-G, Downstate to Zones H-I, Metropolis to Zone J and Big Island to Zone K. All data from day-ahead zonal load commitment reports available from the ISO's website at NYISO (2016a).

[4]Network withdrawal capacity is set to 98% of peak demand in Capitol Valley semiurban and urban networks; 95% in all Downstate and Big Island networks; and 90% in Metropolis.

related parameters obtained from the detailed distribution network modeling experiments in Chapter 2.

Table 4.2: Summary of representative distribution network zones in Enerlandia

	Share of Demand [%]			*Peak Coincident Withdrawal Capacity† [MW]*		
Transmission Zone	Rural	Semiurban	Urban	Rural	Semiurban	Urban
Outer Enerlandia	70	30	0	6660	2860	n/a
Capitol Valley	50	30	20	2200	1180	780
Downstate	0	50	50	n/a	910	910
Metropolis	0	0	100	n/a	n/a	9310
Big Island	0	50	50	n/a	2550	2410

† - Peak coincident injection capacity for each network is 50 percent of withdrawal capacity.

Table 4.3: Summary of key parameters by representative distribution network topology

Parameter Name	Units	GenX Parameter Symbol†	Rural	Semiurban	Urban
Share of Demand in LV	p.u.	$SHARE_z^{mv}$	0.12	0.08	0.09
Loss quadratic LV coefficient	per MW	$LVQUAD_z$	0.0072	0.0025	0.0025
Loss linear MV coefficient	per MW	$MVNET_z$	0.059	0.0337	0.0347
Loss linear LV coefficient	per MW	$LVTOT_z$	0.0063	0.0063	0.0063
Reinforcement cost - LV	$ per MW-yr	$CDCAP_z^{lv}$	27,639	28,143	25,228
Reinforcement cost - MV	$ per MW-yr	$CDCAP_z^{mv}$	7,870	6,274	8,562
Net reduction LV linear coeff.	per MW	$LVCOEF_z^W$	0.2182	0.2236	0.3817
Net reduction LV quadr. coeff.	per MW	$LVCOEF2_z^W$	0.0700	0.0268	0.0376
Net reduction MV linear coeff.	per MW	$MVCOEF_z^W$	0.5297	0.0424	0.7232
Max contribution from MV	p.u.	$\overline{MV}_z^W$	0.642	0.077	0.469
Discount rate for MV	p.u.	$DISCOUNT_z$	0.135	0.091	0.096

† - See Table 3.4.

Note that each distribution network zone is meant to represent multiple networks of similar topology across the transmission zone. For example, peak demand in the Capitol semiurban network zone is nearly 15 times the peak demand in the semiurban test network upon which parameters are based. This network can thus be thought of as representing 15 similar semiurban networks throughout the Capitol Valley region.[5] Effects with linear

[5]Note that demonstrating effective methods for clustering distribution networks into similar groupings

coefficients (e.g. linear terms in the loss and net demand reduction formula) should scale proportionately, and no adjustment is required to reflect the multiple networks represented by the single distribution zone. However, parameters for quadratic terms need to be adjusted appropriately (e.g., $\sum_{i=1}^{n} X^2 \neq (nX)^2$). If we consider that each distribution network zone modeled represents N other similar networks with a total peak demand equal to S-times the peak demand demand in the representative network, then any quadratic term should be adjusted as follows:

$$\sum_{n=1}^{N} \gamma\left(\frac{S}{N}\right)^2 = N\left(\frac{\gamma}{N^2}\right)S^2 = \left(\frac{\gamma}{N}\right)S^2 \tag{4.1}$$

Thus, the quadratic parameters reported in Table 3.4 are each scaled appropriately based on the ratio of peak demand in the zone and the base network capacity for each of the three European test networks modeled in Chapter 2.[6]

The set of utility-scale generation and storage resources that can be installed in each transmission zone is indicated by the set of letters above each zone in Fig. 4-1. Utility-scale (or transmission-level) generator costs are from the National Renewable Energy Laboratory's Annual Technology Baseline 2017 edition NREL (2017) and represent projected costs for 2025. I assume that lithium ion (Li-ion) battery energy storage costs fall 75 percent below 2017 costs (from Lazard (2017)) by 2025, a relatively aggressive but possible cost trajectory for this rapidly improving technology. Performance characteristics for each resource type are from Sepulveda et al. (2018) and fuel costs are 2025 Reference Case values from U.S. EIA (2018).[7] These inputs are summarized in Table 4.4.

In addition to utility-scale resources installed at transmission voltages, the model may choose to install distributed solar PV and Li-ion storage systems at both medium and low

that can be represented by a tractable number of representative network topologies with sufficient accuracy remains a critical research challenge. Demonstrating a process for down-selecting from the full range of real distribution networks within a given power system to a smaller representative set without significant loss of accuracy is necessary if the methods developed in this thesis are to be applied in real-world power system planning contexts. This important piece of future work is discussed in Chapter 5.

[6]The coincident peak network capacities are as follows: 28.3 MW for the rural network, 81.95 MW for the semiurban network, and 68.75 MW for the urban network.

[7]Natural gas costs $4.48 per MMBtu and enriched uranium fuel rods for nuclear plants cost $0.66 per MMBtu of usable reactivity. Note that coal plants are excluded due to lack of economic competitiveness in this context based on test runs with steam coal at $2.28 per MMBtu.

Table 4.4: Summary of utility-scale generator and storage parameters by representative distribution network topology

Resource	Unit size Unit size [MW]	Overnight Cost [$/kW]	Installed Cost Annuity [k$/MW-yr]†	Fixed O&M [k$/MW-yr]	Variable O&M [$/MWh]	Fuel Cost [$/MWh]‡
Nuclear	1000	$5,234	$563.9	$102	$2	$6.90
CCGT	500	$997	$109.0	$10	$3	$28.13
CT	100	$852	$93.1	$12	$7	$40.68
Onshore Wind	∗	$1,276	$139.4	$51	$0	n/a
Solar PV	∗	$781	$126.1	$10	$0	n/a
Li-ion Battery	∗	$437 ($109/kWh)	$52.5	$11	$0	n/a

† - Installed capital costs (inclusive of financing during construction) are converted to an annuity using a weighted average cost of capital of 8.1% (long-run average financial conditions from NREL (2017)) and the following asset life per resource: nuclear 40 years; gas CCGT and CT 30 years; wind and solar 25 years. Financing cost during construction uses an 8% cost of debt and capital outlay formula from NREL (2017) with the following construction times (in years): nuclear 9; CCGT, CT, wind 3; solar, Li-ion: 1.
‡ - Fuel costs per MWh calculated assuming the following heat rates: 10.46 MMBtu/MWh for nuclear; 6.35 MMBtu/MWh for CCGT; 9.36 MMBtu/MWh for CT

∗ - Installed capacity for resources with modular unit size are considered continuous decision variables.

voltage levels in each of the 10 distribution zones. I assume that distributed solar PV systems installed at MV represent systems at the 0.5-5 MW scale that cost an incremental 25 percent more than utility-scale systems, while solar PV at LV represents systems at 10-100 kW scale and are 85 percent more expensive than utility-scale, as per data from Margolis et al. (2018) (summarized in Fig. 1-8). Similarly, distributed Li-ion battery storage systems at MV represent 1-10 MWh scale systems with 40 percent incremental cost relative to utility-scale battery systems and storage at LV is 100-500 kWh scale at 95 percent incremental cost as per data from Lazard (2017) (summarized in Fig. 1-9). Note that I did not include smaller scale solar or storage systems typical of residential installations at the 1-10 kW/kWh scale, as these systems are even more costly (see Figures 1-8 to 1-9). Without any additional locational value relative to larger options that can also be installed at LV, the model will never select this scale of system unless forced to do so (a reality that has significant policy implications, as discussed in Chapter 5). Sensitivity to economies of unit scale and incremental costs for both distributed resources are explored in the cases below.

Based on the average share of price-responsive day-ahead demand bids in the NYISO

system,[8] I assume that 6 percent of demand is price-responsive in any given hour: 1 percent will curtail demand at marginal prices above $250/MWh, 2 percent at prices above $500/MWh, and 3 percent at prices above $1,000/MWh. Beyond this level, if generation scarcity or binding network constraints prevent sufficient supply at any zone, demand can only be balanced via shedding load at a cost of non-served energy of $10,000/MWh. I do not model flexible or time shiftable demand in these cases.

Finally, note that each case is run as a greenfield expansion case, with no preexisting generator and storage capacity.

4.2 Cases

4.2.1 Base Case

This base case uses all of the base parameters described in Section 4.1 and models unit commitment decisions for thermal generators using the integer unit commitment formulation (see Chapter 3, Section 3.3.10), with resources clustered by resource type and zone. Reserve constraints are not included. This case is a mixed integer linear programming problem with 5 transmission zones, 10 distribution zones, 61 eligible resources – 21 at transmission voltage levels of which 12 are thermal units subject to unit commitment constraints and 40 at distribution levels – and 8,760 hourly time intervals. After elimination of redundant constraints and variables via Gurobi's pre-solve routine (Gurobi Optimization Inc., 2016), this results in a large optimization problem with 5.76 million rows, 4.66 million columns and 21.59 million non-zeros elements. There are 3.32 million continuous decision variables and 1.34 million integer variables (of which 1.05 million are binary[9]).

This case and all others are run on the Engaging Supercomputing Cluster located at the

[8] This corresponds to "price cap load" from NYISO (2016a).

[9] These binary variables are related to variables associated with approximation of quadratic transmission and distribution loss terms used to ensure segments of the segment-wise approximation fill in order to prevent phantom losses (see Chapter 3, Sections 3.3.7 & 3.3.8). This accuracy obviously comes at a considerable computational cost, and it may be worth disabling this feature of some degree of error due to phantom losses is tolerable. Future work should explore the importance of phantom losses to important outcomes of interest and explore tradeoffs between accuracy and computational speed.

Massachusetts Green High Performance Computing Center.[10] Each case is run on a single node making use of one Intel Xeon E5 Haswell-EP CPU with 2.1GHz, 16 cores, and 3.1 GB of memory per core and solved with Gurobi v7.5.0. Solutions within a 1 percent MIP gap[11] are considered solved to optimality. In practice, the final solution for this case is solved with a 0.099 percent gap.

Figures 4-2 to 4-3 show the resulting capacity and energy mix for this base case. Technologies that do not see any deployment are excluded from each chart. The first thing to note is that no distributed solar or storage are deployed in this base case. All resources are utility-scale generation and storage at transmission voltage zones and the capacity and energy mix is dominated by combined cycle natural gas plants. Combustion turbines and a small number of utility-scale Li-ion storage systems contribute to capacity needs while utility-scale solar PV generates a little over 3 percent of annual energy. Gas generators are spread throughout the Enerlandia region generally in proportion to demand, as installed costs are identical for each resource regardless of location. The model thus co-locates generators and demand when possible to minimize transmission losses. Cases with more realistic differences in installed costs (due to property values or labor cost differences) or prohibitions on siting would see more dispersion of gas generators and transmission constraints would become more important drivers of siting decisions. Solar meanwhile is deployed to capture the best capacity factor available in the three zones which may host solar (Outer Enerlandia, Capitol Valley and Big Island), although losses appear to be sufficient to split the location of solar across two of these regions, rather than situate all solar assets on Big Island (where utility-scale solar produces 4.7% more on average than an equivalent capacity in Capitol Valley). No wind or nuclear resources are built, due to their relatively high levelized costs and the lack of a policy driving low-carbon or renewable energy resource deployment.

It is notable that no DERs are adopted in the base case. As bulk generators can be located

[10] See http://mghpcc.org/

[11] The 'MIP gap,' or mixed integer programming gap, refers to difference between the current best upper and lower bound solutions which bound the actual optimal feasible integer solution. In this cost minimization context, a 1 percent MIP gap therefore means the best feasible integer solution returned is no more than 1 percent costlier than the linear relaxation that forms the lower bound of the MILP solution algorithm.

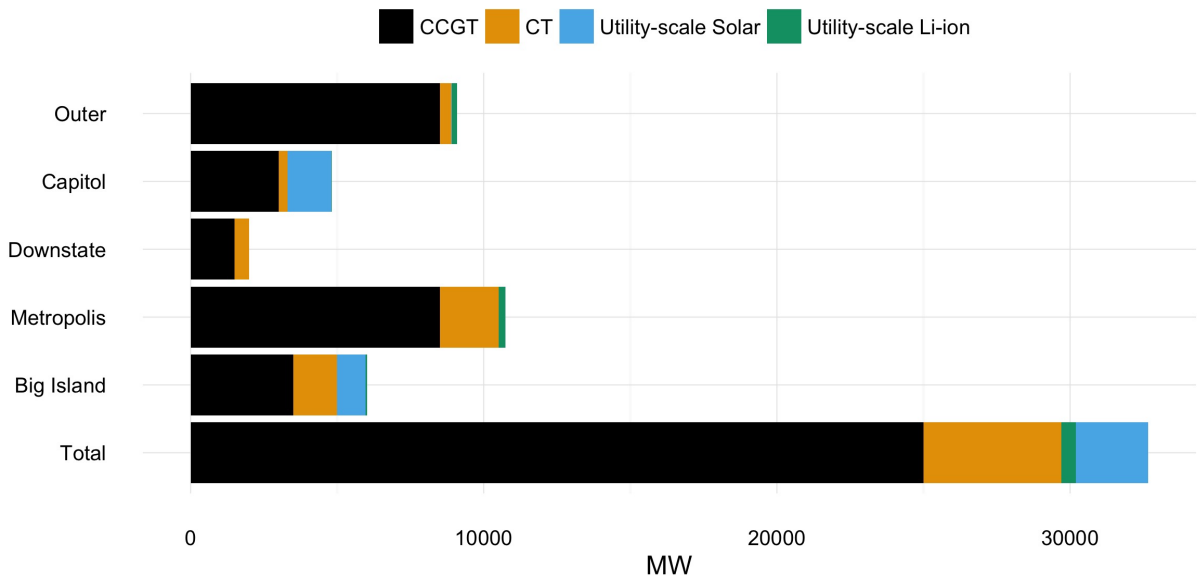

Figure 4-2: Installed capacity by region and resource type - base case with integer unit commitment

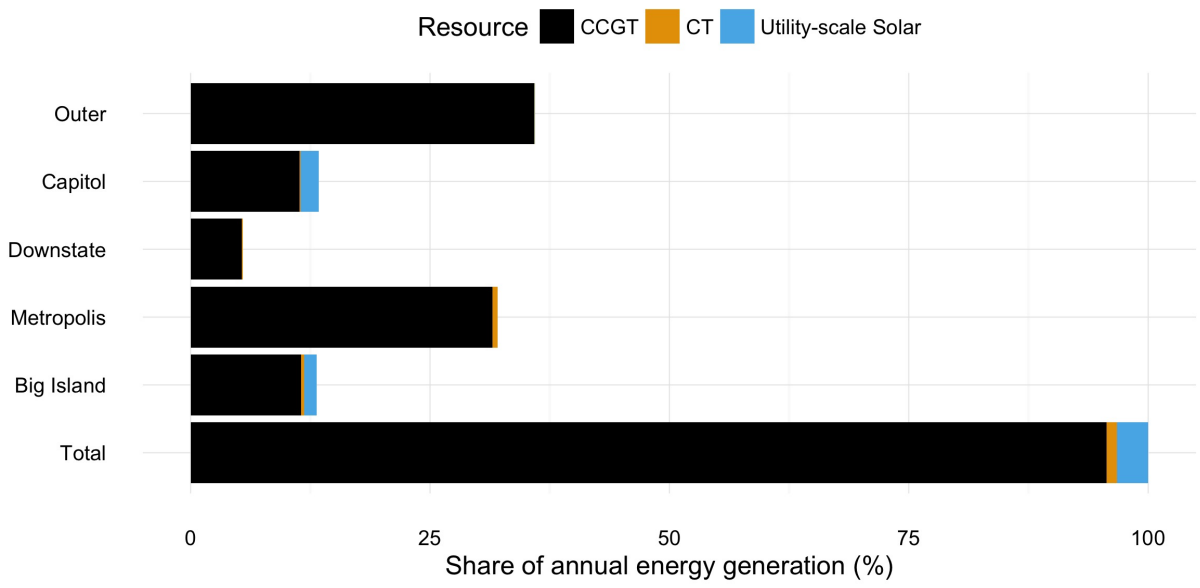

Figure 4-3: Share of annual energy generation by region and resource type - base case with integer unit commitment

in transmission zones near demand, transmission losses or congestions do not provide any additional locational value for DERs in this base case. However, coincident peak demand is greater than initial distribution network capacity in the Capitol Valley semiurban and urban networks and all Downstate, Metropolis, and Big Island distribution zones. Despite this potential source of locational value, the ability to avoid distribution network capacity upgrades does not result in distributed solar or storage adoption, because these resources face a more cost-effective competitor: price-responsive demand. As Figures 4-4 to 4-5 illustrate, reductions in annual demand of less than 0.1 percent below the base demand level is sufficient to avoid all distribution network margin upgrades – and then some. Indeed, price-responsive demand appears to be driven by the ability to avoid costly but poorly utilized generation capacity investments needed only to meet 'superpeak' demand periods that rarely occur throughout the year. Reductions in peak demand to avoid generation investments also coincide with coincident peak withdrawal periods within each distribution network and thus also provide sufficient network margin to avoid any network upgrades. Margin gained from price-responsive demand curtailment (or demand response) in this case thus exceeds needed network margin in all networks.

Without any remaining locational value to capture from network investment deferral, distributed solar and storage are simply too costly relative to utility-scale solar and storage to warrant adoption in this case. The incremental unit cost of solar and storage at MV are 25 percent and 40 percent greater than their utility-scale cousins, and distribution network losses – the only remaining source of locational value here – are not sufficient to justify this cost. Subsequent cases will explore more restrictive assumptions about demand elasticity and sensitivity to economies of unit scale assumptions for solar and storage...

4.2.2 Comparing Integer Unit Commitment and Linear Relaxation

This case explores the impact on accuracy and computational performance associated with using two different formulations to represent the unit commitment constraints and investment decisions for large thermal generators. The first approach is the integer clustering

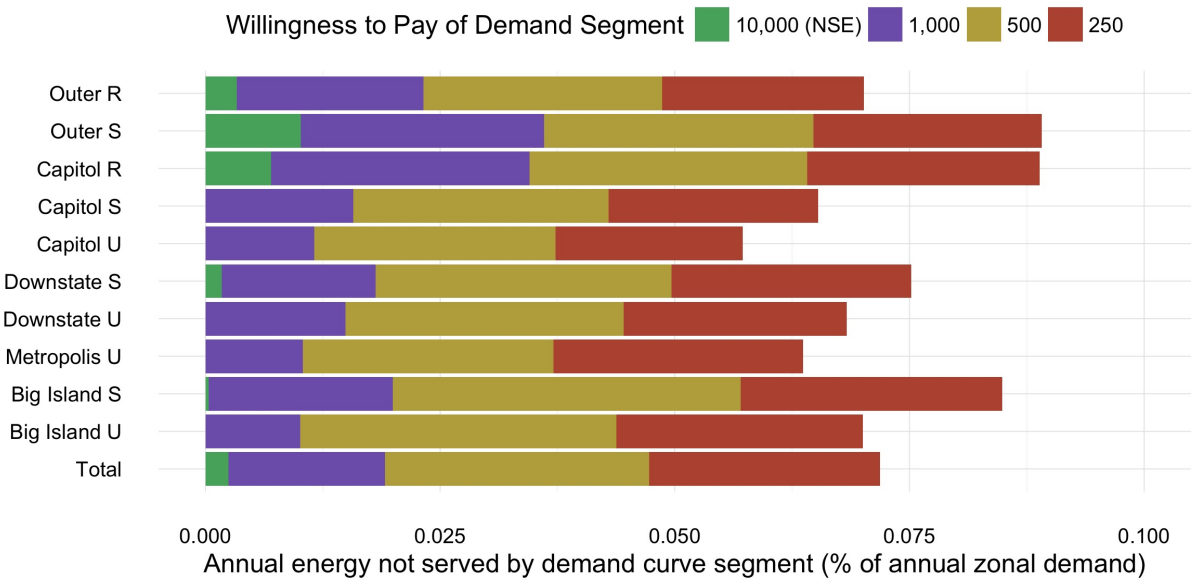

Figure 4-4: Price-responsive demand and non-served energy by region and demand segment - base case with Integer Unit Commitment

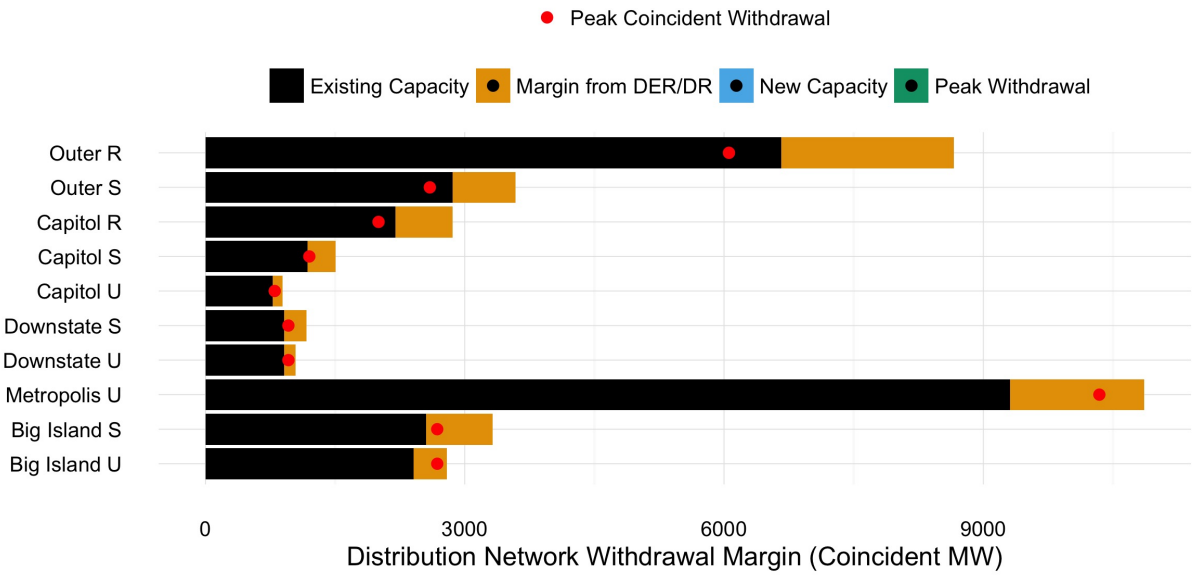

Figure 4-5: Coincident peak withdrawals and sources of distribution network capacity by region - base case with integer unit commitment

method used in the base case above, and the second case applies a linear relaxation of the integer unit commitment constraint set. That is, the second case is a linear program (LP) where the feasible region represents the convex hull of the discrete MILP problem in the base case. By eliminating discrete decision variables, solution time is considerably improved, but the final solution represents an abstraction of the feasible discrete decisions which incurs some measure of error along several important outcome variables. The results below compare the two solutions and quantify performance in terms of abstraction error and solution time.

Dimensionality and Solution Time

The relaxed UC base case is an LP with 2.67 million rows, 3.17 million columns, and 16.63 million nonzero elements after pre-solving and eliminating redundant constraints and variables. The problem solves in 246.54 minutes (approx. 4 hours, 6 mins) using Gurobi's concurrent solution method, which simultaneously applies multiple LP solution methods (simplex, dual simplex, and barrier) in parallel using different computing cores.

In contrast, I was unable to solve the integer UC base case using the concurrent solution method to find the linear relaxation (Gurobi's default) used to bound the MILP solution during the search for an optimal integer solution in under 12 hours (at which point the Engaging cluster ends unfinished tasks). However, by simultaneously running three instance of the integer UC case on different computing nodes, with Gurobi set to use a single LP relaxation search method in each case, I was able to find a solution that satisfied the MIP gap of 1 percent. The instance using the barrier method completed in 371.44 minutes (approx. 6 hours, 11 mins), while the other two methods both failed to find a satisfactory solution within the 12 hour limit.

To create a direct comparison for the integer UC case using the barrier method, I also re-ran the relaxed UC case specifying that Gurobi should use only Barrier method to solve (as this method was also the first to solve the relaxed problem during the concurrent search). This time, the model solved in 225.32 minutes (approx. 3 hours 45 mins, or about 9 percent faster than the concurrent solution method).

Thus, the relaxed UC method not only finds an optimal solution within the 12 hour limit, but it also solves roughly 40 percent faster than the integer UC formulation when directing Gurobi to use only the barrier method to find the LP solution/relaxation. In addition, barrier was the only one of Gurobi's four solution methods was capable of solving the integer UC instances to convergence in under 12 hours. The linear relaxation of the unit commitment constraint set therefore offers a meaningful performance improvement. But at what cost in terms of the accuracy of key outcomes of interest?

Comparison of Results and Abstraction Error

Figures 4-2–4-9 present the key results for the relaxed UC base case. These are all broadly similar to the integer solution. Indeed, Tables 4.5–4.7 present the error between the relaxed and integer UC cases (direction of error reflects the difference (relaxed result − integer results)). Total costs are within 0.1 percent of the integer solution. Individual cost errors are somewhat larger. Without the integrality constraints on larger thermal generators, the relaxed version slightly underestimates fixed costs and overestimates variable costs, but by no more than 0.4 percent of the total cost in either metric.

Table 4.5: Abstraction error from linear relaxation of integer unit commitment decisions: costs

	Cost errors	
	[M$]	[% of total cost]
Total costs	-9.30	-0.1
Fixed costs	-36.71	-0.4
Variable costs	24.93	0.3
Cost of unmet demand	2.55	0.0
Cost of startups	-0.07	0.0
Cost of unmet reserves	0.00	0.0
Cost of network expansion	0.00	0.0
Max error (±)	36.71	0.4

Errors reflect the difference between the relaxed UC case and the integer UC case

As Table 4.6 demonstrates, the differences in fixed and variable costs arise from a slight over-estimation of installed CCGT capacity and underestimation of solar and storage ca-

pacity due to the linear relaxation of the integer build decisions.[12] The continuous solution allows construction of a portion of a CCGT's discrete capacity in four of five zones that is not present in the integer solution, while one zone builds slightly less than the discrete capacity built under the integer case. Since overall CCGT capacity is slightly smaller in the integer case, the solution includes larger quantities of the modular technologies, solar and storage, than in the continuous case. The result is a slightly higher fixed cost (due to more capital-intensive solar and storage) and lower variable costs (due to less CCGT capacity) than the relaxed UC case. However, overall errors in installed capacity and annual energy generation are minor. Capacity results are off by less than half the discrete unit size of a CCGT for any individual resource and zone. Scaled to the size of the system, no single combination of resource and zone has an error of more than 0.66 percent of the total installed capacity with most below 0.2 percent. Errors in annual energy generation are similarly modest, especially when scaled to the size of total annual energy supply.

Finally, errors for the total annual non-served energy – or the sum of both price elastic demand not satisfied (the predominant volume here) and involuntary load shedding – as well as distribution network withdrawal margins gained via this demand-side flexibility are somewhat larger in normalized terms. However, this reflects the much smaller base values used for normalization here. In general, these differences are quite small.

Overall, the linear relaxation of the discrete unit commitment decisions ('relaxed UC') produces results that are accurate (likely within a range similar to the error produced by a 1 percent MIP gap for the MILP problem in fact). At the same time, this approach significantly improves solution time. As not all integer UC cases run will converge within the resource limit on the cluster I am using for a problem of this scale, I use the relaxed UC approach throughout the rest of these cases.

[12]Errors appear to be almost entirely due to relaxation of the discrete unit build decisions, rather than the hourly unit commitment decisions. It is likely that a formulation that retains integer build decisions but relaxes operational decisions may therefore improve further in accuracy, although at the cost of turning a fully continuous problem into a mixed integer linear problem. It would be worthwhile to compare performance of this alternative formulation in future research.

Table 4.6: Abstraction error from linear relaxation of integer unit commitment decisions: capacity and energy

		Capacity Error		Energy Error	
Resource	Zone	[MW]	[% of total MW]	[GWh]	[% of annual GWh]
CCGT	Outer	165	0.51	174	0.10
CCGT	Capitol	10	0.03	377	0.21
CCGT	Downstate	-51	-0.16	-75	-0.04
CCGT	Metropolis	172	0.53	182	0.10
CCGT	Big Island	53	0.16	296	0.17
CCGT subtotal		*349*	*1.07*	*954*	*0.54*
CT	Outer	-40	-0.12	-11	-0.01
CT	Capitol	42	0.13	20	0.01
CT	Downstate	-28	-0.09	3	0.00
CT	Metropolis	-38	-0.12	-123	-0.07
CT	Big Island	12	0.04	10	0.01
CT subtotal		*-52*	*-0.16*	*-79*	*-0.08*
Utility-scale Solar	Outer	-19	-0.06	-43	-0.02
Utility-scale Solar	Capitol	-217	-0.66	-494	-0.28
Utility-scale Solar	Big Island	-138	-0.42	-331	-0.19
Utility-scale Solar subtotal		*-374*	*-1.14*	*-868*	*-0.49*
Utility-scale Li-ion	Outer	-177	-0.54	-63	-0.04
Utility-scale Li-ion	Capitol	-12	-0.04	-4	0.00
Utility-scale Li-ion	Metropolis	-92	-0.28	-29	-0.02
Utility-scale Li-ion	Big Island	-36	-0.11	-10	-0.01
Utility-scale Li-ion subtotal		*-317*	*-0.97*	*-106*	*-0.07*
Max error (±)		217	0.66	494	0.28

Errors reflect the difference between the relaxed UC case and the integer UC case

Table 4.7: Abstraction error from linear relaxation of integer unit commitment decisions: non-served energy and distribution network capacity

	Non-served Energy Error		Distribution Margin Gained Error	
Zone	[MWh]	[% of total NSE]	[MW]	[% of total margin needed]
Outer R	-1463	-12.7	none	none
Outer S	-1686	-14.7	none	none
Capitol R	174	1.5	none	none
Capitol S	214	1.9	0	0.0
Capitol U	154	1.3	0	0.0
Downstate S	-12	-0.1	-1	-0.1
Downstate U	-52	-0.5	1	0.1
Metropolis U	-2256	-19.6	-65	-4.1
Big Island S	-84	-0.7	-83	-5.2
Big Island U	-548	-4.8	-1	-0.1
Max error (±)	2256	19.6	83	5.2

Errors reflect the difference between the relaxed UC case and the integer UC case

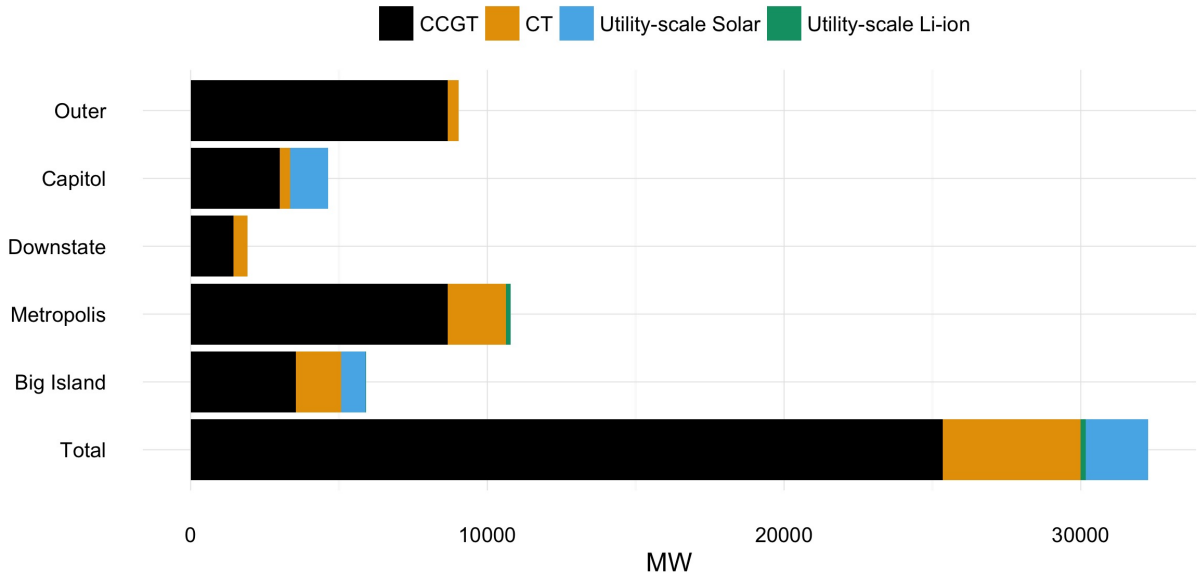

Figure 4-6: Installed capacity by region and resource type - base case with relaxed unit commitment

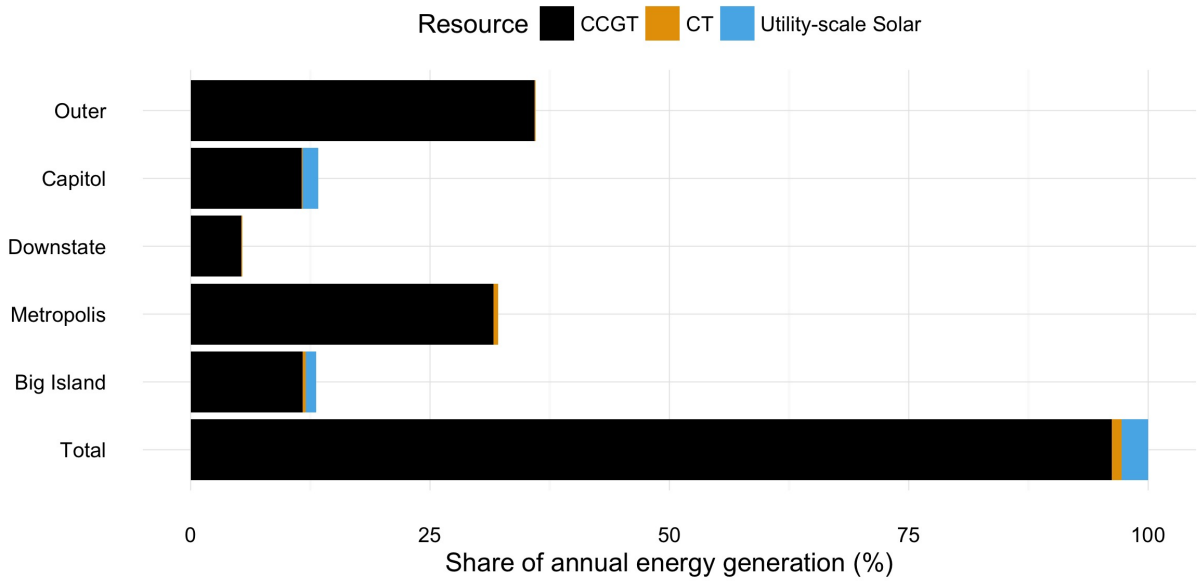

Figure 4-7: Share of annual energy generation by region and resource type - base case with relaxed unit commitment

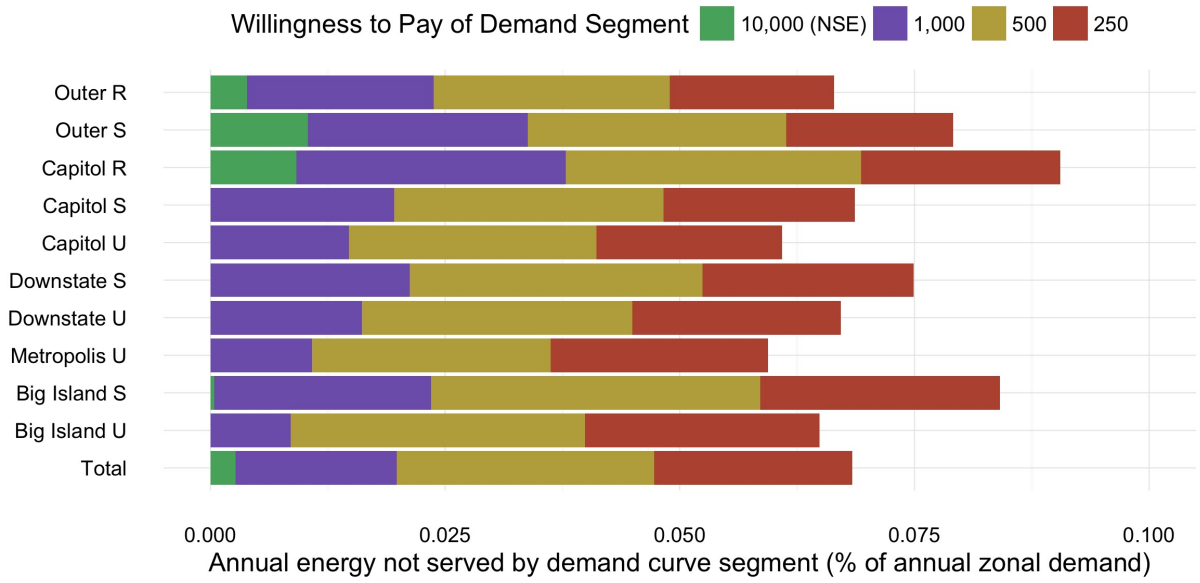

Figure 4-8: Price-responsive demand and non-served energy by region and demand segment - base case with relaxed unit commitment

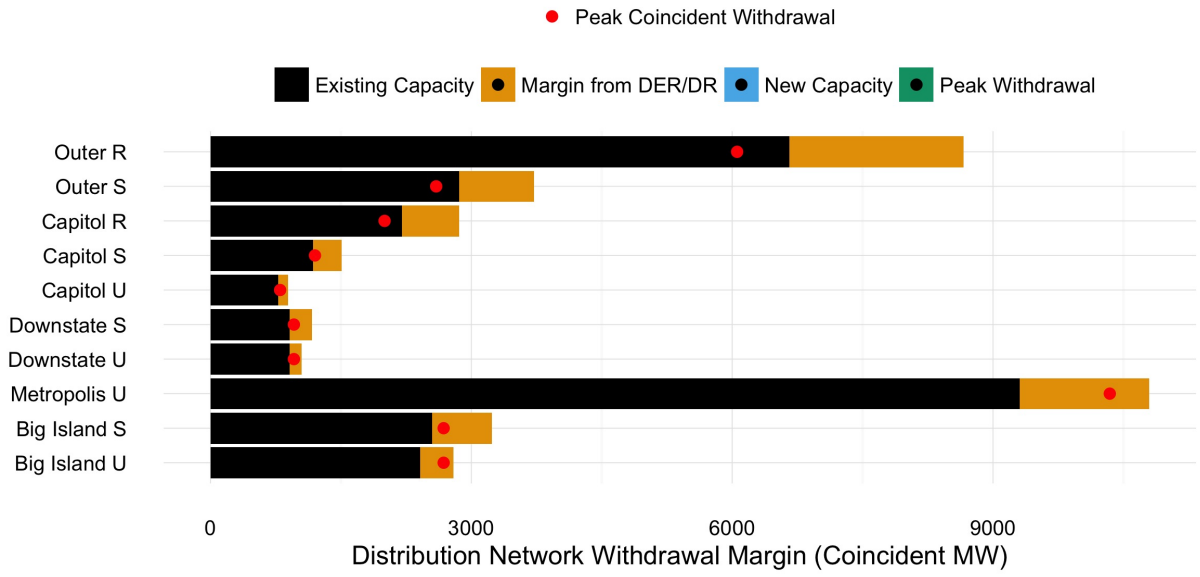

Figure 4-9: Coincident peak withdrawals and sources of distribution network capacity by region - base case with relaxed unit commitment

4.2.3 Does Modeling Distribution Make a Difference?

To determine how much of an impact inclusion of distribution network losses and reinforcements has on planning results, this case re-runs the base case with relaxed unit commitment constraints while ignoring distribution network parameters. All parameters for distribution network losses are set to zero and network reinforcement costs are free, eliminating these factors from the model's objective function.

As Table 4.8 illustrates, omitting distribution network losses and network capacity constraints / expansion costs from the generation and transmission planning problem leads to a systematic underestimation of power system costs. Overall system costs are 11.3 percent lower when distribution network parameters are ignored, or an error of just over $1 billion per year.

Table 4.8: Error due to omission of distribution network losses and expansion: costs

	Cost errors	
	[M$]	[% of total cost]
Total costs	-1060	-11.3
Fixed costs	-490	-5.2
Variable costs	-530	-5.7
Cost of unmet demand	-40.9	-0.4
Cost of startups	-0.57	0.0
Cost of unmet reserves	0.00	0.0
Cost of network expansion	0.00	0.0
Max error (±)	36.71	0.4

Errors reflect the difference between the case excluding distribution network parameters and the relaxed UC base case

Without considering distribution losses, overall capacity and energy are both underestimated by 12.3 percent and 10.2 percent, respectively (Table 4.9). The error in capacity is larger than the error in energy as losses are largest during coincident peak demand periods, which also drive overall capacity needs. Lower total capacity investments and energy dispatched are responsible for the majority of the error in total costs seen above.

By ignoring distribution losses and the ability to avoid distribution network upgrades, this case also undervalues price-responsive demand. As a result, price-responsive demand

curtailment is 26-52 percent lower across each of the segments of elastic demand. Even involuntary non-served energy is 42 percent lower. Lower price-responsive demand reduces total systems costs by 0.4 percentage points below the base case. Furthermore, total utility-scale energy storage capacity is 150 MW larger than in the base case, an 86 percent increase in Li-ion storage capacity. These results indicate that factoring in only the impact on generation and storage capacity and energy costs at the transmission level was insufficient to yield the optimal level of price-responsive demand curtailment and accordingly overestimates the value of energy storage by a substantial degree.

Table 4.9: Error due to omission of distribution network losses and expansion: capacity and energy

		Capacity Error		Energy Error	
Resource	Zone	[MW]	[% of total MW]	[GWh]	[% of annual GWh]
CCGT	Outer	-1169	-3.6	-7785	-4.4
CCGT	Capitol	-331	-1.0	-1862	-1.0
CCGT	Downstate	-151	-0.5	-837	-0.5
CCGT	Metropolis	-916	-2.8	-4941	-2.8
CCGT	Big Island	-236	-0.7	-958	-0.5
CCGT subtotal		*-2804*	*-8.7*	*-16383*	*-9.2*
CT	Outer	104	0.3	16	0.0
CT	Capitol	15	0.0	-21	0.0
CT	Downstate	-60	-0.2	-52	0.0
CT	Metropolis	-342	-1.1	-181	-0.1
CT	Big Island	-392	-1.2	-142	-0.1
CT subtotal		*-676*	*-2.1*	*-379*	*-0.2*
Utility-scale Solar	Capitol	-265	-0.8	-607	-0.3
Utility-scale Solar	Big Island	-372	-1.2	-892	-0.5
Utility-scale Solar subtotal		*-637*	*-2.0*	*-1499*	*-0.8*
Utility-scale Li-ion	Outer	31	0.1	7	0.0
Utility-scale Li-ion	Downstate	20	0.1	4	0.0
Utility-scale Li-ion	Metropolis	25	0.1	5	0.0
Utility-scale Li-ion	Big Island	74	0.2	17	0.0
Utility-scale Li-ion subtotal		*150*	*0.5*	*33*	*0.0*
Total	n/a	-3966	-12.3	-18227	-10.2
Max error (±)		1169	3.6	7785	4.4

Errors reflect the difference between the case excluding distribution network parameters and the relaxed UC base case

4.2.4 Carbon Pricing

In this case, I use all inputs from the base case, but impose a substantial carbon price of $100 per ton CO_2 on emissions from natural gas-fired power plants, which dominate the base case. This more than doubles the cost of natural gas to $9.81 per MMBtu (a 118 percent increase relative to other cases without carbon price). As Figures 4-10 and 4-11 illustrate, the carbon price increases the energy share of solar PV to roughly 28 percent, a nearly ten-fold increase relative to the base case. Crucially, however, *all* of this additional solar capacity is installed at utility scale. In addition, Li-ion battery storage capacity increases dramatically, as its competitiveness as a capacity resource increases relative to gas-fired combustion turbines and the value of energy arbitrage across time increases due to the larger share of solar in the region. Once again, however, all of this additional Li-ion storage capacity is installed at utility-scale in transmission voltages. Note also that price-elastic demand continues to supply any needed distribution capacity margin in this case.

Despite substantially greater value for carbon free generation, there is very little *additional* locational value created by a carbon price. In effect, the only additional locational value related to a carbon price (or equivalent emissions limit) is the marginally larger reduction in carbon-emitting generation per MWh of distributed solar or storage generated, due to the amplifying effect of marginal losses in distribution and transmission. However, this additional benefit is insufficient to justify distributed solar or storage deployment in this case, even at $100 per ton CO_2. This finding is important. Should it be replicated in further research (as I expect), it demonstrates that while DERs are widely viewed as a key part of the strategy for decarbonizing the power sector, the comparative advantage of distributed resources lies in their ability to capture *locational value*. This value is largely orthogonal to the objectives of carbon reduction. In fact, policies to drive DER adoption in the pursuit of clean energy or low-carbon goals may simply increase electricity costs, as illustrated in further cases.

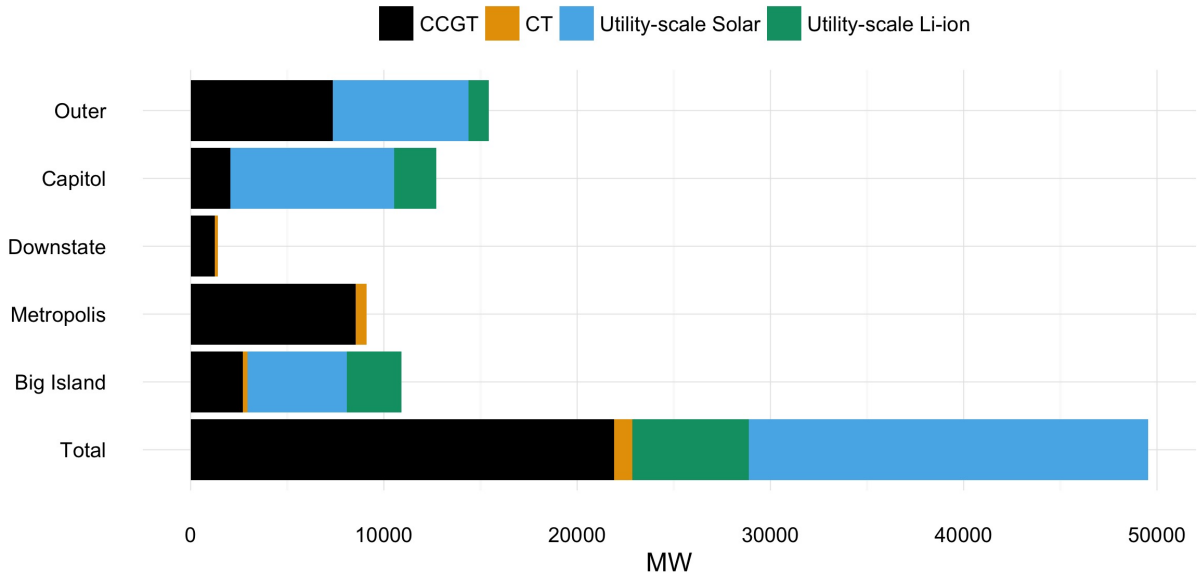

Figure 4-10: Installed capacity by region and resource type - $100 per ton CO_2 carbon price case

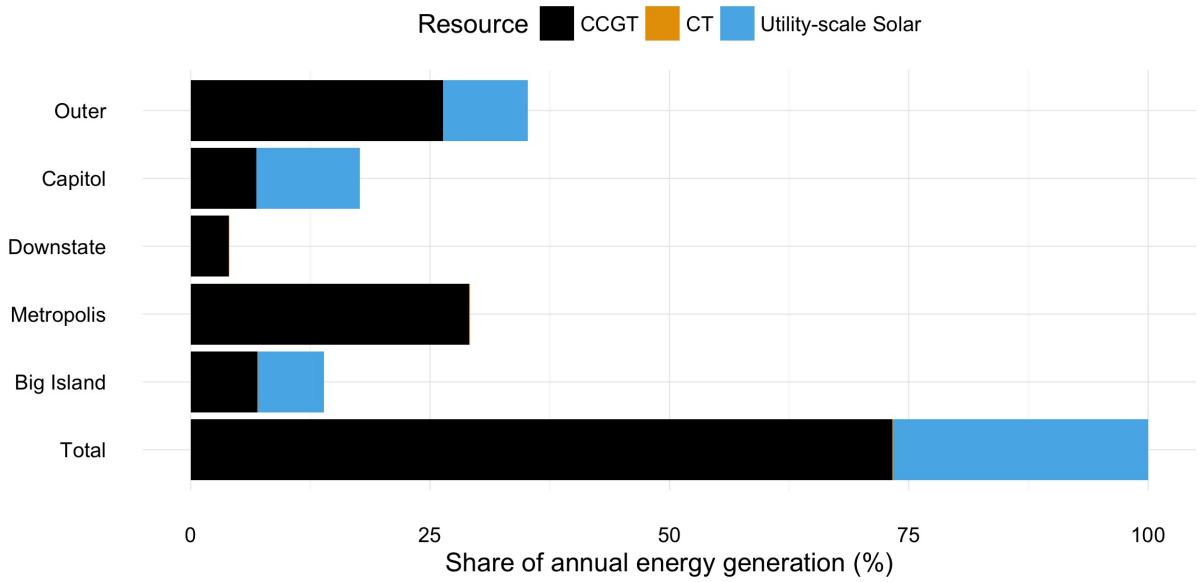

Figure 4-11: Share of annual energy generation by region and resource type - $100 per ton CO_2 carbon price case

4.2.5 Limited Price-Responsive Demand

Given the fact that price-responsive demand captures most of the locational value that might justify distributed solar or storage adoption in the base case, this section describes a series of cases which progressively reduce the share of customers in each segment of price-responsive demand. Table 4.10 describes the set of price-responsive demand segments in each case at each willingness to pay level. In addition, involuntary curtailment of demand at the cost of non-served energy ($10,000/MWh) is always permitted.

Table 4.10: Reduced demand response cases

	Case						
Willingness to Pay	Full DR (Base case)	Limited DR 1	Limited DR 2	Limited DR 3	Limited DR 4	Limited DR 5	No DR
$1000 per MWh	3.0	2.5	2.0	1.5	1.0	0.5	0
$500 per MWh	2.0	1.7	1.3	1.0	0.7	0.3	0
$250 per MWh	1.0	0.8	0.7	0.5	0.3	0.2	0
Total	6.0	5.0	4.0	3.0	2.0	1.0	0.0

As the availability of price-responsive or elastic demand falls across cases, several changes in installed capacity can be observed. First, with less price-response demand during peak consumption periods, total installed capacity of gas combustion turbines (CT) steadily increases (Fig. 4-12). Unsurprisingly, less price elasticity of demand results in larger installed capacity overall and requires additional investment in infrequently utilized 'peakers,' which raises total costs (Fig. 4-16).

Second, the relatively small quantity of Li-ion battery storage systems installed in the base case (about 175 MW) begins to steadily transfer to distribution voltages (Fig. 4-13). These distributed storage systems are predominately installed in the urban Metropolis and Big Island distribution zones. Once total price-responsive demand falls to 3 percent of total demand in each zone or lower, Li-ion storage systems become the next most cost effective solution to avoid any distribution capacity investments needed after exhausting reductions in price-elastic demand. Storage systems therefore become more valuable in distribution zones experiencing more rapid peak demand growth. Where storage can capture locational value

from avoiding distribution network upgrades, this additional value is sufficient to overcome incremental costs due to economies of unit scale given the assumptions used in these cases[13] justifying deployment of storage at distribution voltage levels—at least until the marginal value of network deferral is exhausted. For example, in the case where 3% of demand in each zone is price-responsive, only approximately 80 MW of storage is needed to supplement price-elastic demand and eliminate distribution upgrades. After that, the marginal locational value of distributed storage falls and it no longer makes economic sense to deploy any additional storage at distribution voltage levels. Instead, the model retains another roughly 40 MW of utility-scale storage in this case.

Finally, once total price-responsive demand falls to 1 percent of demand in each zone, distributed storage becomes split between MV and LV (Fig. 4-13). The split between MV and LV storage reflects the maximum contribution of medium voltage net demand reductions to distribution network margins in the urban Metropolis and Big Island zones. In other words, without demand response, distributed battery storage installed at medium voltage levels are the most cost-effective way to accommodate coincident peak demand growth above the existing distribution network capacity in several zones. However, some of the congestions caused by demand growth are located within low voltage circuits or at MV-LV transformers and cannot be relieved by storage at MV. The model therefore installs storage at MV until storage at MV reaches the maximum contribution to network margins (represented by the $\overline{MV}_z^W$ parameter in the model). LV storage is then deployed, but as Fig. 4-15 illustrates, the marginal locational value due to avoided network upgrades apparently falls sufficiently to no longer warrant additional LV storage capacity before fully eliminating necessary network upgrades in the Metropolis zone.

These cases demonstrate the importance of capturing marginal declines in locational value and tradeoffs between economies of unit scale to determining the optimal scale and quantity of distributed resources to deploy (in this case, distributed storage). The placement of storage at medium and low voltage levels in these cases is sensitive to the marginal locational value

[13] In the assumptions used here, medium voltage Li-ion storage systems are 40% more costly to install than utility-scale systems, and low-voltage systems are 95% more expensive to install (see Fig. 1-9).

derived from distribution network deferral, for example.

These cases also indicate that a relatively small share of price-responsive demand during coincident peak demand periods may capture sufficient locational value in distribution networks to eliminate the economic case for investment in any distributed resources (e.g., by eliminating the need for network upgrades). Given the assumptions used herein, it requires only 3 percent of demand to be price-responsive in each zone at prices exceeding $250/MWh in order to eliminate any distributed storage investment (distributed solar is never cost-effective in these cases). This result derives from the greater than 1 MW of peak demand growth accommodated by 1 MW of optimally-sited net demand reduction in distribution networks demonstrated in Chapter 2, Section 2.3. If price-responsive consumers are not ideally located, the required demand reduction may be somewhat larger. However, a meta-review of 63 time-varying electricity rate pilots containing a total of 337 pricing treatments spanning nine countries and four continents (Faruqui et al., 2017) finds that residential electricity customers reduce peak demand by 5 percent on average given a peak-to-off-peak price ratio of 2:1 and by 10 percent at a ratio of 4:1. These figures represent only behavioral responses (i.e., manually turing off devices or adjusting thermostat settings, etc.). When households are equipped with enabling technologies to automate reductions in consumption, such as smart thermostats, peak demand falls by 9 percent on average at a 2:1 price ratio and 16 percent at a 4:1 ratio. Average retail rates are on the order of 5-10 cents per kilowatt-hour, or $50-100/MWh, and price-elastic demand begins to curtail at prices above $250/MWh in this study, representing a marginal energy price at least 2.5 to 5 times larger than the typical retail price. The prices at which demand segments curtail in this study thus represent much higher willingness to pay than evidenced by these real-world time-varying rate pilots. It is therefore quite likely that price-responsive demand could cost-effectively reduce the need for distribution network upgrades in a wide range of settings—if enabled by efficient rate design or other appropriate incentives. If this is the case, the locational value available to DERs will fall substantially.

Finally, given the assumed price-elasticity of demand segments in these cases, comparing

the base case and the case without any price-responsive demand gives a rough sense of the potential social welfare improvements from unlocking greater price-responsive demand. Total costs are $208 million per year or just 2.2 percent higher in the absence of any price-responsive demand than in the base case (with 6 percent of demand in each zone willing to curtail at prices ranging from $250-1000/MWh). The total loss of consumer surplus represented by the curtailed demand in the base case is $42 million, for a net improvement in social welfare of $166 million per year, or 1.8 percent of total expenditures in the base case.

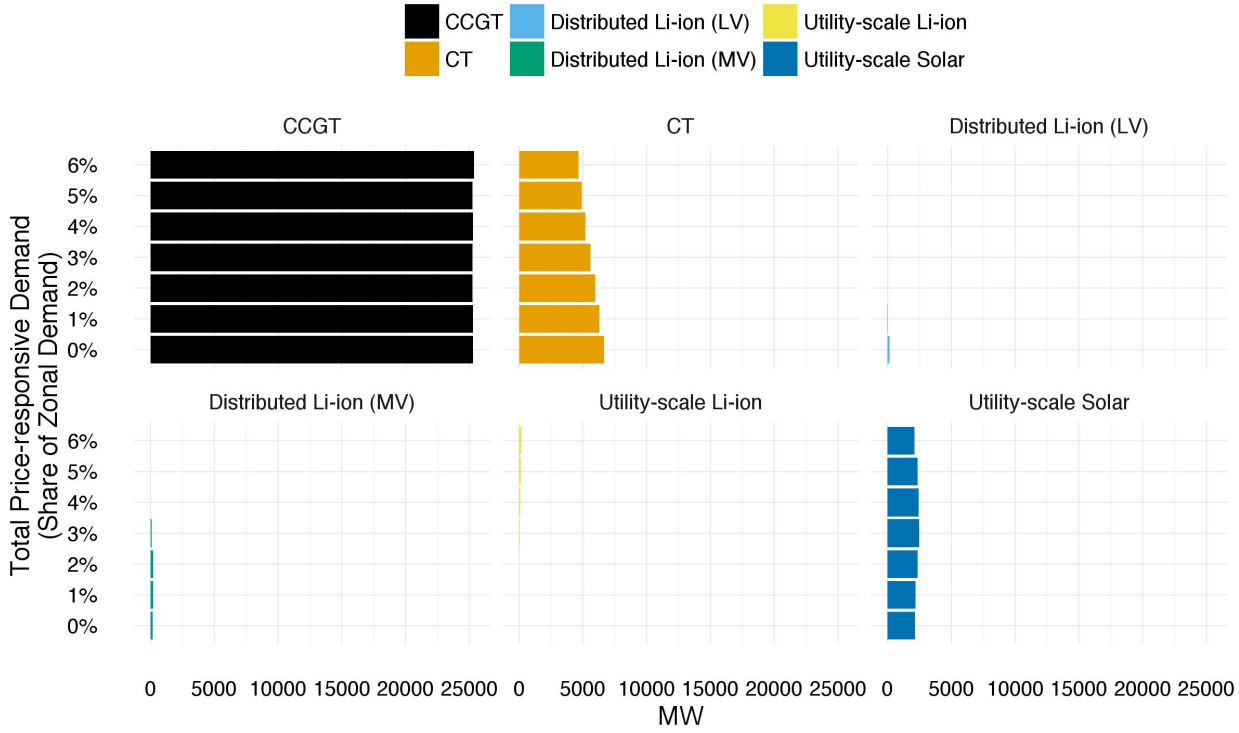

Figure 4-12: Effect of limited price-responsive demand on installed capacity by resource type

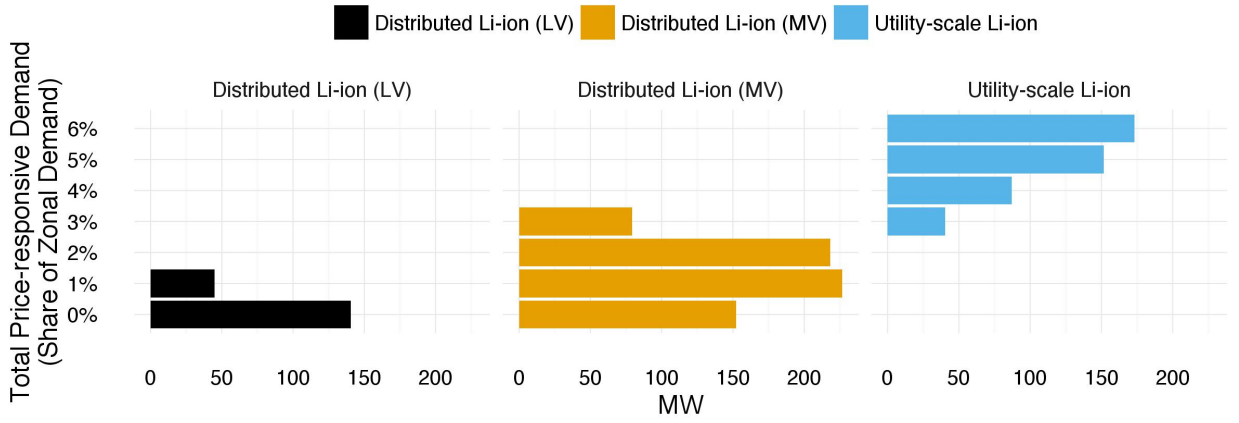

Figure 4-13: Effect of limited price-responsive demand on installed Li-ion storage capacity by voltage level

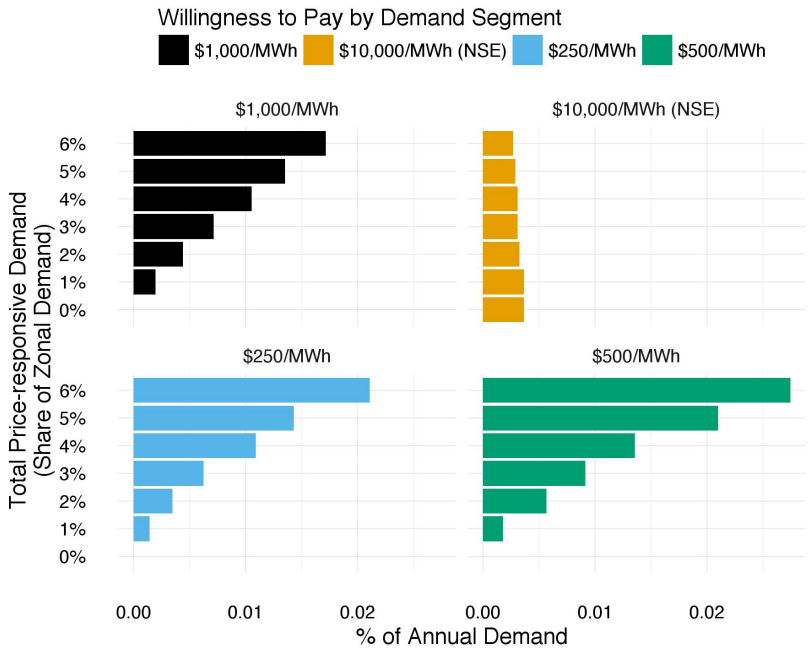

Figure 4-14: Price-responsive demand and non-served energy by demand segment in limited price-responsive demand cases

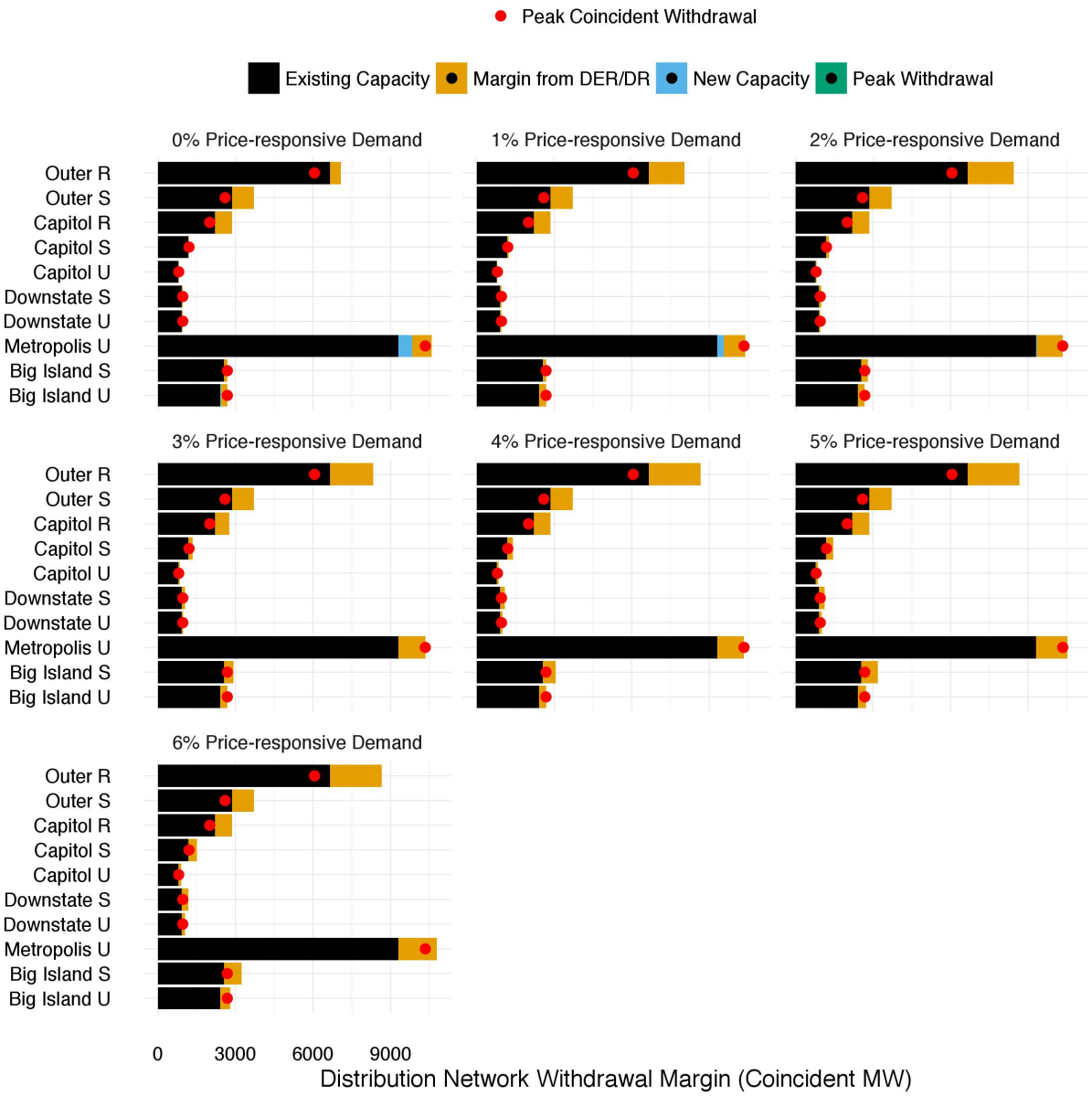

Figure 4-15: Effect of limited price-responsive demand on coincident peak withdrawals and sources of distribution network capacity by region

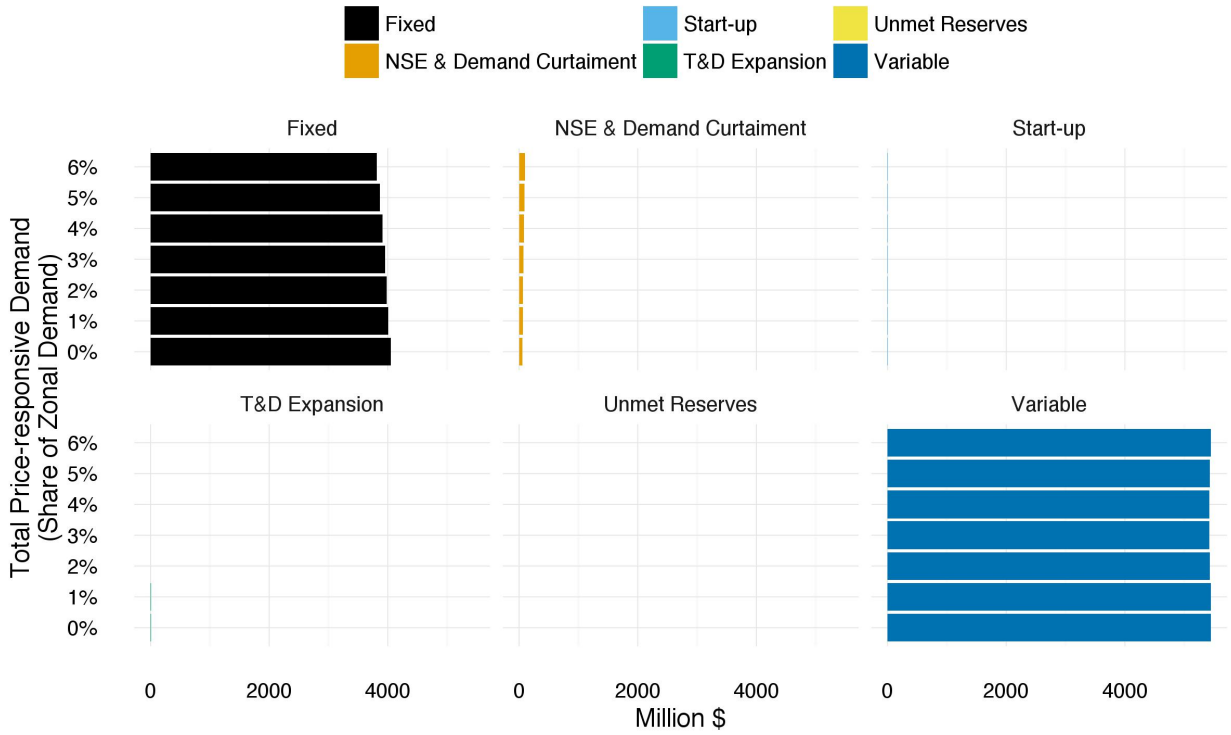

Figure 4-16: Effect of limited price-responsive demand on system costs

4.2.6 The Cost of Distributed Solar Mandates or Incentives

In this case, I force increasing deployment of distributed solar PV at low voltage in each distribution zone to explore the impacts of policies that drive distributed PV adoption above and beyond what is economically justified from a least-cost system optimization perspective. A minimum capacity of distributed solar PV in each zone is specified as a percentage of the peak demand in each distribution network zone and increases from 2% to 100% across the experiment. I run this experiment with both no carbon price and a $100 per ton CO_2 price imposed on natural gas, as per Section 4.2.4.

No Carbon Price

In the absence of a CO_2 price, as the DG solar requirement increases from 2-6 percent, distributed solar at LV distribution voltages directly displaces utility-scale solar capacity and energy shares (Figures 4-17 & 4-18). That is, the only effect of the solar mandate is to displace lower cost utility-scale solar with costlier distributed solar (see Fig. 4-19). The displacement is roughly one for one, indicating that distributed solar's closest competitor is its larger cousin, utility-scale solar.

Higher minimum DG solar requirements begin to increase the overall solar PV capacity, and the larger installed capacity of solar drives several changes in the overall capacity mix (Fig. 4-17). First, Li-ion storage capacity increases, indicating the complementary nature of solar and battery storage. In combination, solar and storage also reduce the total installed capacity of combined cycle gas plants (CCGTs) and combustion turbines (CTs) as well as the energy generation from CCGTs (Fig. 4-18).

At very high penetration levels above 50 percent of each distribution network's peak demand, mandating DG solar installations also drives distributed storage installations. At these levels, distributed solar PV output exceeds the peak injection capacity of each network (set at 50% of maximum demand in these cases). Here I model distributed PV as non-curtailable, as is the case with most behind the meter solar systems. As such, the only way to comply with the injection peak constraint and the distributed solar requirement

simultaneously is to install storage to absorb peak solar output that would otherwise violate the network constraint. Approximately 10.9 GW of distributed storage is therefore required to support DG solar capacity at 100 percent of peak demand in each distribution zone, or nearly 1 GW of storage per 3 GW of DG solar.

At the 100 percent mandate, 30.3 GW of installed DG solar supplies 35 percent of annual energy demand, up 10-fold up from the unconstrained base case. By displacing gas-fired generation, this increase in solar output reduces annual CO_2 emissions by 32 percent. However, this reduction in CO_2 comes at a significant increase in cost (Fig. 4-19). Total system costs increase by 63 percent or $5.9 billion per year under this mandate, for an average cost of $314 per ton of CO_2 displaced.

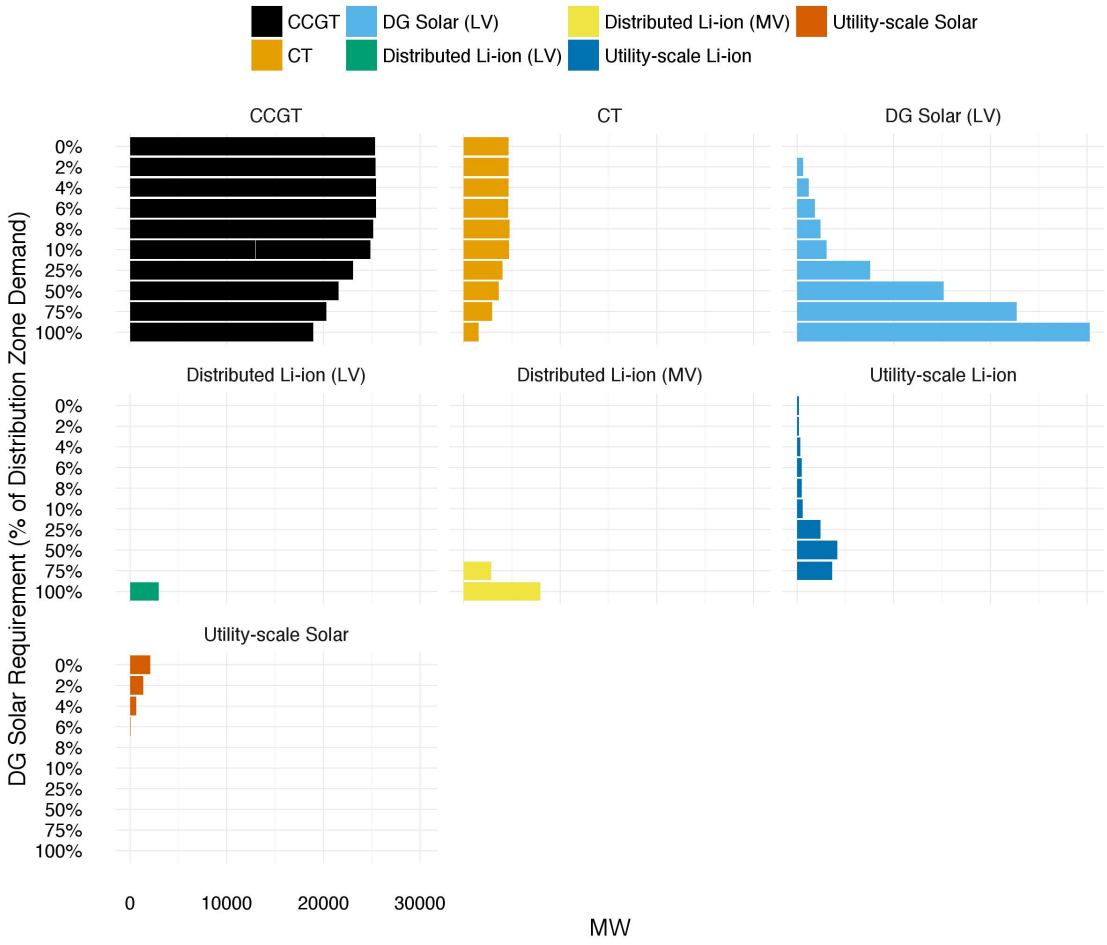

Figure 4-17: Effect of distributed solar requirement on installed capacity by resource type and minimum distributed solar PV requirement

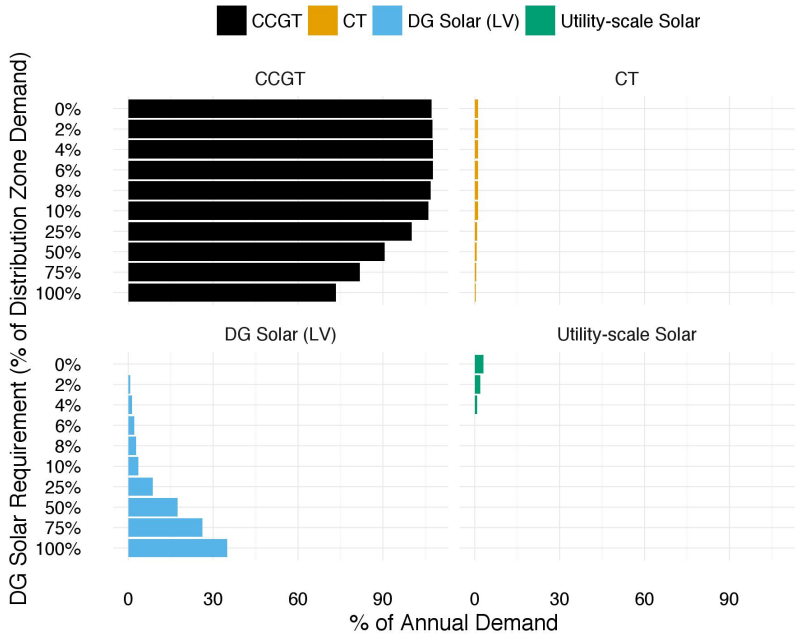

Figure 4-18: Effect of distributed solar requirement on share of annual energy generation by resource type and minimum distributed solar PV requirement

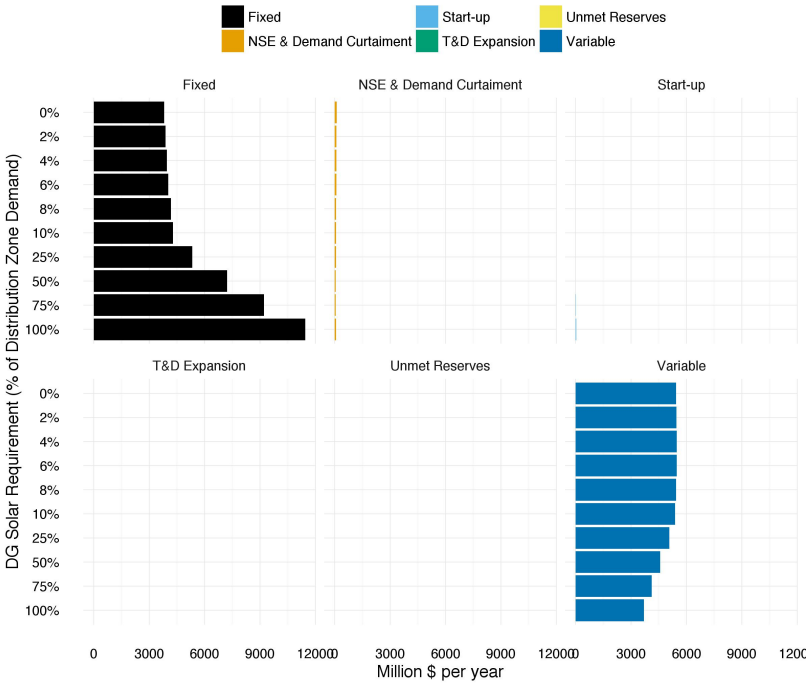

Figure 4-19: Effect of distributed solar requirement on system costs by minimum distributed solar PV requirement

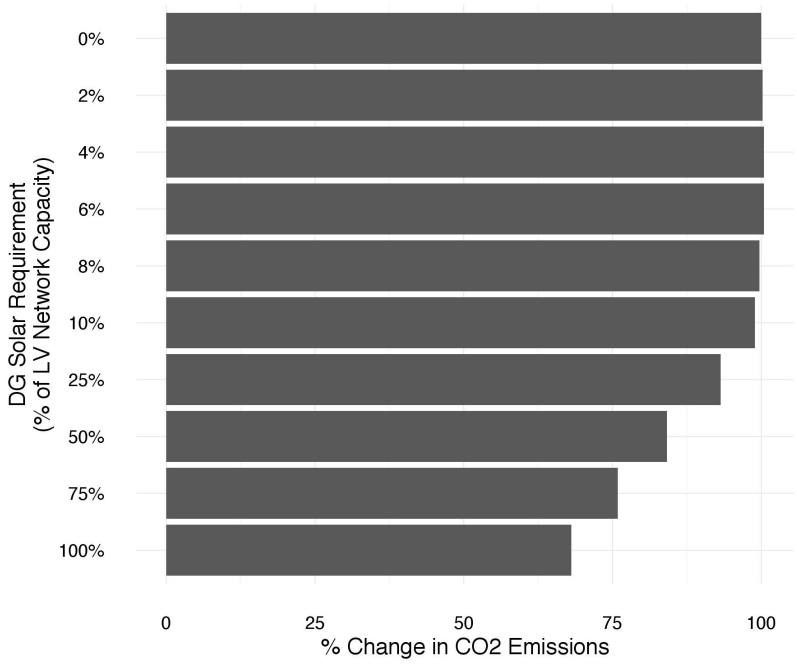

Figure 4-20: Effect of distributed solar requirement on annual CO_2 emissions by minimum distributed solar PV requirement

$100 per Ton CO_2 Price

With a $100 per ton CO_2 price in place and absent a DG solar mandate, utility-scale solar capacity increases to 20.6 GW (Fig. 4-21) and supplies nearly 30 percent of annual demand versus 3 percent in the base case (Fig. 4-22). CO_2 emissions are 14.4 percent lower than the base case absent a carbon price and total system costs are $9.37 billion or 56 percent higher. However, this cost includes $4.43 billion in carbon taxes (or equivalent permit prices in an emissions cap and trading program) paid via higher electricity prices. This revenue can be put to other uses, including recycling back to electricity customers or investment in public purposes. Thus, the total increase in actual electricity system investment and operating costs (e.g., total cost less carbon revenues) is only $838 million, or 9 percent of the base case cost. The average cost of carbon abatement in this case is $58 per ton CO_2 (and the marginal cost is obviously $100 per ton).

In the presence of this substantial carbon price, the distributed solar PV mandate in this set of cases serves to steadily displace utility-scale solar across the entire range of the mandate up to the 75% requirement (Figures 4-21 & 4-22). Capacity and energy shares of other resources are largely unaffected by the DG solar mandate across this range, as is CO_2 (Fig. 4-24). Total costs however increase by $8.5 billion per year (Fig. 4-23) or 90.4 percent higher than in the absence of a DG solar mandate.

Once again, supporting both the 75 and 100 percent DG solar requirements (as a share of each distribution zone's peak demand) necessitates additional distributed Li-ion storage installation to absorb peak injections and avoid distribution network constraints or upgrades. This contributes to higher total system costs as well.

Total system costs when DG solar reaches 100 percent of each distribution network zone's peak demand are $9.9 billion per year or 105 percent higher than in the absence of the DG solar mandate. CO_2 emissions are 4.5 million metric tons lower than without the DG solar mandate, or an additional 7.7 percentage point reduction relative to the base case absent a carbon price or DG solar mandate. However, the average cost of this additional mitigation is a staggering $2,176 per metric ton.

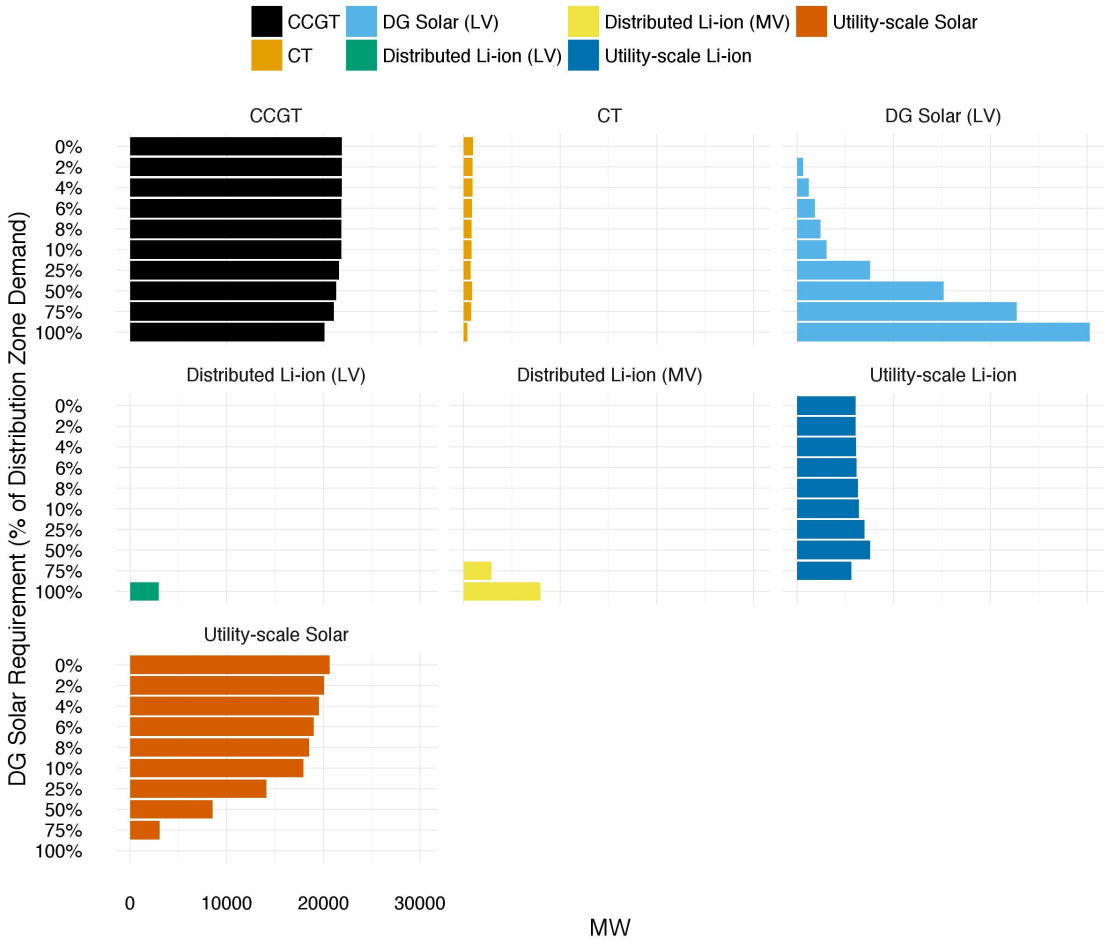

Figure 4-21: Effect of distributed solar requirement on installed capacity by resource type and minimum distributed solar PV requirement - $100 per ton CO_2 price case

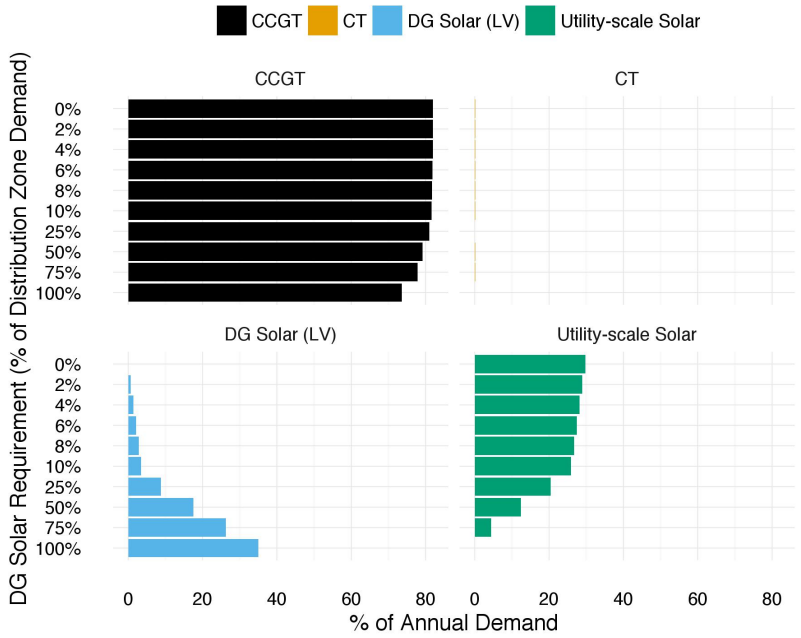

Figure 4-22: Effect of distributed solar requirement on share of annual energy generation by resource type and minimum distributed solar PV requirement - \$100 per ton CO_2 price case

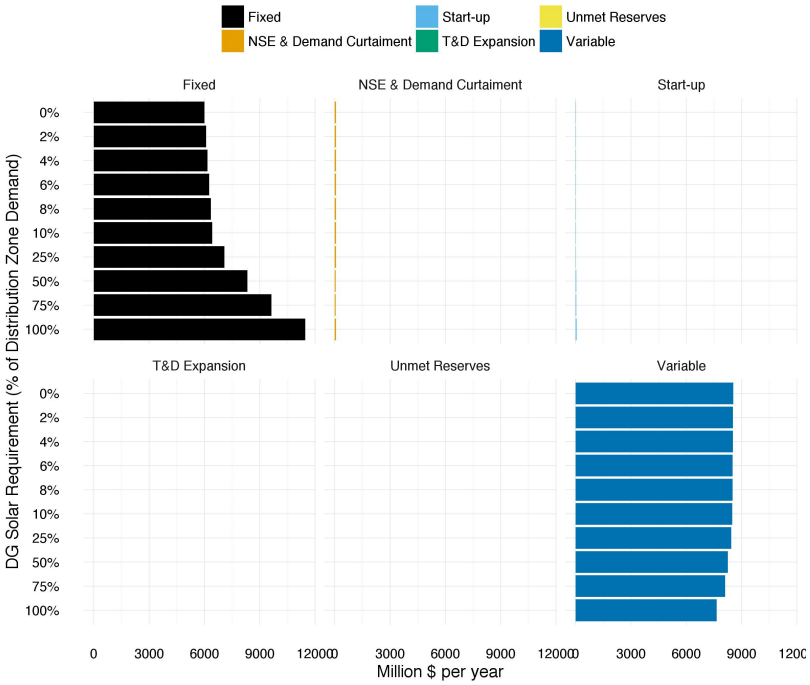

Figure 4-23: Effect of distributed solar requirement on system costs by minimum distributed solar PV requirement - \$100 per ton CO_2 price case

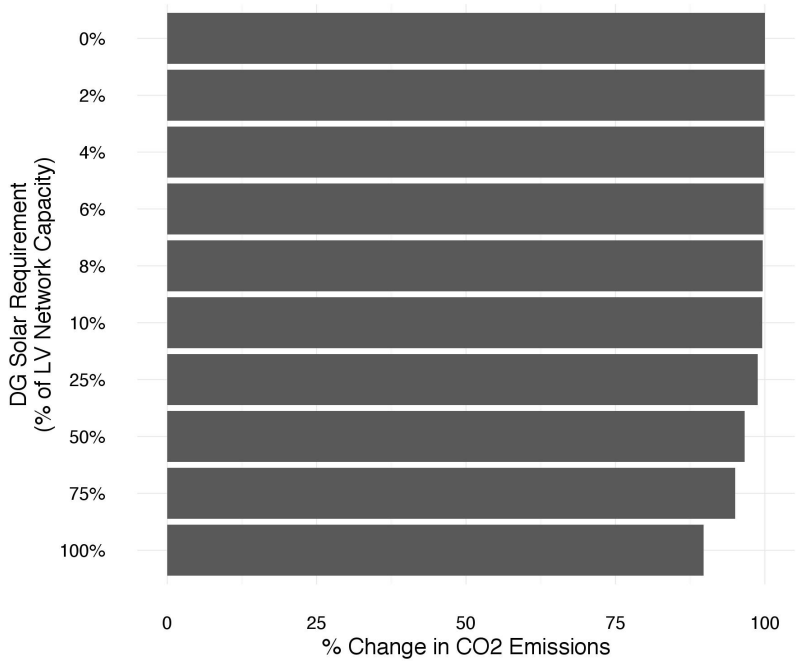

Figure 4-24: Effect of distributed solar requirement on annual CO_2 emissions by minimum distributed solar PV requirement - \$100 per ton CO_2 price case

4.2.7 Lower Economies of Unit Scale: Li-ion Energy Storage

This set of cases explores how reductions in incremental costs due to economies of unit scale can improve the economic attractiveness of distributed Li-ion energy storage systems, relative to utility-scale storage. In each case, I progressively reduce the incremental unit costs of MV and LV Li-ion storage systems by 20 percent of the incremental cost in the base case (40 percent for MV storage and 95 percent for LV storage).

As Fig. 4-25 illustrates, until the incremental cost of distributed storage at low voltage levels falls to on the order of 18 percent of the cost of the utility-scale storage, no distributed storage is deployed. Beyond this level, the small capacity of utility-scale storage is entirely displaced by storage at low voltage. Total storage capacity in this case increases to approximately 700 MW, roughly four times the installed capacity of utility-scale storage in other cases. Interestingly, the distributed storage capacity is installed at LV rather than MV and is installed in the Outer Enerlandia rural and semi-urban networks and the rural Capitol Valley network, neither of which face distribution network withdrawal constraints. Both factors indicate that distributed storage is installed in this case principally to take advantage of the magnifying effect of marginal losses in low voltage levels. This additional storage capacity also reduces price-responsive demand curtailment at the most expensive segment ($1,000 per MWh) as well as slightly reduces involuntary non-served energy (Fig. 4-26). In other words, at an incremental cost of just 18 percent, the locational value of marginal loss reduction (particularly during peak demand periods that drive price-responsive demand at $1,000 per MWh) is sufficient to justify distributed storage at low voltage. Marginal losses in medium voltage are lower, which means distributed storage 'skips over' MV in this case, and is deployed solely at LV, despite the slightly lower costs of MV storage.

At an incremental cost of 4 percent relative to utility-scale storage, Li-ion storage capacity at LV increases further to 1,400 MW. This additional capacity further reduces price-responsive demand curtailment at $1,000/MWh. Utility-scale solar capacity (Fig. 4-25) and annual energy generation also fall by roughly 50 percent. This indicates that once distributed storage has displaced utility-scale storage, it begins to compete with other resources that

provide capacity value in the system. In this case, utility-scale solar appears to be the closest competitor, and the greater locational value captured by storage at low voltage combined with only nominal incremental costs gives storage more of an edge in this competition. Total system costs are largely unaffected by these changes in distributed storage capacity, however (Fig. 4-27).

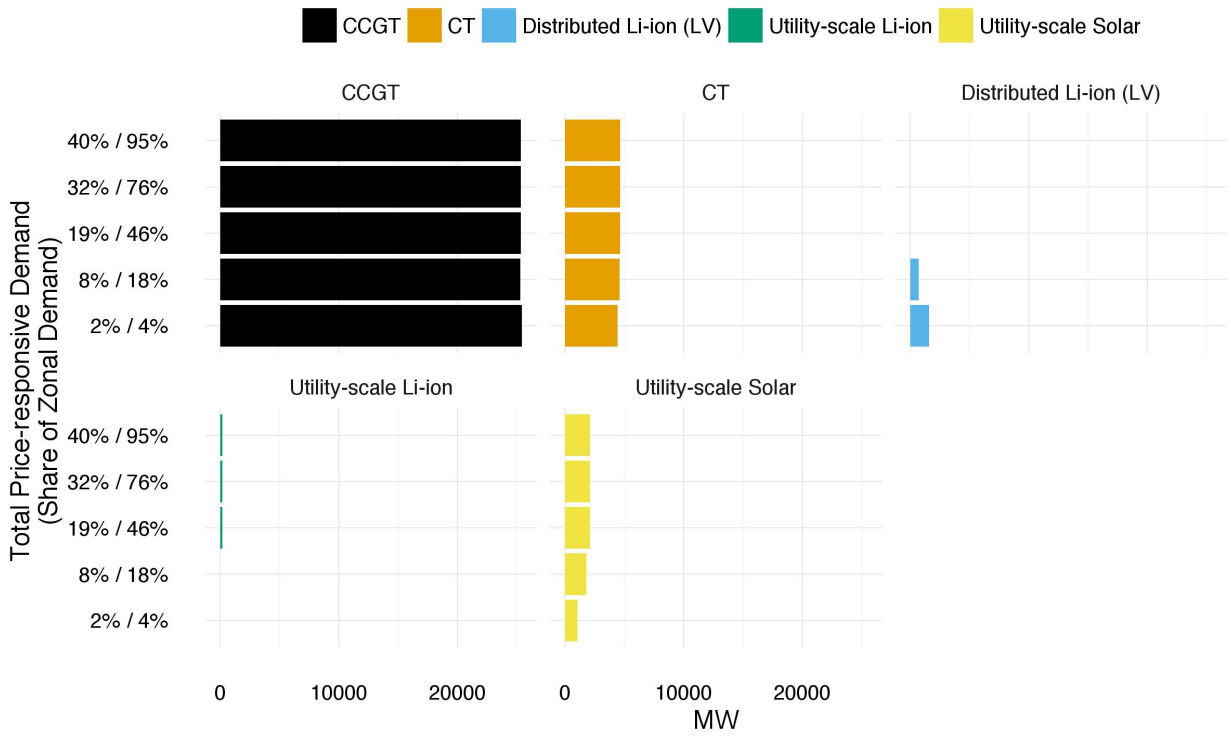

Figure 4-25: Effect of lower economies of unit scale for Li-ion storage on installed capacity by resource type

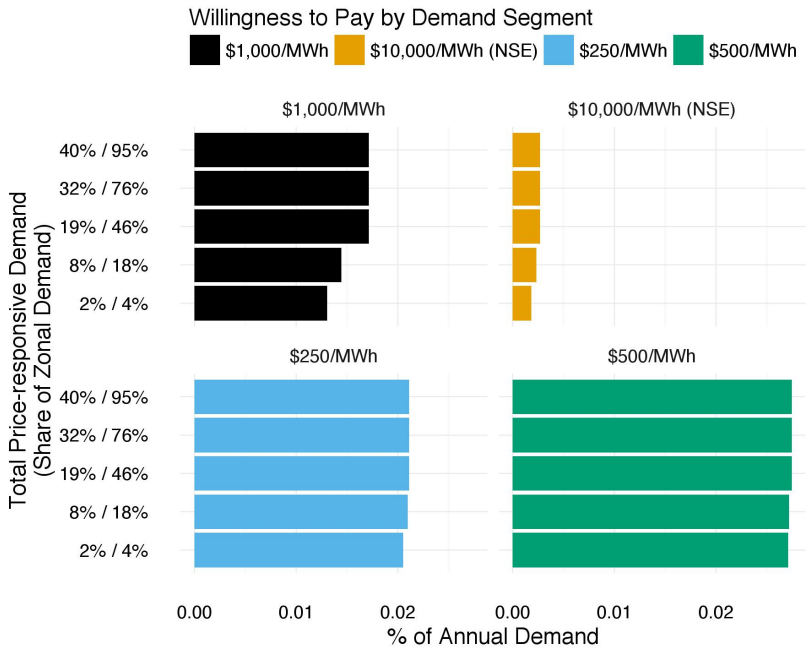

Figure 4-26: Effect of lower economies of unit scale for Li-ion storage on unmet demand by demand segment

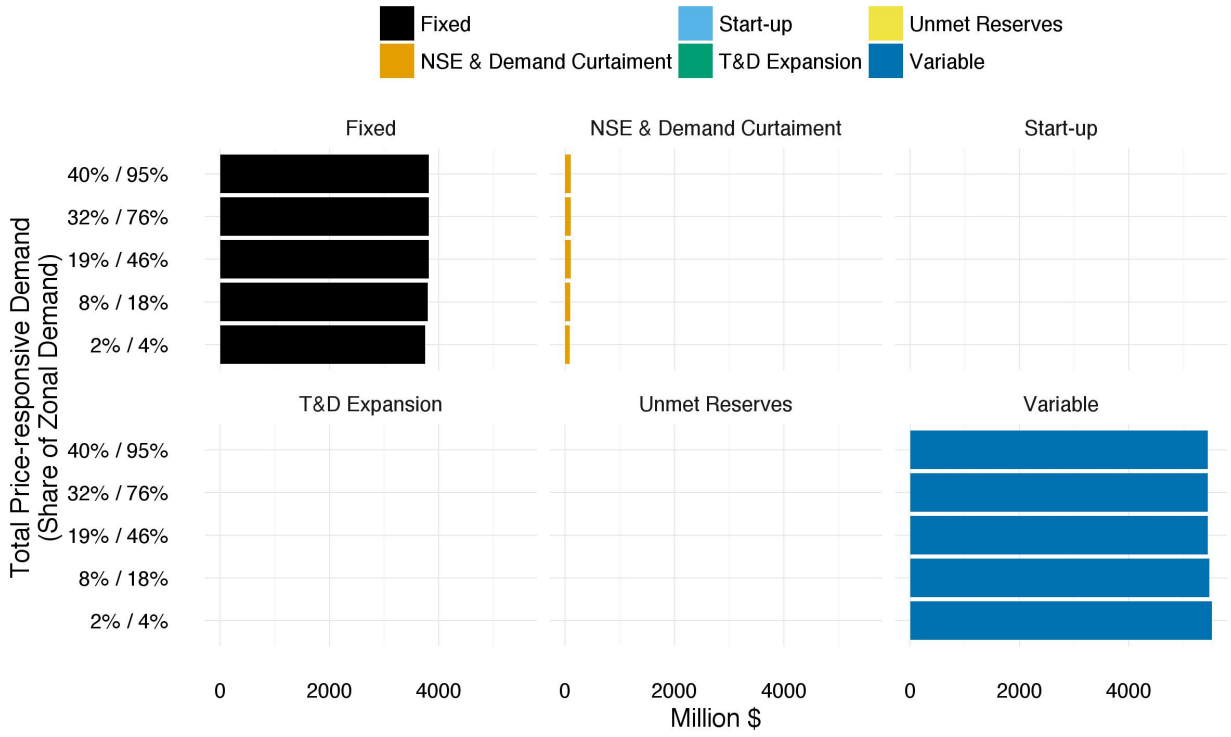

Figure 4-27: Effect of lower economies of unit scale for Li-ion storage on system costs by cost component

4.2.8 Lower Economies of Unit Scale: Solar PV

This set of cases explores how reductions in incremental costs due to economies of unit scale can improve the economic attractiveness of distributed solar PV systems, relative to utility-scale solar. As in Section 4.2.7 above, I progressively reduce the incremental cost of distributed solar at MV and LV (initially 25 percent and 85 percent, respectively) by 20 percent in each successive case.

As in the storage case above, once the incremental unit costs of distributed solar fall to on the order of 16 percent for systems at low voltage, DG solar begins to appear in the least-cost capacity mix (Fig. 4-28). At a 16 percent cost premium, DG solar at LV replaces about a third of the utility-scale solar capacity, and fully displaces utility-scale solar by the time the cost gap falls to a nominal 3 percent. Greater distributed solar capacity helps reduce the amount of non-served energy required (Fig. 4-29), indicating that DG solar has noticeable capacity value in this system (meaning it produces a meaningful amount of energy during peak demand periods that would otherwise trigger high prices that cause elastic demand to reduce consumption).

The capacity of other resources are largely unaffected as DG solar capacity increases (Fig. 4-28), as are total system costs (Fig. 4-30). For the most part, cheaper distributed solar merely swaps for larger-scale solar and some amount of price-responsive demand curtailment without substantially affecting the overall system.

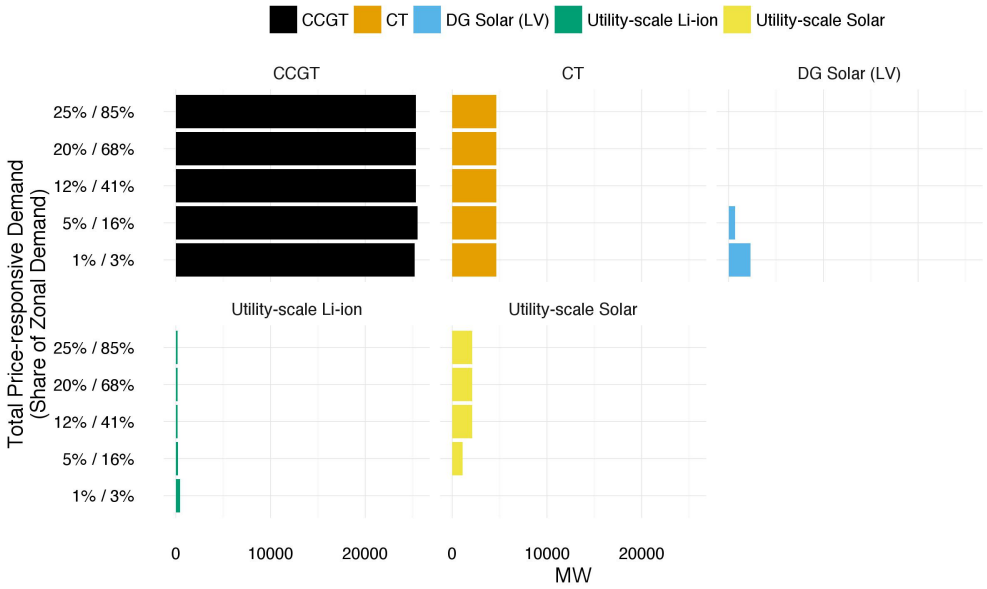

Figure 4-28: Effect of lower economies of unit scale for solar PV on installed capacity by resource type

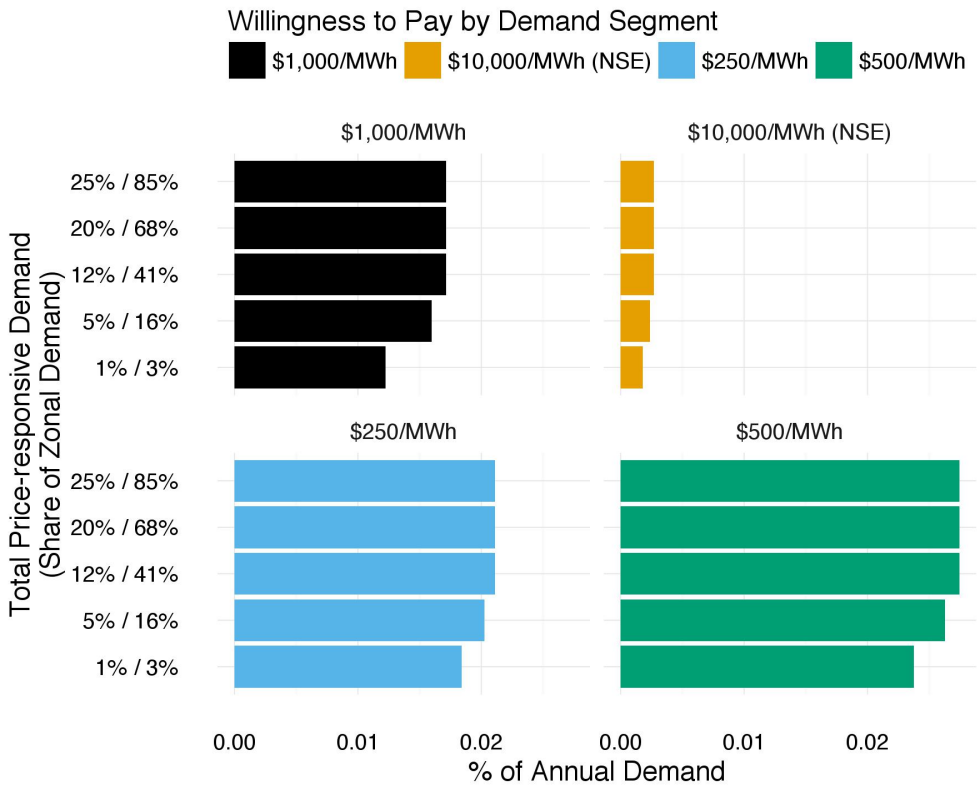

Figure 4-29: Effect of lower economies of unit scale for solar PV on unmet demand by demand segment

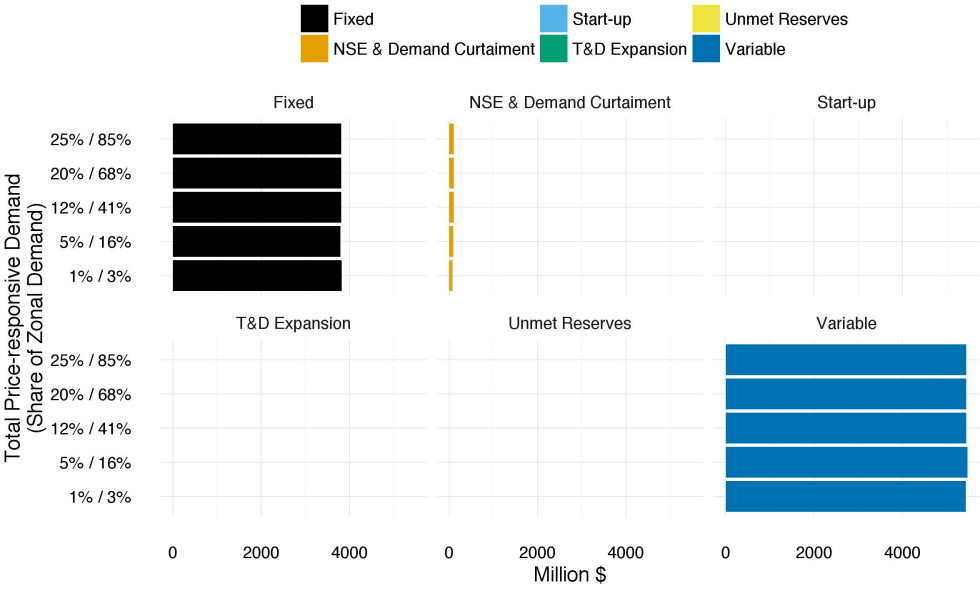

Figure 4-30: Effect of lower economies of unit scale for solar PV on system costs by cost component

Chapter 5

Conclusions

5.1 Summary

This dissertation introduced and demonstrated a novel set of methods for incorporating distributed energy resources (DERs), flexible and price-responsive demand, and distribution network losses and reinforcement costs in an integrated electricity resource capacity planning framework. Methods using simulations of large-scale distribution networks are shown to produce a set of polynomial equations that can accurately represent the aggregate impact of changes in demand or distributed generation on resistive losses and distribution network expansion costs. These equations were incorporated into a state-of-the-art electricity resource capacity planning model, which enables simultaneous optimization of fixed and variable costs of: 'utility-scale' electricity generation and storage; distributed generation and storage installed at multiple scales and distribution voltage levels; flexible and price-responsive electricity demand; and associated transmission and distribution network costs and losses. This planning model captures the primary sources of 'locational value' that may economically justify deployment of DERs and are important to understanding the full value of flexible or price-responsive demand. It also incorporates economies of unit scale tradeoffs associated with the higher costs of smaller-scale distributed resources. The key features of the model were demonstrated through several case studies performed for a fictional regional

power system. Insights on the potential role and value of DERs and flexible demand can be derived from these case studies, which also highlight the utility of this novel planning tool to provide decision support for policy makers, regulators, and electric utility planners.

5.1.1 The (Limited) Role and Value of Distributed Energy Resources

Distributed energy resources enjoy substantial public policy support in a growing number of jurisdictions. Distributed solar PV and battery energy storage, in particular, benefit from direct subsidies, favorable tariff design (such as flat volumetric rates with net metering or non-coincident monthly demand charges), and deployment mandates (e.g., solar 'carve-outs' in renewable portfolio standards or storage mandates). Collectively, these policy and regulatory decisions preferentially remunerate smaller-scale, distributed solar and storage systems, relative to larger-scale solar or storage at transmission voltage levels, and have driven significant penetration of these distributed resources in various locales (Chapter 1, Section 1.1.1).

As this thesis demonstrates, the comparative advantage of distributed resources lies in their ability to locate throughout electricity networks at locations where the delivery of electricity services has higher than average locational value. Locational value emerges from the physical characteristics of electricity networks, including resistive losses, capacity limits of network components, voltage limits at network nodes, and the potential for network failures that may disrupt delivery of electricity services. These network characteristics impact the locational value of three main electricity services: electrical energy; network capacity (or 'non-wires' substitutes for network capacity); and enhanced reliability or resilience. By delivering energy in areas with high marginal losses, providing reliable power injections or reductions in net consumption in constrained portions of the distribution network, or supplying energy during network failures, DERs may be able to deliver greater value than larger, 'utility-scale' counterparts unable to site within distribution networks (see Chapter 1, Section 1.1.3).

However, smaller-scale installations of solar, storage, and other technologies suitable for

deployment at multiple scales incur higher costs per unit by failing to exhaust economies of scale. The installed costs of residential-scale (e.g., under 10 kW) solar PV and Li-ion battery storage systems in the United States are more than double the costs of multi-megawatt, utility-scale installations of the same resources, for example. Larger distributed solar or storage installations can harness greater economies of unit scale and thus incur progressively smaller incremental costs, but all remain more costly than utility-scale counterparts (see Figures 1-8 & 1-9).

The incremental locational value captured by DERs must therefore exceed the incremental unit costs incurred by smaller-scale systems[1] in order for their deployment to deliver a net improvement in social welfare, relative to larger-scale alternatives. Conversely, in cases where incremental unit costs exceed incremental locational value, society incurs a 'distributed opportunity cost' when small-scale DERs are deployed in lieu of more cost-effective, larger-scale installations of the same resource.

These trade-offs between DERs and their larger-scale alternatives are not simply rhetorical. As modeling in Chapter 4 illustrates, distributed solar or storage compete most directly with larger-scale solar and storage, respectively. Greater penetration of distributed storage, for example, reduces the economic value of utility-scale solar by driving down marginal electricity prices at times when larger solar PV systems are also producing the majority of their output. Distributed storage systems can also provide the same range of capacity- reserves- and energy arbitrage-related services as multi-megawatt storage installations,[2] thus pitting these resources against one another in competition for a set of services that exhibit rapidly diminishing marginal value.

Where distributed solar or storage (or other modular technologies) have greater incremental unit costs than the marginal locational value captured by each installation, two outcomes may result from deployment of distributed rather than utility-scale systems. First, DER de-

[1]Both incremental value and cost should be measured relative to any larger-scale alternatives that are available in the same power system.

[2]Changes in electricity markets, rate design, or other regulatory reforms may be needed to unlock the full range of services from distributed storage systems, but all of this is technically feasible with the right policy and regulatory regime.

ployment displaces lower cost, larger-scale alternatives. As Chapter 4, Section 4.2.6 indicates, substitution between technologies of the same resource type but at different scales is likely to be approximately one for one. The result will be a higher cost of delivered energy with an approximately equal share of solar or storage in the overall energy and capacity mix. In other words, the location of storage and solar will shift from transmission voltages to distribution voltages, but without any substantial net increase in overall capacity of each resource.[3] Second, distributed solar/storage installations can be *additional* to utility-scale solar/storage, but *only* if public policy support for utility-scale systems is increased to overcome the decline in marginal value caused by greater penetration of distributed solar/storage.

Further complicating matters, locational value is neither universal nor constant. The effect of losses, congestions, and network reliability on locational value differs dramatically across a given power system region, and even within a single distribution network. Additionally, the marginal value of avoided losses or network reinforcements diminishes as more DERs provide the same services within a given portion of the grid. Resistive losses rise quadratically with current (and thus power flow), for example. The marginal value of network losses avoided by additional injections from DERs therefore diminishes at a rate double the increase in injection. Similarly, DERs may capture significant locational value by generating energy locally when network congestions prevent delivery of lower cost energy or by avoiding or deferring the need for costly network upgrades. But once sufficient energy is supplied to mitigate the congestion or defer the upgrade, the marginal value of additional DER deployment drops precipitously. It is therefore essential that the drivers of locational value are well understood and that policy and economic incentives encourage adoption of DERs where locational value continues to exceed incremental unit costs. This is almost universally *not* the case for the policy and regulatory regimes in place in the vast majority of jurisdictions today.

Additionally, this thesis indicates that the more price-elastic and flexible electricity de-

[3]As annual production from distributed solar systems is generally lower than utility-scale systems, which typically employ tracking arrays and are more optimally sited, there may be an increase in overall solar PV capacity if distributed PV displaces utility-scale PV, but this will not come with an increase in overall solar energy share.

mand becomes, the less valuable DERs are within the power system, all else equal (Chapter 4, Sections 4.2.1 & 4.2.5). Much of the locational value that may be captured by distributed solar, storage, or other DERs derives from avoiding or deferring investments in poorly utilized generation or network capacity that is sized to meet coincident peaks in demand that occur only rarely. However, more price-elastic and flexible electricity demand can obviate the need for much of this under-utilized generation or network capacity. Similarly, reducing consumption during coincident peak demand periods can have a substantial mitigating effect on marginal losses and congestions that may drive higher locational marginal prices at distribution voltages.[4] Reductions in demand can make use of existing assets and only need to be exercised on the infrequent occasions when network or generation capacity are strained. As such, price-responsive or re-schedulable electricity consumption may be a more cost-effective alternative to capture locational value than investment in DERs in many instances. This appears to be true even when demand reductions incur relatively large opportunity costs for electricity consumers (e.g., on the order of hundreds or even thousands of dollars per MWh). Unfortunately, rate designs for the vast majority of electricity customers currently lack temporal or spatial granularity necessary to induce price elastic consumers to reduce or shift consumption during the most valuable time periods and at the most valuable locations within the grid. These same inefficient rate structures also distort the installation and operation of DERs in ways that further diminish their locational value.

Finally, while solar power and energy storage are likely to play a key role in decarbonizing electric power systems and thus mitigating the worst effects of climate change (see de Sisternes et al. (2016); Sepulveda et al. (2018)), the additional benefits of *distributed* solar, storage, or other clean energy resources are almost entirely orthogonal to their climate benefits. As illustrated in Chapter 4, Section 4.2.4, imposing a substantial carbon price on power systems does not noticeably enhance the economic value of DERs, relative to their larger-scale counterparts. The only way in which climate benefits intersect with locational value is via the enhancing effect of marginal losses on the volume of carbon-emitting gen-

[4]Note that I refer to the 'price' here as the shadow price or marginal cost of supply at a given location, whether this cost is accurately reflected in electricity tariffs or market designs or not.

eration displaced by a kWh supplied by a solar or storage system at distribution voltage levels.[5] As such, any additional policies to drive adoption of DERs serve to increase the total cost of decarbonizing the electricity sector. As Chapter 4, Section 4.2.6 demonstrates, this additional cost can be substantial. Policies supporting distributed solar or storage often enjoy strong public support. But unless such policies enhance political support for additional overall public or ratepayer expenditures on climate mitigation or clean energy deployment to an extent that *exceeds* the additional costs imposed by more costly DERs, the net effect would be to impede progress towards a decarbonized power system. In addition, electricity is expected to play a pivotal role in displacing fossil fuel use beyond power generation by electrifying a greater share of end uses, such as transportation, industry, and heating. To the extent that DER adoption increases the marginal cost of electricity, it could also slow substitution of electricity for carbon-emitting fuels in these sectors.

In summary, distributed energy resources *can* deliver real value to power systems where and when they are able to capture greater locational value created by high marginal network losses, the ability to relieve network congestions or defer impending upgrades, or enhance local reliability. However, this value is finite, varies significantly across power systems, and declines marginally as DERs are deployed or flexible demand is unlocked. In addition, driving DER adoption in cases where incremental unit costs exceed marginal locational value incurs real distributed opportunity costs that increase either the cost of delivered electricity or the cost of total policy expenditures (or both). This may also entail very real costs in terms of climate mitigation efforts given political constraints on public willingness to pay for mitigation efforts (see Jenkins (2014)) and the need to substitute a greater share of low-carbon electricity for oil, gas, and coal in transportation, heating, and industrial sectors.

To capture the potential value of DERs and unlock more flexible demand without incurring substantial social costs, policy and regulation must become more sophisticated. Policy incentives for DER adoption should be proportional to the marginal locational value delivered by supported technologies. Incentives need to become much more geographically targeted to

[5]That is, if marginal losses are 20 percent for example, a kWh of solar generated at low voltage distribution displaces 1.2 kWh of fossil generation at transmission voltages.

encourage installation of DERs only where they deliver marginal social benefits. To the degree distributed scale installations of clean energy technologies are preferentially encouraged over utility-scale counterparts, this additional incentive should not exceed their additional locational value. Finally, to avoid replicating the same inefficient utilization of capital assets that characterizes our bulk generation and networks today, electricity rate design and other incentives should encourage price elastic consumers to reduce or shift consumption wherever and whenever the marginal cost of electricity services exceeds the marginal benefit of consumption – and ideally to do so *before* encouraging deployment of DERs.

5.1.2 Enhanced Decision Support via Improved Electricity System Planning Tools

Policy making, regulatory decisions, and utility planning have all historically benefited from a suite of power system modeling tools that can evaluate the potential costs and benefits of pending decisions. Electricity resource planning tools are particularly valuable, as they provide an opportunity to explore hypothetical futures, perform sensitivity analysis, and evaluate the technical and economic impacts of new policies, investments, or technology options.

Unfortunately, existing electricity capacity planning (or generation expansion planning) models are unable to appropriately analyze the value and role of DERs and flexible demand in power systems. These tools are traditionally limited to considering investment in 'utility-scale generation' and (in some cases) transmission. To date, these planning tools have lacked a tractable method for modeling the impacts of DERs and flexible demand on distribution network losses and distribution network reinforcement or expansion costs – two primary sources of 'locational value' in electricity systems. They also lack sufficient granularity to capture important tradeoffs associated with economies of unit scale for resources that can be deployed at multiple scales and voltage levels. DER capacity could be added to such models exogenously, but not co-optimized alongside the rest of the system, and the full impact of these resources on transmission and distribution networks are not modeled. These

important planning tools have therefore become insufficient to provide decision support or policy guidance in cases where DERs or flexible demand play more than a de minimis role in power systems.

To capture the key economic and technical considerations associated with DERs and demand-side flexibility with sufficient accuracy, electricity resource capacity planning models must be enhanced to include four additional features. First, capacity planning tools should endogenously model the largest sources of locational value, including non-linear resistive network losses, impacts of network constraints, and network capacity expansion costs, with all three factors modeled for both transmission and distribution networks. Second, models should allow siting of DERs at multiple scales and voltage levels in order to capture economic tradeoffs associated with economies of unit scale. Third, these models should endogenously account for the potential role of more flexible and price-responsive demand in reducing investment and operating costs, including impacts on both generation and network capacity. Finally, planning models should include endogenous investment decisions for a wide range of the most salient distributed and conventional resources, in order to capture competition and complementary between each of these resources.

5.2 Contributions

This thesis offers a new framework for electricity system capacity planning with distributed energy resources and flexible and price-responsive demand. It extends the current state of the art in capacity planning models by demonstrating a method to represent the salient features of distribution networks, including losses and network reinforcement costs, in a holistic optimization model. This model captures the most important sources of locational value for DERs and flexible or price-responsive demand, allows siting of DERs at multiple scales and distribution voltage levels to capture tradeoffs between locational value and economies of unit scale, considers competition between a wide range of available resources, and simultaneously co-optimizes generation, transmission, distribution, and DER investment and operational decisions. In addition, I apply this modeling framework in a number of initial case studies

to demonstrate its utility and provide initial insight on the potential value and role of DERs in power systems.

In summary, the methodological contributions of this work are to demonstrate:

1. A new approach to using AC power flow simulations to accurately derive the effect of aggregate changes in power withdrawals and injections on resistive network losses in large-scale distribution networks (e.g., a set of primary and secondary feeders home to on the order of 20-100 MW of total peak demand) and represent these effects with a relatively simple polynomial function.

2. A method for adapting AC optimal power flow simulations to identify the minimum quantity of net reductions in coincident peak demand (achieved either by demand flexibility or distributed generation or storage) necessary to accommodate demand growth in the same large-scale distribution networks. This method can be used to accurately estimate the total demand-side flexibility needed to accommodate increases in peak demand without investment in new distribution network assets to increase network capacity – or the potential of so-called 'non-wires' alternatives.

3. A method for using a distribution network planning model to accurately determine the cost of traditional distribution network upgrades required to accommodate an equivalent increase in peak demand.

4. A holistic electricity resource capacity planning model which employs results from the above methods to incorporate distributed energy resources and flexible demand and consider key sources of locational value or cost, including impacts of demand and DERs on transmission and distribution network costs and losses.

Collectively, these methods are an important contribution to updating and expanding the capabilities of power system planning tools to keep pace with a rapidly evolving electricity sector. These methods can be used to perform techno-economic assessment and provide insight on the potential role and value of various DERs or demand flexibility in power

systems, evaluate the benefits or costs of potential policy or regulatory reforms, or provide insight for electricity utility planners.

In addition, initial application of this model to a variety of example case studies herein provides indicative but important insights on the potential role and value of DERs – and their limitations – which can provide guidance for both policy and regulatory decisions and future research directions.

5.3 Future Work

Overall, the modeling framework and methods introduced and demonstrated in this thesis provide a foundation for future research on the value and role of DERs in power systems and the costs of policy and regulatory decisions that either improve or further distort incentives for demand flexibility and adoption and use of distributed resources. This section summarizes several fruitful directions for further research.

First, this thesis demonstrates the initial use of three methods for simulating the effect of electricity demand or power injections on distribution network losses and network reinforcements and deriving polynomial functions to approximate these relationships. However, these simulations were performed for only three synthetic but representative European networks of differing topologies (specifically an urban, semiurban, and rural network). Future work should extend the application of these methods to a wider and more diverse set of networks to determine the diversity and range of results likely to be encountered in real-world power system planning contexts. In addition, European and North American network planning, design practices, and engineering standards differ. It would be fruitful to apply these same methods to networks representative of U.S. systems to discern if there are noticeable differences in the magnitude of the resulting coefficients (or even their functional form, although this is unlikely).

Second, in the case studies herein, single distribution network zones are used to represent anywhere from between 12 and 214 different networks of similar topology. Representing a large number of distinct networks with a single representative distribution network zone

will produce some degree of abstraction error, and this error is likely to be substantial at the high end of that range. Future research could therefore perform the power flow and network reinforcement simulation methods demonstrated in this thesis on a large number of randomly sampled networks from across one or more real-world regional power systems or utility service territories. These results could then be used to both estimate the likely degree of abstraction error that results when using different candidate networks as representatives of a larger cluster of similar networks, as well as to bound the maximum size these clusters can take before resulting errors render the use of simulation results in the holistic system planning model untenable. Ideally, these efforts could also use the sample of networks as a training set and use machine learning methods to identify physical characteristics of distribution networks that can be used to predict clusters of networks that can be represented by similar coefficients with minimal error. If this process yields an accurate predictive method, it may be possible to represent all networks in a large territory with a set of representative networks drawn from a randomized sample without having to reproduce the network simulations for each individual network.

Third, this thesis demonstrates a process to capture two of the three largest drivers of locational value for DERs in power system capacity planning models: losses and network constraints and reinforcements. However, this thesis does not provide a means of representing the additional locational value associated with enhanced reliability that certain DERs may provide (other than to add revenues from this service as an exogenous parameter in sensitivity analysis). If further research can identify a method to capture resilience and reliability benefits of DERs in the same power system planning context, then the accuracy and utility of this modeling framework will be further enhanced.

Fourth, the full power system planning model was demonstrated for a fictional power system with 5 transmission network zones, 10 distribution zones, and 61 individual resource options (as well as 5 segments of price-responsive demand). This thesis demonstrates that a formulation of this model that uses a linear relaxation of unit commitment constraints and investment decisions for discrete thermal generators can reliably produce results for this

scale system in roughly 2-6 hours on a high performance computing cluster. This fictional test system corresponds roughly to the size of the New York Independent System Operator region, which is the smallest ISO in the United States. In addition, NYISO's 11 actual transmission zones were reduced to just 5, and only 10 distribution networks are used to represent the full range of network topologies in the system (e.g., generally 2-3 distribution zones per transmission zone). This scale is probably sufficient to generate qualitative insights for indicative planning or techno-economic analysis. However, generating quantitative insights for real power systems will require expanding the spatial scope and number of network zones (both transmission and distribution) that can be represented. It therefore would be productive to identify the maximum spatial resolution at which this model can be reliably solved with its current formulation, explore opportunities to improve computational performance by changing model formulation, or to judiciously apply further abstraction methods to allow greater geographic resolution (or to incorporate discrete integer decisions such as transmission or distribution substation upgrades or investments in generating units). The capacity planning formulation herein is also amenable to various decomposition methods which may yield a step-change improvement in computational performance and are worth exploring.

Finally, the initial case study results herein indicate that the potential role and value of DERs in power systems may be limited, and that current policy support for DER adoption may outstrip the social value these resources deliver in many contexts. However, this important finding would need to be validated in a more realistic power system context and tested across a wider range of sensitivities and assumptions before offering concrete policy guidance. Such work represents an important and timely further application of the methods introduced in this thesis.

Bibliography

Abdin, I. F. and Zio, E. (2018). An integrated framework for operational flexibility assessment in multi-period power system planning with renewable energy production. *Applied Energy*, 222:898–914.

Anderson, D. (1972). Models for Determining Least-Cost Investments in Electricity Supply. *The Bell Journal of Economics and Management Science*, 3(1):267–299.

Benedict, E., Collins, T., Gotham, D., Hoffman, S., Karipides, D., Pekarek, S., and Ramabhadran, R. (1992). Losses in Electric Power Systems.

Bezanson, J., Edelman, A., Karpinski, S., and Shah, V. B. (2017). Julia: A fresh approach to numerical computing. *SIAM Review*, 59(1):65–98.

Blanford, G. J., Bistline, J. E., Young, D., and Merrick, J. (2016). Simulating Annual Variation in Load, Wind, and Solar by Representative Hour Selection. Technical report, Electric Power Research Institute, Palo Alto, CA.

Braun, M. (2007). Reactive power supplied by PV inverters - Cost-Benefit-Analysis. In *22nd European Photovoltaic Solar Energy Conference and Exhibition*, number September, Milan, Italy. 0.

Brown, T., Jonas, H., and Schlachtberger, D. (2018a). PyPSA : Python for Power System Analysis. *Journal of Open Research Software*, 6(1).

Brown, T., Schlachtberger, D., Kies, A., Schramm, S., and Greiner, M. (2018b). Synergies of sector coupling and transmission reinforcement in a cost-optimised, highly renewable European energy system. *Energy*, 160:720–739.

Cain, M., O'Neill, R., and Castillo, A. (2012). History of Optimal Power Flow and Formulations.

California Public Utility Commission (2015). Distribution Resources Plan (R.14-08-013).

Callaway, D., Fowlie, M., and Mccormick, G. (2018). Location, location, location: The variable value of renewable energy and demand-side efficiency resources. *Journal of the Association of Environmental and Resource Economists*, 5(1):39–75.

Caramanis, M., Ntakou, E., Hogan, W. W., Chakrabortty, A., and Schoene, J. (2016). Co-optimization of power and reserves in dynamic T&D power markets with nondispatchable renewable generation and distributed energy resources. *Proceedings of the IEEE*, 104(4):807–836.

Carpentier, J. (1962). Contribution á l'étude du dispatching économique. *Bulletin de la Société Française des Électriciens*, 8(3):431–447.

Carpentier, J. (1979). Optimal power flows. *International Journal of Electrical Power & Energy Systems*, 1(1):3–15.

CEER (2016). Electricity âĂŞ voltage quality. In *6th CEER Benchmarking Report on the Quality of Electricity and Gas Supply - 2016*, chapter 3, pages 80–137.

Clack, C. T. (2018). Weather-Informed Energy Systems Utilizing the WIS : dom Optimization Model Vibrant Clean Energy , LLC. Technical report, Vibrant Clean Energy, LLC.

Cohen, M. A., Kauzmann, P. A., and Callaway, D. S. (2016). Effects of distributed PV generation on California's distribution system, part 2: Economic analysis. *Solar Energy*, 128:139–152.

de Sisternes, F. J. (2014). *Risk Implications of the Deployment of Renewables for Investments in Electricity Generation*. Phd thesis, Massachusetts Institute of Technology.

de Sisternes, F. J., Jenkins, J. D., and Botterud, A. (2016). The value of energy storage in decarbonizing the electricity sector. *Applied Energy*, 175:368–379.

de Sisternes, F. J. and Webster, M. D. (2013). Optimal Selection of Sample Weeks for Approximating the Net Load in Generation Planning Problems.

Denholm, P. and Hand, M. (2011). Grid flexibility and storage required to achieve very high penetration of variable renewable electricity. *Energy Policy*, 39(3):1817–1830.

Ding, F., Nagarajan, A., Chakraborty, S., Baggu, M., Nguyen, A., Walinga, S., McCarty, M., and Bell, F. (2016). Photovoltaic Impact Assessment of Smart Inverter Volt-VAR Control on Distribution System Conservation Voltage Reduction and Power Quality.

Domingo, C. M. (2018). RNM: Reference Network Model.

Domingo, C. M., Gómez, T., Sánchez-Miralles, Á., Peco, J., and Martínez, A. C. (2011). A Reference Network Model for Large-Scale Distribution Planning With Automatic Street Map Generation. *IEEE Transactions on Power Systems*, 26(1):190–197.

Dunning, I., Huchette, J., and Lubin, M. (2017). JuMP: A Modeling Language for Mathematical Optimization. *SIAM Review*, 59(2):295–320.

EnerData (2016). Energy Efficiency Indicators: Rate of Electricity T&D Losses.

EnerNex (2011). Eastern Wind Integration and Transmission Study.

EPRI (2015). EGEAS User's Guide. Technical report, Electric Power Research Institute, Palo Alto, CA.

Eurelectric (2013). Active Distribution System Management A key tool for the smooth integration of distributed generation. Technical Report February, Union of the Electricity Industry (EURELECTRIC), Brussels, Belgium.

European Commission (2012). Roadmap 2050. Technical Report April, European Commission.

Faruqui, A., Sergici, S., and Warner, C. (2017). Arcturus 2.0: A meta-analysis of time-varying rates for electricity. *Electricity Journal*, 30(10).

Fitiwi, D. Z., Olmos, L., Rivier, M., de Cuadra, F., and Pérez-Arriaga, I. J. (2016). Finding a representative network losses model for large-scale transmission expansion planning with renewable energy sources. *Energy*, 101:343–358.

Frew, B., Becker, S., Dvorak, M., Andresen, G., and Jacobson, M. (2016). Flexibility mechanisms and pathways to a highly renewable US electricity future. *Energy*, 101:65–78.

Frew, B. A. (2014). *Optimizing the integration of renewable energy in the United States*. Phd thesis, Stanford University.

GE Energy (2010). Western Wind and Solar Integration Study: Executive Summary.

Gurobi Optimization Inc. (2016). Gurobi Optimizer Reference Manual. Technical report.

Haller, M., Ludig, S., and Bauer, N. (2012). Decarbonization scenarios for the EU and MENA power system: Considering spatial distribution and short term dynamics of renewable generation. *Energy Policy*, 47:282–290.

Hand, M., Baldwin, S., DeMeo, E., Reilly, J., Mai, T., Arent, D., Porro, G., Meshek, M., and Sandor, D., editors (2012). *Renewable Electricity Futures Study*. National Renewable Energy Laboratory, Boulder, CO.

Haydt, G., Leal, V., Pina, A., and Silva, C. A. (2011). The relevance of the energy resource dynamics in the mid/long-term energy planning models. *Renewable Energy*, 36(11):3068–3074.

Heuberger, C. F., Rubin, E. S., Staffell, I., Shah, N., and Mac Dowell, N. (2017a). Power capacity expansion planning considering endogenous technology cost learning. *Applied Energy*, 204(March):831–845.

Heuberger, C. F., Staffell, I., Shah, N., and Dowell, N. M. (2017b). A systems approach to quantifying the value of power generation and energy storage technologies in future electricity networks. *Computers and Chemical Engineering*, 107:247–256.

Hicks, K. L. (1959). Theory of economic selection of generating units. *Power Apparatus and Systems, Part III. Transactions of the American Institute of Electrical Engineers*, 78(4):1794–1799.

Hirth, L. (2013). The Market Value of Variable Renewables: The Effect of Solar and Wind Power Variability on their Relative Price The Market Value of Variable Renewables. *Energy Economics*, 38:218–236.

Hirth, L. (2017). The European electricity market model EMMA. Technical Report Version 2017-07-12, Neon Neue Energieökonomik GmbH.

Hobbs, B. F. (1995). Optimization methods for electric utility resource planning. *European Journal of Operational Research*, 83:1–20.

Hogan, W. W. (2013). Electricity Scarcity Pricing Through Operating Reserves. *Economics of Energy & Environmental Policy*, 2(2):1–11.

Horowitz, K. A., Palmintier, B., Mather, B., and Denholm, P. (2018). Distribution system costs associated with the deployment of photovoltaic systems. *Renewable and Sustainable Energy Reviews*, 90(February):420–433.

Huneault, M. and Galiana, F. (1991). A survey of the optimal power flow literature. *IEEE Transactions on Power Systems*, 6(2):762–770.

Jenkins, J. D. (2014). Political economy constraints on carbon pricing policies: What are the implications for economic efficiency, environmental efficacy, and climate policy design? *Energy Policy*, 69:467–477.

Jenkins, J. D. and Pérez-Arriaga, I. J. (2017). Improved regulatory approaches for the remuneration of electricity distribution utilities with high penetrations of distributed energy resources. *Energy Journal*, 38(3):63–91.

Jenkins, J. D. and Sepulveda, N. A. (2017). Enhanced decision support for a changing electricity landscape: the GenX configurable electricity resource capacity expansion model.

Joskow, P. and Tirole, J. (2007). Reliability and competitive electricity markets. *Journal of Economics*, 38(1):60–84.

Joskow, P. L. (2008). Capacity payments in imperfect electricity markets: Need and design. *Utilities Policy*, 16(3):159–170.

Kirchmayer, L. K., Mellor, A. G., O'Mara, J. F., and Stevenson, J. R. (1955). An Investigation of the Economic Size of Steam-Electric Generating Units. *Transactions of the American Institute of Electrical Engineers. Part III: Power Apparatus and Systems*, 74(3).

Koltsaklis, N. E. and Georgiadis, M. C. (2015). A multi-period, multi-regional generation expansion planning model incorporating unit commitment constraints. *Applied Energy*, 158:310–331.

Krishnan, V. K., Palmintier, B. S., Hodge, B. S., Hale, E. T., Elgindy, T., Bugbee, B., Rossol, M. N., Lopez, A. J., Krishnamurthy, D., Vergara, C., Domingo, Carlos Mateo, Postigo, F., de Cuadra, F., Gomez, T., Duenas, P., Luke, M., Li, V., Vinoth, M., and Kadankodu, S. (2017). Smart-DS: Synthetic Models for Advanced, Realistic Testing: Distribution Systems and Scenarios.

Lannoye, E., Flynn, D., and O'Malley, M. (2011). The role of power system flexibility in generation planning. In *IEEE Power and Energy Society General Meeting, 2011.*

Lara, C., Mallapragada, D., Papageorgiou, D., Vanketesh, A., and Grossman, I. (2018). Deterministic Electric Power Infrastructure Planning: Mixed-Integer Programming Model and Nested Decomposition Algorithm. *European Journal of Operational Research.*

Lazard (2017). Lazard's levelized cost of storage analysis âĂŤ version 3.0. Technical Report November.

Li, R., Wang, W., Chen, Z., Jiang, J., and Zhang, W. (2017). A review of optimal planning active distribution system: Models, methods, and future researches. *Energies*, 10(11):1–27.

Loulou, R., Goldstein, G., Kanudia, A., Lettila, A., and Remme, U. (2016). Documentation for the TIMES Model Part I. Technical Report July, International Energy Agency, Paris.

MA DOER (2018). Qualified Generation.

MacDonald, A., Clack, C., Alexander, A., Dunbar, A., Wilczek, P., and Xie, Y. (2016). Future cost-competitive electricity systems and their impact on US CO2 emissions. *Nature Climate Change*, 6:526–531.

Mai, T., Barrows, C., Lopez, A., Hale, E., Dyson, M., Eurek, K., Mai, T., Barrows, C., Lopez, A., Hale, E., Dyson, M., and Eurek, K. (2015). Implications of Model Structure and Detail for Utility Planning: Scenario Case Studies Using the Resource Planning Model.

Mai, T., Drury, E., Eurek, K., Bodington, N., Lopez, A., and Perry, A. (2013). Resource Planning Model: An Integrated Resource Planning and Dispatch Tool for Regional Electric Systems.

Mallapragada, D. S., Papageorgiou, D. J., Venkatesh, A., Lara, C. L., and Grossmann, I. E. (2018). Abstract Impact of model resolution on scenario. *Energy*, In press.

Margolis, R., Feldman, D., and Boff, D. (2018). Q4 2017/Q1 2018 Solar Industry Update.

Masse, P. and Gibrat, R. (1957). Application of Linear Programming to Investments in the Electric Power Industry. *Management Science*, 3(October):149–166.

Mateo, C., Prettico, G., Gómez, T., Cossent, R., Gangale, F., Frías, P., and Fulli, G. (2018). European representative electricity distribution networks. *International Journal of Electrical Power & Energy Systems*, 99.

Merrick, J. H. (2016). On representation of temporal variability in electricity capacity planning models. *Energy Economics*, 59:261–274.

Mileva, A., Johnston, J., Nelson, J., and Kammen, D. (2016). Power system balancing for deep decarbonization of the electricity sector. *Applied Energy*, 162:1001–1009.

MIT Energy Initiative (2011). Managing Large-Scale Penetration of Intermittent Renewables.

Morales-Espana, G., Latorre, J. M., and Ramos, A. (2013). Tight and Compact MILP Formulation of Start-Up and Shut-Down Ramping in Unit Commitment. *IEEE Transactions on Power Systems*, 28(2):1288–1296.

Nahmmacher, P., Schmid, E., Hirth, L., and Knopf, B. (2016). Carpe diem: A novel approach to select representative days for long-term power system modeling. *Energy*, 112:430–442.

Nakamura, S. (1984). A review of electric production simulation and capacity expansion planning programs. *International Journal of Energy Research*, 8(3):231–240.

National Electrical Manufacturers Association (2011). ANSI C84.1-2011: Electric power systems and equipmentâĂŤVoltage ratings (60 Hertz). Technical report, American National Standards Institute.

National Grid (2018). National Grid System Data Portal.

Nelson, J., Johnston, J., Mileva, A., Fripp, M., Hoffman, I., Petros-Good, A., Blanco, C., and Kammen, D. M. (2012). High-resolution modeling of the western North American power system demonstrates low-cost and low-carbon futures. *Energy Policy*, 43:436–447.

NREL (2017). 2017 Annual Technology Baseline. Technical report, National Renewable Energy Laboratory, Golden.

Ntakou, E. and Caramanis, M. (2015). Distribution network spatiotemporal marginal cost of reactive power. In *IEEE Power and Energy Society General Meeting*.

NYISO (2016a). NYISO Load Data.

NYISO (2016b). NYISO Operating Study Summer 2016. Technical report, New York Independent System Operator (NYISO), Albany, NY.

Palmintier, B. S. (2013). *Incorporating Operational Flexibility Into Electric Generation Planning: Impacts and Methods for System Design and Policy Analysis*. Phd dissertation, Massachusetts Institute of Technology.

Palmintier, B. S. and Webster, M. D. (2014). Heterogeneous Unit Clustering for Efficient Operational Flexibility Modeling. *IEEE Transactions on Power Systems*, 29(3):1089–1098.

Palmintier, B. S. and Webster, M. D. (2016). Impact of Operational Flexibility on Generation Planning With Renewable and Carbon Targets. *IEEE Transactions on Sustainable Energy*, 7(2):672 – 684.

Penn, I. (2018). California Will Require Solar Power for New Homes.

Pérez-Arriaga, I., Knittel, C., Bharatkumar, A., Birk, M., Burger, S., Chavez, J. P., Dueñas-Martinez, P., Herrero, I., Huntington, S., Jenkins, J., Luke, M., Miller, R., Rodilla, P., Tabors, R., Tapia-Ahumada, K., Vergara, C., Xu, N., Gomez, T., Battle, C., Norford, L., and Draffin, C. (2016). *Utility of the Future: An MIT Energy Initiative response to an industry in transition*. Massachusetts Institute of Technology, Cambridge, MA.

Pérez-Arriaga, I. J. and Linares, P. (2008). Markets vs. regulation: A role for indicative energy planning. *Energy Journal*, 29(SPEC. ISS. #2):149–164.

Perez-Arriaga, I. J. and Meseguer, C. (1997). Wholesale marginal prices in competitive generation markets. *IEEE Transactions on Power Systems*, 12(2):710–717.

Pfenninger, S. and Staffell, I. (2016). Long-term patterns of European PV output using 30 years of validated hourly reanalysis and satellite data. *Energy*, 114:1251–1265.

Pfenninger, S. and Staffell, I. (2018). Renewables.ninja.

Pletka, R., Khangura, J., Rawlines, A., Waldren, E., and Wilson, D. (2014). Capital Costs for Transmission and Substations. Technical Report February, Western Electricity Coordinating Council.

Poncelet, K. (2018). *Long-term energy-system optimization models: Capturing the challenges of integrating intermittent renewable energy sources and assessing the suitability for descriptive scenario analyses*. Phd thesis, KU Leuven.

Poncelet, K., Delarue, E., Six, D., Duerinck, J., and D'haeseleer, W. (2016). Impact of the level of temporal and operational detail in energy-system planning models. *Applied Energy*, 162:631–643.

Poncelet, K., Hoschle, H., Delarue, E., Virag, A., and Drhaeseleer, W. (2017). Selecting representative days for capturing the implications of integrating intermittent renewables in generation expansion planning problems. *IEEE Transactions on Power Systems*, 32(3):1936–1948.

Prettico, G., Gandale, F., Mengolini, A., Lucas, A., and Fulli, G. (2016). Distribution system operators observatory: From European electricity distribution systems to represntative distribution networks. Technical report, European Commission Joint Research Centre.

Pudjianto, D., Aunedi, M., Djapic, P., and Strbac, G. (2014). Whole-Systems Assessment of the Value of Energy Storage in Low-Carbon Electricity Systems. *IEEE Transactions on Smart Grid*, 5(2):1098–1109.

Pudjianto, D. and Strbac, G. (2017). Assessing the value and impact of demand side response using whole-system approach. *Proceedings of the Institution of Mechanical Engineers, Part A: Journal of Power and Energy*, 231(6):498–507.

Robertson, J. G., Harrison, G. P., and Wallace, A. R. (2017). OPF Techniques for Real-Time Active Management of Distribution Networks. *IEEE Transactions on Power Systems*, 32(5):3529–3537.

Schmalensee, R., Bulovic, V., Armstrong, R., Batlle, C., Brown, P., Deutch, J., Jacoby, H., Jaffe, R., Jean, J., Miller, R., O'Sullivan, F., Parsons, J., Pérez-Arriaga, I. J., Seifkar, N., Stoner, R., and Vergara, C. (2015). *The Future of Solar Energy.* Number 3. Massachusetts Institute of Technology, Cambridge, MA.

Schweppe, F. C. and Burke, W. J. (1989). Least-Cost Planning: Issues and Methods. *Proceedings of the IEEE*, 77(6):899–907.

Schweppe, F. C., Caramanis, M. C., Tabors, R. D., and Bohn, R. E. (1988). *Spot Pricing of Electricity.* Springer US.

Sepulveda, N. A. (2016). *Decarbonization of Power Systems: Analyzing Different Technological Pathways by.* Ms thesis, Massachusetts Institute of Technology.

Sepulveda, N. A., Jenkins, J. D., de Sisternes, F. J., and Lester, R. K. (2018). The role of firm low-carbon electricity resources in deep decarbonization of power generation. *Joule*, In press:1–25.

Short, W., Sullivan, P., Mai, T., Mowers, M., Uriarte, C., Blair, N., Heimiller, D., and Martinez, A. (2011). Regional Energy Deployment System (ReEDS).

SRECTrade (2018). Massachusetts SREC-I and SREC-II Update. Technical report, SRECTrade.

Staffell, I. and Pfenninger, S. (2016). Using bias-corrected reanalysis to simulate current and future wind power output. *Energy*, 114:1224–1239.

State of California (2018). About Go Solar California.

Sullivan, M. J., Mercurio, M., Schellenberg, J., and Freeman, S. &. C. (2015). Updated Value of Service Reliability Estimates for Electric Utility Customers in the United States.

The White House (2016). United States Mid-Century Strategy for Deep Decarbonization. Technical Report November, United States White House.

U.S. EIA (2009). The National Energy Modeling System: An Overview 2009. Technical Report October, U.S. Energy Information Administration, Washington, DC.

U.S. EIA (2017). The Electricity Market Module of the National Energy Modeling System: Model Documentation 2016. Technical report, U.S. Energy Information Administration, Washington, DC.

U.S. EIA (2018). Annual Energy Outlook 2018. Technical report, U.S. Energy Information Administration, Washington, DC.

U.S. EPA (2018). Documentation for EPA's Power Sector Modeling Platform v6: Using the Integrated Planning Model. Technical Report May, U.S. Environmental Protection Agency, Washington, DC.

Vallés Rodríguez, M. (2017). *Efficient Implementation and Potential Benefits of Demand Response in Electricity Distribution Networks*. Phd, Comillas Pontifical University, Madrid.

Wilson, R. and Biewald, B. (2013). Best Practices in Electric Utility Integrated Resource Planning. Technical Report June, Regulatory Assistance Project.

Wilson, R. and Peterson, P. (2011). A brief survey of state integrated resource planning rules and requirements. Technical report.

Young, D., Blanford, G., Bistline, J., Rose, S., de la Chesnaye, F., Bedilion, R., Wilson, T., and Wan, S. (2018). US-REGEN Model Documentation. Technical report, Electric Power Research Institute, Palo Alto, CA.

Zhang, F., Hu, Z., and Song, Y. (2013). Mixed-integer linear model for transmission expansion planning with line losses and energy storage systems. *IET Generation, Transmission & Distribution*, 7(8):919–928.

Zhao, J., Wang, C., Zhao, B., Lin, F., Zhou, Q., and Wang, Y. (2014). A review of active management for distribution networks: Current status and future development trends. *Electric Power Components and Systems*, 42(3-4):280–293.

Zibelman, A., Acampora, P., Brown, G., Sayre, G., and Burman, D. (2014). Order Establishing Brooklyn/Queens Demand Management Program.

Zibelman, A., Acampora, P. L., Sayre, G. C., and Burman, D. X. (2015). Order Adopting Dynamic Load Management Filings with Modifications.

Zimmerman, R. D. and Murillo-Sánchez, C. E. (2016). Matpower 6.0 User's Manual. Technical report, Power Systems Engineering Research Center, Cornell University.

Zimmerman, R. D., Murillo-Sánchez, C. E., and Thomas, R. J. (2011). MATPOWER: Steady-State Operations, Planning, and Analysis Tools for Power Systems Research and Education. *IEEE Transactions on Power Systems*, 26(1):12–19.